DOCTOR OF PHILOSOPHY

Investigating the physiological function of BACE1 and its role in metabolism

Gabriel, Jennie Louise

Award date:
2020

University of Dundee

Investigating the physiological function of BACE1 and its role in metabolism

Jennie Louise Gabriel

Thesis submitted for the degree of
Doctor of Philosophy

2020

Table of Contents

List of Figures

List of Tables

Acknowledgements

I would like to thank my supervisor, Mike Ashford for allowing me to conduct my PhD within his lab. I'd also like to thank him for his support and guidance throughout the project.
I would also like to thank both Alzheimer's Society and ARUK for funding this project.

I offer many thanks to the past and present members of the lab (Ashford massive) Paul, Susan, David, Daniella and (labmate 4 lyfe) Beth. You have all offered so much help and support over the past few years. Particular thanks and apologies to Beth for tolerating my maddening ramblings whilst trawling through peptide data and for making the lab such a fun place to work. Claire too, has always been a constant shoulder; sharing the ups and downs of research and both have assisted me greatly in the *in vivo* aspects of my project helping with tissue harvesting and perfuse fixing tissues. Other members of the MCM division have been amazing in their help and encouragement. Particular thanks to Will Fuller and Calum Sutherland who have been incredible in their guidance through the biochemical aspects of my project and for their emotional support through the tough times. Alison McNeilly deserves much gratitude for her consistent support and advice through all things animal and statistical.
Within the School of Life Sciences, Dr Sara Ten Have and Dr Michele Tinti have both offered so much of their time to aid me with this project; teaching me the ins and out of proteomics and bioinformatics as well as conducting individual analyses of the proteomic data. The Fingerprints facility within the university of Dundee were also instrumental in preparing the samples and analysis MS data for protein identification. Dr Susan Bray of the Tayside tissue bank kindly sectioned and stained the mouse tissues and Dr Rachel Toth of the University of Dundee cloning facility created the BACE1 fusion protein constructs for proximity assay. Thanks also go to Yves Rouillé of the Institut Pasteur de Lille for gifting me his leptin receptor construct pCneo-mObRb.

From the University of Aberdeen I must thank Prof. Bettina Platt for allowing the use of her humanised BACE1 knock-in animal model and Dr Claire Hull for

maintaining the animals throughout the dietary intervention. I must also thank Prof. Mirela Delibegovic for allowing use of her PTP1B antibody.

I must thank my husband Lee for his fortitude throughout my PhD and his boundless encouragement. Bath buds Lynette and Naomi have been oases for escapism as well as confidence boosters through the perils of imposter syndrome. Finally, my parents to whom I owe everything.

Candidate's Declaration

I hereby declare that all results described in this thesis, unless otherwise stated, are entirely my own work. I further state that the composition of this thesis was performed by myself and none of the material has been submitted for any other degree. Lastly, I verify that all sources have been appropriately cited. The work was carried out in the School of Medicine, University of Dundee, under the supervision of Professor M. L. J. Ashford.

Jennie Louise Gabriel

Supervisor's Declaration

I certify that Jennie Louise Gabriel has completed 8 terms of experimental research and has fulfilled the conditions of Ordinance 39, University of Dundee, such that she is eligible to submit the following thesis in application for the degree of Doctor of Philosophy.

Professor M.L.J Ashford

Abbreviations

Acronym	Definition
11β-HSD	11-β-dehydrogenase
AAV	Adeno-associated virus
Abcf2	ATP-binding cassette sub-family F member 2
ACE1/2	Angiotensin conversting enzyme
ACTH	adrenocorticotropin hormone
AD	Alzheimer's Disease
ADAM10	Disintegrin and metalloproteinase domain-containing protein 10
AgRP	Agouti-related protein
AICD	Amyloid intracellular domain
AMPA	α-amino-3-hydroxy-5-methyl-4-isoxazolepropionic acid
AMPAR	α-amino-3-hydroxy-5-methyl-4-isoxazolepropionic acid receptor
ANOVA	Analysis of variance
APH1	Anterior pharynx defective 1
APLP	Amyloid precursor like protein
ApoE	Apolipoprotein E
APP	Amyloid precursor protein
APPswe	Amyloid precursor protein; swedish mutation
ARC	Arcuate nucleus
ARF6	ADP-ribosylation factor 6
Arhgap1	RHO GTPase-activating protein 1
ATP	Adenosine triphosphate
Axl	Tyrosine protein kinase receptor UFO
Aβ	Amyloid beta
$A\beta_{1-40}$	Amyloid beta; 1-40
$A\beta_{1-42}$	Amyloid beta; 1-42
BACE1	Beta-site amyloid precursor protein cleaving enzyme 1
BBB	Blood brain barrier
BDNF	Brain derived neurotrphic factor
BirA	Bifunctional ligase/repressor
BLAST	Basic Local Alignment Search Tool
BMI	Body mass index
Bsg	Basigin
CAMKII	Calcium/calmodulin-dependent protein kinase II
CART	Cocaine- and amphetamine-regulated transcript protein
CASK	Calcium/calmodulin-dependent serine **protein** kinase
Cav1	Caveolin 1
CHL1	Cell adhesion molecule like 1
CK1	Casein kinase 1
CNS	Central nervous system
CNTN2	Contactin 2
CPE	Carboxypeptidase E
CRH	corticotropin-releasing hormone
CSF	Cerebral spinal fluid
CTAP	Cell Type specific labeling using Amino acid Precursors
ddH_2O	Double distilled H_2O
DDR	Discoidin domain receptor
DG	Dentate gyrus
DHHC20	Zinc Finger DHHC Domain-Containing Protein 20
DIO	Diet induced obesity

DLG1	Discs Large MAGUK Scaffold Protein 1
DNA	Doeoxyribonucleic acid
DPN	Dorsal premammilllary nucleus
DS	Down syndrome
EC	Entorhinal cortex
ECM	Extracellular matrix
Efr3a	Protein EFR3 homolog A
EGF	Epidermal growth factor
EGFR	Epidermal growth factor receptor
Eif3	Eukaryotic translation initiation factor 3
EPB41L1	Erythrocyte Membrane Protein Band 4.1 Like 1
ER	Endoplasmic reticulum
ErbB	Epidermal growth factor receptor B
ERK	Mitogen activated protein kinase
FA2H	Fatty acid 2-hydroxylase
FAD	Famelial alzheimer's disease
FDR	False discovery rate
FERM	4.1 protein, Ezrin, Radixin and Moesin
Flot2	Flotilin 2
FUCA1	alpha-L-fucosidase
FUT	Fucosyltransferase
GABA	γ-aminobutyric acid
GABAR	γ-aminobutyric acid receptor
Gart	Trifunctional purine biosynthetic protein adenosine-3
GCSFR	Granulocyte colony-stimulating factor receptor
GGA	Golgi-localized, γ-ear-containing, Arf
Gigyf1	GRB10 interacting GYF protein 1
GLUT	Glucose transporter
gp-130	Glycoprotein 130
GPI	Glycosylphosphatidylinositol
GSK3α	Glycogen synthase kinase 3 alpha
GSK3β	Glycogen synthase kinase 3 beta
GWAS	Genome wide association study
HF	High-fat
HFD	High-fat diet
HPRT	Hypoxanthine-guanine phosphoribosyltransferase
HPV	Human Papillomaviruse
HRP	Horse radish peroxidase
ICV	Intracerebroventricular
IHC	Immunohisochemistry
IL-18	Interleukin 18
IL-1β	Interleukin 1 beta
IL-6	Interleukin 6
IP	Intraperitoneal
IPA	Ingenuity pathway analysis
IRS-1	Insulin receptor substrate 1
Jag1	Jagged 1
JAK	Janus kinase
JAK2	Janus kinase 2
Kars	Lysine tRNA ligase
KI	Knock-in
KO	Knock-out

Krt10	Keratin (type I cytoskeletal 10)
KTN1	Kinectin 1
LATE	Limbic-predominant age-related TDP-43 encephalopathy
LDL	Low density lipoprotein
LHA	Lateral hyothalamic area
LIFR	Leukemia inhibitory factor receptor
LOAD	Late onset alzheimer's disease
LRP1	Lipoprotein receptor related protein 1
LTP	Long term potentiation
M6PR	Mannose 6 phosphate
MALDI-TOF	Matrix-assisted laser desorption ionization time-of-flight mass spectrometry
MAP1B	Microtubule-associated protein 1B
MC4R	Melanocortin 4 receptor
MCI	Mild cognitive impairment
MEK	Dual specificity mitogen-activated protein kinase kinase
Mettl16	RNA N6-adenosine methyltransferase
mGluR	Metabotropic glutamate receptor
MMB	Medial mammilary body
MPRIP	Myosin phosphatase Rho-interacting protein
mRNA	Messenger RNA
Myof	Myoferlin
NAP	Nectin and ponsin
$Na_v\beta_2$	voltage-gated sodium channel β_2 subunit
NC	Normal chow
NCAM	Neuronal cell adhesion molecule
NECL	Nectin like protein
NET	Neutrophil extracellular trap
NF-κB	Nuclear factor kappa B
NFT	Neurofibrillary tangle
NLRP3	NLR Family Pyrin Domain Containing 3
NMDA	N-Methyl-D-aspartic acid
NMDAR	N-Methyl-D-aspartic acid receptor
NPY	Neuropeptide Y
NRG	Neuregulin
NRG1	Neureguin 1
NST	Nucleus of the solitary tract
NT	Neurotransmitter
ObR	Leptin receptor
ObRb	Leptin receptor; isoform b
PAM	Peptidylglycine α-amidating monooxygenase
PC1	Pro-hormone convertase 1
PC2	Pro-hormone convertase 2
PCA	Principle component analysis
PCR	Polymerase chain reaction
PDI	Protein disulphide isomerase
Pgrmc2	Progesterone receptor component 2
PI3K	Phosphoinositide 3-kinase
PIGN	Phosphatidylinositol Glycan Anchor Biosynthesis Class N
PKB	Protein kinase B
PLD3	Phospholipase D3
PM	Plasma membrane
POMC	Pro-opiomelanocortin

PPARγ	Peroxisome proliferator-activated receptor γ
PPL	Poly-L-Lysine
PSEN2	Presenilin 2
PSGL1	P-Selectin Glycoprotein Ligand 1
PTM	Post-translational modification
PTP1B	Tyrosine-protein phosphatase non-receptor type 1
PVN	Paraventricular nucleus
Rab	Ras-related proteins
RNA	Ribonucleic acid
RNAi	Interfering RNA
RT PCR	Reverse transcription PCR
SAD	Sporadic Alzheimer's Disease
sAPP	Soluble APP
sAPPα	soluble Amyloid precursor protein alpha
sAPPβ	soluble Amyloid precursor protein beta
ScrP	Scrambled peptide
SEPT	Septin
Sez6	Seizure protein 6
Sez6L1	Seizure protein 6-like 1
Sh3pxd2a	SH3 and PX domain-containing protein 2A
SHP-2	Tyrosine-protein phosphatase non-receptor type 11
Slc	Solute carrier family protein
SLM	Stratum lacunosum moleculare
SNP	Single nucleotide polymorphism
SO	Stratum oriens
SOCE	Store-operated Ca2+ entry
SOCS3	Supressor of cytokine signalling 3
SorLA	Sortilin related receptor 1
Sptbn1	Spectrin beta chain non-erythrocytic 1
SR	Stratum radiatum
STAT	Signal transducer and activator of transcription
STAT3	Signal transducer and activator of transcription 3
SUSPECS	surface-spanning protein enrichment with click sugars
T2D	Type 2 Diabetes
TA	Temporoammonic
TBR1	T-box brain 1
TDP-43	Transactive response DNA binding protein of 43 kDa
TGFB1	Transforming Growth Factor Beta 1
TGN	Trans-golgi network
TMT	Tandem mass tag
TNF-α	Tumour necrosis factor α
TNFR1	TNF receptor 1
TS	Trisynaptic
TXNDC15	Thioredoxin Domain Containing 15
UCP1	Uncoupling protein 1
USP8	Ubiquitin specific peptidase 8
UTR	Untranslated region
VAMP	Vesicle associated membrane protein
Vang1	Vang-like protein 1
VMH	Ventromedial hypothalamus
VPN	Ventral premammillary nucleus
Vps13c	Vacuolar protein sorting associated protein 13c

WAT	White adipose tissue
WT	Wild type
αMSH	alpha melanocyte stimulating hormone

Summary

Dementias are now considered to be the 5th greatest cause of death worldwide and the leading cause of death in the UK. One of the biggest problems facing Alzheimer's Disease (AD) research is the time difference between disease onset and diagnosis in sporadic cases; with many patients only exhibiting symptoms after decades of living with AD pathologies. Due to this, current understanding of the early stages of this dementia is extremely limited but the pathogenic production of amyloid is currently considered the earliest change in AD development.

The presence of neurotoxic amyloid is a hallmark of AD. This peptide aggregates to form the characteristic plaques that are used to diagnose AD post-mortem. The rate limiting step in amyloidogenesis is the activity of the aspartyl protease β-site amyloid precursor protein cleaving enzyme 1 (BACE1). Whilst the function of this enzyme has been well studied within the context of AD, very little is known about its physiological function within healthy organisms. However, studies have identified that BACE1 KO mice are resistant to diet-induced obesity and its co-morbidities and BACE1 protein expression is known to increase in obesity- a known risk factor for AD.

This thesis aims to test the hypothesis that metabolic dysfunction as a result of chronic high-fat feeding leads to changes in BACE1 activity, thereby increasing the susceptibility of developing AD. To do this, proteomic analysis of hippocampal and hypothalamic tissues from chow fed and high-fat fed mice were compared alongside a BACE1 proximity assay to determine novel BACE1 interacting proteins. A further study was designed to test the hypothesis that amyloid peptides lead to leptin resistance- a possible contributor to central memory and metabolic impairment. These studies suggest a role for BACE1 in the regulation of cell connectivity and communication, which may underlie the changes in central metabolic and memory circuitry seen in both obesity and AD.

Chapter 1

Introduction

1.1 Dementia and Alzheimer's Disease

1.1.1 Background

Dementia is an umbrella term describing degenerative diseases of the brain. Alterations in brain function brought about by these conditions result in difficulties in movement, speech, behavioural changes and memory deficits to name but a few. The symptoms vary with the brain region affected and the disease, but pathologies can overlap between dementias within the same individual often making precise diagnoses difficult. For example, individuals with amyloid pathology (associated with Alzheimer's disease) may also exhibit lewy body pathology (associated with Parkinson's disease). These diseases represent abnormal brain function as a result of dysfunctional neurochemistry such as; deficiencies in neurotransmitter release, blood flow or brain atrophy.

Over 850,000 people are suspected of living with a dementia in the UK, more than 520,000 of which have Alzheimer's disease (AD). The number of dementia cases is expected to rise to over 2 million by 2050 leading to a financial impact of £55bn by 2040 in the UK alone (Prince et al., 2007). As the leading cause of death in the UK, research into the causes and treatments for dementias are urgently needed (ARUK, 2017).

Alzheimer's disease (AD) is the most common form of dementia worldwide with 2 out of 3 dementia diagnoses resulting from this disease (ARUK, 2018). Alzheimer's disease was first reported in 1906 by Alois Alzheimer- a psychiatrist and neuroanatomist who described a 50 year old woman presenting paranoia, sleep disturbances, memory deficits, aggressiveness and confusion. Upon her death, Alzheimer discovered distinctive plaque and tangle morphology within her brain which are still used today as diagnostic markers of AD (Hippius & Neundörfer, 2003). AD is widely considered a disease of the hippocampus and cerebral cortex. AD associated atrophy within the hippocampus results in loss of long-term potentiation (LTP) and, as a result, the ability to form new memories whilst memories from youth remain unaffected until later stages with severe atrophy. This inability to form new memories is the hallmark of AD and is one of the first symptoms to manifest. Other symptoms include impaired problem solving, behavioural and personality changes as well as difficulties with speech in later stages of the disease. AD progression was classified by Braak & Braak (1995). They categorised six stages of AD (I-VI) with each showing increasing

pathology and progressing atrophy throughout the hippocampus, limbic structures and the neocortex in a predictable pattern relating to behavioural changes observed with advancement of the disease. The pathology used by Braak & Braak in their classification of AD was the presence of neuro-fibrillary tangles (NFTs). NFTs form within neuronal cells and increase in number throughout AD progression. They are formed when the microtubule associated protein tau becomes hyper-phosphorylated, leading to accumulation of this protein into aggregates. The resultant loss of functional tau protein leads to instability within the microtubules which then disassemble, causing changes in cell morphology and eventual death of the cell. This pathology correlates well with cognitive decline and is a good aid in the determination of disease progression, however it is not considered the initiating factor of AD. Whilst NFT pathology can be identified in early Braak stages and is considered to begin approximately 10 years before cognitive symptoms manifest; changes in amyloid- another AD associated pathology - are predicted to occur up to 25 years before diagnosis and may be a key initiator in AD onset (Bateman et al., 2012).

Whilst AD is still largely considered a disease of the hippocampus and cerebral cortex, neuroimaging studies have identified atrophy within other brain regions. Indeed, grey matter abnormalities have been identified in the amygdala, striatum and hypothalamus of healthy individuals that later go on to develop AD (Hall, Moore, Lopez, Kuller, & Becker, 2008; Loskutova, Honea, Brooks, & Burns, 2010). Furthermore, metabolic characteristics such as accelerated weight loss and low body weight in the elderly are associated with early stage AD (Johnson, Wilkins, & Morris, 2006b; White, Pieper, Schmader, & Fillenbaum, 1996).

1.1.2 Amyloid in Alzheimer's Disease

The amyloid cascade hypothesis in AD was first proposed by Hardy & Higgins (1992). They proposed that accumulation of the β-amyloid (Aβ) peptide and its neurotoxic effects are the cause of AD and that this pathology preceded NFTs and even caused this second pathology. A dogma of AD pathogenesis is that the oligomerisation and aggregation of amyloid proteins into amyloid plaques leads to this neurotoxic effect however, this theory is beginning to be challenged. Aβ peptides are small 4kDa fragments and exist as small soluble oligomers, fibrils and large plaques aggregates (Chen & Glabe, 2006; Cleary et al., 2005). Recent

studies have indicated that soluble oligomers have greater neurotoxic and LTP inhibitory effects than larger amyloid species suggesting that Aβ aggregation may in fact be a protective mechanism against the toxicity of smaller species (Cizas et al., 2010; Cleary et al., 2005; Walsh et al., 2002). Whilst these studies provide important and valuable insight into the causes of cell death within AD, many of them lack physiological relevance. *In vivo*, Aβ plaques are known to contain a multitude of proteins in addition to amyloid which may confer effects not accounted for in *in vitro* amyloid oligomerisation methods. Proteomic analysis of amyloid plaques by Liao *et al.* (2004) revealed 488 proteins within these aggregates.

The amyloid cascade hypothesis (Figure 1.1) states that Aβ production is the result of sequential cleavages of the amyloid precursor protein (APP). APP, a type I transmembrane protein, contains multiple cleavage sites for secretases. Under non-AD conditions, initial cleavage of APP is predominantly conducted by an α-secretase enzyme, typically A disintegrin and metalloproteinase domain-containing protein 10 (ADAM10) as the main α-secretase within the brain (S Lammich et al., 1999). ADAM10 cleaves APP at Lys^{687} and Leu^{688}. This cleavage results in release of a soluble APP fragment (sAPPα) into the extracellular space and leaves an N-terminally truncated APP within the membrane. A subsequent cleavage by the γ-secretase complex within the transmembrane domain completes processing and releases a small P3 fragment ($Aβ_{17-40/42}$) into the extracellular space and the C-terminal domain (AICD) into the cytosol. The physiological purpose of this processing has yet to be determined but some studies have indicated that products of APP processing play an important role in neuronal physiology and survival.

Studies into the physiological effects of APP cleavage by-products have been contradictory with sAPPα having been shown to both attenuate and promote LTP in neurons. Further evidence suggests that it may behave as a growth factor in the regulation of glucose uptake in skeletal muscle (Hamilton et al., 2014; Taylor et al., 2008). The $Aβ_{17-40/42}$ fragment (Figure 1.2) does not form fibrillar oligomers as full length Aβ species do. However, pre-amyloid aggregates containing $Aβ_{17-40/42}$ are a known component of senile plaques in AD in Down's syndrome (DS) patients. A feature of which is increased APP expression due to trisomy of

chromosome 21. Whilst pre-amyloid lesions may be prolific in DS patients, their presence is not associated with neuronal death and cerebral dysfunction as observed with amyloid plaques in AD. More recent studies have suggested roles for the N-truncated Aβ peptides such as $Aβ_{17-40/42}$, including calcium signalling interference and proinflammatory effects (Szczepanik, Rampe and Ringheim, 2001; Jang *et al.*, 2010). The function of the AICD peptide is largely debated with some studies suggesting no or little function for this APP fragment and others implicating it as a transcriptional regulator of genes such as *GSK3β, ACE1/2, EGFR* and *LRP1*. The regulation and theorised functions of AICD have been extensively reviewed by Müller *et al*. (2008).

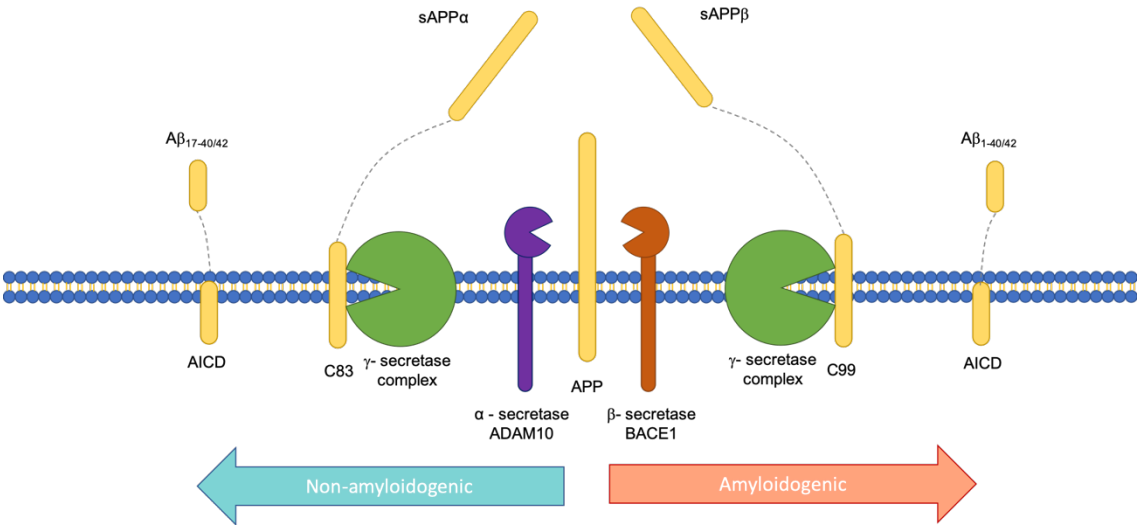

Figure 1.1 APP processing under healthy and AD conditions. Under normal conditions APP is proteolytically cleaved first by an α-secretase such as ADAM10, then by a γ-secretase complex. This results in the release of extracellular sAPPα and a small 3kDa $Aβ_{17-40/42}$ fragment by a non-amyloidogenic process. The AICD fragment is released into the cytosol. In the amyloidogenic pathway, the initial cleavage by the β-secretase BACE1 leads to the release of extracellular sAPPβ and the neurotoxic peptides $Aβ_{1-40/42}$ upon γ-secretase cleavage. Increases in amyloidogenic processing of APP are characteristic of AD.

In AD patients, there is reduced processing of APP through non-amyloidogenic mechanisms and increased processing via an alternative, amyloid-producing mechanism (Nistor et al., 2007). (Figure 1.1) This increase in amyloidogenesis is the result of increased expression and activity of the β-site APP cleaving enzyme 1 (BACE1); an aspartyl protease that cleaves APP 16 amino acids N-terminal of the α-secretase cleavage site between Met^{671} and Asp^{672}. BACE1 expression has been shown to increase with age whilst ADAM expression remains stable, suggesting a possible cause of increased amyloidogenic APP processing leading to AD (Nistor et al., 2007). BACE1 processing of APP leads to a shorter sAPPβ peptide being released and full-length amyloid ($Aβ_{1-40/42}$) being produced upon γ-

secretase cleavage (Figure 1.2). Unlike sAPPα, sAPPβ is not involved in LTP (Taylor et al., 2008) but, like sAPPα, has been shown to promote dendritic growth but not axonal length (Chasseigneaux et al., 2011). Both forms of sAPP have been shown to activate NF-κB and increase interleukin 1β (IL-1β) expression in microglia and sAPP treatment of co-cultures of microglia and primary neurons showed increased neurotoxicity in the presence of these peptides (Barger & Harmon, 1997). Further indications of the neurotoxic effects of APP peptides lie in a study showing that N-terminal fragments of APP bind to death receptor 6 resulting in activation of caspase-dependent cell death pathways (Nikolaev, McLaughlin, O'Leary, & Tessier-Lavigne, 2009).

APP contains a second BACE1 cleavage site (the β' site) between Tyr^{681} and Gln^{682}. This site is within the full-length Aβ peptide and cleavage here leads to an N-terminal truncation and the $Aβ_{11\text{-}40/42}$ peptide (Figure 1.2). This peptide does not exhibit the neurotoxic effects observed with full-length Aβ species but is a known component of senile plaques. A novel, pyroglutamate amyloid species ($pAβ_{3\text{-}X}$) has also been identified as a large component of senile plaques (Mori, Takio, Ogawara, & Selkoe, 1992). $pAβ_{3\text{-}X}$ represents a minor amyloid species and is becoming increasingly researched for its pathological effects within the brain. This truncation leads to dehydration of the N-terminal glutamic acid to form pyroglutamate by glutaminyl cyclase- a process that is known to be upregulated in AD (Schilling et al., 2008). This modification results in rapid aggregation as a result in increased N-terminal hydrophobicity, resistance to proteolytic degradation and increased neurotoxicity of this peptide (Piechotta et al., 2017; Russo et al., 2002).

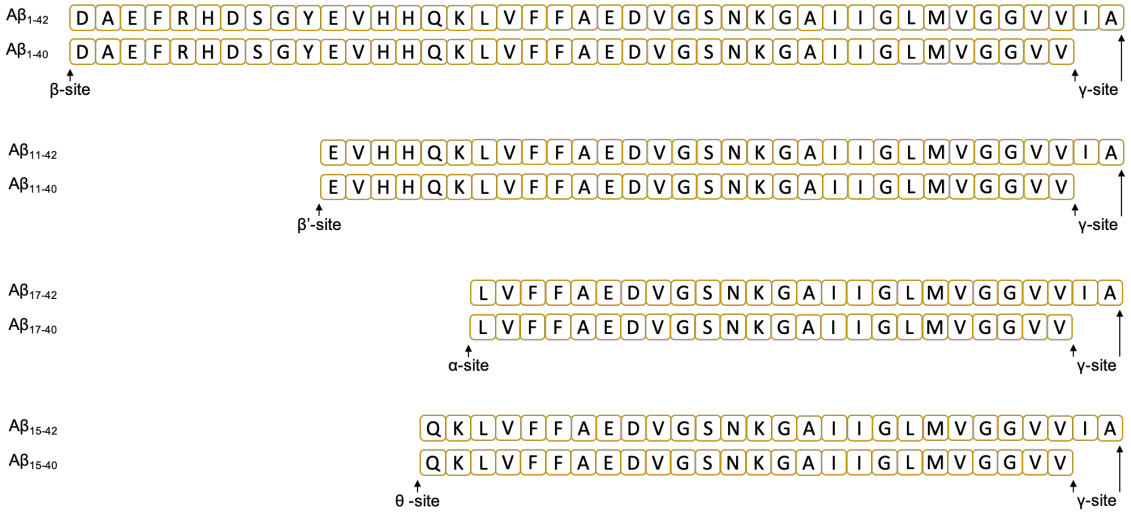

Figure 1.2 Sequences and cleavage points of the common amyloid species. The length of amyloid peptide varies with APP cleavage site. APP processing by β-secretase BACE1 forms the longest peptide of the amyloid species' $Aβ_{1-40}$ and $Aβ_{1-42}$. $Aβ_{1-42}$ is considered to aggregate the most readily of the amyloid peptides suggesting that the IA amino acids not present in $Aβ_{1-40}$ contribute to aggregation. BACE1 processing at the β' site leads to $Aβ_{11-40}$ and $Aβ_{11-42}$ peptides that are less abundant than $Aβ_{1-40}$ and $Aβ_{1-42}$. α-secretases such as ADAM10 lead to the formation of smaller $Aβ_{17-40}$ or $Aβ_{17-42}$ amyloid species and caspase processing of APP at the θ-site produces the peptides $Aβ_{15-40}$ and $Aβ_{15-42}$.

Plant *et al.* (2003) showed that inhibition of BACE1 in primary rat neurons induced cell death. Furthermore, this effect could be overcome with $Aβ_{1-40}$ treatment at pM concentrations. Effects of BACE1 inhibition were diminished with $Aβ_{1-42}$ whilst $Aβ_{25-35}$ offered no protection from cell death. In addition, immunodepletion of amyloid peptides *in* vivo resulted in reduced long and short-term memory as a result of inhibition of LTP. These effects can be overcome with human oligomeric $Aβ_{1-42}$ overall suggesting that these peptides play an important physiological role within the brain under physiological conditions (Garcia-Osta & Alberini, 2009; Puzzo et al., 2011). Aβ peptides have been suggested to contain antimicrobial properties through binding of fibrillar species to pathogens resulting in pore formation and bacterial perforation (Kagan et al., 2012). Furthermore, amyloid peptides have been shown to bind viruses such as HPV and influenza, preventing cell infection (Brothers, Gosztyla, & Robinson, 2018). These studies are supported by Aβ targeting drugs inducing hippocampal atrophy, cognitive decline and increased infections (Brothers et al., 2018). All support the hypothesis that Aβ plays an important physiological role and that efficient clearance of Aβ peptides suppresses the potential immune and neuroprotective functions they confer.

The length of Aβ peptide appears to have a great effect upon its pathophysiology. $A\beta_{1-42}$ is the most commonly studied as it has been shown to oligomerise more readily and form larger aggregates than any other amyloid species. It is also the most common form of amyloid within Aβ plaques. $A\beta_{1-40}$ is also commonly studied but the lack of residues 41 and 42 result in preference towards smaller, trimeric or tetrameric species that do not go on to form fibrillar structures (Bitan et al., 2003). $A\beta_{1-40}$ is the most abundant of the amyloid species though expression of this peptide does not correlate to AD progression as well as $A\beta_{1-42}$. However, with recent studies identifying smaller, oligomeric amyloid structures as the most neurotoxic, interest in $A\beta_{1-40}$ is increasing.

The C-terminal length of Aβ peptides is determined by the γ-secretase complex made up of four integral membrane proteins: Presenilin (PSEN), anterior pharynx defective 1 (APH1), nicastrin and presenilin enhancer 2 (PEN-2) (Kimberly et al., 2003; Wolfe et al., 1999; G. Yu et al., 2000). Two homologues exist of Presenilin, PSEN1 and PSEN2 which share 67% sequence identity (Levy-Lahad et al., 1995). PSEN proteins represent the catalytic subunit of the complex with two aspartic acid residues catalysing proteolysis of substrates (Wolfe et al., 1999). Evidence indicates that the predominant forms of Aβ within the brain are $A\beta_{X-40}$ indicating a preference for cleavage at 40 by the γ-secretase complex (Mori et al., 1992). Current thinking is that the C-terminal length of amyloid is determined as a result of cleavages of a larger, $A\beta_{X-49}$ peptide with sequential release of tetrapeptides but the mechanisms dictating the stopping point has not been determined (Takami et al., 2009; Tomita et al., 1999).

The extent of aggregation of Aβ has also been shown to depend on the secondary structure. Aged Aβ peptides exhibit increased β-sheet conformation which leads to greater aggregation and a propensity towards fibrillar oligomerisation. Less β-sheet conformation in Aβ peptides results in smaller, more diffuse plaques (similar to the proamyloid $A\beta_{17-40/42}$ plaques observed in DS brains) (Urbanc et al., 2004; Viet, Ngo, Lam, & Li, 2011). Whilst the larger Aβ aggregates were once thought to be the main cause of AD, it is now considered that smaller, oligomeric structures may be more neurotoxic than the fibrillar forms, suggesting that Aβ with less β-sheet conformation may play a greater role in AD (Ahmed et al., 2010). As the $A\beta_{17-40/42}$ fragment forms smaller, oligomeric species without the resulting

neurotoxicity it may be suggested that the N-terminal cleavage site of Aβ plays a key role in the pathological effects of amyloid peptides; possibly as a result of secondary structural changes. This idea is supported by identification of folding differences between $A\beta_{1-40}$ and $A\beta_{1-42}$ that may affect the availability of hydrophobic regions within the peptide, thus influencing the propensity towards oligomerisation (Urbanc et al., 2004).

Recently, a new form of AD-like dementia has been characterised termed limbic-predominant age-related TDP-43 encephalopathy (LATE). LATE patients exhibit late-stage clinical symptoms comparable to AD but is a result of proteinopathy of transactive response DNA binding protein of 43 kDa (TDP-43) (Nelson et al., 2019). Early stages of LATE occur within the amygdala and are identified by increased phosphorylation and ubiquitination of TDP-43. This is accompanied by translocation from the nucleus to the cytoplasm whereby TDP-43 containing, tau negative inclusions form. In later stages, these inclusions are also present in the entorhinal cortex and dentate gyrus (DG) (Kadokura, Yamazaki, Lemere, Takatama, & Okamoto, 2009).

A major obstacle in AD research is the lack of animal models that can be used as a representative of sporadic AD (SAD). Whilst canine, feline and even some cetacean cases of AD have been documented, cases have not been identified in rodents (Chambers et al., 2015; E. Head, 2013; Sarasa & Pesini, 2009). This has led to a plethora of rodent models of AD, all of which have mutations in one or more of the APP, PSEN1 or Tau genes to induce AD-like phenotypes but are not true representations of non-genetic AD. Whilst rodents do express all of the amyloidogenic machinery and do produce Aβ peptides, even aged rodents do not exhibit the amyloid and tau pathologies associated with AD. This may be due, in part, to the sequence differences in APP between humans and rodents. Mouse Aβ varies from human in only 3 amino acids R5G, Y10F and H13R (Lv et al., 2013). These amino acid changes result in a 20% reduction in β-sheet folding compared to human $A\beta_{1-42}$. The extent of β-sheet conformation may then influence the ability of amyloid to aggregate (Viet et al., 2011). Due to these differences, there is currently no accurate physiological model for SAD.

1.1.3 Hippocampal function and Alzheimer's Disease

The hippocampus is the main brain region involved in learning and memory. Current thinking in neuroscience suggests that memories are retained and maintained through the regulation of synaptic sensitivity to neurotransmitters- a process known as synaptic plasticity. The neuronal processes of LTP and long-term depression (LTD) are thought to be an integral part of maintaining synaptic plasticity. In LTP, high-frequency stimulation of neurons leads to enhanced synaptic strength through increased post synaptic potential thereby increasing signal transmission in the postsynaptic neuron (Bliss & Lømo, 1973). The effects of LTP can be long lasting with evidence suggesting that LTP can still be detected 1 year after stimulation; however these effects were dependent upon environmental enrichment (Abraham, Logan, Greenwood, & Dragunow, 2002). Furthermore, neurons which have undergone high-frequency stimulation are more susceptible to LTP with future stimulation indicating sensitisation of this process.

Conversely, low frequency signals lead to LTD whereby synaptic strength is weakened and can reduce effect size of high-frequency stimulation on LTP. Habituation to this process can lead to synapse loss and desensitisation of neurons. To prevent this; neurons undergo a homeostatic process whereby continuous LTP or LTD stimulation leads to changes in neuronal sensitivity and the reduction or elevation (respectively) of synapse strength to keep synaptic sensitivity within a sustainable physiological range. The suggested mechanisms for this process have been reviewed by Vitureira and Goda (2013). Synaptic dysfunction is a known attribute of AD and AD models. Transgenic mice over-expressing APP have been shown to exhibit impaired LTP as well as increased sensitivity to LTD compared to WT controls, a result that has been replicated with application of Aβ peptides to hippocampal slices *ex vivo* (Nomura, Takechi, & Kato, 2012; Walsh et al., 2002; Wang et al., 2002).

Multiple mechanisms have been proposed for how LTP and LTD occur but the form most commonly associated with learning and memory is NMDA receptor (NMDAR) activation. NMDAR is a neuronal receptor for the most common excitatory neurotransmitter in the brain- glutamate. NMDARs are both receptors and ion channels and are integral in synaptic plasticity by initiating Ca^{2+} influx upon persistent glutamate release (high frequency stimulation) into the synaptic

cleft. NMDAR activation is a slower response than that seen in action potential transmission, which is primarily the function of faster acting glutamatergic ion channels- AMPA receptors (AMPAR) and kainate receptors. One of the downstream effects of NMDAR activation is the translocation of further AMPAR to the post-synaptic terminal, thereby increasing synaptic sensitivity to further presynaptic glutamate release. Another modulatory mechanism behind synaptic strength is though the G-protein coupled glutamate receptors mGluRs. These receptors regulate LTP through activation of MAPK signalling (amongst others) that promote transcription of genes such as BDNF that regulate synaptic strength (Viwatpinyo & Chongthammakun, 2009). Interestingly, activation of the same mGluR (mGluR5) promotes APP translation (Westmark & Malter, 2007). Furthermore, oligomeric amyloid species have been shown to bind to mGluR5 leading to over-stabilisation and clustering within the post-synaptic membrane. This increased mGluR5 signalling and led to Ca^{2+} influx and synaptotoxicity (Renner et al., 2010). Aβ peptides have also been implicated in NMDAR dysfunction as oligomeric species have been suggested to activate NMDARs (Texidó, Martín-Satué, Alberdi, Solsona, & Matute, 2011; Wu, Anwyl, & Rowan, 1995).

Whilst BACE1 activity and Aβ production is increased in the hippocampus in AD, amyloidogenesis is still active in cognitively normal adults. This indicates that low concentrations of amyloid are likely to have a physiological function. It is therefore plausible that oligomeric amyloid accumulation within the synapse leads to excitotoxicity that may contribute to the cognitive impairment observed in AD rather than mere presence of Aβ. This would suggest that increased BACE1 activity within the neurons is a key switch from essential APP expression within the cell to synaptotoxic amyloid accumulation.

1.1.4 Mutations associated with Alzheimer's Disease

AD onset is usually sporadic but can also occur as a result of genetic abnormalities as familial AD (FAD). Sporadic AD, also known as SAD, has no known cause and the biggest risk factor is age with one in 14 developing SAD over the age of 65 and one in 6 over the age of 80 (Prince et al., 2007). FAD occurs as a result of mutations in proteins involved in APP processing that increase cleavage by either BACE1 or γ-secretase. Over 52 mutations have been

identified within APP itself that are suspected to influence AD risk, most of which increase processing by BACE1. Over 180 point mutations have been found within the PSEN1 subunit of the γ-secretase complex which alter the $A\beta_{1\text{-}40/42}$ ratio or lead to increased $A\beta_{1\text{-}40/42}$ production. From this point forward, mentions of AD refer to SAD.

1.2 Metabolic risk factors associated with Alzheimer's Disease

1.2.1 Background

The main risk factor associated with AD is age but increasing evidence is implicating metabolic dysfunction with this dementia. Some describe AD as 'type 3 diabetes' in reference to the insulin resistance known to occur within the brain and many features are common to obesity (and its comorbidities) and AD (Talbot et al., 2012) (Figure 1.3). Neuroimaging studies have identified grey matter loss and limbic atrophy in type 2 diabetics affecting areas known to be most at risk in AD. Furthermore, cognition has been shown to be negatively influenced by long-term high-fat diet (HFD) in rodents (Beckett et al., 2015; Farr et al., 2008; Moran et al., 2015; G Winocur & Greenwood, 1999). Interestingly, the detrimental effects of HFD could be diminished by environmental enrichment in early life indicating that environmental factors likely play a role in combination to biochemical dysfunction (Gordon Winocur & Greenwood, 2005).

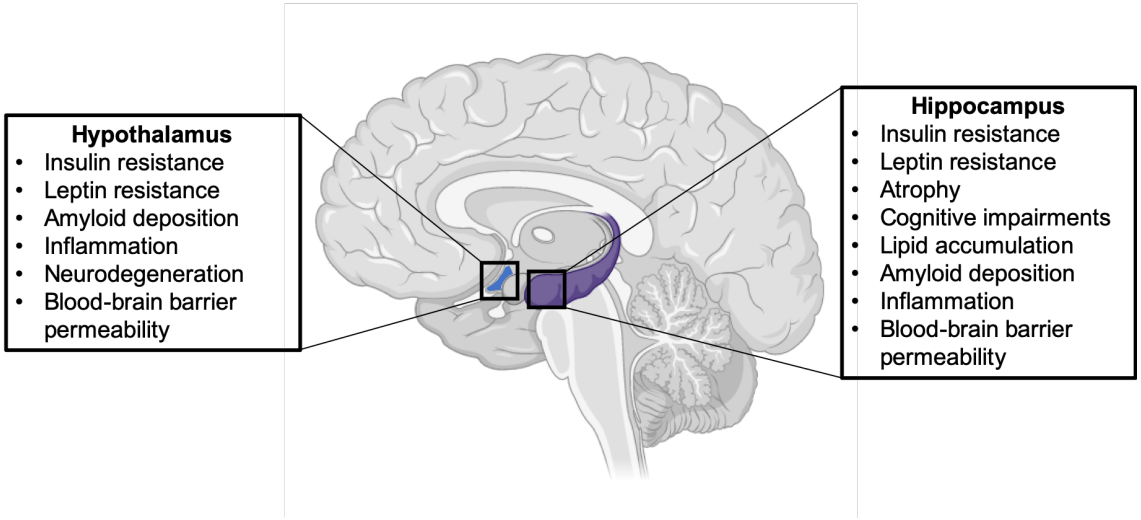

Figure 1.3 Diagram of common features between obesity and Alzheimer's disease. Pathologies within the brain associated with both obesity and AD in the hippocampus and hypothalamus. Figure was created using BioRender.com.

Obesity, both type 1 and 2 diabetes and cardiovascular disease have all been identified as risk factors for AD but the mechanisms behind this these associations have yet to be confirmed (Jolivalt et al., 2010; Stampfer, 2006). Many hypotheses exist to explain this association. Alterations in lipid profile and metabolism have been suggested which may be irrespective of ApoE4 genotype (a known genetic risk factor for AD). A little-discussed hallmark of AD is the presence of lipid inclusions within brain glial cells; first noted by Alois Alzheimer, these suggest that lipid storage and metabolism may be either a contributor or an effect of AD (Foley, 2010). Lipidomic studies have identified changes in both plasma and brain lipid profiles in both AD and MCI, implying that this pathology may occur at an early stage within the disease (Snowden et al., 2017; Wood et al., 2016). Changes in lipid metabolism within the brain has been shown to diminish stem cell proliferation- a phenomenon that contributes to learning and memory in adults (Hamilton et al., 2015). Furthermore, lipid accumulation is suspected to occur in the brains of rodents as a result of HFD however further studies are required to determine whether the changes in brain lipid profile with obesity lead to AD-like changes in brain function (Borg, Omran, Weir, Meikle, & Watt, 2012).

The cholesterol hypothesis suggests that high plasma cholesterol contributes to the amyloid deposition. (Pappolla et al., 2003) Epidemiological studies have identified a reduced risk of developing AD in patients on the cholesterol lowering drugs- statins (Shepardson, Shankar, & Selkoe, 2011). However, the majority of studies indicating an association between plasma cholesterol and amyloid production have been performed *in vitro* leading to questions regarding the physiological reproducibility of this result. One of the main confounding factors may be that whilst cholesterol may directly influence amyloid production, cholesterol does not easily cross the blood-brain barrier and the majority of cholesterol present within the brain is produced there through *de novo* synthesis (Balazs et al., 2004; Wood, Li, Müller, & Eckert, 2014). This could severely limit the effects of high plasma cholesterol on the brain unless cholesterol transport is increased due to increased blood-brain barrier (BBB) permeability (Saeed et al., 2014). However, this has not been proven either in the context of AD or obesity and cholesterol within the CSF has in fact been shown to be reduced in AD whilst plasma cholesterol is increased; suggesting that increased plasma cholesterol

may not correlate to increased cholesterol transport into the brain (Popp et al., 2013). However, high dietary cholesterol has been shown to increase amyloid production within the brains of animal models possibly as a result of increased gene expression of BACE1 and reduced ADAM10 (Sharman et al., 2013). These studies suggest a more complex system whereby high plasma cholesterol contribute to altered brain cholesterol synthesis and activation of AD-associated genes within the brain tissue through a mechanism that has yet to be identified.

Another key hypothesis behind amyloidogenesis is through inflammation. Central inflammation has been associated with both AD and metabolic diseases such as obesity and types 1 and 2 diabetes (Miller & Spencer, 2014; Ratter et al., 2017). Furthermore, increased inflammatory markers within the brains of type 2 diabetics has been associated with decreased cognitive function (Heyer, Mergeche, Bruce, & Connolly, 2013). In mice, a possible synergism has been identified between obesity and amyloid exposure to increase brain inflammatory signalling and glial activation indicating a cumulative effect on immune signalling within the hippocampus (Barron et al., 2016). The inflammation hypothesis suggests that amyloid production occurs in response to a pathogenic challenge- either real or perceived by the body. Therefore under conditions that illicit a chronic inflammatory response- such as metabolic disease- amyloid production becomes persistent and itself, becomes damaging (Moir, Lathe, & Tanzi, 2018).

Insulin is not the only metabolic hormone implicated in AD. Both leptin and ghrelin, appetite regulatory hormones produced in adipose and stomach tissues respectively, are suspected of having actions within the hippocampus that contribute to memory formation, learning and inflammation (Burguera et al., 2000; Ghamari-Langroudi, Srisai, & Cone, 2011). Indeed, leptin has been shown to contribute to the inflammatory response and is considered a cytokine due to similarities in structure between leptin and IL-6 as well as their receptors.
Supraphysiological doses of leptin have been shown to stimulate monocyte activation and release of cytokines TNF-α and IL-6, both of which are known markers of chronic inflammation and part of the innate immune response (Santos-Alvarez, Goberna, & Sánchez-Margalet, 1999; Zarkesh-Esfahani et al., 2004). However, these cytokines have also been associated with induction of leptin secretion so the exact nature of the relationship between these proteins

remains uncertain. Leptin has also been shown to induce IL-1β release from glial cells, though whether this is through a Signal transducer and activator of transcription 3 (STAT3) dependent or independent mechanism is unconfirmed (Hosoi, Okuma, & Nomura, 2000, 2002; Pinteaux et al., 2007). These studies all indicate a relationship between leptin and innate immunity and it may be that leptin resistance in obese individuals contributes to their chronic inflammatory state. It has also been shown that BACE1 contains a NFκB transcription factor binding site (Sambamurti, Kinsey, Maloney, Ge, & Lahiri, 2004) suggesting transcriptional control of BACE1 through this inflammatory pathway.

1.2.2 Metabolic dysfunction and Alzheimer's Disease

In 2018, 26% of the English population is classed as obese with a further 35% classed as overweight and in Scotland almost one third of the population is classed as obese (29%) with a further 36% being overweight (Baker, 2018). Excess weight with body mass index >30 is associated with metabolic diseases such as type 2 diabetes (T2D), cardiovascular diseases and stroke. One of the hallmarks of T2D is insulin resistance whereby prolonged hyperinsulinemia leads to diminished insulin response and therefore reduced glucose control leading to increased appetite, frequent urination with increased thirst and fatigue. Left untreated, T2D may lead to nerve damage, this in combination with reduced wound healing and vascular dysfunction can result in limb loss as wounds become gangrenous (American Diabetes Association, Complications). Due to lack of a sufficient energy store within the brain, circulating glucose is the main form of energy in the CNS making it very sensitive to changes in glucose homeostasis. Metabolic dysfunction in AD has now been strongly linked to changes in central insulin sensitivity and central insulin is considered the main regulator of glucose transport into the brain. AD patients exhibit signs of insulin resistance both within the hypothalamus and the hippocampus and a recent study has identified the insulin receptor as a possible substrate for BACE1 within the liver (Meakin, Mezzapesa, et al., 2018).

Insulin is secreted from the pancreas and crosses the BBB into the brain by receptor mediated transcytosis (Duffy & Pardridge, 1987). Binding of insulin to its receptor activates the PI3-kinase (PI3K) and MEK/ERK signalling cascades that mediate glycogenesis, lipogenesis and cell growth and survival (Guo, 2014).

Activation of insulin signalling promotes the storage of glucose as glycogen within the liver as well as increasing energy usage within cells by promoting energy expensive processes such as protein synthesis. Central PI3K pathway activation by insulin results in anti-apoptotic effects and may contribute to neuroprotection (Ryu, Ko, Jou, Noh, & Gwag, 1999). Furthermore, insulin has been shown to maintain BBB integrity by regulating endothelial expression of P-glycoprotein- a BBB transporter that regulates efflux of toxins (Liu et al., 2009). Insulin may also play a role in neurotransmitter signalling as it has been shown to inhibit serotonin receptor 5-HT_{2c} through regulation of MAP kinase signalling (Hurley et al., 2003). In addition, insulin has been shown to promote dopamine release in the nucleus accumbens, an effect that is diminished by diet induced obesity (DIO) and possibly a contributor to reward-seeking behaviour and over-eating (Stouffer et al., 2015). The brain is reliant on glucose as its primary source of energy whilst peripheral tissues, upon glycogen depletion are more capable of utilising both fats and proteins- albeit less efficiently- to maintain function. The brain, lacking in fat or glycogen stores, is reliant on circulating glucose to provide sufficient energy to function. As such the brain is sensitive to changes in blood glucose as a result of peripheral hyperglycemia, as is the case in diabetics.

Recent studies have revealed that leptin resistance too, may be a causal factor in AD progression and contribute towards the association between metabolic disease and dementia (Bonda et al., 2014; Meakin, Jalicy, et al., 2018).
Leptin is an adipokine, released into the circulation from adipocytes upon eating whereby it mediates a variety of effects on many organs. Leptin receptors are expressed in pancreas, muscle, brain and immune cells amongst other tissues (Burguera et al., 2000; Guerra et al., 2007; Lord et al., 1998; Morioka et al., 2007). Due to similarities between leptin and the cytokines IL-6, 11 and 12 as well as structural and signalling similarities of the leptin receptor to type I cytokine receptors such as gp-130 subunit of the IL-6 receptor, granulocyte colony-stimulating factor receptor (GCSFR), and leukemia inhibitory factor receptor (LIFR), leptin is a presumed cytokine (Baumann et al., 1996) (Figure 1.4). However, the best characterised roles for leptin are in energy homeostasis both through peripherally and centrally driven effects.

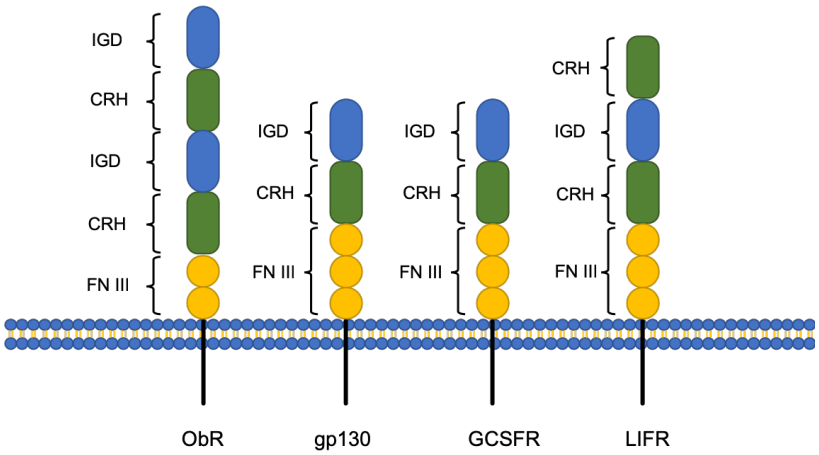

Figure 1.4 Structure of type I cytokine receptors. The leptin receptor (ObR) structural similarity with type I cytokine receptors such as the gp130 subunit of the IL-6 receptor, the GCSF receptor (GCSFR) and the LIF receptor (LIFR). All contain Ig domains (IGD), cytokine receptor homology domain (CRH) and Fibronectin type III like domains. For this reason, ObR is considered a cytokine I receptor.

1.2.3 Leptin signalling

Leptin has been implicated in neuronal development and the leptin receptor (ObR) has been identified in brain regions outside of the hypothalamus such as the neocortex, amygdala, hippocampus and cerebellum (Burguera et al., 2000; Huang, Koutcherov, Lin, Wang, & Storlien, 1996; Mercer et al., 1996). The human leptin receptor exists in 5 different isoforms, all varying in the length of their c-terminal cytoplasmic domain. It has been shown that only isoform b (ObRb) contains all of the phosphorylation and binding sites required to initiate leptin signalling and regulate energy homeostasis (Tartaglia, et al. 1995). ObRb proteins form homodimers in order to function and phosphorylation at Y985, Y1077 and Y1138 regulates the activation of downstream pathways as well as providing binding sites for negative regulators allowing for feedback inhibition within the pathway.

The intracellular domain of ObRb contains the binding sites for janus kinase 2 (JAK2)- the initiator that leads to the activation of the signal transducer and activator of transcription 3 (STAT3), phosphoinositide 3-kinase (PI3K) and Ras-extracellular signal-regulated kinase (ERK) signalling responses upon leptin binding (Banks, Davis, Bates, & Myers, 2000; Niswender et al., 2001). Phosphorylation of STAT3 at Y705 is used as an indicator of leptin receptor activation as it is a requirement of JAK-STAT pathway activation and activated by few other receptor tyrosine kinases. STAT3 phosphorylation occurs when JAK2 binds to ObRb leading to the phosphorylation of the leptin receptor at Y985

and Y1138; this allows binding of STAT3 and Src homology region 2 domain-containing phosphatase-2 (SHP-2) to the leptin receptor and permits JAK2 mediated tyrosine phosphorylation of both. pSTAT3 then dimerises and translocates to the nucleus whereby it prevents transcription of orexigenic peptides agouti-related protein (AgRP) and neuropeptide Y (NPY) as well as initiating transcription of energy regulatory neuropeptides such as anorexigenic polypeptide pro-opiomelanocortin (POMC) as well as suppressor of cytokine signalling 3 (SOCS3) which inhibits the JAK2-STAT3 pathway (Figure 1.5) (Gong et al., 2008; Swart, Jahng, Overton, & Houpt, 2002; A. W. Xu, Ste-Marie, Kaelin, & Barsh, 2007). pSHP-2 activates Ras-ERK signalling upon binding to its cofactor growth factor receptor-bound protein 2 (GRB2) (Banks et al., 2000). The role of SHP-2 in leptin signalling is complex with confounding studies claiming both attenuation and amplification of leptin's effects with SHP-2 depletion (Carpenter et al., 1998; Li & Friedman, 1999). More recent studies suggest that SHP-2 regulates downstream pathways of leptin receptor activation through diminishing JAK-STAT signalling by dephosphorylating JAK2 and promoting ERK activation (Zhang, Chapeau, Hagihara, & Feng, 2004). Leptin signalling is negatively regulated by proteins such as SOCS3 and protein tyrosine phosphatase 1B (PTP1B). SOCS3, upon leaving the nucleus, binds to the leptin receptor at Y985. This may block both binding and activation of SHP-2 and prevent further phosphorylation of STAT3 through direct inhibition of JAK2 under prolonged periods of leptin receptor activation (Bjorbak et al., 2000; Sasaki et al., 1999). PTP1B is a phosphatase that acts on JAK2; upon phosphate removal JAK2 is inactivated and thereby prevents further JAK-STAT signal transduction (Lund, Hansen, Andersen, Møller, & Billestrup, 2005). (Figure 1.5)

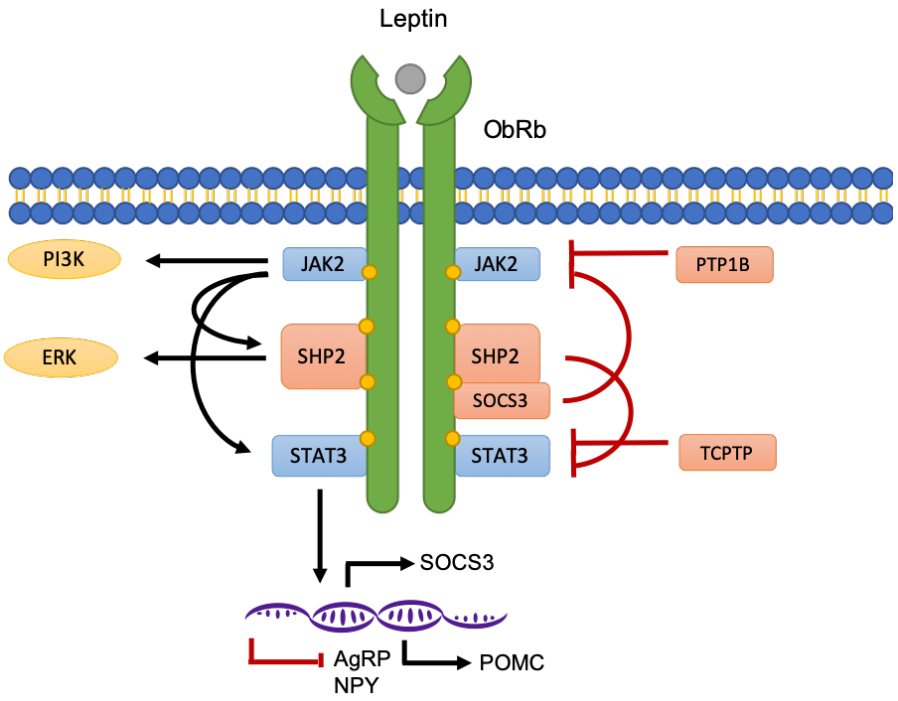

Figure 1.5 Simplified schematic of signalling downstream of activation of the long form of the leptin receptor (ObRb) by leptin. Activation of ObRb results in phosphorylation of JAK2 thereby activating the PI3K and STAT3 signalling pathways. JAK2 also results in activation of SHP-2, which then stimulates a signalling cascade activating ERK. Phosphorylation of STAT3 by JAK2 leads to translocation to the nucleus whereby STAT3 acts as a transcription factor for the transcription of energy regulatory protein, anorexigenic peptide POMC in addition to turning off transcription of orexigenic peptides AgRP and NPY. STAT3 activates a feedback mechanism by stimulating transcription of SOCS3, which leaves the nucleus and binds to JAK2-inhibiting further activation of PI3K and STAT3. PTP1B and TCPTP phosphatases regulate leptin signalling be dephosphorylating JAK2 and STAT3 respectively.

Leptin signalling within the brain is a key regulator of energy homeostasis. Released from adipocytes, leptin enters the circulation and initiates energy regulatory effects within peripheral tissues and the brain. Leptin is able to cross the blood brain barrier where it exerts its metabolic effects through the hypothalamus. Leptin binds to its receptor (ObRb) on first order AgRP/NPY and POMC/CART neurons in the arcuate nucleus (ARC) of the hypothalamus (Figure 1.6) (Allison, Myers, & Jr., 2014). Activation of leptin signalling in POMC/CART neurons activates the JAK-STAT pathway leading to the production of Pro-opiomelanocortin (POMC); POMC is highly processed within the hypothalamus leading to the production of many signalling peptides including α-melanocyte stimulating hormone (αMSH) (Sohn, 2015). POMC cleavage by prohormone convertase 1 (PC1) creates a N-terminal fragment (N-POMC (1-77)), adrenocorticotropin hormone (ACTH) and a c-terminal fragment (β-lipotropin; β-LPH). Subsequent cleavages of ACTH by prohormone convertase 2 (PC2), carboxypeptidase E (CPE) and peptidylglycine α-amidating monooxygenase (PAM) respectively result in active αMSH (reviewed by Cawley, Li, & Loh, 2016).

Secreted αMSH binds to melanocortin-4 receptors (MC4R) on anorexigenic second order neurons in the paraventricular nucleus (PVN) of the hypothalamus. (Girardet & Butler, 2014) These anorexigenic neurons project into the nucleus of the solitary tract (NST), a nerve bundle which descends the spinal cord as well as the pituitary gland to regulate both nervous and hormonal responses. The NST initiates peripheral responses to reduce appetite and increase sympathetic activity to drive glucose uptake into tissues and increase energy expenditure via central effects (Blouet & Schwartz, 2012; Verberne, Sabetghadam, & Korim, 2014). Simultaneously, leptin pathway activation in AgRP/NPY neurons leads to signalling of these neuropeptides in the PVN by inverse agonism of the MC4R (Nijenhuis, Oosterom, & Adan, 2001). This attenuates the food-seeking behaviours that these peptides bring about via orexigenic neurons in the lateral hypothalamic area (LHA) (Verberne et al., 2014). (Figure 1.6)

Obese individuals enter a state of leptin resistance whereby leptin fails to activate the JAK-STAT pathway. This leads to aberrant energy regulation which exacerbates the obese state. The mechanisms behind diet-induced leptin resistance are contested but studies have implicated changes such as reduced POMC post-translational processing, reduced blood-brain barrier transport of leptin and defects in leptin receptor activation. (Cakir et al., 2013; El-Haschimi, Pierroz, Hileman, Bjørbaek, & Flier, 2000; Van Heek et al., 1997)

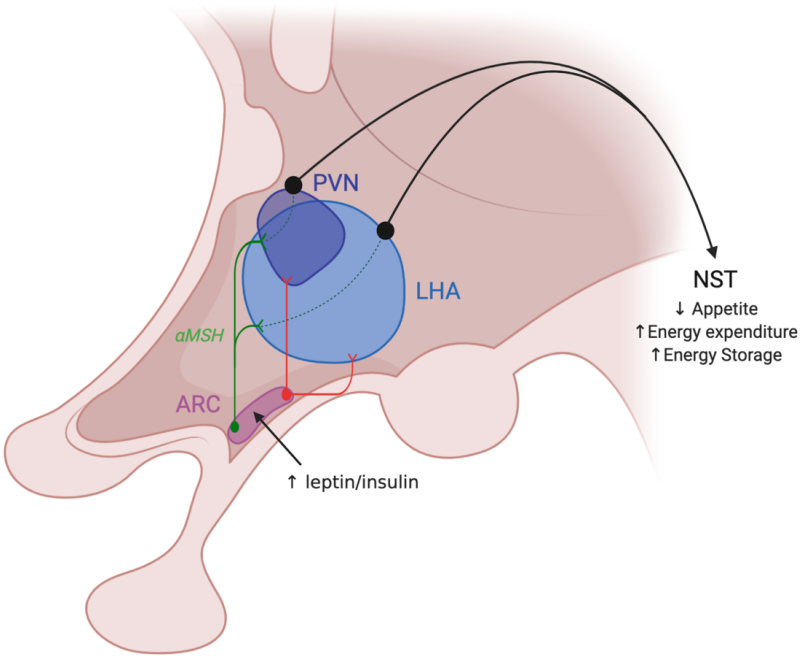

Figure 1.6 Schematic diagram of the effects of leptin within the hypothalamus on energy homeostasis. Binding of leptin or insulin to their respective receptors on POMC/CART neurons (green) in the arcuate nucleus (ARC) of the hypothalamus leads to the production and release of αMSH from synapses in the paraventricular nucleus (PVN). Second order neurons in the PVN extend axons into the nucleus of the solitary tract (NST) and release anorexigenic factors. The NST then co-ordinates an increase in sympathetic signalling resulting in reduced appetite, increased energy expenditure and increased energy storage. Leptin/insulin binding to AgRP/NPY neurons (red) leads to a reduction in the production of these neuropeptides and amelioration of their orexigenic effects. Figure was created using BioRender.com.

Leptin is not released from all adipocytes equally and different fat depots have been shown to release leptin differently. Brown adipocytes do not express leptin whereas white adipocytes do. Expression of leptin is reciprocal to UCP1 and so increased browning in white adipose tissues (WAT), and therefore increased UCP1 expression, leads to decreased expression of leptin (Cancello, Zingaretti, Sarzani, Ricquier, & Cinti, 1998). This relationship can be driven by centrally administered leptin (Commins, Watson, Levin, Beiler, & Gettys, 2000). Additionally, visceral fat accumulation does not result in increased leptin mRNA and does not correlate to increased circulating leptin whereas subcutaneous fat accumulation does (Banerji, Faridi, Atluri, Chaiken, & Lebovitz, 1999; Montague, Prins, Sanders, Digby, & O'rahilly, 1997; T. R. Nagy et al., 1997; Russell et al., 1998). This is important when considering the relationship between obesity and neurodegenerative diseases such as AD. As it has been shown that increased adiposity increases the risk of developing AD, however this correlation is far more pronounced in those with increased central adiposity in mid-life as defined by sagittal abdominal diameter (Whitmer et al., 2008; Whitmer et al., 2005). High waist-hip ratio and high body fat percentage have been associated with grey

matter atrophy as well as reduced volume within brain regions such as the pallidum and nucleus accumbens as well as cortical thinning in males (Hamer & Batty, 2019; Kim et al., 2014). This relationship may also be influenced by ApoE4 genotype (Zade et al., 2013). Interestingly, increased adiposity is associated with protection against AD in the elderly indicating an age-dependent effect (Hughes, Borenstein, Schofield, Wu, & Larson, 2009). Greater waist-to-hip ratio is associated with increased visceral fat within the body cavity as opposed to subcutaneous fat accumulation which is more equally distributed about the waist and hips. It may therefore be that increased central adiposity represents lower circulating leptin levels in these individuals and therefore a reduction in the protective effects that leptin offers.

Besides metabolism, leptin has been shown to contribute to reproduction, cognitive development and inflammation (Chehab, Lim, & Lu, 1996). Indeed, circulating leptin is known to differ between sexes with women exhibiting greater levels than men. However, fluctuations in circulating leptin occur throughout the menstrual cycle suggesting a relationship between sex hormones and leptin (Ahrens *et al.*, 2014). However, post-menopausal women appear to express comparable circulating leptin to premenopausal women indicating that the role of sex hormones in leptin regulation may not be simple (Bednarek-Tupikowska et al., 2006). In addition to this, the leptin deficient mouse (*ob/ob*) has been shown to be sterile due to lack of ovulation and spermatogenesis, a condition that is overcome with daily intraperitoneal (IP) leptin administration (Chehab et al., 1996; Mounzih, Lu, & Chehab, 1997). These differences in metabolism with sex may be important in studying the connection between metabolic dysfunction and dementia. There are almost twice the number of women with dementia living in the UK than men indicating sex is a risk factor for these diseases (Prince et al., 2007).

1.2.4 Leptin in memory and cognition

Obese individuals have elevated plasma (approximately 2.5nM vs. 0.6nM in obese and lean individuals respectively) and cerebral spinal fluid (CSF) leptin (approximately 21pM vs. 16pM in obese and lean individuals respectively) (Adeyemi & Abdulle, 2000; Nam et al., 2001). They also exhibit metabolic dysfunction and leptin resistance whereby high concentrations of leptin fail to

implement the energy regulatory mechanisms required to maintain energy homeostasis (Caro et al., 1996; Enriori et al., 2007; Frederich et al., 1995). Studies have associated disruption in many aspects of leptin signalling with increased weight gain. *Ob/Ob* and *db/db* mice- transgenic animals deficient in leptin and *ObRb* leptin receptor isoform respectively are regularly utilised as murine models of obesity. More recent studies have utilised these animal models to study the neurological effects of obesity finding that ObR deficient animals exhibit reduced spatial memory abilities, decreased anxiety, locomotor deficits and increased psychosis behaviours with age (Li et al., 2002; Sharma et al., 2010).

Whilst AD is most commonly associated with atrophy of the cortex and hippocampus resulting in characteristic changes in memory, learning and reasoning skills; evidence is emerging that the hypothalamus is also subject to atrophy in this dementia (Callen, Black, Gao, Caldwell, & Szalai, 2001). Studies have shown that the hypothalamus exhibits amyloid pathology similar to that seen in the hippocampus and cortex in both mild cognitive impairment (MCI) and AD. (Iwatsubo, Saido, Mann, Lee, & Trojanowski, 1996; McDuff & Sumi, 1985). Animal model studies into the physiology of AD have identified that transgenic mice exhibiting increased amyloid production have metabolic phenotypes including decreased body weight associated with reduced fat mass, increased resting metabolic rate and decreased plasma leptin. These mice exhibit reduced *POMC* and *CART* mRNA in the hypothalamus as well as reduced responsiveness to leptin stimulation in NPY neurons. (Ishii, Wang, Racchumi, Dyke, & Iadecola, 2014) This suggests that metabolic dysfunction in AD may not be due to just hypothalamic atrophy, but also aberrant leptin signalling due to increased amyloid. Obesity and it's co-morbidities have been shown to increase the likelihood of developing AD; twin studies by Xu *et al*. (2011) found that AD patients were 70% more likely to have been overweight or obese in midlife compared with cognitively normal individuals. With obesity becoming a global epidemic, the effects of nutrient excess on the brain must be better understood as these dementias may become more commonplace as the current population ages.

Leptin has been researched as a neuroprotectant; serum leptin positively correlates with hippocampal volume in the elderly and individuals with higher circulating leptin appear to be at reduced risk of cognitive decline (Holden et al., 2009; Narita, Kosaka, Okazawa, Murata, & Wada, 2009). Leptin is known to assist with working memory as rodents deficient in the leptin receptor have been shown to exhibit impaired LTP and LTD in CA1 neurons and performed poorly in spatial memory tests compared to controls (Li et al., 2002). It is thought that leptin receptor activation within the hippocampus leads to increased transport of AMPA receptors (AMPARs) to and from the synapse via a PI3K dependent mechanism thereby regulating LTP and LTD (Moult et al., 2010; Moult, Milojkovic, & Harvey, 2009). Leptin is also thought to modulate NMDA receptor function and through this, enhances LTP (Shanley, Irving, & Harvey, 2001). Metabolic studies in dementia have identified central leptin dysfunction in these neurological diseases by reduced leptin sensitivity and decreased circulating leptin in later stages of AD (Lieb et al., 2009).

Weight loss is commonly associated with AD. A clinical study identified that weight loss of greater than 4% over 4 years gives rise to a 3-fold greater likelihood of AD from MCI in aged individuals; whilst weight loss from mid-life may be an indicator of MCI (Alhurani et al., 2016; Cova et al., 2016). However, the cause and effect of this relationship has yet to be established. It has been suggested that circulating leptin concentrations in individuals with AD is lower than that of their cognitively healthy counterparts but studies are conflicting (Maioli et al., 2015; Power, Noel, Collins, & O'Neill, 2001). There is little evidence of a difference associated with MCI (Oania & McEvoy, 2015). Whilst evidence has been published claiming that increased circulating leptin associates with reduced incidence of AD, some studies have suggested that plasma leptin is not a predictor of AD risk in those with MCI however CSF leptin provided a better predictor of AD development (Lieb et al., 2009; Oania & McEvoy, 2015). Bonda *et al.* (2014) found that whilst AD patients exhibited higher CSF and hippocampal leptin concentrations, mRNA for the leptin receptor was reduced and immunohistochemistry (IHC) and colocalization staining revealed localisation of ObRb to both NFTs and neuritic plaques. This suggests that whilst leptin concentrations are high, signal transduction is impaired. Further studies have indicated that brain leptin signalling is altered in AD patients even when CSF

leptin is unchanged due to reduced ObRb expression (and therefore reduced leptin signalling) in the hippocampus as well a shift in leptin and ObRb localisation from neurons to reactive astrocytes (Maioli et al., 2015). Furthermore, this study showed that $A\beta_{1-42}$ exposure increases leptin receptor synthesis in both neurons and astrocytes thereby associating BACE1 activity to leptin signalling within the brain.

It has been proposed that leptin may reduce the targeting of BACE1 to lipid rafts by altering the lipid composition of the rafts (Fewlass et al., 2004; Ruth, Proctor, & Field, 2009). As targeting to lipid rafts is a requirement for BACE1 endocytosis, reductions would lead to accumulation of BACE1 at the cell membrane and reduced expression within endosomal compartments- compartments which are known to provide more favourable environment for BACE1 catalysis and produce the majority of secreted amyloid peptides (Ellis & Shen, 2015). It has also been proposed that leptin may mediate BACE1 activity through induction of peroxisome proliferator-activated receptor γ (PPARγ) expression (Sastre et al., 2006). They identified BACE1 as containing PPARγ response elements within the BACE1 promotor and found that BACE1 is downregulated by this nuclear receptor. Human data indicate that PPARγ protein expression and its binding to BACE1 is reduced in the AD prefrontal cortex however BACE1 expression was increased (Sastre et al., 2006). Furthermore, neuron-specific PPARγ knock-out in mice leads to reduced weight gain on HFD, reduced food intake, increased energy expenditure and increased leptin sensitivity (Lu et al., 2011). Interestingly, STAT3 is also a suggested regulator of BACE1 transcription with p25/CDK5 leading to BACE1 accumulation and increased amyloid production through a proposed STAT3 dependent mechanism (Wen et al., 2008).

Leptin has also been suggested to improve amyloid pathology. It has been shown that leptin increases ApoE-dependent amyloid uptake in SH-SY5Y and Neuro2a cells (Fewlass et al., 2004). This study also found that APPswe/PSEN1 transgenic mice exhibited reduced plasma leptin compared to WT littermates thereby suggesting a feedback mechanism between amyloid and leptin. This role for leptin has also been shown in hippocampal slices with leptin treatment reducing both secreted $A\beta_{1-40}$ and $A\beta_{1-42}$ (Marwarha, Dasari, Prasanthi, Schommer, & Ghribi, 2010). However, the concentrations of leptin (1-3nM) used

within the study were supraphysiological with typical CSF and plasma leptin levels being approximately 46pM and 312pM respectively in healthy individuals (Wong et al., 2004). Therefore, further *in vivo* or *ex vivo* validation is required. Overall, this has led to the suggestion of leptin as a therapeutic agent for AD.

1.2.5 BACE1 and metabolism

An increasing body of evidence implicates BACE1 as a regulator of metabolic homeostasis. Studies have indicated that BACE1 knock-out (KO) mice are protected from diet-induced obesity when challenged with a HFD. This is accompanied by protection from metabolic disease with retention of insulin signalling and leptin sensitivity with nutrient excess whilst wild-type (WT) controls become insulin resistant and show diabetic phenotypes (Meakin et al., 2012; Meakin, Jalicy, et al., 2018). It has also been shown that chronic nutrient excess by way of 20 week HFD led to increased BACE1 expression in both central and peripheral tissues (Meakin et al., 2012; Meakin, Jalicy, et al., 2018; Thirumangalakudi et al., 2008; Wang et al., 2013b). In contrast, BACE1 knock-in (KI) mice exhibited dysfunctional glucose homeostasis from 4 months of age, impaired glycogen storage and fatty liver. These mice have a small increase in forebrain BACE1 expression through the addition of the human *BACE1* gene under the CamKII promotor in the HPRT locus (Plucinska et al., 2014). These mice also exhibited lipid accumulation within the brain and hypothalamic dysfunction shown by elevated *POMC* and *MC4R* gene expression. However, the increases in metabolic gene expression in the hypothalamus did not lead to decreased food intake compared to WT controls suggesting greater energy efficiency with increased BACE1 expression (Plucińska et al., 2016).

A HFD study on the AD model APP/PSEN1 showed an inflammatory phenotype that exacerbated AD pathologies. Upon reversal of the HFD, these pathologies were ameliorated (Walker, Dixit, Saulsberry, May, & Harrison, 2017). One of the key pathologies associated with AD is the formation of extracellular amyloid plaques. In addition to increased BACE1 expression, chronic HFD leads to increases in β-site APP processing in transgenic mouse models of AD suggesting increased BACE1 activity with dietary stress as BACE1 is the rate limiting step in amyloid production (Julien et al., 2010). This may contribute to a feedback loop as increased amyloid has also been implicated in metabolic dysfunction.

Neuroimaging studies have identified correlations between amyloid burden within the brains of AD patients and decreased glucose metabolism (Adriaanse et al., 2014; Carbonell et al., 2016). Clarke *et al.* (2015) show that acute, central administration of amyloid oligomers alters skeletal muscle glucose uptake, adipose inflammation as well as causing glucose and insulin intolerance. Amyloid treated mice expressed increased adipose leptin mRNA but increased weight gain as well as increased hypothalamic *AgRP* and *NPY* mRNA. This study also showed reduced glucose clearance in APP/PSEN1 transgenic mice offering strong evidence for a metabolic dysfunction as a result of raised oligomeric amyloid within the brain.

1.3 BACE1 biochemistry

1.3.1 Introduction to BACE1

BACE1 was discovered in 1999 by 4 different teams investigating potential β-secretase enzymes responsible for β-amyloid production (Hussain et al., 1999; Sinha et al., 1999; R Vassar et al., 1999; Riqiang Yan et al., 1999). These teams validated APP as a true substrate for BACE1 through colocalization, *in vivo* and *in vitro* protease assays providing strong evidence for it being the sought-after β-secretase.

BACE1 is a type I transmembrane protein of 501aa; it has a large, 435aa extracellular domain containing both catalytic aspartic acid residues required for proteolytic activity. BACE1 contains a very small cytoplasmic domain of only 22aa, however this domain contains four potentially palmitoylatable cysteines and a phospho-serine. (Figure 1.7) Mouse and human BACE1 sequences have 96.41% identity and sequence conservation can be observed throughout evolution with BACE1 orthologues having been identified in marine invertebrates such as hydra. Furthermore, BACE1 from the marine invertebrate *Branchiostoma* has been shown to cleave APP at the β site indicating a strong conservation of function. Interestingly, APP evolution occurs much later that BACE1. This conservation of BACE1 outside of APP evolution indicates an important role for this protein outside of amyloid formation (Moore et al., 2014b).

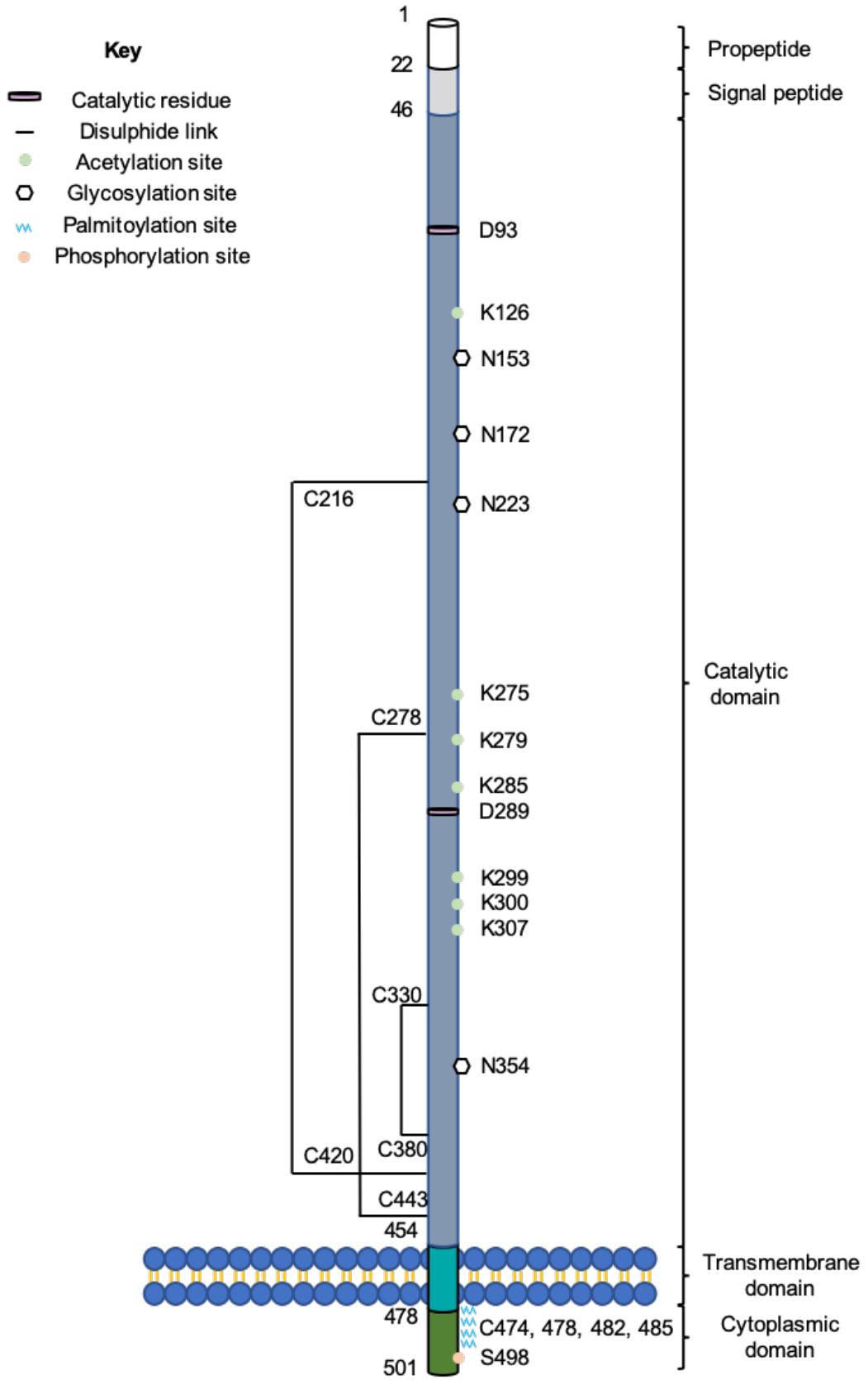

Figure 1.7 Schematic of post-translational modifications of the BACE1 protein. The BACE1 transcript encodes a signal and pro peptide, catalytic domain, transmembrane domain and cytoplasmic domain. D93 and D289 are the catalytic residues required for aspartyl protease activity. BACE1 is phosphorylated at S498, palmitoylated at C474, 478, 482 and 485, glycosylated at N354, 223, 172 and 153 and is acetylated at K307, 300, 299, 285, 279, 275 and 126. Disulphide linkages connect C443-278, C420-216 and C380-330.

However, whilst APP occurs much later in evolution, the APLP proteins have been identified in earlier evolutionary branches than BACE1. This could suggest that the BACE1-APLP association may be of more physiological importance than BACE1-APP (Moore et al., 2014a). The BACE1 paralogue, BACE2, cleaves APP within the β site but exhibits higher preference to a θ site that is downstream of the α site; thereby cleaving within the Aβ sequence and producing a truncated $Aβ_{15-40/42}$ peptide (Farzan, Schnitzler, Vasilieva, Leung, & Choe, 2000; Sun et al., 2005; R Yan, Munzner, Shuck, & Bienkowski, 2001). (Figure 1.2) These two homologs exhibit 75% sequence identity (45% identical) (Sun et al., 2005).

Interestingly, genotypic analyses have yet to identify and validate polymorphisms in the BACE1 gene that influence susceptibility to AD (Todd et al., 2008) but genome-wide association studies (GWAS) on AD and non-demented controls have identified the BACE1 single nucleotide polymorphise (SNP) rs650585 associates with reduced plasma $Aβ_{1-40}$ (Chouraki et al., 2017). The relevance of this mutation in AD risk has yet to be determined. Another GWAS study identified the rs1047964 mutation within the 3' UTR of BACE1 as significantly increasing the risk of death by CVD in women with migraine (Schürks, Buring, Ridker, Chasman, & Kurth, 2011). The SNP rs535860 within the 3' UTR has been associated with increased risk of T2D but interestingly results in decreased BACE1 expression in HEK 293 cells (Hoffmeister et al., 2013). The rs638405 mutation in BACE1 has been associated not only with increased risk of AD in combination with the ApoE4 allele, but increased risk of Parkinson's Disease (PD) (Kirschling et al., 2003; Lange et al., 2015; Murphy et al., 2001; Nowotny et al., 2001). Many studies have focused on this 1239G/C SNP within exon 5 of BACE1, but have produced conflicting results as to whether the G or C variant increases the risk of developing AD (Clarimon et al., 2003; Jo et al., 2008; J. Shi et al., 2004; M. Yu, Liu, Shen, Lv, & Zhang, 2016). This SNP doesn't result in variability at the peptide level at both the G and C variants encode valine and no mechanisms have been identified as to why this SNP may affect AD risk. Furthermore, this SNP appears to have no influence over CSF amyloid or sAPP levels in AD patients (Sjölander, Zetterberg, Andreasson, Minthon, & Blennow, 2010). It must also be mentioned that the majority of studies into BACE1 variants use AD cases, it may be that BACE1 SNPs have a greater effect in other diseases. However, the lack of SNPs in BACE1 resulting in functional variation

should perhaps be unsurprising considering the high degree of conservation in this gene, further supporting the idea that BACE1 plays in integral physiological role.

1.3.2 BACE1 KO mouse models

BACE1 KO mice have been a primary model for studying the neurological and physiological functions of BACE1. BACE1 KO mice have been shown to be viable and exhibit few phenotypes (Luo et al., 2001). One group identified increased neonatal mortality in the BACE1 KO line (Dominguez et al., 2005). Others have identified hyperactivity, increased muscle tone, neuronal hypomyelination, seizures and schizophrenia within these mice however these phenotypes are not consistent between studies and different BACE1 KO models appear to exhibit these effects to varying degrees, if at all (Dominguez et al., 2005; Harrison et al., 2003; Hitt, Jaramillo, Chetkovich, & Vassar, 2010; Hu et al., 2006; Roberds et al., 2001).

BACE1-/-BACE2-/- double KOs have been created in order to identify whether BACE2 may compensate for BACE1. This model exhibited greater risk of early life mortality compared to single BACE1 KO mice (Dominguez et al., 2005). This leads to questions regarding the evolutionary advantage that BACE1 must offer and the reason for the strict conservation of this protein throughout evolution.

1.3.3 Transcriptional and translational regulation of BACE1

BACE1 transcription is mediated through a variety of transcription factors which are involved in processes such as inflammation, development and physical/emotional stress responses. Proposed transcriptional regulation sites include progesterone response element, glucocorticoid, retinoic acid recognition and NFκB binding sites within the promotor region (Sambamurti et al., 2004). However, mRNA expression of BACE1 does not reflect protein activity as BACE1 mRNA expression within the pancreas is high but enzymatic activity against APP substrates is low, this is contrary to the brain where BACE1 mRNA expression is moderate but activity high (Sinha et al., 1999; Riqiang Yan et al., 1999). There must, therefore, be alternative mechanisms outside of gene expression, that regulate BACE1 activity towards APP.

BACE1 has a large, 446 nucleotide 5' UTR with high (77%) GC content that is thought to act as a translational regulator of BACE1 protein expression. The 3' UTR does not appear to regulate BACE1 translation (Sven Lammich, Schöbel, Zimmer, Lichtenthaler, & Haass, 2004). The BACE1 5' UTR also contains multiple upstream ATGs that may influence the translational start site for BACE1 (De Pietri Tonelli et al., 2004; Rogers, Edelman, & Mauro, 2004). It has been shown that whilst BACE1 protein levels increase in AD patients, mRNA expression remains unchanged (Fukumoto, Cheung, Hyman, & Irizarry, 2002; Holsinger, McLean, Beyreuther, Masters, & Evin, 2002; Preece et al., 2003). It is therefore plausible that translational regulation of BACE1 is the key mechanism regulating BACE1 protein expression in a dementia context. Interestingly, BACE1 mRNA has been shown to increase in mice challenged with chronic HFD suggesting that dietary intervention or exposure to a chronic stressor may be required for transcriptional regulation of BACE1 expression (Meakin, Jalicy, et al., 2018).

1.3.4 BACE1 activity

BACE1 is a type 1 transmembrane protein and aspartyl protease. Aspartyl protease enzymatically cleave substrates through a hydrolytic reaction with catalytic aspartic acid residues within the active site. Aspartic acids at amino acids 93 and 289 are responsible for the proteolytic activity of BACE with mutation of either residue resulting in decreased cleavage of APP (Hussain et al., 1999) Both Asp residues are required for proteolytic activity; whilst one acts as a proton acceptor from a water molecule thereby initiating hydrolysis, the other stabilises the carboxyl group of the phosphate backbone in the substrate. (Figure 1.8) This allows electron transfer within the peptide substrate leading to proteolysis. BACE1 activity has been shown to increase in acidic environments such as in the endo/lysosomal compartments (Vassar et al., 1999). However, unlike typical aspartyl proteases, BACE1 is poorly inhibited by the broad-spectrum aspartyl protease inhibitor pepstatin suggesting as an alternative chemistry to proteolysis by this protein even compared to its closest evolutionary relative, cathepsin D (Ahmed et al., 2010).

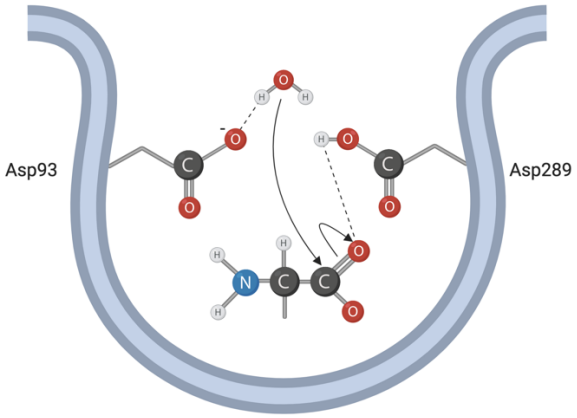

Figure 1.8 Mechanism of proteolysis by aspartyl proteases. The aspartic acid residues within aspartyl proteases catalyse the proteolysis of substrates. One catalytic residue stabilises the peptide substrate whilst the second oxidises a water molecule which targets the phosphate backbone of the substrate leading to proteolysis. Figure was created using BioRender.com.

Since its identification as the β-secretase, BACE1 has been a key drug target in the treatment and prevention of AD. The premise for its targeting being that inhibition of BACE1 would lead to reductions in amyloid production and thereby protect an individual from amyloid pathology and AD. Whilst some would argue that amyloid burden does not always result in AD, the emergence of the Icelandic mutation- an A673T substitution within APP- indicates that a 40% reduction in amyloid offers protection against this form of dementia (Jonsson et al., 2012). Whilst many BACE1 inhibitors have made it to clinical trial stages, none yet have progressed further. One of the first challenges in BACE1 inhibitor development is designing a drug that will cross both the BBB and cellular membranes to act upon compartmentalised BACE1. Inhibitors have been developed through multiple mechanisms including small molecules, peptides and antibodies, each have shown varying degrees of success. The most successful peptide strategies have exhibited reductions in plasma amyloid but failed to produce significant results within the CSF in Phase I clinical trials (Sankaranarayanan et al., 2009). This suggests poor transport across the BBB as a confounding factor with this form of therapy. Small molecule inhibitors were explored and effective pharmacophores; acylguanidine, aminopyridine, and isothiourea identified that exhibit inhibitory properties on both catalytic aspartic acid residues. Compared to previous peptide-based inhibitors, these small molecules have a low molecular weight and have high binding affinity (Coimbra et al., 2018). Testing of small molecule inhibitors led to the development of the LY2811376 BACE1 inhibitor- an isothiourea- by Merck. However, trials in rodents led to the discovery of glial and

neuronal degeneration as well as retinal degeneration caused by accumulations of autofluorescent granules. However, these effects were also identified in BACE1 KO mice given this compound indicating that they are off-target and should not be expected from all BACE1 targeting inhibitors (May et al., 2011).

Perhaps the most promising BACE1 targeting treatment is the dual-specific antibodies to both BACE1 and the transferrin receptor to improve uptake into the brain (Atwal et al., 2011; Yu et al., 2011). Whilst some agents have passed initial testing and made it to clinical trials, ultimately BACE1 inhibitors have not been shown to significantly reduce CFS amyloid concentrations.

The BACE1 inhibitors that have shown great success in reducing central amyloid concentration with few side effects were extremely successful in treating amyloid pathology and associated cognitive decline in rodent models of FAD. However, despite many successes in BACE1 inhibition in animal studies, many exhibit either side effects or are ineffective against SAD in human trials. This may be, in part, due to animal models being based upon the genetics of FAD rather than conditions associated with SAD (Volloch & Rits, 2018).

1.3.5 BACE1 and APP trafficking

Whilst both BACE1 and APP are considered cell surface proteins, evidence is emerging that the BACE1-APP interaction occurs elsewhere within the cell. APP expression has been shown predominantly within the golgi and secretory pathway (Caporaso et al., 1994). Unshed APP has been shown to spend relatively little time at the cell surface before being internalised within minutes to endosomes (Koo, Squazzo, Selkoe, & Koo, 1996; Marquez-Sterling, Lo, Sisodia, & Koo, 1997). APP is internalised via clathrin mediated endocytosis and contains a consensus motif (NPTY) within the cytoplasmic domain. Once in the endo/lysosomal system, APP can then be recycled back to the plasma membrane (PM) or targeted to the lysosome for degradation (Nordstedt, Caporaso, Thyberg, Gandy, & Greengard, 1993; Yamazaki, Koo, & Selkoe, 1996). There is evidence to suggest that endocytosis of APP is a requirement for amyloid production, therefore implicating the endosomal system as a major site of APP processing by BACE1 (Koo & Squazzo, 1994). Expression of APP within

clathrin coated pits has led to the suggestion that APP is a cell-surface receptor however the short expression time of APP at the PM suggests otherwise.

BACE1 processing occurs in a similar manner. After translation, BACE1 undergoes multiple post-translational modifications including propeptide cleavage and glycosylation in order to produce mature, active protein (Capell et al., 2000). The maturation of BACE1 is further discussed in section 1.3.6. Upon activation BACE1 is expressed in the secretory pathway whereby it is targeted to the plasma membrane (PM) through the trans-golgi network (TGN). Within the PM, BACE1 is targeted to lipid rafts and then undergoes clathrin mediated endocytosis upon binding of Golgi-localized, γ-ear-containing, Arf (GGA) proteins to the c-terminal domain (Shiba et al., 2004; Toh, Chia, Hossain, & Gleeson, 2018). BACE1 enters sorting endosomes where, like APP, it can be targeted back to the PM, the TGN or enter the lysosome for degradation (Udayar et al., 2013). BACE1 can also be transported directly to early endosomes from the TGN by association with sortilin and retrograde transport from early endosomes to the TGN may be mediated by the same protein as c-terminal truncation of sortilin leads to accumulation of both proteins within endosomes (Finan, Okada, & Kim, 2011).

Multiple studies have implicated sub-cellular localisation of BACE1 as a regulator of APP processing suggesting that the proteins responsible of BACE1 targeting could be important drug targets to reduce amyloid pathology in AD (Finan et al., 2011). APP endocytosis occurs after flotillin and cholesterol-dependent clustering and utilises the AP2 adaptor protein complex to internalise in a clathrin-dependent manner (Perez et al., 1999; Schneider et al., 2008). BACE1, however utilises an ARF6 dependent mechanism suggesting, perhaps, different methods of endocytosis and therefore differing PM localisations and vesicles (Prabhu et al., 2012; Sannerud et al., 2011). This suggests that the first point of contact between these proteins from the PM would be early endosomes.

1.3.6 BACE1 modification

Maturation of BACE1 is heavily reliant on post-translational modifications. Translated BACE1 contains both a propeptide and signal peptide. To produce mature BACE1, the propeptide is cleaved within the endoplasmic reticulum (ER)

and is a suspected requirement for correct BACE1 folding conferring no effect on BACE1 activity if left intact. (Shi et al., 2001) The signal peptide targets BACE1 to the TGN for anteriograde transport, it is here that the propeptide is cleaved by a furin-like protease (Bennett et al., 2000; Capell et al., 2000). Throughout maturation 7 BACE1 lysine residues become acetylated within the ER, this modification adds stability to the folding protein and once folded, deacetylation occurs within the golgi (Ko & Puglielli, 2009). Unfolded BACE1 is degraded through a pathway involving PCSK9 (Jonas, Costantini, & Puglielli, 2008). Acetylation, and therefore folding of BACE1, has been shown to be influenced by the lipid secondary messenger ceramide (Costantini, Ko, Jonas, & Puglielli, 2007; Puglielli, Ellis, Saunders, & Kovacs, 2003). Ceramides are significantly elevated in AD patients from very early stages of the disease (Holtzman, McKeel, Kelley, & Morris, 2002). As such it may be that increased stability of BACE1 through increased acetylation may be a contributing factor to the switch from non-amyloidogenic to amyloidogenic processing of APP.

Phosphorylation of BACE1 at Ser498 by casein kinase I (CK1) modulates sub-cellular trafficking of BACE1 (Walter et al., 2001). Using WT, S498D and S498A BACE1, it has been shown that this post-translational modification of BACE1 is a key regulator in cellular trafficking of the protein. The S498D, a mimic of phosphorylated BACE1 was found to move freely throughout the TGN and endosomal systems whereas non-phosphorylatable S498A BACE1 mutants accumulated within early endosomes. Whilst internalisation of BACE1 from the PM was not affected by phosphorylation state, cycling from early endosomes back into the TGN or late endosomes was only possible in phosphorylated WT BACE1 or the S498D BACE1 mutant. The Ser498 phosphorylation site is directly adjacent to the di-leucine (LL) motif at amino acids 499 and 500 meaning that steric effects on this motif by the phosphate group could be possible (Pastorino, Ikin, Nairn, Pursnani, & Buxbaum, 2002; Wahle et al., 2005). The LL motif is a well characterised regulator of protein trafficking, particularly away from the PM by interactions with clathrin associated proteins (John, Meister, Banning, & Tikkanen, 2014). In BACE1, the LL motif is known to regulate transport from the PM into the endosomal system. LL to AA mutation of this motif leads to accumulation of BACE1 at the cell membrane however S498A mutation did not alter BACE1 trafficking thereby suggesting that phosphorylation at this site does

not hinder the function of the LL motif (Pastorino et al., 2002) and must modulate BACE1 trafficking through an alternative mechanism. BACE1 contains a characteristic GGA protein binding motif at residues 496-500 therefore the serine phosphorylation site is contained within this motif. GGA proteins are adaptor proteins that regulate the movement of receptors such as the mannose-6-phosphate receptor between the endosomal system and the TGN. Cycling similar to that observed with BACE1. Moreover, phosphorylation of BACE1 at S498 has been shown to increase GGA1 binding and siRNA knockdown of GGA1 results in significant reductions in BACE1 co-expression with Rab11- a marker of recycling endosomes (Shiba et al., 2004; Toh et al., 2018).

Plausible CK1 targeting sites have been previously identified not only in BACE1, but in subunits of the γ-secretase complex including PSEN1 and PSEN2 and the microtubule binding protein Tau (Chen et al., 2017; Flajolet et al., 2007; Li, Yin, & Kuret, 2004). Transcription of CK1δ been shown to increase in the brains of AD patients (Yasojima, Kuret, DeMaggio, McGeer, & McGeer, 2000) therefore suggesting an increase in BACE1 phosphorylation and possibly increased cycling of BACE1 through the secretory pathway.

Palmitoylation of BACE1 has been shown to be integral to lipid raft targeting and amyloid production (Andrew et al., 2017; Vetrivel et al., 2009). It occurs on four cysteine residues within the cytosolic domain C474, C478, C482, C485. The palmitoyl-transferase DHHC20 has been largely attributed with the process however other DHHC proteins such as 3, 4, 7 and 15 have also been suggested suggesting that palmitoylation of BACE1 may occur within the golgi, ER and PM (Cho & Park, 2016; Vetrivel et al., 2009). Targeting of BACE1 to lipid rafts may be another method by which BACE1 substrates are determined. Lipid rafts typically contain lipidated and GPI anchored and transmembrane proteins within a domain high in cholesterol, saturated phospholipids, sphingolipids and glycolipids resulting in a hydrophobic, ordered and rigid membrane nanodomain (Sezgin, Levental, & Eggeling, 2017). Lipid rafts are also important in the cycling of BACE1 throughout the cell as they are key target areas for endocytosis (Nichols, 2003; Pelkmans, 2005). The process of internalisation is known to be responsible for retrograde transport of BACE1 away from the cell surface. Interesting, APP is not as readily targeted to lipid rafts and therefore

palmitoylation of BACE1 may separate it from this substrate thereby leading to non-amyloidogenic APP processing (Ehehalt, Keller, Haass, Thiele, & Simons, 2003). APP is also transported directly from the golgi into early endosomes and its transport throughout the cell may be influenced by its homodimerization which, in turn, influences the ability of APP to interact with sorting proteins LRP1 and SorLA (Eggert et al., 2018). Transport into early endosomes through both of these mechanisms may enable BACE1 to come into contact with APP in this environment rather than at the cell surface thereby providing a preferable environment for BACE1 cleavage of this substrate.

N-glycosylation of BACE1 occurs at four residues N153, N172, N223, N354 all of which are contained within the ectodomain (Capell et al., 2000; Haniu et al., 2000). (Figure 6) A study by Charlwood *et al.* (2001) suggested that glycosylation of BACE1 is important for catalytic activity as their unglycosylated BACE1 mutants exhibited a reduction in BACE1 activity towards a APPswe peptide substrate; however these data were not published with a WT BACE1 control.

More recent evidence indicates that BACE1 undergoes bisecting GlcNAcylation, the addition of N-acetylglucosamine within a fork in the branched sugar, and that this modification delays BACE1 degradation with non-glycosylated BACE1 showing greater targeting to the endo-lysosome system (Kizuka et al., 2015). However, this increase in BACE1 targeting for degradation was shown using a KO model of the enzyme responsible for GlcNAcylation (GnT-III), rather than a BACE1 specific reduction in GlcNAcylation. It has been shown that GnT-III AD and GnT-III KO/hAPP mice exhibit reduced amyloid production (K. Akasaka-Manya et al., 2010; Kizuka et al., 2015). Interestingly, this study also indicated that GlcNAcylation bestows anti-amyloidogenic effects through modified APP. However there is also evidence that this type of sugar modification is increased in APP with the London and Swedish mutations that result in increased amyloid production and are associated with FAD (Keiko Akasaka-Manya et al., 2008).

BACE1 is ubiquitinated at Lys residues 63 and 501 (Kang, Cameron, Piazza, Walker, & Tesco, 2010). Lys501 has been shown to become mono-ubiquitinated as well as polyubiquitinated in a Lys-63-linked manner; whilst Lys63 is predominantly Lys-63-linked polyubiquitinated. Furthermore, ubiquitination of

BACE1 is a requirement for activation of GGA3 mediated lysosomal targeting of BACE1 as this protein binds to ubiquitin rather than the LL-motif of BACE1. Inducing a K501R mutation within BACE1 leads to increased half-life but does not influence BACE1 endocytosis or retrograde transport to the TGN; but does lead to accumulation within early endo-lysosomal systems with increased expression having been identified in early and late endosomes as well as lysosomal compartments (Kang, Biscaro, Piazza, & Tesco, 2012; Kang et al., 2010). The type of ubiquitination that may be responsible for this processing has yet to be identified. The deubiquitinase responsible for removing lysosomal targeting signals on BACE1 is Ubiquitin Specific Peptidase 8 (USP8). RNAi knockdown of USP8 has been shown to reduce BACE1 protein expression due to increased ubiquitination and increased targeting to the endo-lysosomal compartments (Yeates & Tesco, 2016). BACE1 has also been shown to undergo SUMOylation at K501 as well as K275 and that is modulated by the presence of SUMO-conjugating enzyme UBC9. Interestingly, SUMOylation of K501 has been shown to increase BACE1 stability and activity. Injection of AAV BACE1 K501R into the hippocampus of APP/PS1 transgenic mice decreases amyloid deposition as well as cognitive decline (Bao et al., 2018). However, both SUMO and ubiquitination studies use the same negative control of the BACE1 K501R mutant as both modifications occur at the same site. Therefore, further experiments are required to determine which modification is responsible for which regulatory effects.

BACE1 exists as three alternatively spliced isoforms within the human brain as well as full length transcript. Transcripts with deletions of 132, 75 and 207 nucleotides at 146-189, 190-214 and 146-189 & 190-214 respectively lead to prepro-BACE1 proteins 457, 476 and 432aa in length. These deletions occur between the catalytic aspartic acid residues and lead to significant reductions in the production of both $A\beta_{40}$ and $A\beta_{42}$ as well as proteolytic activity towards an APPswe substrate (Tanahashi & Tabira, 2001). It has been suggested that these truncations cause loss of activity by altering the morphology of the active site (Bodendorf, Fischer, Bodian, Multhaup, & Paganetti, 2001; Ehehalt et al., 2002). An animal study by Zohar *et al.* (2005) indicated that full-length BACE1 expression was predominant throughout the brain and is higher in APPswe mice

compared to WT controls. However, expression decreases with age in the transgenic animals whilst all BACE1 isoforms increased in WT with age.
As previously mentioned, BACE1 expression within the pancreas is higher than then the brain, whilst activity here towards APP substrates is significantly lower than the CNS (Sinha et al., 1999; Vassar et al., 1999). It has been shown that expression of non-enzymatic BACE1 isoforms is high in the pancreas and may? be the cause of this expression-activity discrepancy (Holsinger, Goense, Bohorquez, & Strappe, 2013; Tanahashi & Tabira, 2001).

These BACE1 isoforms have been detected within the pancreas in high levels. Further splice variants have been identified such as a truncated 127aa form containing an early termination codon and another lacking exon 4, however no further studies have substantiated the existence and characterisation of these isoforms (Mowrer & Wolfe, 2008; Tanahashi & Tabira, 2007).

Finally, it has been suggested that BACE1 may, in fact, be a substrate for the α-secretase ADAM10 and cleavage results in shedding of the BACE1 ectodomain. The effects of BACE1 shedding on amyloid pathology have yet to be determined with evidence indicating both increased $A\beta_{1-40}$ (but not $A\beta_{1-42}$) production or no effect on APP β-processing (Benjannet et al., 2001; Hussain et al., 2003)

1.3.7 BACE1 substrates

APP, whilst being the best characterised of the BACE1 substrates, is known to be a poor substrate to BACE1. Molecular dynamic simulations and fluorescence resonance energy transfer experiments have identified that binding affinity and catalytic activity of BACE1 to APP is lower than other substrates such as Neuregulin 1 (NRG1) (Halima et al., 2016).

Though the amyloid cascade hypothesis has become central to AD research, the relevance of amyloid peptides to this disease is still contested. Whilst research has focussed heavily on the $A\beta_{1-42}$ peptide due to its propensity for aggregation and its increased production in AD, the neurotoxic effects of this peptide have yet to be proven *in vivo*. Since genetic analyses in FAD has provided strong evidence for APP mutations in AD onset, it may be that alternative processing pathways are equally, if not more important in the contribution to AD than the BACE1-APP

relationship. Formative studies by Lu *et al.* (2000) and Gervais *et al.*, (1999) show that APP is also a substrate for members of the caspase family of cysteine aspartases and that APP processing by this family of enzymes is upregulated in neurons in AD. Caspases are proteolytic enzymes that are best known for their role in cell death mechanisms. Teams identified APP as a substrate to caspases 3, 6 and 8 whilst caspase 9 was only identified *in vitro*. Caspase 3 had been previously described as cleaving APP at Asp^{664} however caspases 8 and 9 were also suggested to cleave at this site producing a c-terminal C31 fragment (Barnes et al., 1998; Pellegrini, Passer, Tabaton, Ganjei, & D'Adamio, 1999; Weidemann et al., 1999). The C31 fragment was shown to induce cell death and apoptosis in cultured 293T and N2A cells respectively. Lu et al. also showed pro-apoptotic effects of the C99 fragment- the c-terminal peptide produced as a result of BACE1 cleavage of APP (Figure 1.1) and suggest that both the C99 and C89 c-terminal fragments could be substrates for caspases for further processing. They identified active caspase-9 in synaptosomal preparations from brain tissues and found that the C31 APP fragment was present in AD cases but not controls. Gervais *et al.* identified upregulation of caspase 3 cleavage of APP not only in AD patients but in brain injury- a known risk factor for AD as well as identifying the APPswe mutation as improving the preference for APP cleavage by caspase 6 by 3-fold however no other caspases were able to cleave APP with this mutation. This team also showed that peptide products of caspase cleavage of APP are present within amyloid plaques. Additional studies have corroborated the role of caspases 3, 6, 8 and 9 in APP processing and their actions in neurodegenerative diseases including AD and motor neuron disease (LeBlanc, Liu, Goodyer, Bergeron, & Hammond, 1999; Lu, Soriano, Bredesen, & Koo, 2003; Pellegrini et al., 1999; Rehker et al., 2017; Tamayev, Akpan, Arancio, Troy, & D'Adamio, 2012). The role of alternative APP processing in AD has been previously hypothesised. Volloch and Rits (2018) discuss the successes of BACE1 inhibitors in models of FAD and the relative failures of the same drugs in SAD cases and suggest alternative mechanisms for increased amyloid in AD- possible through an alternative translation initiation site just upstream of the C99 coding region. However, due to the necessity of caspases in programmed cell death and inflammation, it makes them a much less attractive drug target than BACE1.

Cathepsins have also been identified as APP proteases. Cathepsins B, D and L (CatB, CatD & CatL respectively) have all be identified as APP proteases and it is known that expression of all but CatL are increased in aged brains. (Mackay *et al.*, 1997; Wang *et al.*, 2015). Interestingly, brain CatL expression is reduced with age (Nakanishi et al., 1994). Prior to the discovery of BACE1 as the β-secretase, it was hypothesised that CatD may have been involved in either β or γ processing of APP due to its ubiquitous tissue expression and localisation within the endo-lysosomal system where the majority of amyloid production occurs (Saftig et al., 1996). It, like BACE1, is an aspartyl protease and generic inhibition of aspartyl protease activity was shown to reduce amyloidogenesis. However, this hypothesis was disproven when CatD null primary neurons were identified as secreting β -secretase cleavage products (Saftig et al., 1996). CatD has been shown to be increased in the cortex of AD patients (Chai et al., 2019). Enzymatic studies have indicated that in acidic conditions, CatD has greater affinity for APP than CatB and C, this affinity was even greater for the APP_{swe} peptide substrate spanning Glu^{668} to Phe^{675} of the APP β-site (Ladror, Snyder, Wang, Holzman, & Krafft, 1994). CatB has received particular attention for APP processing as studies have indicated that inhibition or attenuation of CatB activity results in reduced amyloid secretion from both hippocampal neurons and chromaffin cells. Furthermore, inhibition of CatL led to increased $Aβ_{1-42}$ but not $Aβ_{1-40}$ or total amyloid (Klein, Felsenstein, & Brenneman, 2009). CatB and CatL are cysteine proteases and cysteine protease inhibition has been shown to effectively reduce amyloid production and increase α-secretase activity (Hook, Kindy, & Hook, 2007). However, it has also been suggested that CatB facilitates amyloid degradation by cleaving $Aβ_{1-42}$ into non-toxic species suggesting a protective function against amyloid pathology (Mueller-Steiner et al., 2006). The role of cathepsins in AD is therefore complex and their precise contribution to pathogenesis has yet to be determined.

Whilst the contributions of BACE1 to APP processing and cytotoxicity remain debatable, the physiological function of BACE1 remains elusive. In order to better understand the role that BACE1 plays in a non-disease context, studies have been designed to profile its substrates. One of the key difficulties in identifying BACE1 substrates is the promiscuity of this enzyme. The BACE1 active site is large and evidence suggests that BACE1 is an atypical member of the pepsin

family and conveys biochemical differences even to its most similar homolog CatD. The first large-scale study to identify BACE1 substrates was conducted by Hemming *et al.* (2009). This study utilised quantitative proteomics with stable isotope labelling with amino acids in cell culture (SILAC) on the conditioned medium of both HEK 293 and HeLa cell lines overexpressing human BACE1, in effect analysing the secretome of these cells. This study identified 68 putative BACE1 substrates which included known substrates APP, APLP1/2 and LRP (von Arnim et al., 2005). This led to follow up studies confirming and characterising the interactions of BACE1 with novel substrates such as Sez6L, Jag1 and NCAM1. However, these studies have only identified mechanisms through which BACE1 may contribute to disease rather than a physiological function in healthy individuals. Further studies to identify the BACE1 secretome conducted by Kuhn *et al.* (2012) and Dislich *et al.* (2015) confirmed many previous findings but again, failed to suggest a physiological role for BACE1.
Further -omics studies have identified BACE1 substrates by monitoring changes in the neuronal cell surface proteome. Using surface-spanning protein enrichment with click sugars (SUSPECS). Based on click-chemistry, labelling glycoproteins with N-azidomannoseamine, the glycoproteins could then be biotinylated using an alkyne-containing biotin compound (sulfo-dibenzylcyclooctyne-biotin) that covalently binds to the azide group of the glycoprotein label. These glycoproteins could then be identified using MS. The team used this method to determine that overexpression of BACE1 in living neurons results in strong increases in BACE1 substrates APP, APLP1, Sez6, Sez6L, CNTN2 and CHL1 as well as the multipass protein PLD3 (Herber et al., 2018).

A limitation to many of these studies lies in the requirement for overexpression of BACE1 in order to achieve quantifiable or detectable outcomes due to low BACE1 expression or activity in the chosen model. However, increased BACE1 is characteristic of diseased or stressed conditions such as metabolic stress, inflammation or hypoxia and are therefore not representative of normal physiological conditions and may identify substrates only representative of disease. In addition to this, many validation studies are conducted *ex vivo* and therefore offer no insight into the compartmentalisation effects of BACE1 on the substrate.

It must be noted that these studies focus on the proteolytic function of BACE1 whilst it has been shown that BACE1 may, in fact, exert non-enzymatic functions. Including control on voltage gated K^+ channels through interaction with α-subunits and regulating expression, localisation and gating of channels (Lehnert et al., 2016). These are regulators of neuronal excitability and tie in to signal propagation and LTP. This finding builds upon the previous finding of non-catalytic BACE1 isoforms expressed highly within the pancreas as discussed in section 1.3.5; the function of which has yet to be established. However, proteomic studies so far would exclude these interactions and focus purely on the sheddase function of BACE1 since its discovery as the β -secretase.

BACE1 exhibits a varied substrate profile with validated targets including the Notch ligand Jagged-1 (Jag-1), the integrin binding protein Neuregulin-1 (Nrg-1) and the voltage-gated sodium channel β_2 subunit ($Na_v\beta_2$) (Wanxia He, Hu, Xia, & Yan, 2014; Wong et al., 2005).This is perhaps unsurprising when one considers the large and open nature of the BACE1 binding pocket offering no structural selectivity for substrates. The promiscuity of BACE1 has therefore implicated it in many cellular processes, adding further difficulty to establishing the physiological function of this enzyme.

Through cleavage of Jag1, BACE1 is implicated as a regulator of cell fate. Activation of Notch by its binding partners Delta-1, Jagged 1 or Jagged 2 during development determine the differentiation of neural stem cells into astrocytes, neurons or glia (Grandbarbe et al., 2003). BACE1 KO models exhibit significantly elevated notch signalling by reduced ectodomain shedding of Jag1. Increased notch activation by Jag1 has been shown increase astrocyte formation within the hippocampus but reduce neurogenesis in early stage development (Xiangyou Hu, He, Luo, Tsubota, & Yan, 2013). Regulation of Jag1 by BACE1 opens up the possibility of a role for BACE1 in development and cell fate mechanisms. Despite BACE1 KO mice exhibiting no significant increases in lethality during gestation, and no significant increase in BACE2 as a compensator, the effects of double knock-out of BACE1 with other known jagged proteases, such as ADAM17, have not been investigated.

Another well characterised substrate is with the integrin binding protein neuregulin-1 (Nrg-1). This protein has many functions and structures within the brain which have been extensively reviewed by Mei and Xiong (2008). There are 6 types of Nrg-1 isoforms which are expressed differentially throughout tissues and cell types and regulated by alternative splicing and alternative promotor sequences within the gene (Tan et al., 2007). 5 of the 6 types of Nrg-1 are membrane anchored and shedding by a protease, such as BACE1, results in activation of the protein as a growth factor (Wang, Miller, & Falls, 2001). Research into this protein focuses mainly on schizophrenia with the discovery of an Icelandic population that exhibit mutations within the Nrg-1 gene leading to this condition due to its effects on neurotransmitter receptors such as NMDARs. (Stefansson et al., 2002). Interestingly, some BACE1 KO models are known to express a schizophrenic like phenotype (Savonenko et al., 2008). BACE1 cleaves Nrg1 types I and III which are known to bind to ErbB receptor tyrosine kinases.

Whilst BACE1 may regulate synaptic glutamate through indirect mechanisms, there is evidence to suggest that the ion channel $Na_v\beta_2$ subunit is a substrate of BACE1. Due to the presence of an Ig loop within the β-subunits they are classified as cell adhesion molecules and are part of the same superfamily as cadherins, selectins and integrins (Isom & Catterall, 1996). BACE1 overexpression may therefore prevent cell surface expression of the sodium channels by cleaving the β-subunit; this could resulted in reduced sodium current density and could cause reduced depolarisation of neurons thereby reducing the likelihood of an action potential within the neuron (Kim et al., 2007).

From these few substrates we know that BACE1 regulates a wide variety of cellular processed through multiple mechanisms; the maturation and activation of proteins to initiate signalling cascades, inhibition of signalling by shedding of ligands and the regulation of cell surface expression of ion channels covering cell functions such as synaptogenesis, cell fate and neuronal signal transduction.

1.4 Project aims

The aims of this project were to better understand how changes in BACE1 expression and activity influence, and are influenced by, metabolic stress and the physiological role of BACE1. This was conducted through three studies:

An *in vivo* study into the effects of BACE1 expression on the brain proteome. This study monitored changes in protein expression within the hippocampus and hypothalamus of transgenic mice with either a global BACE1 KO or an approximately 2-fold over-expression of the human BACE1 gene under the CamKII promotor in order to make it brain-specific (BACE1 KI). The BACE1 KI mice exhibit a diabetic phenotype even without dietary intervention suggesting a role for BACE1 in energy homeostasis and glucose control (Plucinska et al., 2014; Plucińska et al., 2016).

A cell-based proximity assay was developed in order to identify BACE1 interacting proteins. This assay was based around the Bio-ID method whereby a fusion protein was made of BACE1 with the *E.coli* biotin ligase BirA (R118A). This enabled biotinylation of proteins within 10nm radius of BACE1/BirA. Development of this assay would enable future experiments to identify whether known stressors, such as a HFD or chronic inflammation lead to changes in the BACE1 interactome.

Finally, this project followed previously published work into the effects of Aβ exposure on leptin signalling. *In vivo* data using intracerebroventricular (ICV) infusion of amyloid peptides into the brains of WT mice indicate that central exposure to these peptides induces hypothalamic leptin resistance (Meakin, Jalicy, et al., 2018). This study used leptin responsive cell lines including hypothalamic neurons (GT1-7) to determine the effects of simulated ‘chronic’ amyloid exposure at physiological concentrations on leptin sensitivity and signalling components. Known regulators of leptin signalling were determined in order to detect a possible mechanism by which amyloid peptides may induce leptin resistance.

Chapter 2

Materials & methods

2.1 Common chemicals and methods

2.1.1 Chemicals

All chemicals utilised were obtained from Sigma Aldrich unless otherwise stated. Bromophenol blue and D-Glucose were obtained from Fisher Scientific. 30% polyacrylamide was obtained from National diagnostics. Butanol, Ethanol, Isopropanol, Methanol, PBS tablets, Sodium chloride and sucrose were obtained from VWR international.

2.1.2 Commonly used solutions

Commonly used buffers and solutions are represented in table 2.1.

2.1.3 Antibodies and probes

All primary and secondary antibodies and RT PCR probes utilized within this thesis are represented in table 2.2.

Solution	Component	Concentration
Lysis buffer (pH 7.4)	Tris HCl pH 7.4	25mM
	NaF	50mM
	NaCl	0.1M
	EDTA	1mM
	EGTA	5mM
	NaPPi	10mM
	Triton X-100	1% (v/v)
(added at time of use)	Sucrose	92mg/ml
	β-Mercaptoethanol	1µl/ml
	NA3OV4	1mM
	Benzamidine	1mM
	PMSF	0.1mM
4x Sample Buffer (12ml)	Tris HCl pH 6.8	4ml
	Glycerol	3.2ml
	20% SDS	3.2ml
	β-Mercaptoethanol	1.6ml
	Bromophenol blue	pinch
10x SDS-PAGE running buffer	Tris HCl	190mM
	Glycine	2M
(added at time of use)	10% SDS	0.01% (v/v)
SDS-PAGE transfer buffer	Methanol	20% (v/v)
	Tris HCl	48mM
	Glycine	39mM
Tris-buffered saline (TBS)	Tris HCl pH 7.4	20mM
	NaCl	150mM
TBS+ Tween (TBST)	TBS as above	
	Tween-20	0.01% (v/v)
Stripping buffer pH 2.2	Glycine	200µM
	10% SDS	0.1% (v/v)
	Tween 20	1% (v/v)
COMSR buffer (pH10.4)	Urea	7M
	Thiourea	2M
	Tris HCl	40mM
	C7BzO	1% (w/v)
Bio-ID lysis buffer	SDS	0.1%w/v
	Triton X-100	1%
	PBS	1x
	NA3OV4	1mM
	Benzamidine	1mM
	PMSF	0.1mM
Bio-ID digestion buffer	Urea	1M
	Ammonium bicarbonate	100mM

Table 2.1 Commonly used solutions

Primary Antibodies for Western Blotting				
Antibody	**Supplier**	**Code**	**Concentration**	**Blocking Agent**
Actin	Sigma	A2066	1:5000	5% BSA TBST
BACE1	Cell Signalling Technologies	5606S	1:1000	5% BSA TBST
EPB41L1	ThermoFisher Scientific	PA563352	1:500	5% BSA TBST
EPB41L1	Abcam	ab179453	1:1000	5% BSA TBST
FUCA1	R&D Systems	MAB7039-SP	1:1000	5% BSA TBST
HA-tag	Cell Signalling Technologies	3724S	1:2000	5% BSA TBST
pSHP2 Y542	Cell Signalling Technologies	3751	1:1000	5% BSA TBST
pSHP2 Y580	Cell Signalling Technologies	3703	1:1000	5% BSA TBST
pSTAT3 Y705	Cell Signalling Technologies	9131S	1:1000	5% BSA TBST
PTP1B	Supplied by Prof. Mirela Delibegovic		1:1000	5% BSA TBST
SHP2	Cell Signalling Technologies	3397	1:1000	5% BSA TBST
SOCS3	Cell Signalling Technologies	2923	1:1000	5% BSA TBST
STAT3	Cell Signalling Technologies	9139	1:1000	5% BSA TBST
Streptavidin-HRP	Cell Signalling Technologies	3999S	1:2000	5% BSA TBST
TXNDC15	Thermo Fisher Scientific	PA548583	1:1000	5% BSA TBST
Primary Antibodies for Immunoflourescence Staining				
BACE1	Cell Signalling Technologies	5606S	1:100	3% BSA TBST
EPB41L1	ThermoFisher Scientific	PA563352	1:50	3% BSA TBST
HA-tag	Cell Signalling Technologies	3724S	1:200	3% BSA TBST
M6PR	Abcam	ab2733	1:100	3% BSA TBST
Primary Antibodies for Immunohistochemistry				
EPB41L1	ThermoFisher Scientific	PA563352	1:200	
BACE1 (human)	GeneTex	N1C2	1:500	
BACE1 (mouse)	Sigma	B0681	1:200	
NeuN	Merck	ABN90P	1:500	
Secondary Antibodies for Western Blotting				
IgG-HRP rabbit anti-mouse	Thermofisher Scientific	31450	1:5000	5% BSA TBST
IgG-HRP goat anti-rabbit	Sant Cruz Biotechnology	sc-2004	1:10,000	5% BSA TBST
Secondary Antibodies for Immunofluorescence				
Alexa Fluor 488	Life Technologies	A21200	1:500	3% BSA TBST
Alexa Fluor 594	Life Technologies	A11012	1:500	3% BSA TBST

Table 2.2 Antibodies used in both immunoblotting and immunostaining along with dilutions and blocking conditions.

2.1.4 Western Blotting

2.1.4.1 Sample preparation

Upon completion of the experiment, lysates were produced for analysis. Cells were washed with ice-cold PBS in order to stop cellular processes and ice-cold lysis buffer (table 2.1) was added to the well or plate. The volume of lysis buffer used varied with cell line and the size of culture vessel. Cells were scraped on ice and lysates were transferred to a 1.5ml microcentrifuge tube and stored at -20°C.

Tissues were lysed using 5ml tight-fit glass homogenisers (Fisher). Tissues were kept in liquid nitrogen until required whereupon they were transferred immediately into an ice-cold homogeniser containing 500μl (hippocampus and cortex) or 150μl (hypothalamus) of lysis buffer. The tissue was then allowed to defrost in lysis buffer and homogenised until no visible tissue remained. The lysed tissue was transferred into a clean 1.5ml microcentrifuge tube and stored at -20°C.

2.1.4.2 Determination of protein content and sample preparation

Protein content of each lysate was established by Bradford Assay (Bradford, 1976). Lysates were prepared for western blot analysis by defrosting on ice and centrifugation at 10,000g for 15 minutes at 4°C. The supernatants were transferred to a new 1.5ml microcentrifuge tube and the pellets stored at -20°C. The Bradford assay was conducted on a 96-well plate containing 1μl of supernatant and 250μl Bradford reagent (Thermo Fisher Scientific, Pierce™). Colorimetric analysis was conducted on an EnVision 2104 Multilabel plate reader (Perkin Elmer) using a protocol that shook the plate for 30 seconds, incubated the plate for 5 minutes at 37°C and shook the plate for a further 30 seconds prior to reading the optical density at 595nm. A standard curve was generated using serial dilutions of BSA (Thermo Fisher Scientific, Pierce™) in Bradford reagent and used to determine the protein content of each lysate supernatant.

200μg of supernatant was diluted in ddH_2O to establish equal concentrations of protein within the samples of each replicate. Samples were made by adding 25% 4x sample buffer (table 2.1) to the diluted lysate. Samples were heated to 95°C

for 5 minutes and cooled on ice prior to brief centrifugation in order to collect the sample within the tube.

2.1.4.3 SDS -Page

Gels were cast using the Mini-PROTEAN® Tetra Handcast Systems (BIO-RAD) using 1mm spacer plates. Samples were run on 10% acrylamide separating gels unless otherwise stated with a 4% acrylamide loading gel. (table 2.3) Plates were cleaned using 70% ethanol and loaded into the casting stand. The separating gel was made with ammonium persulphate (APS) added just prior to casting. The gel was added to the plates using a Pasteur pipette to a level marked approximately 50mm below the comb. A 50:50 (v/v) ddH_20, n-butanol mix was pipetted onto the surface of the loaded gel to remove bubbles and ensure the gel surface remains level. Once set, the ddH_20, butanol mix was removed and the gel washed with ddH_20. The plates were dried using filter paper and the loading gel was applied. 10 or 15 well combs were inserted and the gel allowed to set.

Amyloid oligomerisation was determined using 7-20% gradient gels. These were cast using the and Mini-PROTEAN® 3 Multi-Casting Chamber with 0.75mm spacer plates. (table 2.3)

Complete gels were transferred into the buffer tank and filled with running buffer. (table 2.1) 20μg of protein sample was loaded into each well with 5μl SeeBlue™ Plus2 (Thermo Fisher Scientific; LC5925) protein standard used as a molecular weight marker. Gels were run at 150V for approximately 1.5hrs.

	Separating Gel		**Gradient Gels**		**Loading Gel**
Percentage acrylamide **Component**	*10%*	*15%*	*7%*	*20%*	*4%*
ddH2O	4.15ml	2.27ml	18.03ml	2.10ml	2.8ml
1.5M Tris HCl ph 8.8	3.15ml	3.15ml	8.97ml	7.38ml	-
0.5M Tris HCl pH 6.8	-	-	-	-	1.25ml
30% Acrylamide	3.75ml	5.6ml	8.34ml	19.6ml	0.85ml
10% SDS	110μl	110μl	358.65μl	295.04μl	50μl
TEMED	11μl	11μl	2.49μl	2.49μl	5.35μl
20% APS	55μl	55μl	49.85μl	31.4μl	50μl

Table 2.3 Composition of tris-glycine gels for protein separation.

2.1.4.4 Transfer onto membranes

Gels were transferred onto 0.45μm nitrocellulose (Amersham Bioscience) unless otherwise stated using the Mini Trans-Blot® Cell (BIO-RAD) wet transfer system. Gels were prised apart using a plastic spatula and the loading gel gently removed. The transfer cassettes were placed in a trough of transfer buffer (table 2.1) and a pre-soaked sponge and filter paper added to the black side. The gel was gently prised off the glass and onto the filter paper in the cassette. Nitrocellulose was wetted with transfer buffer and carefully aligned on top of the gel ensuring no bubbles are trapped between the gel and the membrane. Pre-soaked filter paper followed by a sponge were placed on top of the nitrocellulose and the cassette carefully closed. Cassettes were placed into the transfer tank with an ice pack and the tank was filled with transfer buffer. The transfer took place at 100V for 1 hour.

2.1.4.5 Immunoblotting

Post transfer, nitrocellulose membranes were removed from the cassette and air-dried for 1 hour. When dry, the membranes were stained using Ponceau-S solution and washed with ddH2O to observe the bands. Membranes were cut into a maximum of 3 pieces to allow multiple proteins to be observed. Ponceau-S solution was washed off with TBS and the membranes were blocked in TBS containing 10% skimmed milk powder (Marvel). Membranes were blocked for 1 hour. Following blocking, membranes were washed briefly in TBS to remove excess milk and incubated in primary antibody solution (table 2.2) overnight at 4°C on a rocker at 35 osc./min. The following day, the blots were washed 5x 5minutes in TBST and incubated in secondary antibody solution (table 2.2) for 1 hour at RT on a rocker at 35 osc./min. The membranes were then washed 5x 5 minutes with TBST and stored in TBST at 4°C prior to visualisation.

2.1.4.6 Membrane stripping

Once phospho-proteins had been blotted for, membranes were stripped and re-probed for total proteins. Membranes were washed thoroughly in TBST to remove ECL and incubated in enough stripping buffer (table 2.1) to cover the membrane for 2x 10mins. Membranes were then washed twice in PBS for 10 minutes and

twice in TBS for 5 minutes. Membranes were then blocked and re-probed as per the protocol previously stated.

2.1.4.6 Analysis

Blots were visualised on film using ECL western blotting substrate (Thermo fisher Scientific, Pierce™; 32106) made and applied as per manufacturer recommendations. 2ml were applied to a whole membrane or 500µl to cut membranes. Membranes were blotted dry on tissue paper and placed into an X-ray film cassette and covered with clear acetate. X-ray film (Fisher; 34089) was applied to the membranes in a dark room and film was developed in a Konica Minolta SRX-101A table top processor.

Blots were scanned (Epson Perfection 2400 Photo) and quantified using ImageJ densitometry software on inverted images.

2.1.4.6 Statistical Analysis

All densitometry data were normalised to actin loading controls. Total proteins were then normalised to a control and the fold change represented graphically. Phospho-proteins are represented as a ratio of ratios to total protein expression. This was then normalised to the control sample within the study to give a fold change and represented graphically. Graphs indicate each data point with the bar representing the mean for each group. Error bars indicate the standard error of the mean. Statistical analysis was achieved through the non-parametric Kruskall-Wallis test and Dunn's multiple comparison test used to compare groups. $p \leq 0.05$ was considered significant (*), $p \leq 0.01$ (**) and $p \leq 0.001$(***).

2.1.5 Gene expression analysis

2.1.5.1 Sample preparation

Tissues were lysed in the same manner as with sample preparation for western blot however each tissue was lysed in 1ml TRI Reagent (T9424; Sigma Aldrich). Samples were then stored at -80°C until RNA extraction.

2.1.5.2 RNA extraction

Samples were defrosted on ice then allowed to stand at room temperature (RT) for 5 minutes. Phase separation was carried out by adding 200µl RT chloroform and shaken by hand for 1 minute. Samples were then allowed to stand at RT for

a further 15 minutes before centrifugation at 12000rpm for 15 minutes at 4°C. The RNA containing aqueous phase was then removed to a clean 1.5ml microcentrifuge tube. 0.5ml of RT isopropanol was added to each sample and inverted to mix. The samples were left at RT for 10 minutes followed by centrifugation at 12000rpm for 5 minutes at 4°C. The supernatant was removed and pelleted RNA washed with 1ml 75% ethanol at RT. Samples were mixed by pipetting to ensure resuspension of the pellet and centrifuged at 12000rpm for 5 minutes at 4°C. The ethanol was carefully removed and the purified RNA pellet air dried for 15 minutes in a fume hood. The RNA was resuspended in 30µl of nuclease-free water (Ambion) and mixed by pipetting. The purity and concentration of the RNA was determined using a nanodrop ND-8000 Spectrophotometer and Nanodrop 8000 V2.3.2 Software. The spectrophotometer was cleaned prior to use and blanked using nuclease-free water. The concentration of RNA was determined at 260nm and DNA:RNA ratio determined adequate at 260/280nm of >1.7. RNA was stored at -80°C until cDNA synthesis.

2.1.5.3 cDNA synthesis

cDNA libraries were created from the purified RNA of each sample using the SuperScript™ II reverse transcriptase (Invitrogen; 10864014). For each sample, 1µl total RNA was combined with 3µg of random primers (Invitrogen; 48190011) and 1µl dNTP mix (10mM each) (Invitrogen; 18427013) and nuclease-free water added to a total volume of 13µl in a sterile microcentrifuge tube. This solution was incubated at 65°C for 5 minutes and placed on ice before adding 4µl of 5x first-strand buffer and 2µl of 0.1M DTT. This was mixed gently before the addition of 200U SuperScript™ II reverse transcriptase followed by further mixing. The cDNA synethsis took place at 42°C for 50 minutes and the reverse transcriptase denatured with a 70°C incubation for 25 minutes. The cDNA library was diluted to 5ng/µl and stored at -20°C.

2.1.5.4 Real-time PCR

RT PCR was conducted using the Taqman® gene expression analysis system (Applied Biosystems). This system used the FAM™ reporter dye attached to a gene-specific probe. The PCR reactions were prepared in sterile 96-well plates (Nunc). Each reaction contained 2.5µl cDNA, 10µl of mastermix (applied

biosystems) , 1µl of probe and 6.5µl of nuclease-free water. An actin control for each sample was included in every plate. The plate was briefly centrifuged to ensure collection of each reaction mix in the bottom of each well and sealed. RT PCR was conducted using the 7900HT fast RT PCR system. The cycling conditions included an activation step of 95°C for 10 minutes followed by 40 cycles of: 95°C for 15 seconds, 60°C for 2 minutes. The copy number determined by the RT PCR system was used to calculate RNA expression and normalised to the actin control. The probes used are detailed in table 2.4.

Probe Name	Code
Actin	Mm00438023_m1
Caspase1	Mm00434226_m1
IL-18	Mm00434228_m1
IL-1β	Mm00446190_m1
IL-6	Mm00840904_m1
NLRP3	Mm00545913_s1
SOCS3	Mm00443260_g1
TNFα	Mm00438023_m1

Table 2.4 Table of Taqman® RT PCR probes used in gene expression analysis

2.1.6 Cell maintenance

Cell lines were maintained under aseptic conditions and cultures at 37°C and 5% atmospheric CO_2. All plasticware used was purchased from Nunc.

All cell lines used and their culture media are presented in table 2.5. All cells were passaged 2-3 times weekly upon reaching 70-80% confluency. The passage ratios for each cell line are indicated in table 2.5. Cells were passaged by removing the cell culture medium and adding 2.5ml 0.05% Trypsin-EDTA (Gibco; 25300054) to the T75 culture flask. Cells were incubated in trypsin for 3-5 minutes in a cell culture incubator. Cell dissociation was established by observing the cells through a microscope. The trypsin was then deactivated by the addition of cell culture medium and cells were dispersed by gentle pipetting. 10ml cell culture medium was added to a clean T75 flask and the cell suspension added.

2.1.7 Cell storage

Cells stocks were stored in 1ml aliquots in liquid nitrogen. To freeze cells for storage and 70 - 80% confluent T75 flask was washed with warm, sterile PBS and trypsinised with 2.5ml 0.05% Trypsin-EDTA. Cells were incubated in trypsin

for 3-5 minutes in a cell culture incubator until cells had dissociated from the flask. 5ml of normal culture medium was added and transferred to a sterile 15ml centrifuge tube. Cells were pelleted by centrifugation at 800rpm for 4 minutes with a slow deceleration. Whilst cells were spinning a freezing medium was made by combining 4ml of normal culture medium with 1ml sterile DMSO. (Sigma Aldrich; D2650-5X5ML) When the cells had pelleted the medium was removed and the pellet flicked to begin resuspension. 2ml of normal culture medium was added to the cells and the suspension pipetted to achieve a single cell suspension. 2mls of freezing medium was added to the suspension and gently mixed. 1ml of the cell suspension was added to each of 4 cryovials and frozen in a Mr Frosty freezing container at -80°C overnight. Once frozen, the cryovials were transferred into liquid nitrogen for long-term storage.

To thaw cells from storage the cryovials were placed in a 37°C water bath until almost completely defrosted. The cryovial was then removed from the water bath and the cells transferred into a T25 containing 5ml of normal culture medium. The cells were gently pipetted to achieve a single-cell suspension and incubated in a cell culture incubator overnight. Once adhered the following day, the medium was removed and the cells washed with warm, sterile PBS. 5ml culture medium was then added to the cells which were then left to grow in a cell culture incubator until confluent. When confluent, cells were transferred into a T75 flask and cultured as described in 2.1.5.

Cell Line	Passage ratio	Medium	Supplements	Provider
Wild-type Hek 293	1:10	DMEM, No Glucose (Gibco; 11966025)	Fetal bovine serum 50U/ml Penicillin-Streptomycin 4mM L-Glutamine 25mM/10mM D-Glucose	Seralab; EU-000-S Gibco; 15140122 Gibco; 25030081
mObRb Hek 293	1:10	DMEM, No Glucose (Gibco; 11966025)	Fetal bovine serum 4mM L-Glutamine 10mM D-Glucose + 200µg/ml Geneticin™ (maintenance) + 500µg/ml Geneticin™ (selection)	Seralab; EU-000-S Gibco; 25030081 Gibco; 10131027
N46	1:5	DMEM/F-12 GlutaMAX (Gibco; 31331093)	Fetal bovine serum 50U/ml Penicillin-Streptomycin	Seralab; EU-000-S Gibco; 15140122
mHypoA 2/22	1:5	DMEM, High Glucose (Gibco; 41965039)	Fetal bovine serum 50U/ml Penicillin-Streptomycin 4mM L-Glutamine	Seralab; EU-000-S Gibco; 15140122 Gibco; 25030081
GT1-7	1:4	DMEM, High Glucose (Gibco; 41965039)	Fetal bovine serum 4mM L-Glutamine + 200µg/ml Geneticin™ (maintenance) + 500µg/ml Geneticin™ (selection)	Seralab; EU-000-S Gibco; 25030081 Gibco; 10131027
HT-22	1:10	DMEM, High Glucose (Gibco; 41965039)	Fetal bovine serum 50U/ml Penicillin-Streptomycin 4mM L-Glutamine	Seralab; EU-000-S Gibco; 15140122 Gibco; 25030081

Table 2.5 Cell culture media composition for each cell line

2.2 Animal models

2.2.1 Maintenance of mouse lines

Animal procedures were performed in accordance with Home Office guidelines under the project licences of Michael Ashford PPL 60/4280 (prior to September 2016), PPL 70/9068 from September 2016 within the University of Dundee. Animal procedures within the University of Aberdeen were performed under the project license of Prof. Mirela Delibegovic (P94B395E0) and personal license of Claire Hull (PIL I9EAD51F20). Regulated procedures were carried out by multiple personal license holders. Claire Sneddon (PIL I156E6B55) and Bethany Coull (PIL ID046E63B) conducted fixing of tissues. Paul Meakin (PIL I50789083) and Bethany Coull were responsible for the changing and maintaining of diets.

All animals were maintained in a 12-hour light/dark cycle in a temperature-controlled facility at 21°C. Mice were allowed *ad libitum* access to either normal chow (NC) diet (7.5% fat, 75% carbohydrate, 17.5% protein content by energy; RM1 diet, Special Diet Services) or 45% high-fat (HF) diet (45% fat, 35% carbohydrate, 20% protein content by energy; 824053, Special Diet Services) and water. Mice used for staining, proteomics and validation were male whilst preliminary studies were conducted from female BACE1 KO and KI cortices. Mice used in the proteomic study were fasted overnight to reduced variability in metabolic protein expression as a result of inconsistencies in time since last feed. This allowed identification in basal protein levels. By fasting overnight, it is presumed the animals enter a catabolic state whereby all postprandial signalling has returned to baseline and blood glucose variability is minimised. Mice were weighed weekly and handled daily.

2.2.2 BACE1 -/- mouse line

BACE1-/- mice were generated by GlaxoSmithKline on a C57BL/6J background and maintained in-house at Ninewells Hospital & Medical School, University of Dundee. The mice used in this study were >97% C57BL/6J due to a historical back-cross with 129P mice and subsequent breeding back on to C57BL/6J. BACE1 -/- mice were produced by the insertion of the *LacZ* reporter gene in place of exon 1 of BACE1. (S M Harrison et al., 2003)

2.2.3 Genotyping of BACE -/- mice

BACE1-/- mice were genotyped by PCR amplification within BACE1 and LacZ genes. Once weaned, ear notches were taken. DNA was extracted by combining 100µl of extraction solution (Sigma; E7526) and 25µl of tissue preparation solution. (Sigma, T3073) The ear notch was submerged in the extraction solution and incubated at room temperature for 10 minutes followed by 95°C for 3 minutes. 100µl of neutralisation solution B (Sigma; N3910) was added and the mix placed on ice. Once cool, DNA extractions were stored at -20°C until required. PCR was conducted using KOD hot start DNA polymerase (Merck Millipore; 71086) in two reactions for the BACE1 and LacZ separately. BACE1 was identified using the forward primer 5'-CGC TGC ACT GGC TCC TGC TAT GGG-3' and reverse primer 5'-TCT CCA CAT AGT CCT GGC CGG-3'. LacZ was identified using the forward primer 5'-GAC CAG CCC TTC CCG GCT GTG CCG-3' and the reverse primer 5'-GCC GAC CAC GGG TTG CCG TTT TCA-3'. Contents of the PCR reactions contained 1x KOD buffer, 1.5mM MgSO4, 0.2mM dNTPS (each), 0.02U/µl KOD Hot-start DNA polymerase and 0.15µM forward and reverse primers. Reactions were made up to 50µl total volume using sterile, nuclease-free H2O. Thermocycler conditions are stated in table 2.6. PCR products were analysed by horizontal gel electrophoresis on a 1% agarose gel containing 10% v/v SYBR™ Safe DNA Gel Stain (Invitrogen; SS33102). Samples were prepared by adding 10µl of 6x blue/orange loading dye (Promega; G1881) and a well loaded with 10µl of 100bp DNA ladder (Promega; G2101). Gels were run at 120V for 45 minutes in TAE buffer (Sigma; T9650) and visualised on a Bio-rad ChemiDoc MP XRS+ Imaging System. BACE1 bands are present at 200bp whilst the *LacZ* band occurs at 299bp. (Figure 2.1) KO mice were identified by the absence of the BACE1 band in addition to a *LacZ* band. Heterozygous mice exhibited a band for both genes and WT mice exhibited only a BACE1 band.

Step	Temperature (°C)	Duration
Polymerase activation	95	2 min
35 cycles:		
Denaturation	95	20s
Annealing	62	15s
Extension	70	7s
Hold at 4°C		

Table 2.6 PCR conditions for amplification of the BACE1 gene from genomic mouse DNA.

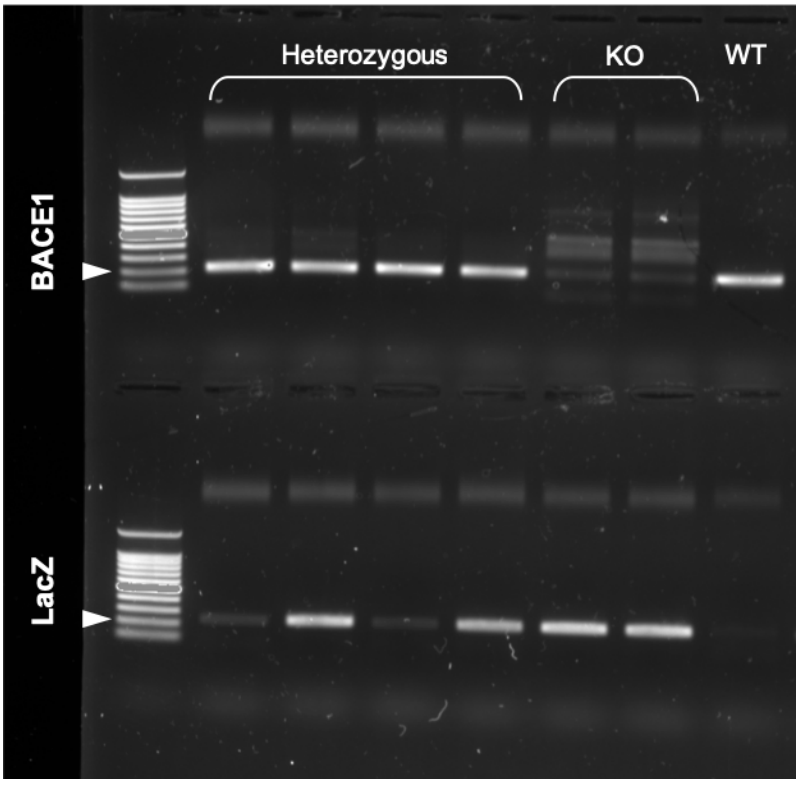

Figure 2.1 Gel representing the amplified fragments from PCR reactions to detect the BACE1 and LacZ genes from genomic DNA extracted from ear notches. White arrow represents the 200bp marker in a 100bp DNA ladder. Heterozygous mice exhibit a band in both the BACE1 and LacZ reactions, BACE1 KO mice exhibit a band in LacZ and a characteristic laddering in the BACE1 reaction, WT mice exhibit a band in the BACE1 reaction and nothing in the LacZ.

2.2.4 hBACE1 Knock-in mouse line

hBACE1 knock-in mice were generated and maintained by Prof. Bettina Platt at the University of Aberdeen as described by Plucińska et al. (2014). Knock-in mice exhibit a ~2- fold increase in forebrain BACE1 expression through the addition of the human BACE1 gene addition to the HPRT locus under a CamKIIα promotor. Mice were singly housed. The diet was administered in the same way as with the BACE KO and WT animals kept in Dundee and tissues were collected by the

same individuals. The same batch of HFD was used and RM1 diet was given to the WT NC controls.

2.2.5 Diet-induced obese mice

WT C57BL/6J were used as a diet-induced obese (DIO) model due to their susceptibility to weight gain when challenged with a HFD. Animals were group housed (≤3 per cage). At 8 weeks the mice were weighed and their food changed to a 50:50 mix of NC and HFD. After one week the mice were weighed again and their diet changed to 100% HFD and their weight monitored weekly for a further 11 weeks. NC controls were weighed weekly but were kept on RM1 diet for the duration of the dietary challenge. By utilising HF fed animals instead of transgenic obese models this study could utilise a model comparable to the majority of obese human cases as the high-fat, high-sugar diet of western populations is the greatest contributor to human obesity. However, by comparing HFD to NC animals one neglects the effects of other nutritional contributors. In order to maintain the calorific density of the diet (eg.14.74Mj/kg), the protein and carbohydrate content of the HFD must be reduced and this must be considered when evaluating the data.

Animals were considered obese if their weight gain in grams at the end of the study was greater than 3 standard deviations of the average weight gain of the NC controls therefore all WT high-fat (HF) mice exhibited weight gain of at least 9.82g over 12 weeks of HFD. Two mice were removed from the study with weight gains of 3.6g and 4.1g over the 12 week HF dietary challenge.

2.3 Brain Proteomics

2.3.1 Tissue preparation

Animals were killed by cervical dislocation and major artery laceration. Brains were dissected on ice and tissues snap-frozen before storage at -80°C prior to proteomic analysis. Tissues were homogenised in 200µl COMSR buffer (Table 2.1) and protein concentrations determined by bradford assay. Lysates were precipitated in acetone for 1 hour at -20°C and centrifuged at 15000RPM for 20 minutes at 2°C to pellet.

100µg of acetone-precipitated protein pellets were resuspended with 100µL of 100mM TEAB. 20µL of the trypsin storage solution was added to the lyophilised

trypsin and incubated for 5 minutes before adding 2.5µg of trypsin to each protein pellet. Samples were digested overnight at 37°C.

2.3.2 TMT labelling

Tandem mass tag (TMT) isobaric labelling of sample digests was performed using the TMT10plex™ Isobaric label reagent set as per protocol. (ThermoFisher Scientific; 90110) Tissues from individual mice were processed separately so that each label represented a single mouse. Three TMT10plex™ kits were utilised. The first used hippocampal samples from 3 WT NC mice, 3 WT HF mice and 3 BACE1 KO HF mice, the second used hypothalamic samples from the same mice.

2.3.3 LC/MS

Samples were fractionated into 24 fractions using a high pH reversed phase C18 on an Orbitrap Q Exactive Plus mass spectrometer for 160 minutes. Each sample was separated into 24 fractions, the top 15 ions were selected for sequencing. Each sample was run through MS at 70,000 resolution and tandem MS (MS/MS) at 17,500 resolution using data dependent acquisition. Peptides were assigned to proteins by comparison to the Uniprot database using MaxQuant (v1.6.0.13) software with a peptide false discovery rate of 0.01. Occam's razor was employed to assign peptides that encode multiple proteins. This tool determined which protein was most likely to be a true identified hit based on parameters such as peptide coverage and reporter ion intensities. The unidentified peptide was then assigned to that protein as the most probable source of the peptide. False discoveries were excluded by matching peptide data, reverse hits and scrambled hits to a contaminant database.

2.3.4 Statistical analysis

Analysis of the proteomic data was conducted using both quantitative and qualitative methods.

2.3.4.1 Method 1

This analysis was conducted by Dr Sara Ten-Have of the fingerprints facility at the University of Dundee. Analysis was conducted using MaxQuant (v1.6.0.13) software and ion scores for each protein were normalised to the median log intensity of each sample and compared to the mouse UniProt database. The false

discovery rate (FDR) was set to 0.01 for both peptide and protein. Volcano plots were produced to identify statistically significant changes in the brain proteome with both HFD and BACE1 KO. In order to increase the number of hits, the protein reporter intensity ratios were grouped into similar values into a pre-defined data range (eg. 0.05-0.14, 0.15-0.24 ect.) by a process called binning. This produced a normalised distribution of reporter intensities. From here proteins outwith 2 standard deviations of the median were considered significant. This method increased the tolerance of the analysis and resulted in many more hits.

2.3.4.1 Method 2

This analysis was conducted by Dr Michele Tinti a bioinformatician at The University of Dundee. He normalised the data using the CONSTANd method. Normalisation of the data allowed for statistical analysis by t-test using the Bonferroni correction to account for false discoveries. This method of analysis was only compatible with the WT NC, WT HF and KO HF groups as comparison is not possible between TMT10plex™ kits due to potential batch effects and differences between kits.

2.4 Testing proteomic validity

2.4.1 Determination of relative protein expression

Protein abundance for each proteomic hit was conducted by western blotting as described in section 2.1.4. Protein 4.1N (EPB41L1) expression was determined in both hippocampal and cortical samples. TXNDC15 and FUCA1 expression were determined in hypothalamic and cortical samples. All data were normalised to the mean of the WT NC control. Testing the validity of hits utilised tissue lysates from the same animal cohorts as that used for proteomic analysis. Due to a shortage of tissue, it was not possible to use hypothalamic lysates from proteomic animals for validation purposes but tissues from other animals under each condition in the study were used.

2.4.2 Fixing tissues

The brains of NC and HFD mice were perfuse fixed prior to embedding and sectioning. Animals were killed using a schedule 1 procedure (CO_2 in a rising concentration). Once dead, the chest was opened and a needle inserted in the left ventricle of the heart and the right atrium incised to allow perfusion of the

circulatory system. 10ml of ice cold PBS was injected into the ventricle to clean the tissues. After cleaning, 10ml of 4% PFA was injected into the ventricle to fix the tissues. Once fixed, the whole brain was removed and transferred into 4% PFA for 24 hours then transferred to 70% ethanol for storage. Brains were stored at 4°C for 1 week before embedding.

2.4.3 Embedding tissues

Prior to processing, mouse brains were incubated in 70% ethanol for 8 hours. Brains were then halved along the sagittal plane and a hemibrain from each mouse was processed and paraffin embedded. Tissues were processed using the Shandon Citadel 1000 and embedded using Shandon HistoCentre 3. All tissues were processed on the same settings, at the same time.

2.4.4 Processing of murine tissues for staining

Sectioning, antigen retrieval and IHC was performed by Dr Susan Bray of Tayside Tissue Bank. All sections were treated using the same reagents at the same time to negate batch differences.

7 micron sections from paraffin embedded tissue were cut on a Leica RM 2135 microtome onto Superfrost® plus slides (VWR International Ltd) and dried for 1 hr at 60 °C. Antigen retrieval and de-paraffinisation was performed using DAKO EnVision™ FLEX Target Retrieval solution (high pH) buffer (50x conc) (K8004) in a DAKO PT Link for 20 minutes at 97°C.

Immunostaining used Vectastain® Elite® ABC HRP kit (Peroxidase, Rabbit IgG) (PK-6101) with a DAKO Link Autostainer with initial staged conducted by hand:
Sections were washed in Flex Wash Buffer (K8006) then blocked using Flex Peroxidase-Blocking Reagent (SM801) for 5 mins then 10%(v/v) goat serum blocking solution from stock avidin solution (Vector Labs) (SP-2001) for 15 mins. Secions were incubated overnight at 4°C with rabbit anti human EPB41L1 primary antibody, at 1/200 dilution or rabbit anti human BACE-1 primary antibody, at 1/1000 dilution in Flex Antibody Diluent (K8006) including 10%(v/v) stock biotin solution (Vector Labs) (SP-2001)

Using the automated platform:

Sections were incubated in biotinylated anti-rabbit antibody for 30 min followed by Vectastain® Elite ABC reagent for 30 min, Flex DAB+ working solution (SM803) for 2 x 5 minutes, copper sulphate solution for 5 minutes and flex haematoxylin (SM806) for 5 minutes.

In between each step, sections were rinsed with flex wash buffer with a final wash ddH2O. Sections known to stain positively were included in each batch and negative controls were prepared by replacing the primary antibody with DAKO antibody diluent. Slides were manually washed in tap water before being rinsed in graded concentrations of alcohol, with a final rinse in Xylene and glass coverslips were applied.
Sections were all imaged on the same day, on the same microscope using the same settings and magnifications between replicates.

2.4.5 Human tissue data

Human cortical sections were obtained from Edinburgh brain bank who granted ethical approval for the use of these samples. Sex, age and BMI data for cortical tissues are indicated in table 2.7. All AD tissues were from individuals at Braak stage VI. Hippocampal sections were obtained from the south west dementia brain bank who granted ethical approval for the use of these samples. Details of sex, age and AD progression are indicated in table 2.8. The Braak stage of these sections were unavailable.

Sex	Age	BMI
Control		
F	59	23
F	45	23
F	37	21.5
M	57	22.8
Obese		
F	57	36.1
F	46	38
F	40	38.8
M	57	31.4
Aged control		
F	65	21.5
M	76	29
M	84	NA
F	74	30.9
Alzheimer's Disease		
M	76	NA
M	78	NA
M	80	NA
F	85	NA

Table 2.7 Sex, age and BMI of individuals from whom cortical sections were obtained

Age	Sex	AD Diagnosis
Control		
F	80	NA
M	90	NA
F	89	NA
F	78	NA
M	80	NA
M	73	NA
M	77	NA
F	87	NA
Alzheimer's Disease		
F	74	AD
F	88	AD
F	78	AD
M	86	Mild AD
F	86	AD
M	74	Severe AD
M	78	Mod/Sev AD
M	95	Probable AD

Table 2.8 Sex, age and AD diagnosis of individuals from whom hippocampal sections were obtained

2.4.6 Processing of human tissues for staining

Antigen retrieval was conducted by Dr Susan Bray of Tayside tissue bank as previously described (section 2.4.3).

Immunostaining using DAKO EnVision™ FLEX system was performed using a DAKO Link Autostainer with initial staged conducted by hand:
Sections were initially washed in Flex Wash Buffer (K8006) followed by:
5-minute incubation in Flex Peroxidase-Blocking Reagent (SM801) then incubation overnight at 4°C with rabbit anti human EPB41L1 primary antibody, (Invitrogen Fisher) at a dilution of 1/200 or rabbit anti human BACE-1 (NIC1) primary antibody, (GeneTex) at a dilution of 1/250 in Flex Antibody Diluent (K8006)

Using the automated platform:
Sections were incubated with Flex/HRP labelled polymer (SM802) for 20 minutes, Flex DAB+ working solution (SM803) for 2 x 5 minutes, copper sulphate solution for 5 minutes followed by Flex Haematoxylin (SM806) for 5 minutes.

In between each step, sections were rinsed with Flex Wash Buffer with a final wash dH2O. Sections known to stain positively were included in each batch and negative controls were prepared by replacing the primary antibody with DAKO antibody diluent. Slides were manually washed in tap water before being rinsed in graded concentrations of alcohol, with a final rinse in Xylene. Glass coverslips were then applied.
Sections were imaged on the same day, on the same microscope using the same settings and magnifications between replicates.

2.5 BioID

2.5.1 Site-directed mutagenesis

Site-directed mutagenesis was utilised to insert the BACE1 signal peptide and pro-peptide into the N-terminal BirA vector pcDNA3.1 mycBioID upstream of the BirA gene (Figure 2.2). This was done using the Q5® site-directed mutagenesis kit. (New England Biolabs; E0554S) Primers (table 2.9) were designed with a region complementary to the empty vector and a 5’ non-binding section

containing the complementary sequence to half of the insert sequence. The vector was then amplified by PCR using the KOD hot-start DNA polymerase as described in table 2.10 and 2.11. The amplified products were then circularised using the kinase, ligase, DpnI (KLD) reaction. 2µl of the PCR product was added to 10µl of 2X KLD buffer, 2µl of 10X KLD enzyme mix and 6µl of nuclease-free water. The reaction was incubated at room temperature for 5 minutes. The KLD product was transformed into NEB 5-alpha competent *E.coli.* The cells were defrosted on ice and 25µl of cell suspension added to a sterile 5ml snap-cap round bottomed tube. (Fisher Scientific; 14-959-11A). 2.5µl of the KLD reaction mix was added to the cells, mixed, and incubated on ice for 30 minutes. The bacteria were then heat shocked at 42°C for 30 seconds and returned to ice for 5 minutes. 475µl of SOC medium was added to the tube and cultured were incubated at 37°C for 1 hour in a shaking incubator at 220rpm. Cells were plated on LB selection plates containing 100µg/ml ampicillin and incubated at 37°C overnight. All colonies were selected the following day and a miniprep performed as described in section 2.5.6. A sample of each miniprep was sent for Sanger sequencing using the sequencing primers indicated in table 2.14 in order to identify successful mutants. When unsuccessful, site directed mutagenesis was then conducted using a 2-step reaction to add the signal and pro-peptides in separate reactions. The primers and reaction components are indicated in tables 2.12 and 20.13 respectively.

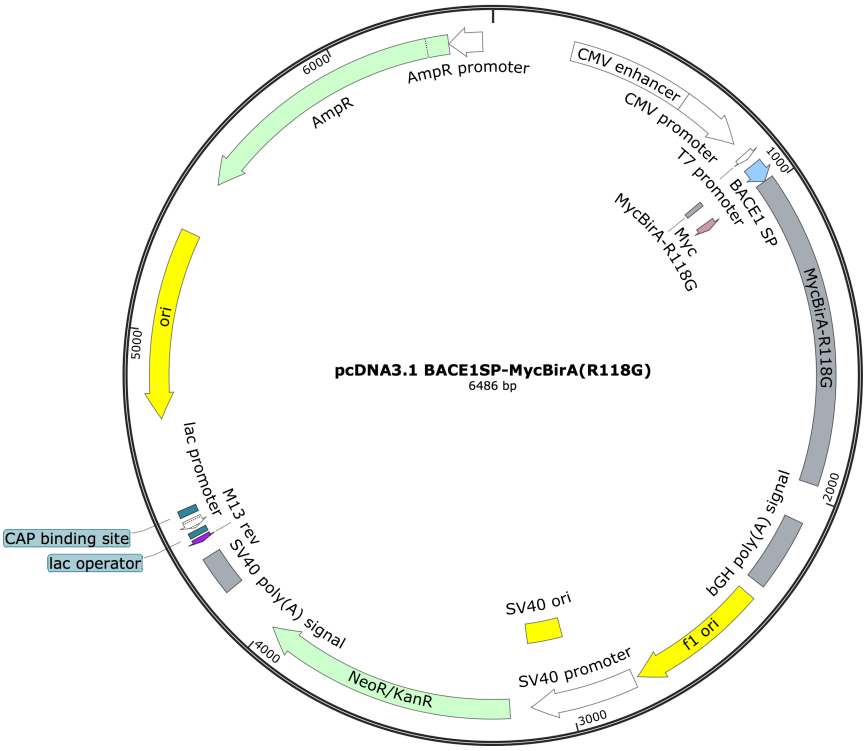

Figure 2.2 Plasmid map of empty pcDNA MycBirA(R118G) plasmid with the BACE1 signal peptide insert 5' of the BirA gene.

The BACE1 gene was amplified from a BACE1 construct using primers to add 5' NheI and 3' BamHI restriction sites using primers cycling conditions outlined in table 2.11 and 2.12 respectively. PCR products were precipitated to remove the polymerase and PCR components from the solution. To do this an equal volume of sodium acetate (0.3M, pH 5.2) followed by 0.7 volumes of isopropanol were added to the PCR reaction mix. The mixture was then centrifuged at 15,000g for 30 minutes at 4°C. The supernatant was removed and the pellet resuspended in 1ml 70% ethanol. The suspension was centrifuged at 15,000g for a further 15 minutes at 4°C. The supernatant was removed and the pellet air dried for 20 minutes or until no ethanol remained. The pellet was then resuspended in 50µl of nuclease-free water. BACE1 inserts were digested using NheI and BamHI restriction enzymes (NEB; R0131S, R0136S). The reaction mix contained 1x NEBuffer 2.1, 10U of NheI, 100ng purified BACE1 and nuclease-free water to a total reaction volume of 50µl. The digest was carried out at 37°C for 15 minutes followed by heat-inactivation at 65°C for 20 minutes. 10U of BamHI restriction enzyme was then added and the reaction mix digested for a further 15 minutes at 37°C. Digest were then purified by horizontal gel electrophoresis using a 1% agarose gel and excision of the BACE1 band. This was purified using the

QIAquick PCR and gel purification kit, (QIAGEN; 28506) resuspending in 30μl nuclease-free water.

Q5 site-directed mutagenesis primers			
PCR primer pair	**Direction**	**Primer sequence 5' - 3' (bases in bold are complementary)**	**Tm**
1	Forward	ACC CAG CAC GGC ATC CGG CTG CCC CTG CGC AGC GGC CTG GGG GGC GCC CCC CTG GGG CTG CGG CTG CCC CGG **CAA GCT GGC TAG CCA C**	50
	Reverse	GCC GTG GGC AGG CAG CAC TCC CGC GCC CAT CCA CAG CAG GAG CCA GGG CAG GGC TTG GGC CAT **GGT CTC CCT ATA GTG A**	
2	Forward	ACC CAG CAC GGC ATC CGG CTG CCC CTG CGC AGC GGC CTG GGG GGC GCC CCC CTG GGG CTG CGG CTG CCC CGG **ACA AGC TGG CTA GCC AC**	50
	Reverse	GCC GTG GGC AGG CAG CAC TCC CGC GCC CAT CCA CAG CAG GAG CCA GGG CAG GGC TTG GGC CAT **GGT CTC CCT ATA GTG A**	
3	Forward	ACC CAG CAC GGC ATC CGG CTG CCC CTG CGC AGC GGC CTG GGG GGC GCC CCC CTG GGG CTG CGG CTG CCC CGG **AAG CTG GCT AGC CAC CAT GG**	60
	Reverse	GCC GTG GGC AGG CAG CAC TCC CGC GCC CAT CCA CAG CAG GAG CCA GGG CAG GGC TTG GGC CAT **CTC CCT ATA GTG AGT CGT ATT AAT TTC GAT AAG CC**	

Table 2.9 Site-directed mutagenesis primers for the addition of both the BACE1 signal and pro peptides to the empty and melting temperatures

Component	Concentration		
KOD buffer	1X		
MgSO4	1.5mM	2mM	2.25mM
dNTPs	0.2mM each		
Primers	0.3μM each		
Template DNA	10ng		
KOD polymerase	0.02U/μl		
DMSO	0μl	2μl	3μl
Total volume:	**50μl**		

Table 2.10 Reaction composition for site-directed mutagenesis

Step	Temperature (°C)	Duration
Polymerase Activation	95	2m
20 or 30 cycles:		
Denaturation	95	20s
Annealing	Tm	10s
Extension	70	2m 43s
Hold at 4°C		

Table 2.11 Cycling conditions for site-directed mutagenesis

2-step Q5 site-directed mutagenesis primers			
PCR primer pair	**Direction**	**Primer sequence 5' - 3'**	**Tm**
Signal peptide	Forward	ATG GGC GCG GGA GTG CTG CCT GCC CAC GGC **GAA CAA AAA CTC ATC TCA GAA GAG GAT C**	50
	Reverse	CCA CAG CAG GAG CCA GGG CAG GGC TTG GG**C CAT GGT GGC TAG CCA GCT**	
Propeptide	Forward	CTG GGG GGC GCC CCC CTG GGG TTA CGG CTG CCC CGG **GAA CAA AAA CTC ATC TCA GAA GAG GAT CTC GAC AAG G**	60
	Reverse	GCC GCT GCG CAG GGG CAG CCG GAT GCC GTG CTG GGT **GCC GTG GGC AGG CAA CAC**	

Table 2.12 Primers for site directed mutagenesis in a 2-step process to add the BACE1 signal peptide and pro-peptides in separate reactions

Component	Concentration
KOD buffer	1X
MgSO4	1.5mM
dNTPs	0.2mM each
Primers	0.3µM each
Template DNA	10ng
KOD polymerase	0.02U/µl
DMSO	2µl
Total volume:	**50µl**

Table 2.13 Reaction composition for 2-step site directed mutagenesis

BACE1 peptide insert sequencing primers	
Direction	**Primer sequence 5' - 3'**
Forward	GGC GTG TAC GGT GGG AGG
Reverse	GGG CGA TCA GCT TCA GGG

Table 2.14 Sequencing primers for detecting the BACE1 gene

2.5.2 Restriction cloning

Restriction cloning was attempted using the pcDNA3.1 MCS-BirA(R118G)-HA vector to create a BACE1-BirA fusion protein. The BACE1 gene was amplified from a BACE1 construct using primers designed to create 5' NheI and a 3' BamHI restriction sites (Table 2.15). PCR conditions as described in tables 2.16 and 2.17. BACE1 inserts were produced and purified using methods described in section 2.5.1.

The pcDNA3.1 MCS-BirA(R118G)-HA vector was precipitated by isopropanol DNA precipitation as previously described and linearised by sequential digestion with NheI and BamHI restriction enzymes in a reaction mix containing 1x NEBuffer 2.1, 10U of restriction enzyme, 1μg vector DNA and nuclease-free water to a total reaction volume of 50μl. NheI digestion was carried out at 37°C for 1 hour followed by heat inactivated at 65°C for 20 minutes. BamHI was then added and digestion carried out for a further hour at 37°C. Following digestion, purification was carried out by horizontal gel electrophoresis and the QIAquick PCR and gel purification kit as described in section 2.5.1.

Ligation was carried out using the LigaFast system. (Promega; M8221) In a microcentrifuge tube 100ng of linear vector DNA and 46ng of BACE1 insert were added to 1x rapid ligation buffer and 3 Weiss units of T4 DNA ligase with nuclease-free water to a total reaction volume of 10μl. Ligations were incubated at room temperature for 5, 10 or 15 minutes. The ligase was then heat inactivated by incubation at 70°C for 10 minutes. Ligation products were transformed into NEB 5-alpha competent *E.coli* as described in section 2.5.1 as well as XL-1 blue *E.coli* (Agilent; 200249) transformed as per recommended protocol. Remaining ligation reaction was analysed by horizontal gel electrophoresis with empty vector, BACE1 insert and 1kb DNA ladder (NEB; N3232) to offer an indication of ligation efficiency. (Figure 2.3)

	BACE1 amplification primers	
Direction	**Primer sequence 5' - 3'**	**Tm**
Forward	GTA CGC TAG CGG GAG ACC GAC GAA GAG C	50
Reverse	GTA CGG ATC CAA CTT AAG CTG GAG ACC G	
Forward	GCG CTA GCC ATG GCC CAA GCC CTG	55
Reverse	GCG GAT CCG CGA TGG TCG ACG GCG C	

Table 2.15 Primers for the amplification of the BACE1 gene from a BACE1 containing plasmid.

Component	Concentration
KOD buffer	1X
MgSO4	1.5mM
dNTPs	0.2mM each
Primers	0.3µM each
Template DNA	10ng
KOD polymerase	0.02U/µl
DMSO	2µl
Total volume:	**50µl**

Table 2.16 Reaction components for the amplification of BACE1 by PCR

Step	Temperature (°C)	Duration
Polymerase Activation	95	2m
25 cycles:		
Denaturation	95	20s
Annealing	Tm	10s
Extension	70	30s
Hold at 4°C		

Table 2.17 Cycling conditions for the PCR of BACE1 from plasmid DNA

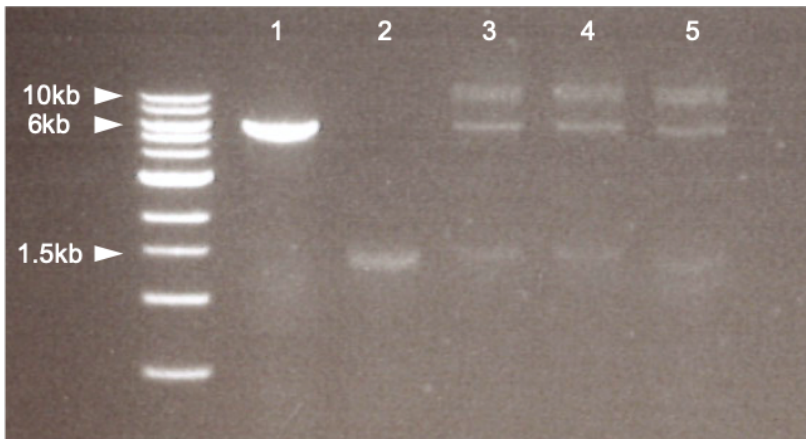

Figure 2.3 DNA gel of ligation products from restriction cloning of a BACE1 into the pcDNA3.1 MCS-BirA(R118G)-HA vector. Lane 1: empty vector. Lane 2: PCR amplified BACE1. Lanes 3, 4 and 5 represent 5, 10 and 15 minute ligation reactions respectively. Each ligation reaction contain fragments that correspond to both the empty vector and the insert indicating the ligation may have been incomplete. A larger band at approximately 10kbp may represent the ligated plasmid.

2.5.3 In-Fusion cloning

Cloning the C-terminal BACE1-BirA fusion protein was attempted using the In-Fusion® HD Cloning Plus system. (TaKaRa; 638909) The BACE1 gene was amplified from a construct using the CloneAmp™ HiFi PCR Premix included in the cloning kit. PCR reaction mix contained 1x CloneAmp HiFi PCR premix, 0.3μM of forward and reverse primers (Table 2.18), 50ng BACE1 template DNA and sterile Nuclease-free water to a total reaction volume of 25μl. The cycling conditions for amplification are indicated in table 2.19. Once amplified, the template DNA was removed by DpnI digest. The reaction contained 1x CutSmart® Buffer, 1U DpnI restriction enzyme and nuclease-free water to a total reaction volume of 50μl. Digests were incubated at 37°C for 1 hour followed by heat deactivation at 80°C for 20 minutes. The pcDNA3.1 MCS-BirA(R118G)-HA vector was linearised by AgeI (NEB; R3552L) restriction digest. 2μg were digested at 37°C overnight in a reaction mix containing 1x NEBuffer 1.1, 2U AgeI-HF in nuclease-free water to a total volume of 50μl. Following digestion the restriction enzyme was denatured by heating to 65°C for 20 minutes. The digests and linearised vector were then cleaned using the QIAquick PCR and gel purification kit as directed in the protocol and eluting into nuclease-free water. The In-Fusion cloning was performed by combining 46ng of BACE1 insert, 100ng of linearised vector and 1x In-Fusion Enxyme Premix to a total volume of 10μl with nuclease-free water. The contents was pipetted to mix and incubated at 50°C for 15 minutes and then placed on ice. The clones were transformed into library efficiency DH5α competent *E.coli* as described in section 2.5.4 and plated onto LB + 100μg/ml ampicillin plates. Plates were incubated overnight at 37°C. No colonies were produced from this method.

In-Fusion Primers			
PCR Primer pair	**Direction**	**Primer sequence 5' - 3'**	**Tm**
1	Forward Reverse	AGG CCT GTT AAC CGG ATG GCC CAA GCC CTG C GAG ACG TAC GAC CGG CTT CAG CAG GGA GAT GTC AT	58
2	Forward Reverse	ACT GGA CTA GTG GAT CAG GAG ACC GAC GAA GAG CCC G GAG ACG TAC GAC CGG CTT CAG CAG GGA GAT GTC AT	58
3	Forward Reverse	ACC CAA GCT GGC TAG ATG GCC CAA GCC CTG CCC TGT TGT CCT TGG ATC CTT CAG CAG GGA GAT GTC ATC AGC	60

Table 2.18 Primers for the In-fusion cloning of BACE1 into empty pcDNA3.1 MCS-BirA(R118G)-HA vector

Step	Temperature (°C)	Duration
30 cycles:		
Denaturation	95	10s
Annealing	55	15s
Extension	72	10s
Hold at 4°C		

Table 2.19 Cycling conditions for the In-fusion cloning of BACE1

2.5.4 Transformation

BACE1 inserts were commercially synthesised by Sigma Aldrich and inserted into pcDNA5D FRT vectors through restriction cloning by Dr Rachel Toth of the University of Dundee cloning facility (Figure 2.4). With the c-terminal BirA fusion protein, a 10bp linker was added between the BACE1 and BirA encoding regions. Transformation of the constructs was conducted using Library efficiency DH5α competent *E.coli* in aseptic conditions. (Invitrogen; 18263012) LB agarose plates were made by heating LB medium until melted. The LB was allowed to cool until the bottle was able to be handled. 10ml LB per plate was inoculated with 100μg/ml ampicillin and poured into sterile 10cm dishes. Once the medium had set the plates were transferred to an incubator at 37°C to dry.

Cells were defrosted on ice and 50μl of cell suspension added to a sterile 5ml snap-cap round bottomed tube. (Fisher Scientific; 14-959-11A) 100ng of DNA was added to the cells and flicked to mix. The cells were then incubated on ice for 30 minutes. Following incubation the cells were heat-shocked in a water bath at 42°C for 45 seconds before returning to ice for a further 2 minutes. 250μl of sterile SOC medium (Invitrogen; 15544034) was added and the cultured incubated at 37°C in a shaking incubator at 220rpm for 1 hour. The cultures were plated into the LB dishes by adding 50μl, 100μl or 200μl to 3 plates. Colonies were allowed to grow in an incubator overnight at 37°C.

A

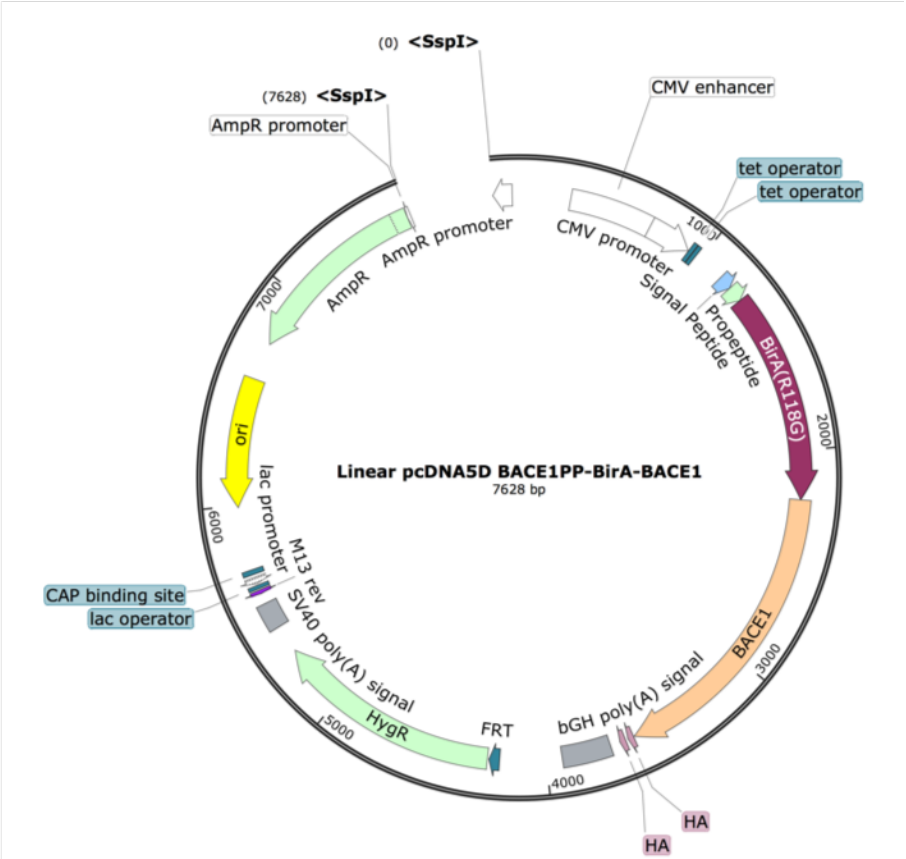

B

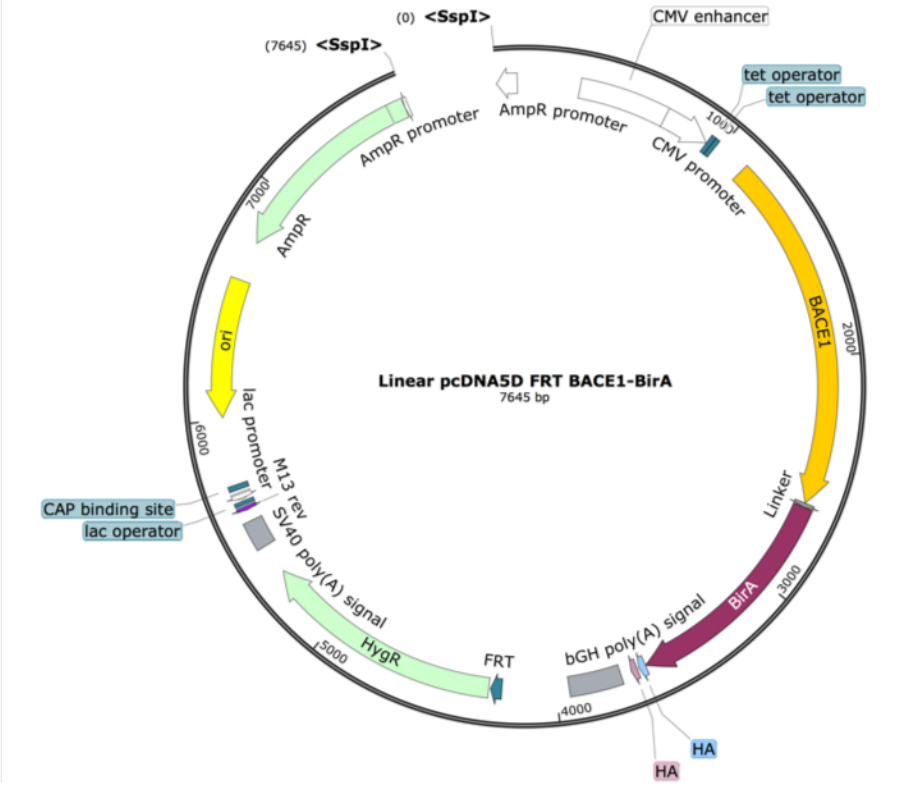

Figure 2.4 Plasmid maps of BACE1 fusion proteins (A) BirA-BACE1 and **(B)** BACE1-BirA fusion protein plasmids. Figures were created using SnapGene molecular biology software.

2.5.5 Colony PCR

Prior to miniprep, the 10 largest, separated (without satellite colonies) colonies were selected. Colonies were exposed to 50μl sterile H_2O in a clean microcentrifuge tube prior to addition to LB medium for miniprep. The cells were lysed in the H_2O by incubating the tubes to 95°C for 5 minutes. The lysates were then used as template DNA for a PCR reaction to detect BACE1. The protocol and primers used for this reaction are described in 2.2.3.

2.5.6 Miniprep

Overnight bacterial cultures were made from transferring the colonies into 2ml LB growth medium supplemented with 100μg/ml ampicillin. Cultures were incubated for 18 hours in a shaking incubator at 37°C and 220rpm. 1.5ml of the culture was miniprepped as instructed in the recommended protocol using a QIAGEN Plasmid Mini Kit. (QIAGEN; 12125) The remaining 500μl of bacterial culture was combined with 500μl sterile Glycerol and stored at -80°C as a glycerol stock.

2.5.7 Midiprep

Overnight bacterial cultures were made from stabs of glycerol stock or 1ml of miniprep culture in 200ml LB growth medium supplemented with 100μg/ml ampicillin. Cultures were incubated for 18 hours in a shaking incubator at 37°C and 220rpm. Midipreps were conducted as per the recommended protocol using a QIAGEN Plasmid Midi Kit. (QIAGEN; 12143) The pellet was resuspended in 100μl nuclease-free H2O. (Ambion; AM9939).

2.5.8 Linearisation

The purified pcDNA5D FRT BACE1-BirA(R118A) plasmid was linearised within the ampicillin resistance gene promotor region by SspI-HF (New England Biolabs; R3132S) restriction digest (Figure 2.4). The concentration of DNA within the sample was established through nanodrop microvolume spectrophotometer set to ‘DNA’. Purity was considered sufficient when the 260/280 ratio ≥1.9. 20μl of purified plasmid was retained and stored at -20°C. The remaining DNA was digested overnight at 37°C in a reaction mix containing: 20μg DNA, 1x CutSmart® buffer, 20U SspI-HF®, nuclease-free H2O to a total reaction volume

of 200μl. Following digestion, the restriction enzyme was denatured by heating the reaction mix to 65°C for 20 minutes. A sample of linearised plasmid was run on a 1% agarose gel alongside uncut control and 1kbp DNA ladder (Thermofisher Scientific; SM0311) to determine whether linearization was successful. (Figure. 2.5)

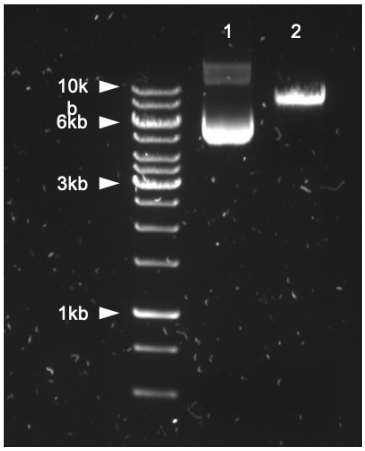

Figure 2.5 Gel of linearization digest product. Circular (lane 1) and linear (lane 2) pcDNA5D FRT BACE1-BirA(R118A) plasmid. pcDNA5D FRT BACE1-BirA(R118A) is approximately 7.6kbp in size and runs close to the 8kbp DNA marker.

2.5.9 Transfection

Cells were transfected using the FuGENE HD (Promega; E2311) transfection reagent. 3x 10cm dishes were seeded with $1x10^6$ or $0.5x10^6$ GT1-7 or HT-22 cells respectively and left to adhere overnight. The following day, the Fugene was allowed to warm to room temperature and Opti-MEM™ medium (Gibco; 31985070) supplemented with 100U/ml Penicillin-Streptomycin (Gibco, 15140122) was warmed to 37°C alongside the normal culture medium and sterile PBS. In a sterile tube the transfection mix contained 18μl of linear BACE1-BirA plasmid (containing 100ng/μl DNA), 423μl Opti-MEM medium and 36μl FuGENE HD. A control transfection mix was made containing 414μl Opti-MEM with 36μl FuGENE HD. The transfection mixes were incubated at RT for 15 minutes. The cells were washed with 2ml warm PBS and 10ml of fresh culture medium was added to each dish. After incubation, 415μl of transfection mix was added to two plates and an equal volume of the control mix to the third plate. Cells were incubated at 37°C, 5% CO_2 for 24 hours.

2.5.10 Proximity assay

After 24 hours the transfected cells were biotin loaded. Biotin was suspended in DMSO and diluted to 50mM in sterile H_2O. Biotin was aliquoted and stored at -20°C until required. To biotin load the cells an aliquot of biotin was heated to 65°C for 1hr to resuspend the precipitate. The transfected cells were washed three times with PBS warmed to 37°C and 10ml of warm culture medium added to the culture. When the biotin was in solution, 10μl was added to each dish. The cells were biotin loaded for 24 or 48 hours in a cell culture incubator. Untransfected cells were incubated for 48 hours.

Once biotin treated, cells were washed three times with warm PBS and lysed in 500μl Bio-ID lysis buffer. (table 2.1, page 49) Cells were scraped and lysis aided by pipetting. Lysates were incubated on ice for 15 minutes then cell debris was removed by centrifugation at 17,000g for 5 minutes. 50μl of soluble lysate was retained for western blot. In a LoBind microcentrifuge tube (Sigma; Z666505) 30μl per lysate of Streptavidin-sepharose beads (GE Healthare; 17511301) were washed in 300μl BioID lysis buffer. The beads were centrifuged at 2g for 5 minutes to sediment and washed with a further 300μl of BioID lysis buffer. This was removed and the remaining soluble lysate was added to the equilibrated beads. The soluble lysate was left on a rotator overnight at 4°C. Following incubation with streptavidin beads, the unbound fraction was removed. The beads were washed 5 times in 1ml lysis buffer followed by 5x 1ml washes with BioID digestion buffer (table 2.1, page 49); sedimenting between each wash by centrifugation. The washed beads were resuspended in 100μl of digestion buffer and 1μl 50mM trypsin gold (Promega; V5280) reconstituted in 50mM acetic acid. The digests were incubated overnight in a thermomixer at 37°C, 1000rpm. Peptides were recovered by centrifugation and transfer of the protein digest into a LoBind microcentrifuge tube using a sterile gel loading tip to minimise bead transfer. Digests were stored at -20°C until sent to an external facility for protein identification.

15μl of soluble lysate and unbound fraction was combined with 5μl of 4x sample buffer. These samples were then analysed by western blot for biotinylated

proteins using streptavidin-HRP antibody and for transfection efficiency using a HA-tag antibody.

2.5.11 Protein identification

Peptides of biotinylated proteins were identified through MALDI-TOF MS/MS and analysed using Mascot software. The identified peptides were compared to the Swiss-prot mouse database of known mouse proteins in order to identify BACE1 interactors. Peptides were assigned an ion score based on peptide abundance and probability of occurrence based on the mouse proteome database. Peptides with an ion score below 36 were discarded. Protein scores were determined as the sum of ion scores of all peptides identified.

Upon identification of proteins within a sample, the BACE1-BirA transfected lysates were compared to the control for each replicate. Any protein identified within the control was removed as a hit from that assay. The replicates were then compared to generate a list of proteins that were identified as hits in 2/3 replicates and 3/3 replicates. The 2/3 and 3/3 protein lists were then compared between 24hr and 48hr biotin loads to identify hits present in 3/3 at both time points and any proteins present in 2/3 replicates in both time points (representing a hit in at least 4/6 replicates). All of the protein hits were submitted for pathway analysis with the Reactome online pathway analysis program generating pathway hits at both 24 and 48 hour timepoints using over-representation analysis whereby software identifies enrichment of specific pathways within input data. This leads to the calculation of a probability score that uses the Benjamani-Hochberg method for FDR correction. Pathway topology mapping was also conducted whereby the interactions between proteins were considered. This method gives an indication of the proportion of a pathway that is present within the given hit list. The top 25 pathways were identified at both timepoints based on the FDR corrected over-representation probability score.

2.5.12 Cell Fixation

13mm cover slips were placed into a 12-well plate and sterilised with 1ml 70% ethanol for 15 minutes. The cover slips were washed with 1ml PBS and all liquid removed. The coverslips were treated with 100μl 0.1mg/ml PLL pipetted into the centre of the coverslip. The plate was covered and left for 1 hour. Following PLL

treatment the coverslips were washed with 1ml PBS and transfected GT1-7 SALK cells seeded at 75,000 cells/well in 500µl normal cell culture medium. The cells were allowed to adhere overnight at 37°C, 5% CO_2.

The following morning, all culture medium was removed and the cells were washed with 1ml ice-cold PBS. The cells were then treated with 500µl ice-cold 4% PFA for 15 minutes followed by washing with 1ml ice-cold PBS. Half of the plate was permeabilised by the addition of 0.1% Triton X-100 PBS for 5 minutes followed by washing in 1ml PBS. Coverslips were stored in PBS at 4°C for up to 1 week.

2.6 Leptin sensitivity experiments

2.6.1 Cell line generation

The pCneo-mObRb construct used to generate leptin sensitive cells was a kind donation from Yves Rouillé, Institut Pasteur de Lille. GT1-7 immortalised mouse hypothalamic and HEK 293 human kidney cells were used to generate stable cells lines overexpressing the mouse leptin receptor B isoform (mObRb). GT1-7 and HEK 293 cells were plated in 5 wells of a 6-well plate at $1x10^6$ and $0.5x10^6$ respectively. Cells were allowed to adhere overnight prior to transfection. Once adhered, the media were replaced with 3ml of warm normal culture medium. The FuGENE HD transfection reagent was allowed to come to room temperature and OptiMEM medium was warmed in a 37°C water bath. Once warm, transfection mixes were made according to table 2.20 and incubated at room temperature for 15 minutes. 125µl of transfection mix was added to each of the wells so that each plate contained 4 different ratios of FuGENE HD to DNA and a control well (table 2.20). Plates were incubated for 48 hours in a cell culture incubator. After transfection the cells were washed with warm, sterile PBS and 3ml of normal culture medium added to each well for 24 hours to allow cells to recover. Once recovered, 3ml of cell-specific selection medium containing G418 antibiotic was added to each well (table 2.5). Selection medium was changed daily until all of the cells in the control well had died. The surviving cells from each transfection were transferred into a T25 and cultured in cell-specific maintenance medium (table 2.5) until confluent. The cells were then maintained in T75 flasks in the maintenance medium and stocks frozen for storage in liquid nitrogen.

	Ratio FuGene HD: DNA				
	4:1	**3:1**	**2:1**	**1:1**	**4:0 (Control)**
Opti-MEM	135µl	138µl	141µl	144µl	138µl
DNA (100ng/µl)	3µl	3µl	3µl	3µl	-
FuGENE HD	12µl	9µl	6µl	3µl	12µl

Table 2.20 Transfection mix composition for each Fugene HD:DNA ratio tried in the transfection of cells with pCneo-mObRb

2.6.2 Leptin dose response in amyloid exposed cells

β-amyloid$_{1-42}$ and Scrambled β-amyloid$_{1-42}$ (Bachem; 4035885, 4064853) control peptides were made into 0.1mg/ml stock solutions in DMSO and stored at -20°C until required. Peptides were diluted in sterile ddH_2O to stock concentrations of 11nM and 100nM. GT1-7 mObRb cells were plated into 2 6-well plates at a seeding density of 1x10^5 cells/well and allowed to adhere overnight. HEK 293 mObRb cells were plated into 2 T25 flasks at 1.5x10^5 cells/flask and allowed to adhere overnight. The following day Aβ$_{1-42}$ and scrambled Aβ$_{1-42}$ (ScrP) medium were made by transferring maintenance culture medium into a T25 flask and adding the peptide at a 1:1000 dilution to a final concentration of either 11pM or 100pM peptide. Serum-free medium was also prepared in the same way. Cells were washed twice with warm PBS and the amyloid medium added to the well or plate. Cells were transferred back to the cell culture incubator for 2 days. All amyloid media were stored in a T25 in the cell culture incubator for the duration of the experiment. After 2 days, the GT1-7 cell medium was replaced with fresh amyloid medium. The HEK 293 mObRb cells were trypsinised as described in section 2.1.5 and transferred into a T75 flask in fresh amyloid medium. The GT1-7 mObRb cells were incubated for a further 2 days in the cell culture incubator after which the amyloid medium was refreshed once more. The HEK 293 mObRb were incubated for 2 days and then plated into sterile 10cm dishes at 1.5x10^5 cells/dish. The cells were placed back into the cell culture incubator overnight. The following morning the cells were washed with warm sterile PBS and the culture medium replaced with serum-free medium containing amyloid. The 11pM amyloid exposed cells were incubated in serum-free medium for 4 hours. At 100pM amyloid the cells were serum starved for 2 hours after which all cells were stimulated with leptin (R&D systems; 498-OB). Stocks of leptin were made at 0.5mM, 1mM, 2mM and 3mM by dilution in sterile PBS. Stocks were stored at -

20°C until required and defrosted in the cell culture hood shortly before requirement. Leptin was added to the cell medium at final concentrations of 0.5nM, 1nM, 2nM and 3nM as well as a PBS control. The plates were swirled to distribute the leptin and the cells were placed back into the cell culture incubator for 30 minutes. After stimulation, the cells were prepared for western blot analysis as described in section 2.1.4.

Chapter 3

Metabolic and inflammatory changes in the cerebral cortex of BACE1 knockout mice

3.1 Introduction

BACE1 is the rate limiting step in the production Aβ from APP. In healthy individuals, BACE1 expression is low and its contribution to APP processing is small. It is supposed that with onset of AD, α-secretase processing of APP is reduced and BACE1 expression and activity increases leading to overproduction of Aβ and the initiation of neurodegeneration with it. Despite our understanding of APP processing in AD, the cause of the increase in BACE1-mediated cleavage is still unknown. BACE1 activity is influenced by stress pathways such as the up-regulation of NF-κB signalling as an activator of the innate immune response, oxidative stress, hypoxia and both hyper and hypoglycaemia. (Chen et al., 2012; Guglielmotto et al., 2009; Mouton-Liger et al., 2012; O'Connor et al., 2008) This leads to the hypothesis that changes in BACE1 expression is a stress response and that chronic stresses such as obesity, diabetes and chronic inflammation may lead to persistently increased BACE1 activity.

Both obesity and type 2 diabetes are known risk factors for AD with suggestions that insulin resistance within the brain may be a major contributing factor for this dementia (reviewed: Neth & Craft (2017)). However the order in which these events occur has not been established. BACE1 knockout mouse models have been shown to present resistance to diet-induced obesity, retention of insulin sensitivity with HFD and no impairment of glucose homeostasis in contrast to wild-type littermates (Meakin et al., 2012; Plucińska et al., 2016). BACE1 expression has also been shown to increase with chronic HFD suggesting that BACE1 upregulation may be a response to the stress of nutrient excess.

This study aimed to identify whether changes in BACE1 expression lead to changes in metabolic and inflammatory markers. It utilised two transgenic BACE1 animal models; a global BACE1 KO and a forebrain specific BACE1 KI with the human BACE1 gene added under the CamKII promoter (Harrison et al., 2003; Plucinska et al., 2014). Samples of the cerebral cortex were analysed for protein and mRNA changes in known markers of metabolic signalling and inflammation.

3.2 Results

3.2.1 Changes in metabolic and inflammatory factors with BACE1 expression

Cortical samples from NC fed, WT BACE1 Knock-out (KO) and BACE1 knock-in (KI) non-fasted mice were analysed by immunoblot and RT-PCR for metabolic and inflammatory markers. Western blot showed no difference in PI3K p85 or PKB expression (Figure 3.1A and B respectively) but serine phosphorylation of PKB was significantly increased in the BACE1 KI model. Gene expression analysis also revealed a trend towards a 50% decrease in SOCS3 mRNA in the BACE1 KI model. This result was not significant however this is likely to be due to low numbers of replicates. (Figure 3.2). No differences were observed in protein expression of GSK3α or GSK3β nor in their tyrosine phosphorylation (Figures 3.3E, 3,3F, 3.3A and 3.3B). However, serine phosphorylation of both GSK3α and GSK3β was significantly increased in the BACE1 KI mice with GSK3α exhibiting a 2-fold and GSK3β a 3-fold increase in phosphorylation compared to WT controls. The BACE1 KO mice showed a trend towards a 50% reduction in serine phosphorylation of both GSK3α and GSK3β but this was not significant- most likely due to the low number of replicates (Figures 3.3C and 3.3D). Serine phosphorylation of both GSK3 α and β has been shown to inhibit GSK3 activity therefore these results suggest reduced GSK3 activity in in the BACE1 KI mice (Fang et al., 2000; Sutherland, Leighton, & Cohen, 1993). Kinase assay (conducted by Prof. Calum Sutherland, University of Dundee) on affinity purified cortical GSK3α and GSK3β revealed no significant changes in GSK3 activity. However, a trend is apparent towards reduced GSK3β activity in the BACE1 KI and increased GSK3β activity in the BACE1 KO. This trend is not present in GSK3α activity despite similar changes in phosphorylation between the two isoforms. (Figure 3.4A and 3.4B)

Inflammatory markers neutrophil elastase and IKBα were unchanged between the BACE1 models but Caspase 1 protein expression was significantly elevated in the BACE1 KI mice. (Figures 3.5B, 3.5C, 3.5D and 3.5A respectively) No changes were observed in NF-κB proteins p105, cREL or p85 (Figures 3.6A, 3.6B and 3.6C) Gene expression analysis revealed no significant changes in inflammatory cytokines IL-1β, IL-18 or IL-6 (Figures 3.7A. 3.7B and 3.7C).

However, a trend was observed towards increased IL-6 mRNA expression in both the BACE1 KO and BACE1 KI mice. Interestingly, caspase 1 mRNA expression was unchanged despite the observed increase in protein expression (Figure 3.7D). A trend towards increased NLRP3 mRNA expression was observed in the BACE1 KI, however this was not significant (Figure 3.7E). TNFα mRNA expression was significantly increased in the BACE1 KI cortex compared to the BACE1 KO. The KI showed a trend towards elevated mRNA compared to WT and the KO a trend towards reduced TNFα mRNA but neither were significant. (Figure 3.7F)

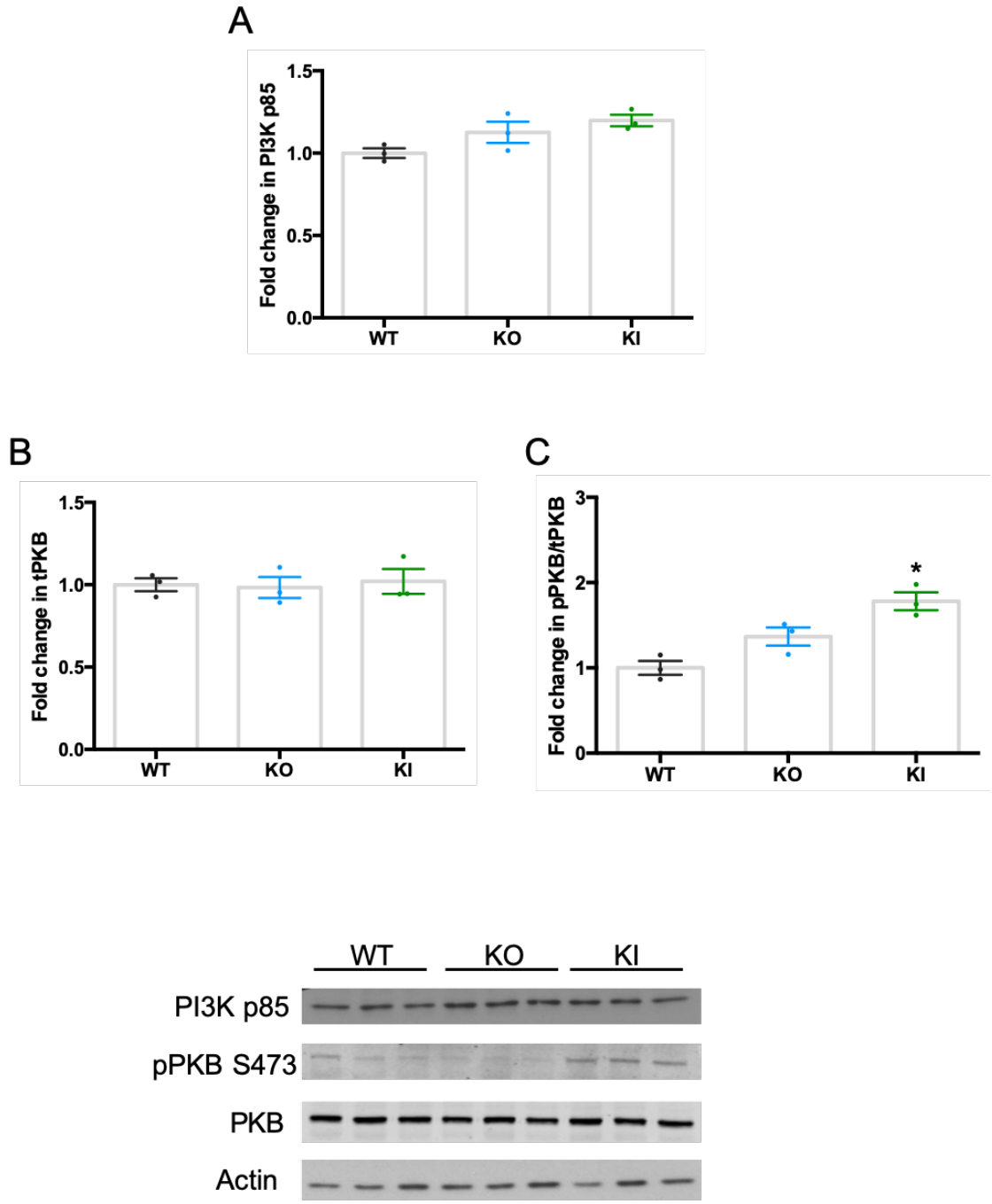

Figure 3.1 Expression and phosphorylation of PI3K pathway proteins with BACE1 KO and KI. Relative change in PI3K P85 (**A**), PKB (**B**) and serine pPKB (**C**) compared in BACE1 KO and forebrain specific BACE1 KI cortices compared to WT controls. No change was present in total PKB of PI3K expression. One-way ANOVA by Kruskall-Wallis test identified significantly increased pPKB in the BACE1 KI cortices compared to WT controls but not the BACE1 KO. n=3 per group. Individual data points indicate the range of data. Standard error indicated by error bars, * = $p<0.05$

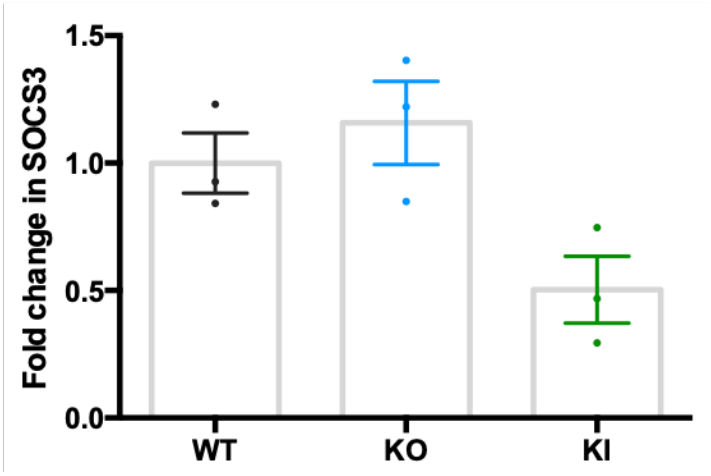

Figure 3.2 Gene expression of SOCS3 with BACE1 KO and KI. mRNA expression of the SOCS3 gene in the cortical tissues of forebrain specific BACE1 KI mice compared to both WT and BACE1 KO tissues. One-way ANOVA by Kruskall-Wallis test revealed no significant change in SOCS3 gene expression between the WT and BACE1 KO mice but a trend towards reduced SOCS3 was observed in the BACE1 KI compared to both the WT and KO. n=3 per group. Individual data points indicate the range of data. Standard error indicated by error bars, * = $p<0.05$

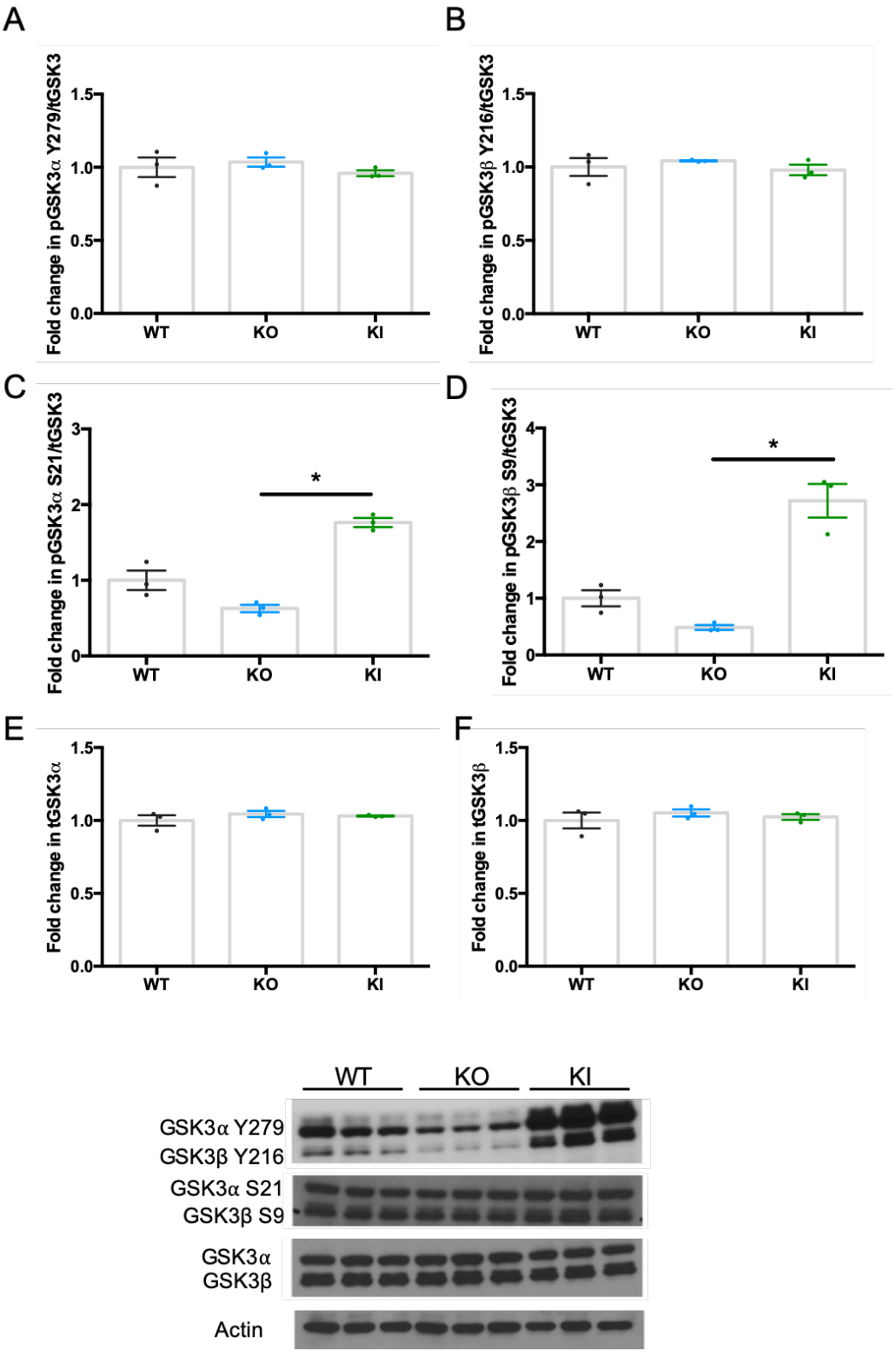

Figure 3.3 Expression and phosphorylation of proteins with BACE1 KO and KI. Protein expression of total GSK3α and GSK3β in the cortices of WT, BACE1 KO and forebrain specific BACE1 KI mice. (**E**, **F**) as well as phosphorylation states at both serine (**C**,**D**) and tyrosine (**A**,**B**) sites. One-way ANOVA by Kruskall-Wallis test revealed neither total GSK3α and GSK3β nor tyrosine phosphorylation changed with BACE1 expression. Serine phosphorylation at S21 and S9 of GSK3α and GSK3β respectively was significantly increased with BACE1 KI compared to BACE1 KO. BACE1 KO cortices exhibited a trend towards reduced phosphorylation at serine sites but this was not significant. n=3 per group. Individual data points indicate the range of data . Standard error indicated by error bars, * = $p<0.05$

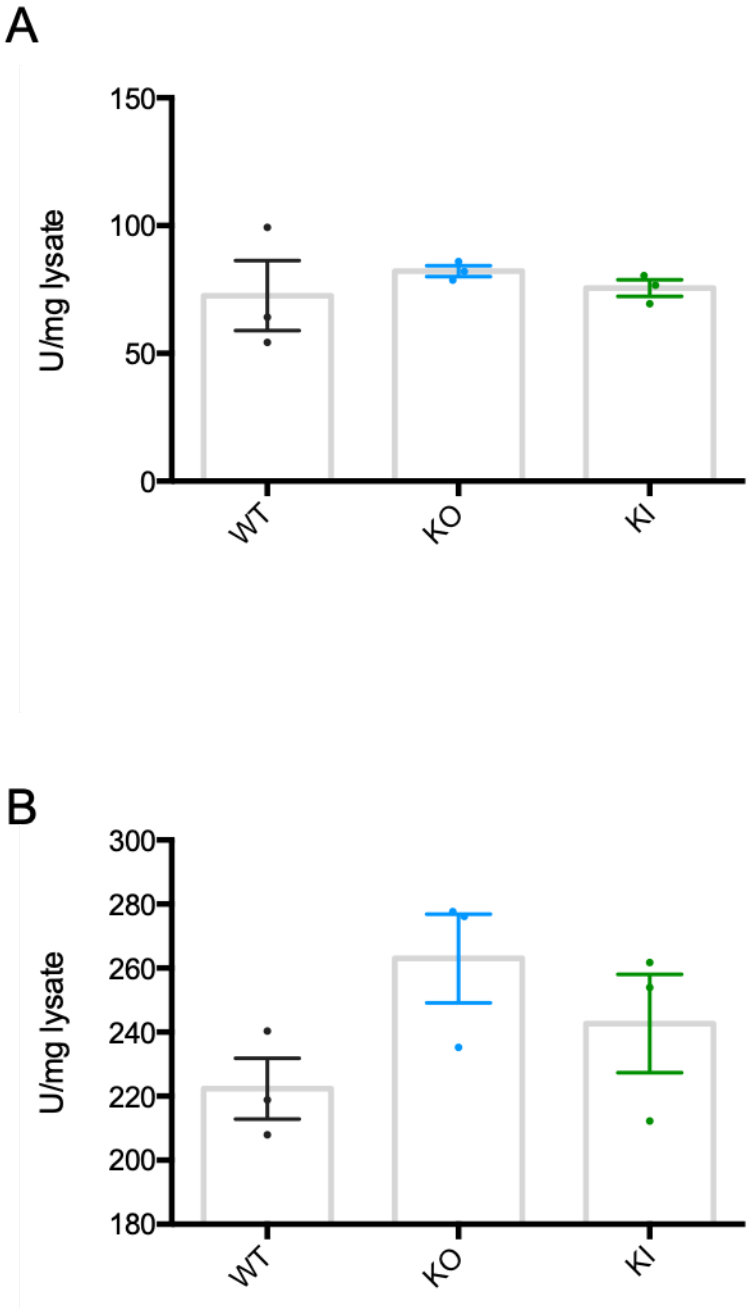

Figure 3.4 Activity of GSK3 proteins with BACE1 KO and KI. Kinase activity of affinity purified GSK3α and GSK3β from cortex lysates of WT, BACE1 KO and forebrain specific BACE1 KI tissues. Despite increases in serine phosphorylation with BACE1 KI, One-way ANOVA by Welch's test and revealed no difference was seen in GSK3α (**A**) or GSK3β (**B**) activity. n=3 per group. Individual data points indicate the range of data. Standard error indicated by error bars.

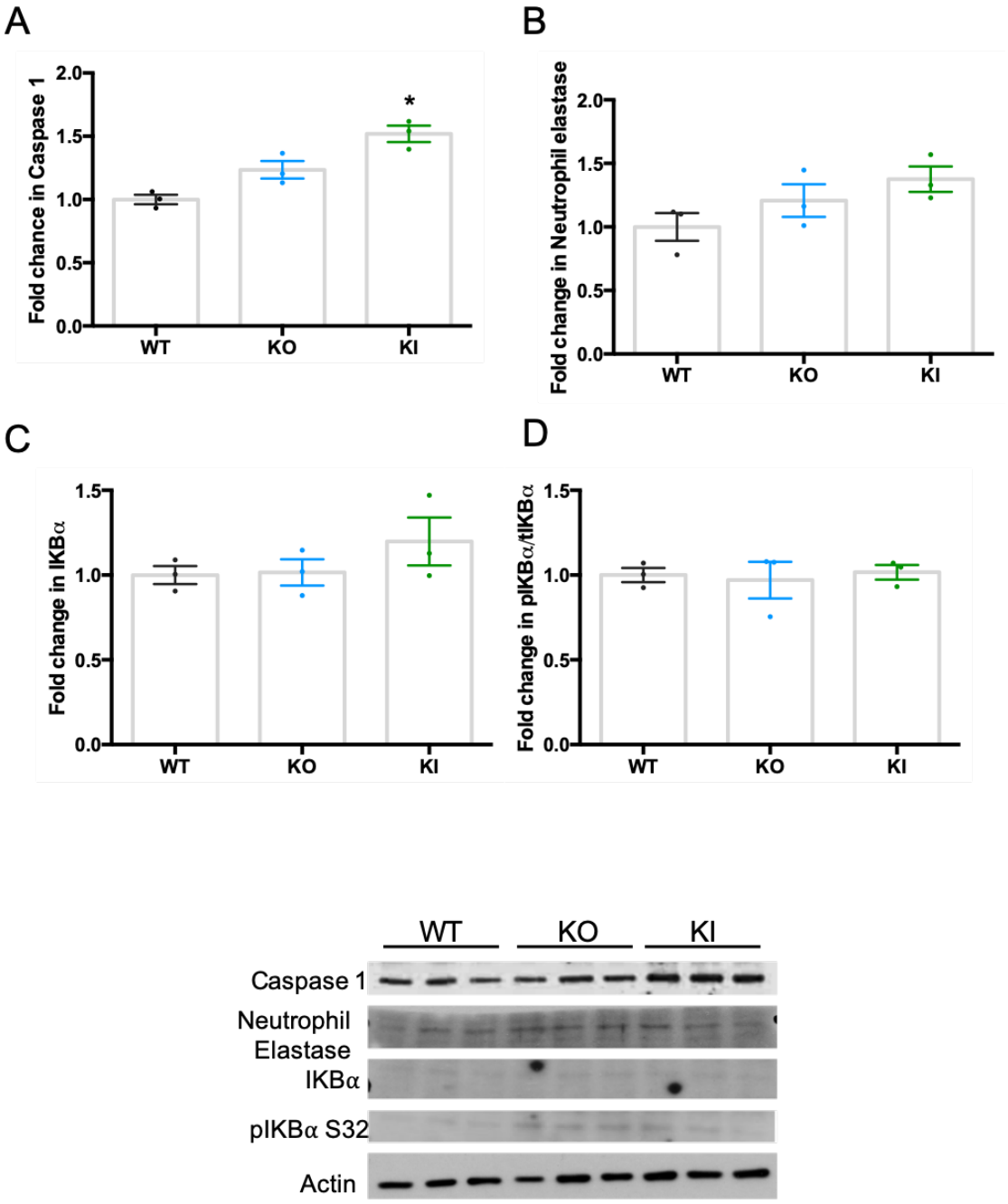

Figure 3.1 Expression and phosphorylation of immune proteins with BACE1 KO and KI. Protein expression of cortical immune markers: Caspase 1 (**A**), Neutrophil elastase (**B**) and IKBα (**C**) as well as phosphorylated IKBα (**D**). One-way ANOVA by Kruskall-Wallis test revealed significantly increased Caspase 1 expression with forebrain specific BACE1 KI but no change with BACE1 KO. No other immune markers showed changes with BACE1 expression. n=3 per group. Individual data points indicate the range of data. Standard error indicated by error bars, * = $p<0.05$

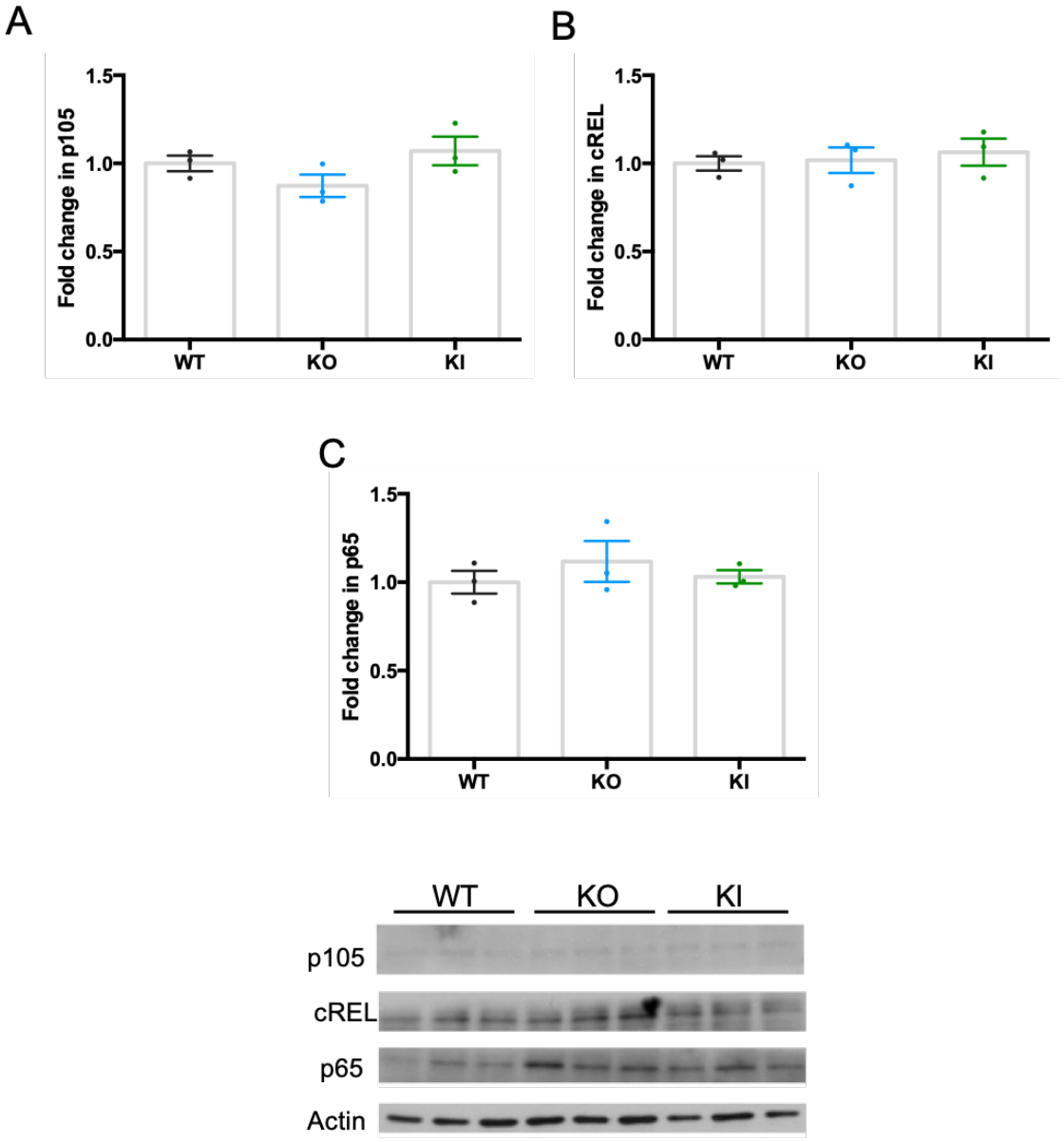

Figure 3.2 Expression and phosphorylation of NF-κB pathway proteins with BACE1 KO and KI. Changes in protein expression of p105 (**A**), cREL (**B**) and p85 (**C**). One-way ANOVA by Kruskall-Wallis test revealed no significant changes in these proteins with BACE1 KO or forebrain specific BACE1 KI in the cortex. n=3 per group. Individual data points indicate the range of data. Standard error indicated by error bars.

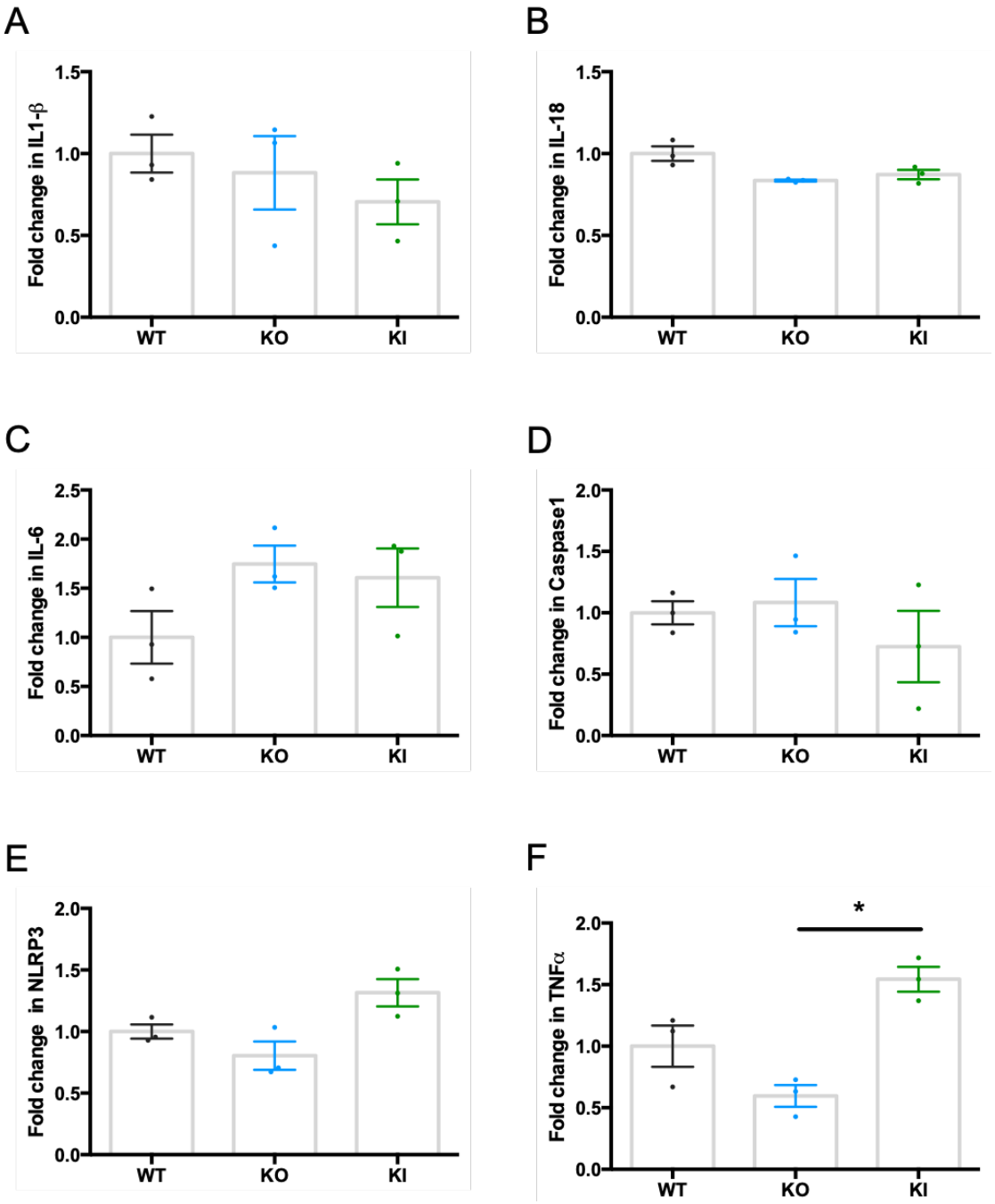

Figure 3.3 Changes in gene expression of immune proteins with BACE1 KO and KI. RT PCR in the cortex of WT, BACE1 KO and forebrain specific BACE1 KI of inflammatory markers. One-way ANOVA by Kruskall-Wallis test revealed no changes in gene expression of inflammatory cytokines IL1-β, IL-18 or IL-6 (**A**, **B** and **C** respectively). Caspase 1 and NLRP3 mRNA were also unchanged with BACE1 expression. (**D** and **E** respectively) TNFα mRNA was significantly increased in the BACE1 KI cortex compared to BACE1 KO with a trend towards greater gene expression compared to WT controls. BACE1 KO exhibited a trend towards reduced TNFα compared to WT. (**F**) n=3 per group. Individual data points indicate the range of data. Standard error indicated by error bars, * = $p<0.05$.

3.3 Discussion

3.3.1 BACE1 expression regardless of diet influences expression of metabolic and inflammatory markers

This study was conducted on stored cortical samples from female, non-fasted WT, BACE1 KO and BACE1 KI mice. These samples were used as they had not been utilised in previous studies therefore remained in -80 storage as whole tissue samples. This study permitted identification of changes in cortical metabolic and inflammatory status as a product of altered BACE1 expression. As changes in insulin signalling within the brains of AD patients has been well documented, preliminary data included analysis of proteins involved in the insulin signalling pathway to determine the effects of BACE1 on signal transduction in cortical samples (Figure 3.8). Changes in PKB have been previously published with BACE1 KO mice exhibiting reduced pPKB with insulin stimulation in liver tissue but no change compared to WT when unstimulated, therefore our data support this previous finding (Meakin et al., 2012). It has also been identified that BACE1 KI mice exhibit a trend toward increased pPKB compared to WT in whole brain lysates as observed here (Plucińska et al., 2016). GSK3 data are contrary to previous BACE1 KI data that indicate that the KI line exhibits a trend towards reduced GSK3β expression in whole brain lysate whereas data from this study shows a marked increase in both GSK3α and β (Plucińska et al., 2016). However, this discrepancy may be due to regional changes as opposed to whole brain or due to fasted vs non-fasted tissues being used. Previous studies have indicated no difference in SOCS3 mRNA expression between BACE1 KO mice and WTs which is supported by data in this study (Meakin, Jalicy, et al., 2018). Whilst no significant change was observed in PI3K p85 subunit or PKB expression in either BACE1 model, serine phosphorylation of PKB, a downstream effector of PI3K pathway activation, was significantly increased in the BACE1 KI mice. As these mice were not fasted it cannot be determined whether these mice have increased basal phosphorylation of PKB thereby suggesting increased sensitivity to insulin or whether they are exhibiting a greater post-prandial insulin response and therefore better glucose stimulated insulin secretion. As no data have been published with regards to plasma insulin levels or insulin tolerance in the BACE1 KI mice, this cannot be determined but increased PTP1B and IRβ contribute to the idea of central insulin resistance in these mice (Plucińska et al., 2016). Further

suggestion towards dysfunctional insulin signalling came from a significant reduction in SOCS3 gene expression in the BACE1 KI mice. This suggests reduced inhibition of IRS which could be an indication of improper regulation of insulin signalling in this model. This is further corroborated by substantially elevated serine phosphorylation of both GSK3α and GSK3β in the BACE1 KI mice. This effect was accompanied by a trend towards reduced serine phosphorylation in the BACE1 KO mice as expected due to the inhibitory nature of this phospho-site. However, this effect was not significant. Whilst many of these changes may be considered as indicators of altered insulin signalling with BACE1 expression, it must be noted that changes to PKB, GSK3 and SOCS3 are also part of cytokine signalling such as leptin and IL-6, acting through their specific receptors. As such, these changes may in fact be independent of the insulin signalling pathway.

These data indicated that BACE1 may play a role in GSK3 inhibition. To confirm the effects of BACE1-mediated serine phosphorylation of GSK3 on activity, a kinase assay was performed which showed that whilst serine phosphorylation suggests decreased activation of GSK3, this had no effect on GSK3α or GSK3β activity towards a muscle glycogen synthase (GS2) isoform target peptide in the BACE1 KI mice. However, decreased S9 phosphorylation led to a trend towards increased GSK3β activity. This change was not present in GSK3α. Due to this, questions must be raised as to the physiological effects of the differences in phosphorylation in this pathway. It may be that activity assay using a known brain substrate may provide more information about the inhibitory nature or substrate selectivity of serine phosphorylation of GSK3 within the brain. GSK3β inhibition decreases BACE1 expression and activity through NFκB signalling (Ly et al., 2013) but no evidence indicates a direct role for BACE1 regulation of GSK3 activity (Avrahami et al., 2013). However, GSK3 characterisation in 5xFAD mouse models overexpressing mutant APP and PS1 showed increased activity of both GSK3α and β suggesting that elevated $A\beta_{1-42}$ may increase GSK3 activity (Avrahami et al., 2013). Furthermore, oligomeric amyloid species have been identified as activators of GSK3β in transgenic APP mouse primary neurons (DaRocha-Souto et al., 2012; Kirouac, Rajic, Cribbs, & Padmanabhan, 2017). However, these studies identify GSK3 activation through decreased serine phosphorylation- while this study indicated that GSK3 phosphorylation may not

be a good indicator of catalytic activity. GSK3 expression and activity is known to be elevated in the brains of patients with AD including the hippocampus and cerebral cortex (Blalock et al., 2004; Leroy, Yilmaz, & Brion, 2007). Furthermore, GSK3 is known to phosphorylate the AD-associate protein Tau and contribute to the hyperphosphorylation that leads to NFT formation (Sperbera, Leight, Goedert, & Lee, 1995).

It must also be considered that whilst both the BACE1 KO and BACE1 KI transgenic lines have been bred into the C57bl/6J mouse line, the BACE1 KO mice had been back-crossed with 129P mice therefore some genetic differences are likely to be present. Without the presence of a WT control for the BACE1 KI line, it was not possible to determine whether these effects are the result of background genetic differences, environmental factors or BACE1 expression.

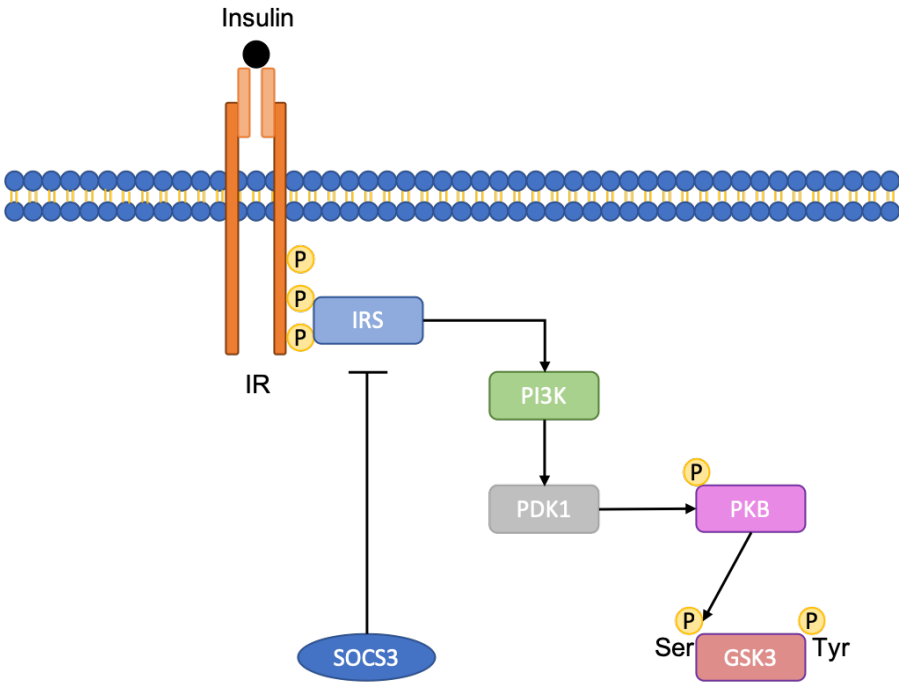

Figure 3.8 Simplified schematic of the insulin signalling pathway. Insulin binds to homodimeric insulin receptor (IR) at the plasma membrane. This brings about autophosphorylation of IR and binding of insulin receptor substrate (IRS). IRS phosphorylation activates the PI-3 kinase (PI3K) pathway by which PI3K phosphorylates Phosphoinositide dependent kinase 1(PDK1) which, in turn, phosphorylates protein kinase B (PKB/AKT) at serine 473. Activation of PKB then leads to phosphorylation of glycogen synthase kinase 3 (GSK3) at serine 21 or serine 9 for GSK3α or GSK3β respectively. SOCS3, transcribed as a result of JAK-STAT pathway activation, inhibits further insulin signalling by competitively inhibiting IRS binding to IR.

Differences were also observed in inflammatory markers. Protein expression of neutrophil elastase remained unchanged indicating no difference in neutrophil

activation in the cortices of these mice. Whilst neutrophils are prevented from entering the brain in healthy individuals by the presence of the BBB, it has been shown that changed in BBB integrity as a result of inflammation results in circulating immune cell entry into the CNS (Joice et al., 2009). Neutrophil invasion has been shown to occur in the brains of AD model mice and humans where they target to amyloid plaques and produce neutrophil extracellular traps (NETs)(Zenaro et al., 2015). These traps are an anti-microbial response that result in tissue damage when activated in a sterile environment and a key component to their formation is chromatin unravelling by neutrophil elastase (Papayannopoulos, Metzler, Hakkim, & Zychlinsky, 2010).

The BACE1 KI mice exhibited increased Caspase 1- a marker of innate immune response- compared to WT mice. Caspase 1 is a key protease in the NLRP3 inflammasome pathway and is responsible for the maturation and release of pro-inflammatory cytokines IL-1β and IL-18 (Winkler & Rösen-Wolff, 2015). Furthermore, Caspase-1 expression and NLRP3 activation has been shown to be elevated in the brains of AD patients whilst Caspase-$1^{-/-}$ and $NLRP3^{-/-}$ APP mice are protected from cognitive deficits (Heneka et al., 2013). In addition to this, microglia derived ASC specks (adaptor protein to NLRP3) have been suggested to seed amyloid deposition (Venegas et al., 2017). However, as this result was not accompanied by a change in Caspase 1 mRNA, this result should be treated with caution. No other changes in inflammatory markers were identified including regulators and members of the NF-κB signalling pathway: IKBα, p105, cREL and p65. Inflammatory cytokine IL-1β and IL-18 mRNA were unaffected by BACE1 expression and inflammasome NLRP3 mRNA was unchanged. IL-6 mRNA expression exhibited a trend towards increasing in both the BACE1 KO and BACE1 KI mice. This may be due to both the pro- and anti-inflammatory nature of IL-6 which may be dependent on the method of IL-6 pathway activation. An assay of soluble IL-6 may provide insight into the pro-inflammatory pathway activation of IL-6 (Scheller, Chalaris, Schmidt-Arras, & Rose-John, 2011). No change in TNFα mRNA was apparent between the BACE1 transgenic mice and WT controls. However, TNFα was significantly increased in the BACE1 KI mice compared to BACE1 KO. There were also trends towards elevation TNFα in the KI compared to WT and reductions in the KO mice compared to WT. As TNFα is a potent NF-κB pathway activator, it is somewhat

surprising that increased transcriptional regulation of TNFα did not result in changes in NF-κB proteins. However, it may be that sub-cellular fractionation would be required for detailed insight into NF-κB as these data were taken from total lysates and represent both cytosolic and nuclear proteins. Alternatively, in this instance TNFα may be exerting effects through an TNFR1- an apoptotic pathway that does not encompass NF-κB and signals via caspases to induce cell death mechanisms. TNFα has been shown to be elevated in AD brains as a result of increased microglial activation, leading to neurotoxic effects, possibly through glutamate release (Takeuchi et al., 2006). Furthermore, HFD has been shown to increase TNFα in muscle and adipose tissues (Borst & Conover, 2005). Therefore, it may be that BACE1 may contribute to this effect in both circumstances. Once again, the genetic background of these mice must be considered, as it may be that the BACE1 KI line exhibit higher basal TNFα production.

3.3.2 Conclusions

These data indicate that BACE1 expression alone can contribute to changes in metabolic signalling and inflammation without the presence of an environmental stressor such as dietary excess. Whilst elevated phosphorylation of both PKB and GSK3 and reduced SOCS3 suggest that central increase in BACE1 expression contributes to PI3K signalling activation, activity assay of GSK3 indicated that phosphorylation of these proteins is not necessarily indicative of activation. As such, further experiments are required to identify whether BACE1 KI mice do exhibit increased PI3K activation and whether this is linked to insulin sensitivity.

Changes in inflammatory markers between the models proved inconsistent as the results do not indicate clear activation of specific pathways. This provides little evidence to suggest whether inflammatory pathways are influenced by BACE1 expression. However, the changes in metabolic markers suggest a role for BACE1 regulation of energy homeostatic mechanisms within the brains of these mouse models. This provided sufficient evidence for proteomic analysis to be conducted of brain tissues between these models. The addition of HFD to the study allowed the determination of the effects of chronic dietary stress, as it is known that chronic HFD leads to increased BACE1 expression which may be a

factor towards the increased risk of AD with obesity (Meakin et al., 2012). It is known that HFD leads to chronic inflammation both centrally and peripherally, oxidative and ER stress and central metabolic dysfunction through both leptin and insulin resistance (Cakir et al., 2013; Meakin, Jalicy, et al., 2018; Stępień et al., 2014; Thaler, Guyenet, Dorfman, Wisse, & Schwartz, 2013). All of which are also observed in AD and contribute to cognitive decline (De Felice & Ferreira, 2014; McGrath et al., 2001; Meakin, Mezzapesa, et al., 2018; Siegel, Bieschke, Powers, & Kelly, 2007). A study was therefore designed to offer insight into the contributions of BACE1 to these effects and determine whether BACE1 is part of their contributions to cognitive decline.

Chapter 4

Effects of HFD and different levels of BACE1 expression on the brain proteome

4.1 Introduction

This project intended to shed light on the pathway/s through which dietary stress increases the risk of AD. Here it was hypothesised that chronic exposure to stresses- such as dietary stress by way of prolonged HFD- may contribute to changes in BACE1 activity and targeting within the brain (Meakin et al., 2012; Meakin, Jalicy, et al., 2018; Plucińska et al., 2016). Furthermore, evidence (as shown in chapter 3) indicate that BACE1 expression alone may lead to changes in metabolic signalling the brain. It known that nutritional excess and HFD lead to chronic inflammation, hyperlipidemia and glucose dyshomeostasis as well as increased BACE1. Therefore, changes in BACE1 expression may provide a link between dietary stress and these effects.

This proteomic study was designed to investigate whether dietary induced increases in BACE1 expression leads to changes in the brain proteome. Whilst in previous studies dietary stresses employed a 20-week HFD to induce metabolic disease within the animals; concerns over the survival of the BACE1 KI mice for this duration of time led to a shortening in the dietary intervention to 12 weeks (Personal communication; Platt lab, University of Aberdeen).

Protein hits were analysed for possible BACE1-dependent changes driven by nutritional excess. Two methods of analysis were conducted on the proteomic data. Method 1 produced more, less statistically robust hits through a less stringent statistical method. This method used median sweep normalisation and hits were initially identified by volcano plot of protein reporter ion intensities- cumulative signal strength of identified peptides assigned to a protein. In order to increase the number of proteins identified, proteins were grouped (‘binned’) by ratio of reporter ion intensities as described in section 2.3.4. Ratios were represented by histogram and proteins with a ratio outwith two standard deviations of the median were considered significant. This threshold was chosen as Gaussian distribution of data indicate that points greater or less than two standard deviations of the median represent a statistical confidence of 95% in the probability that the protein hit is different between groups. As this method of hit identification is much less stringent it will be referred to hereon as ‘semi-quantitative analysis’. (Figure 4.1) Method 1 analyses were conducted by Dr Sara

Ten-Have of the Fingerprints facility (University of Dundee). Method 2 applied the most stringent statistical approach in a fully quantitative analysis in order to determine the most statistically significant hits, this analysis was conducted by Dr Michele Tinti (University of Dundee) and incorporated the comprehensive method of normalisation tailored to isobaric labelling methods- CONSTANd (Maes et al., 2016). This method of analysis also incorporated bias such as changes in conditions between MS runs and technical errors and will be referred to as quantitative analysis.

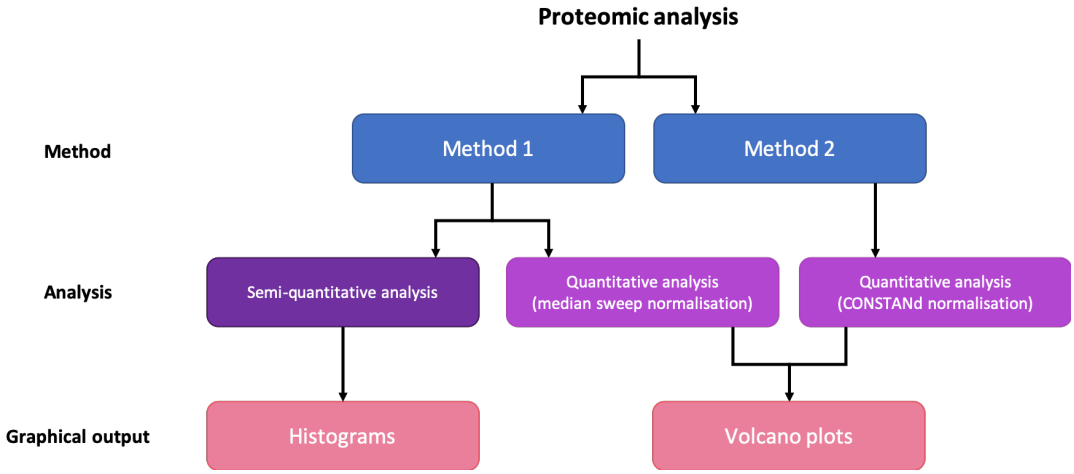

Figure 4.1 Flow diagram of proteomic data analysis

4.2 Results

4.2.1 Comparison of Wild-type mouse lines

As BACE1 KO breeding resulted in a low yield of KO mice, it was not possible to include a KO NC group within this study. Due to limitations in the number of samples allowed by TMT labelling kits it would not have been possible to include this group within the proteomics analysis and for this reason BACE1 KI mice were not used in proteomics either. However, these tissues were utilised in validation attempts therefore wild-type controls from both the BACE1 KO (WT[KO]) and BACE1 KI (WT[KI]) mouse lines were compared for metabolic phenotype. The mice began their dietary challenge at 8 weeks and weights were taken weekly in order to determine their weight gain in response to HFD. After 12 weeks of dietary intervention, mice were fasted overnight prior to culling and tissue harvest. WT mice from both lines exhibited comparable weekly weights over the 12-week

dietary intervention on both the NC and HFD. (Figure 4.2A) However, WT[KI] mice were consistently heavier than WT[KO] mice and a significant difference in weight between the two was observed at the end of the study (Figure 4.2B). This difference was not observed between the mouse lines on NC diet. Weight change (calculated as weight (g)- weight at 12 weeks of age (g)) was comparable between the two WT lines on both diets over the 12 weeks (Figure 4.2C) and no significant difference was observed in % weight gain between animal lines at the end of the study (Figure 4.2D)

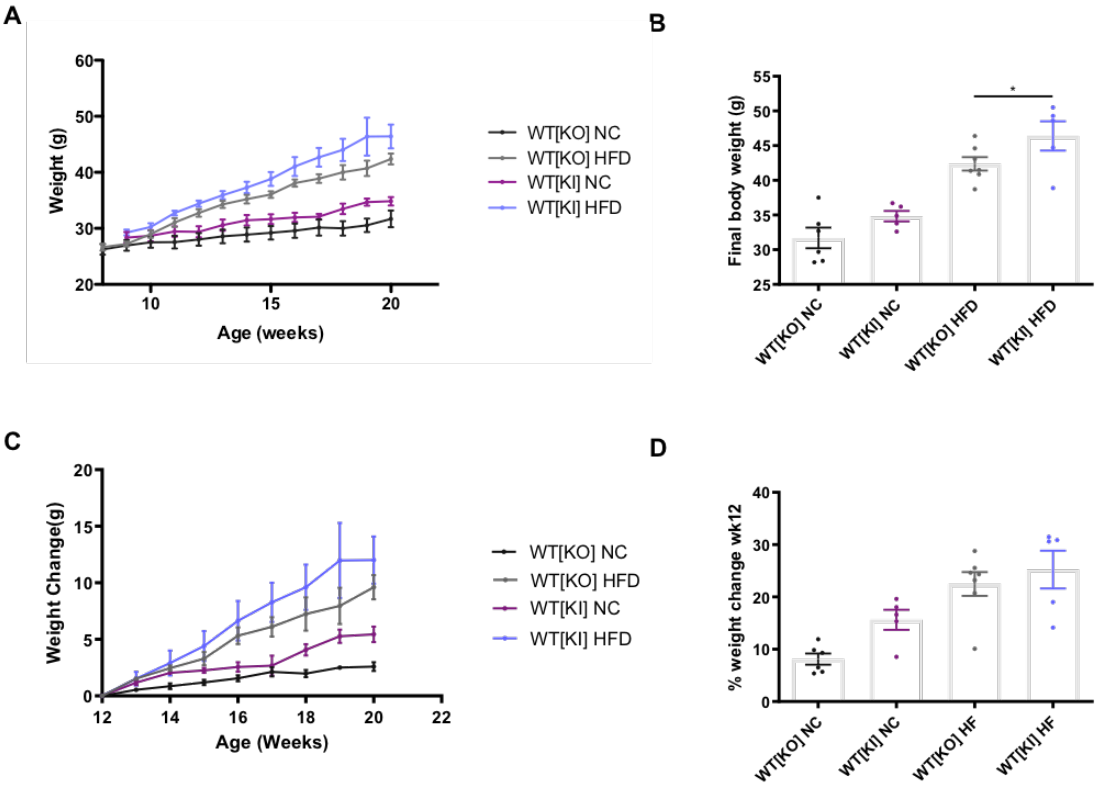

Figure 4.2 Comparison of Wild-type mice of the BACE1 KO line with BACE1 KI line when challenged with 12 weeks of HFD or normal chow. **A**) Body weight over 12-week dietary intervention. **B**) Final body weight after 12-week dietary intervention indicated a significant difference with both genotype and diet with grouped 2-way ANOVA. ($p = 0.0076$, $p < 0.0001$ respectively) Bonferroni's multiple comparison test identified a significant difference between the genotypes on HFD. **C**) Body weight change from 12 weeks of age to the end of the study **D**) Percentage body weight change after 12 weeks of dietary intervention compared to 12 weeks of age. Grouped 2-way ANOVA identified significant differences in percentage body weight change with both genotype and diet ($p = 0.0073$, $p < 0.0001$ respectively) but no significant differences were identified with multiple comparison. n=5-7 per group. Individual data points indicate the range of data.

4.2.2 Weight gain in BACE1 KO and BACE1 KI models with HFD

Mice were weighed weekly in order to monitor the effects of HFD in both the WT mice and determine how the BACE1 genotype influences the response to dietary stress. BACE1 KI mice showed comparable weights to WT mice on HFD whilst WT mice on NC were consistently lighter than their HF counterparts. Whilst BACE1 KO mice were generally heavier than the WT NC controls, they were still generally lighter than the WT HF mice. (Figure 4.3A) After 12 weeks of dietary intervention, the HFD resulted in significant weight gain in WT animals compared to NC controls. BACE1 KO ameliorated the effects of HF with this group being significantly lighter than the WT HF group and showed no significant difference to WT NC controls. KI HF mice exhibited comparable body weights to the WT HFD group and were significantly heavier than WT NC controls. (Figure 4.3B) Over the study every group exhibited a similar trend of weight gain in response to HF whilst the NC group exhibited consistently less weight gain each week. Both BACE1 KO and BACE1 KI mice exhibited a trend towards decreased weekly weight gain compared to WT NC controls (Figure 4.3C) however after 12 weeks of dietary intervention, only the BACE1 KO exhibited significantly reduced % weight change compared to WT HF mice. BACE1 KI NC mice showed increased weight gain compared to WT NC controls but were comparable to WT HF mice in their % weight gain over the course of the study. WT HF mice showed significantly greater % weight gain over the 12 weeks. (Figure 4.2D)

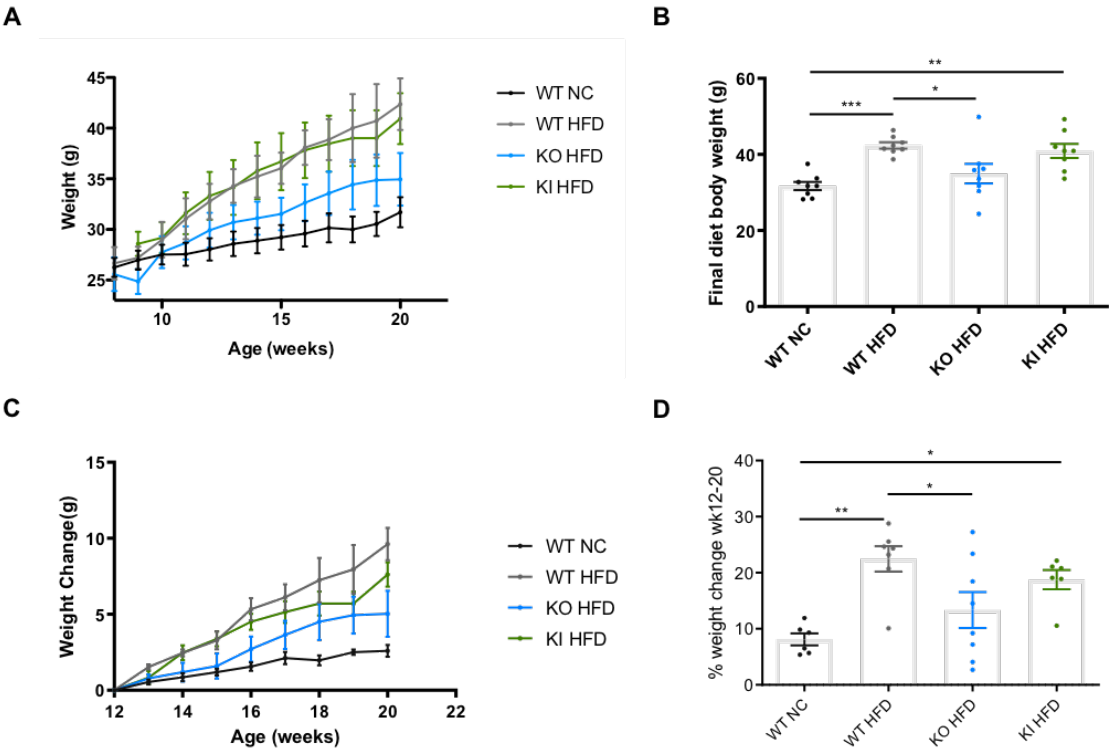

Figure 4.3 Comparison of Wild-type, normal chow fed mice (WT NC) with WT mice, BACE1 KO and forebrain specific BACE1 KI body weights when challenged with 12 weeks of HFD. A) Body weight over 12-week dietary intervention. **B**) Final body weight after 12-week dietary intervention indicated significant differences with both genotype and diet using Two-way ANOVA. Tukey's multiple comparison showed both WT HF and KI HF groups to be significantly heavier than WT NC controls whilst KO mice were significantly lighter than WT mice on the HFD after 12 weeks of dietary intervention. **C**) Body weight change from 12 weeks of age to the end of the study **D**) Percentage body weight change at end of study compared to 12 weeks of age. Two-way ANOVA and Tukey's multiple comparison test showed both WT HF and KI HF groups to have gained significantly more weight than WT NC fed controls. BACE1 KO mice gained significantly less weight than WT HF fed mice. n=8 per group. Individual data points indicate the range of data. Standard error indicated by error bars, * = p<0.05, ** = p<0.01, *** = p<0.001.

4.2.3 Analysis of biological replicates

Samples for this study were not pooled and each replicate represented the brain region from a single mouse. 3 mice per group were randomly selected for analysis and labelled as indicated in table 4.1. BACE1 KO WT littermates were utilised for controls. A total of 72,491 peptides were identified in the hippocampal samples whilst 57,550 peptides were identified in the hypothalamus.

		TMT label									
	Tissue	**126**	**127N**	**127C**	**128N**	**128C**	**129N**	**129C**	**130N**	**130C**	**131**
10Plex 1	Hippo	WT NC 1	WT NC 2	WT NC 3	WT HF 1	WT HF 2	WT HF 3	KO HF 1	KO HF 2	KO HF 3	
10Plex 2	Hypo	WT NC 1	WT NC 2	WT NC 3	WT HF 1	WT HF 2	WT HF 3	KO HF 1	KO HF 2	KO HF 3	

Table 4.1 Allocation of proteomic tissues to TMT labels. 3 TMT 10plex kits were used. 10Plex 1 consisted of hippocampal samples from wild-type normal chow (WT NC), wild-type high-fat (WT HF) and BACE1 KO HF mice- 3 mice per group. 10Plex 2 consisted of hypothalamic samples from WT NC, WT HF and KO HF mice- 3 mice per group. 10Plex 3 consisted of both hippocampal and hypothalamic tissues from 3 BACE1 KI mice.

Pearson correlation was conducted to determine the similarity between biological replicates in their protein expression profile. Correlation was calculated between samples in each TMT10plex™ as statistical comparison between 10plex's is not yet accurate. Pearson's coefficient was calculated. Method 1 analysis produced Pearson's coefficients >0.99 for each correlation in both the hippocampus and hypothalamus with one exception. Whilst all replicates exhibited very significant correlation in the hippocampus on HFD (Supplemental figure S1), replicate 2 showed less similarity to both replicate 1 and 3 in the hypothalamus with both comparisons producing a coefficient of 0.98. Whilst this still indicates great similarity in the hypothalamic proteome within this group and is not sufficient to exclude this replicate from analysis, it suggests that the proteome of mouse HFD 2 is less similar to the others within that group (Figure S1B). Analysis by method 2 produced pearson's coefficients >0.99 for all correlations in the hippocampus. (Supplemental figure S2). In the hypothalamus, HFD2 replicate again exhibited greater proteome variation compared to HFD replicates 1 and 3. In this analysis HFD replicate 2 produced a Pearson's coefficient of 0.96 when compared to the two other replicates in this group. All other coefficients in this 10plex were greater than 0.99 (Supplemental figure S3).

In addition to Pearson's correlation, principle component analysis (PCA) was conducted in order to compare replicates. PCA using method 1 analysis data identified distinct clusters of samples representing the hippocampal and hypothalamic tissues. Both tissues varied in component 1 but exhibited little variability in component 2 (Supplemental figure S4A). The hippocampal samples showed greatest variability in the hippocampus with PCA by quantitative analysis (Supplemental figure S4B). These samples exhibited variability in both components across all sample groups. Hypothalamic samples showed very little variability in component 1 but greater variability in component 2 (4C). Once again, HFD replicate 2 hypothalamus exhibited greater variability in than the others of that group showing itself to differ from the other hypothalamic samples predominantly in component 1. Both PCA analyses failed to indicate grouping of samples by condition based on these components indicating little variability in samples of genetic and dietary groupings.

4.2.4 Protein hits from method 1

Volcano plots from method 1 indicated no significant change in the hippocampal or hypothalamic proteomes of WT mice with 12 weeks HFD compared with NC fed controls (Figures 4.4A and 4.5A). However, 19 and 15 protein hits were observed between WT NC and KO HFD in the hippocampus and hypothalamus respectively. 12 and 9 hits were identified comparing WT HFD and KO HFD in the hippocampus (Figures 4.4B and 4.4C) and the hypothalamus. (Figures 4.5B and 4.5C) These hits are listed in tables 4.2 and 4.3 respectively.

In order to increase the number of hits between the WT NC, WT HFD and KO HFD groups, reporter ion ratios between groups were allocated to bins as described in section 2.3.4 and a histogram produced of reporter ion ratios. From this a normal distribution of ratios was created. The standard deviation was calculated and hits were determined as any protein with a ratio out-with two standard deviations of the median (Figures 4.6 and 4.7). This method of analysis increased the number of proteins significantly affected by both diet and BACE1 expression in both brain regions with hippocampal hits increasing to 146, 183 and 67 hits in the hippocampus (WT NC vs KO HF, WT HF vs KO HF and WT NC vs WT HF respectively). These hits can be viewed via the following link in a google

browser:
[https://drive.google.com/open?id=1SjsiknW9rk5hIfGgqcKK4NREgBravPXC]
In the hypothalamus the number of hits increased to 256, 150 and 598 (WT NC vs KO HF, WT HF vs KO HF and WT NC vs WT HF respectively). These hits can be viewed via the following link in a google browser: [https://drive.google.com/open?id=1WAD0G4sSRuyTkscVQTaI801ECZBEN1d2]
The proteins identified through this method and all significant hits along with reporter ion ratios can be viewed via the following link in a google browser: [https://drive.google.com/open?id=1GqHikFdA_oQJcP1ona0ZwwjoTxn-6Lzg].

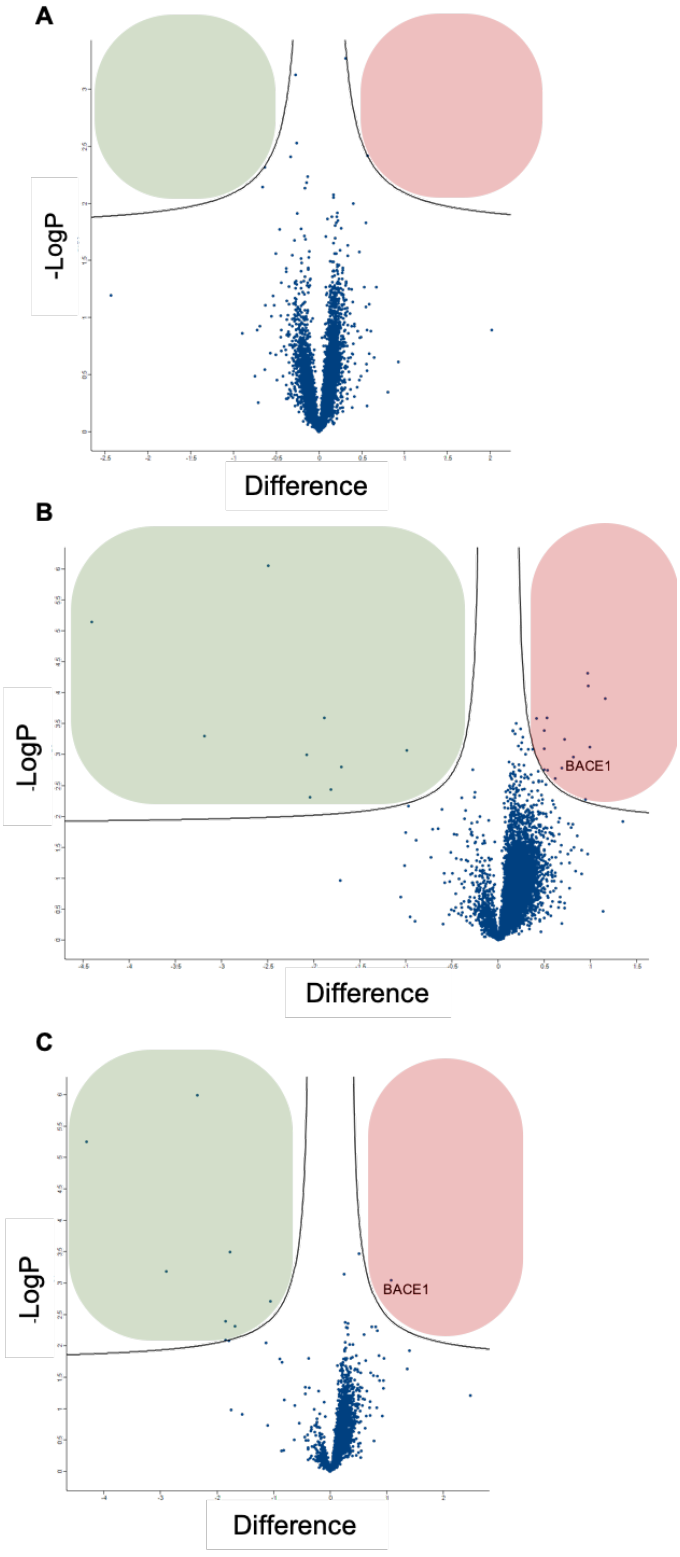

Figure 4.4 Volcano plots of hippocampal protein reporter ion intensity ratios between (**A**) Wild-type normal chow vs Wild-type high-fat where points within the green region indicate proteins upregulated with high-fat diet and points within the red region indicate proteins downregulated with high-fat diet (**B**) Wild-type normal chow vs BACE1 Knock-out high-fat where points within the green region indicate proteins upregulated with BACE1 KO and high-fat diet and points within the red region indicate proteins downregulated with BACE1 KO and high-fat diet (**C**) Wild-type high-fat vs BACE1 Knock-out high-fat where points within the green region indicate proteins upregulated with BACE1 KO and points within the red region indicate proteins downregulated with BACE1 KO. Hits were identified by one-way ANOVA. These hits were identified using method 1 using median sweep normalisation and represent hits prior to post-hoc correction.

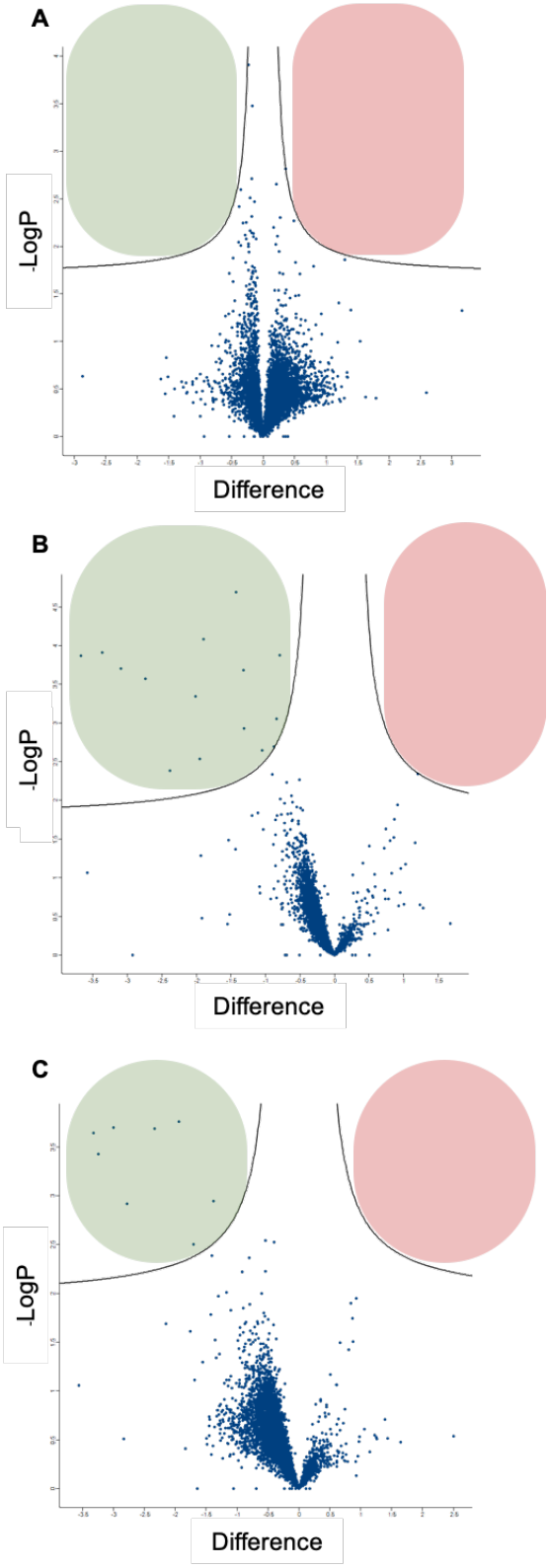

Figure 4.5 Volcano plots of hypothalamic protein reporter ion intensity ratios between (**A**) Wild-type normal chow vs wild-type high-fat where points within the green region indicate proteins upregulated with high-fat diet and points within the red region indicate proteins downregulated with high-fat diet (**B**) Wild-type normal chow vs BACE1 knock-out high-fat where points within the green region indicate proteins upregulated with BACE1 KO and high-fat diet and points within the red region indicate proteins downregulated with BACE1 KO and high-fat diet (**C**) Wild-type high-fat vs BACE1 knock-out high-fat where points within the green region indicate proteins upregulated with BACE1 KO and points within the red region indicate proteins downregulated with BACE1 KO. Hits were identified by one-way ANOVA. These hits were identified using method 1 using median sweep normalisation and represent hits prior to post-hoc correction.

WT NC Vs KO HFD				WT HFD Vs KO HFD			
Gene name	Protein name	log2 difference	-log10 p-value	Gene name	Protein name	log2 difference	-log10 p-value
Map1b	**Microtubule-associated protein 1B**	**-4.39**	**5.49**	**Map1b**	**Microtubule-associated protein 1B**	**-4.04**	**4.63**
Atp2b2	**Plasma membrane calcium-transporting ATPase 2**	**-3.20**	**3.21**	**Atp2b2**	**Plasma membrane calcium-transporting ATPase 2**	**-2.77**	**3.18**
Epb41l1	**Protein 4.1N**	**-2.51**	**6.16**	**Epb41l1**	**Protein 4.1N**	**-2.25**	**5.91**
Caskin1	Caskin-1	-2.11	2.99	Caskin1	Caskin-1	-1.78	2.44
Akr1b10	Aldo-keto reductase family 1 member B10	-2.06	2.36	Tmsb15b	Thymosin beta	-1.71	2.16
Serpina3k	**Serine protease inhibitor A3K**	**-1.90**	**3.75**	**Serpina3k**	**Serine protease inhibitor A3K**	**-1.70**	**3.51**
Ptpns1	**Tyrosine-protein phosphatase non-receptor type substrate 1**	**-1.84**	**2.47**	**Ptpns1**	**Tyrosine-protein phosphatase non-receptor type substrate 1**	**-1.62**	**2.28**
Tmsb15b	Thymosin beta	-1.72	2.75	Adck5	Uncharacterized aarF domain-containing protein kinase 5	-1.00	2.73
Adck5	Uncharacterized aarF domain-containing protein kinase 5	-1.03	2.92	Tefm	Transcription elongation factor, mitochondrial	0.50	3.89
Hars	Histidine--tRNA ligase	-1.02	2.25	Ppp1r11	E3 ubiquitin-protein ligase PPP1R11	0.69	2.46
Mug1	Murinoglobulin-1	-0.65	2.69	Gabra2	Gamma-aminobutyric acid receptor subunit alpha-2	0.75	2.49
S100a6	Protein S100-A6	0.44	2.84	Bace1	Beta-secretase 1	1.02	3.05
Iah1	Isoamyl acetate-hydrolyzing esterase 1	0.44	3.78				
Srp54c	Signal recognition particle 54 kDa protein	0.60	2.71				
Hsd11b1	Corticosteroid 11-beta-HSD 1	0.73	2.70				
Bace1	Beta-secretase 1	0.87	2.88				
Igk	Kappa light chain	0.87	3.27				
Igh	Immunoglobulin heavy constant gamma 2C	0.88	3.24				
HC	11D8 anti-human butyrylcholinesterase (BChE) heavy chain	1.05	5.45				

Table 4.2 Significantly regulated proteins within the hippocampus of wild-type normal chow, high-fat and BACE1 knock-out high-fat fed mice. Determined by method 1 and volcano plot. Highlighted proteins indicate hits across both comparisons whilst proteins in bold indicate hits across all comparisons in both brain regions. Proteins highlighted green are hits in WT NC Vs BACE1 KO HF in both brain regions.

WT NC Vs KO HFD				WT HFD Vs KO HFD			
Gene name	Protein name	log2 difference	-log10 p-value	Gene name	Protein name	log2 difference	-log10 p-value
Atp2b2	**Plasma membrane calcium-transporting ATPase 2**	**-3.66**	**4.07**	**Map1b**	**Microtubule-associated protein 1B**	**-3.16**	**3.62**
Map1b	**Microtubule-associated protein 1B**	**-3.37**	**4.10**	**Atp2b2**	**Plasma membrane calcium-transporting ATPase 2**	**-3.10**	**3.56**
Epb41l1	**Protein 4.1N**	**-3.10**	**3.86**	**Epb41l1**	**Protein 4.1N**	**-2.87**	**3.71**
Ccdc93	Coiled-coil domain-containing protein 93	-2.75	3.79	Arhgap5	Rho GTPase-activating protein 5	-2.67	**3.00**
Akr1b10	Aldo-keto reductase family 1, member B10	-2.42	2.46	Ccdc93	Coiled-coil domain-containing protein 93	-2.25	3.70
Serpina3k	**Serine protease inhibitor A3K**	**-2.04**	**3.54**	**Ptpns1**	**Tyrosine-protein phosphatase non-receptor type substrate 1**	**-1.86**	**3.82**
Dfna5	Gasdermin-E	-2.01	2.60	**Serpina3k**	**Serine protease inhibitor A3K**	**-1.65**	**2.54**
Ptpns1	**Tyrosine-protein phosphatase non-receptor type substrate 1**	**-1.92**	**4.11**	Adck5	Uncharacterized aarF domain-containing protein kinase 5	**-1.32**	**3.06**
Adck5	Uncharacterized aarF domain-containing protein kinase 5	**-1.46**	**4.87**	Mmrn2	Multimerin-2	-1.29	2.61
Retsat	All-trans-retinol 13,14-reductase	-1.35	4.34				
Trp53bp1	TP53-binding protein 1	-1.34	2.97				
Tcaf2	TRPM8 channel-associated factor 2	-1.07	2.68				
Serpina3n	Serine protease inhibitor A3N	-0.92	2.74				
C9	Complement component C9	-0.88	3.03				
CD59A	CD59A glycoprotein	-0.83	3.67				

Table 4.3 Significantly regulated proteins within the hypothalamus of wild-type normal chow, high-fat and BACE1 knock-out high-fat fed mice. Determined by method 1 and volcano plot. Highlighted proteins indicate hits across both comparisons whilst proteins in bold indicate hits across all comparisons in both brain regions. Proteins highlighted green are hits in WT NC Vs BACE1 KO HF in both brain regions.

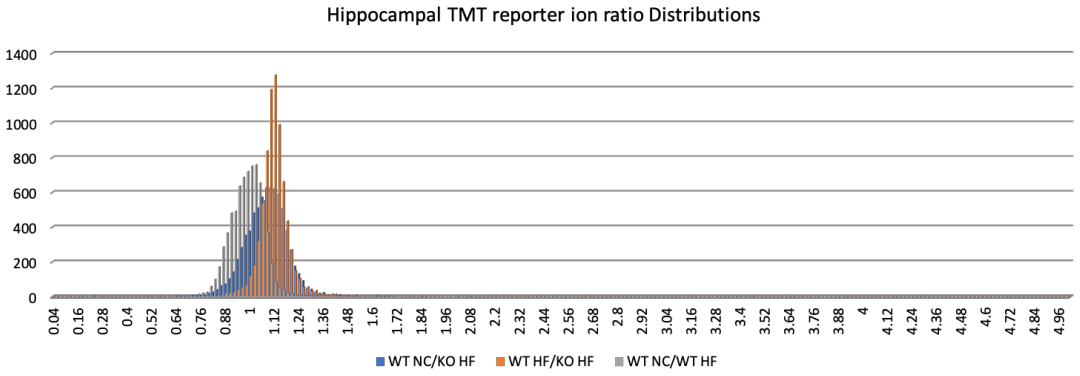

	WT NC/KO HF	WT HF/KO HF	WT NC/WT HF
median	1.075727408	1.105253751	0.972971973
Standard dev	0.148330502	0.104125453	0.102687932
Upper cut-off	1.372388411	1.313504657	1.178347837
Lower cut-offf	0.779066405	0.897002845	0.76759611

Figure 4.6 Histograms of reporter ion ratio distributions in the hippocampus. Wild-type normal chow vs Wild-type high-fat (WT NC/WT HF), Wild-type normal chow vs BACE1 knock-out high-fat (WT NC/ KO HF) and Wild-type high-fat vs BACE1 knock-out high-fat (WT HF vs KO HF). The median reporter ion intensity, standard deviation and upper and lower threshold for significant proteins are indicated.

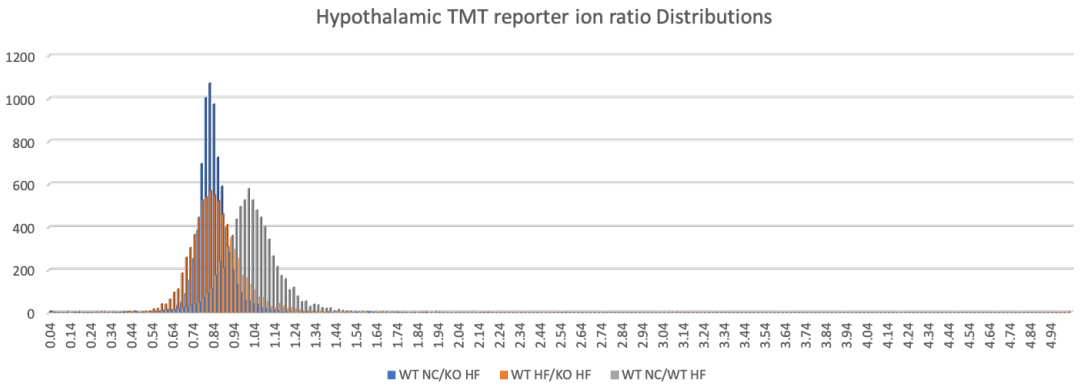

	WT NC/KO HF	WT HF/KO HF	WT NC/WT HF
median	0.81887152	0.82627241	0.996308354
Standard dev	0.110877578	0.21825058	0.175208643
Upper cut-off	1.040626675	1.26277357	1.34672564
Lower cut-offf	0.597116364	0.389771249	0.645891069

Figure 4.7 Histograms of reporter ion ratio distributions in the hypothalamus. Wild-type normal chow vs Wild-type high-fat (WT NC/WT HF), Wild-type normal chow vs BACE1 knock-out high-fat (WT NC/ KO HF) and Wild-type high-fat vs BACE1 knock-out high-fat (WT HF vs KO HF). The median reporter ion intensity, standard deviation and upper and lower thresholds for significant proteins are indicated.

Pathway analysis was conducted on these data to identify enriched pathways in the significant proteins. Enriched pathways from each comparison in the hippocampus and hypothalamus are presented in tables 4.4 and 4.5 respectively. Pathway diagrams can be found via the link in a google browser: [https://drive.google.com/open?id=1OMKh1AY_AvDQtSrq08B-SyujgGHsUG2o]

Pathways implicated in lipid metabolism and nervous system development were identified as changing with HFD in both the hippocampus and the hypothalamus. Whereas neurological disease and cell death pathways were identified as being over-represented in the hippocampus: nervous system development and function, connective tissue disorder, cell signalling, cell assembly, cell-cell signalling, cardiovascular, carbohydrate metabolism, protein trafficking, cell cycle, protein folding, post-translational modifications (PTMs), amino acid metabolism, cell movement, connective tissue disorder, free radical scavenging, small molecule biochemistry and cancer pathways were identified in the hypothalamus that were not present in the hippocampus. Pathways regarding: small molecule biochemistry, lipid metabolism, molecular transport, cellular assembly and organisation, endocrine system disorders, GI disease and nervous system development and function were over-represented in both the hippocampus and hypothalamus of BACE1 KO mice compared to WT HF controls. The hippocampus exhibited changes in: amino acid and carbohydrate metabolism, cell-cell signalling and organisation, immunological disease, protein synthesis and trafficking, PTMs, energy production, cellular response to therapeutics, cardiovascular development and function, cell morphology, inflammatory response, hematological system development and function, connective tissue disorders and organismal injury and abnormalities pathways that were not present in the hypothalamus. The hypothalamus exhibited over-representation of cellular assembly and organisation, metabolic disease, cellular function and maintenance, small molecule transport, cancer, nucleic acid metabolism, molecular transport and cellular movement pathways- all of which were not present in the hippocampus. Both hippocampus and hypothalamus exhibited changes in inflammatory response, neurological disease, nervous system development and cellular growth and proliferation pathways between the WT NC and BACE1 KO groups. Whilst the hippocampus exhibited changes in cellular morphology, organisation and assembly, auditory disease, hereditary

disease, cell mediated immune response, cellular assembly and organisation, GI disease, hepatic disease, carbohydrate metabolism and nucleic acid metabolism the hypothalamus indicated over representation of lipid metabolism, metabolic disease, tissue morphology, cellular function and maintenance, cell death and survival, cancer and organismal injury and abnormalities pathways.

Pathways that appear to change with both diet and BACE1 expression in the hippocampus are lipid metabolism and nervous system development. In the hypothalamus; nervous system development and function, cellular assembly and organisation, cellular movement, small molecule biochemistry and cancer pathways appear to be influenced by both HFD and BACE1 expression.

Hippocampus					
WT NC vs WT HF		**WT NC vs KO HF**		**WT HF vs KO HF**	
Pathway	**Figure**	**Pathway**	**Figure**	**Pathway**	**Figure**
Lipid Metabolism	IPA 11	Cellular morphology, organisation and assembly	IPA 14	Amino acid and carbohydrate metabolism, small molecule biochemistry	IPA 1
Neurological Disease	IPA 12	Neurological disorders	IPA 15	Lipid metabolism, molecular transport	IPA 2
Cell Death/ Nervous system development	IPA 13	Auditory disease, hereditary disease	IPA 16	Cell-cell signalling and organisation, cellular assembly and organisation	IPA 3
		Cell morphology, cell mediated immune response	IPA 17	Endocrine system disorders, GI disease, immunological disease	IPA 4
		Cellular assembly and organisation	IPA 18	PTMs, Protein synthesis and protein trafficking	IPA 5
		GI disease, hepatic disease	IPA 19	Nervous system development and function, amino acid metabolism, PTMs, Energy production	IPA 6
		Inflammatory response	IPA 20	Cellular response to therapeutics, cardiovascular system development and function, cell morphology	IPA 7
		Carbohydrate metabolism	IPA 21	Cell-cell signalling, hematological system development and function, inflammatory response	IPA 8
		Nervous system development	IPA 22	Cell-cell signalling, inflammatory response, hematological system development and function	IPA 9
		Nucleic acid metabolism, cellular growth and proliferation	IPA 23	Connective tissue disorders, inflammatory disease, organismal injuries and abnormalities	IPA 10

Table 4.4 Over-represented pathways within the hippocampus. Wild-type normal chow, high-fat and BACE1 knock-out high-fat fed mice as determined by semi-quantitative analysis and histogram of reporter ion ratios

Hypothalamus					
WT NC vs WT HF		**WT NC vs KO HF**		**WT HF vs KO HF**	
Pathway	**Figure**	**Pathway**	**Figure**	**Pathway**	**Figure**
Nervous system development	IPA 40	Nervous system development, lipid metabolism, inflammatory response	IPA 33	Cellular assembly and organisation, metabolic disease	IPA 24
Connective tissue disorders	IPA 43	Metabolic disease	IPA 34	Cellular function and maintenance	IPA 25
Nervous system development and function	IPA 44	Nervous system development and function	IPA 35	Lipid metabolism, small molecule transport	IPA 26
Cell signalling PTMS	IPA 45	Lipid metabolism	IPA 36	Endocrine system disorders	IPA 27
Cellular assembly and organisation	IPA 46	Tissue morphology	IPA 37	Cancer	IPA 28
Cell-cell signalling	IPA 47	Cellular growth and proliferation	IPA 38	Cellular function and maintenance, nucleic acid metabolism, molecular transport	IPA 29
Cardiovascular system development and function	IPA 48	Neurological disease	IPA 39	Cancer, endocrine disorders, GI disease	IPA 30
Carbohydrate metabolism	IPA 49	Cellular function and maintenance	IPA 40	Cellular movement, nervous system development and function	IPA 31
Protein trafficking and cell cycle	IPA 50	Cell death and survival, Nervous system development and function	IPA 41	Lipid metabolism, small molecule biochemistry	IPA 32
PTMs, Protein folding	IPA 51	Cancer, organismal injury and abnormalities	IPA 42		
Amino acid metabolism, PTMs	IPA 52				
Cellular movement, hypersensitivity response	IPA 53				
Connective tissue disorders	IPA 54				
Free radical scavenging, small molecule biochemistry	IPA 55				
Cell signalling	IPA 56				
Connective tissue disorders	IPA 57				
Cancer	IPA 58				
Lipid metabolism	IPA 59				

Table 4.5 Over-represented pathways within the hypothalamus. Wild-type normal chow, high-fat and BACE1 knock-out high-fat fed mice as determined by semi-quantitative analysis and histogram of reporter ion ratios

4.2.5 Protein hits from method 2

Method 2 employed a comprehensive statistical analysis using a method of peptide normalisation that addresses technical errors such as loading variations and systematic errors such as batch effects (Maes et al., 2016). The data were then corrected using the Bonferroni post-hoc test using the total number of peptides identified in each 10-plex. Whilst this method provides much better statistical evidence for hits found, it substantially reduces the number of significant hits. Analysis by this method showed no significant changes in either the hippocampus or hypothalamus with diet (Figures 4.8A and 4.9A respectively) . This method led to the identification of one significantly altered protein in the hippocampus- Protein 4.1N (Gene: EPB41L1) which was different between in both WT NC Vs KO HFD (p= 0.003, Difference= -2.61) and WT HFD Vs KO HFD (p= 0.01, Difference= -2.47). This protein was significantly changed when comparing the BACE1 KO data to both the WT NC and WT HF data sets. (Figures 3.20B and 3.20C) Within the hypothalamus, two proteins were identified as significantly changing with BACE1 KO comparison to both WT NC and WT HF. (Figures 3.21B and 3.21C) These proteins were thioredoxin domain containing protein 15 (TXD15) (p= 0.0007, Difference= -2.82 and p= 0.03, Difference= -2.81 in WT NC Vs KO HF and WT HF Vs KO HF respectively) and alpha-L-fucosidase 1 (FUCA1) (p= 0.0007, Difference= -2.82 and p= 0.001, Difference = -2.59 in WT NC Vs KO HF and WT HF Vs KO HF respectively).

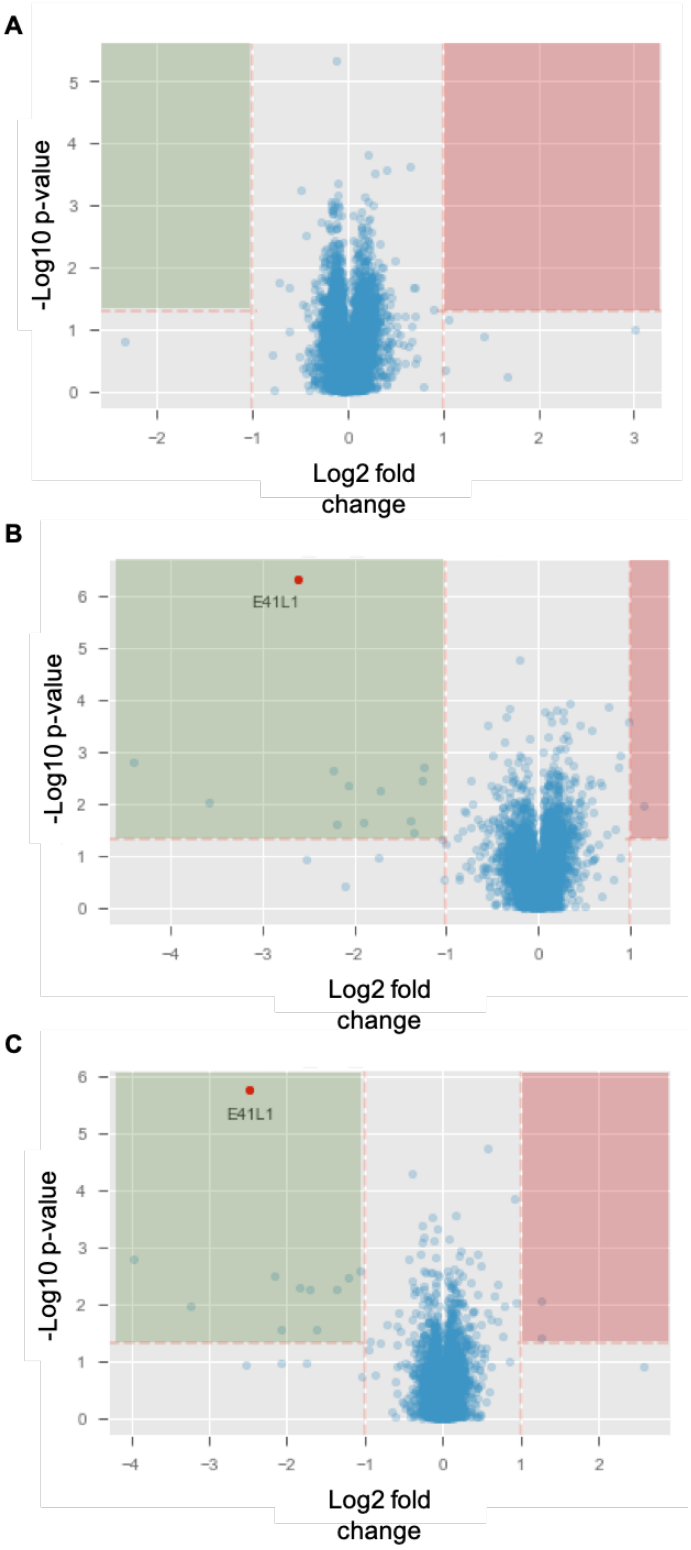

Figure 4.8 Volcano plots map protein reporter ion intensities within the hippocampus between (**A**) Wild-type normal chow vs Wild-type high-fat where points within the green region indicate proteins upregulated with high-fat diet and points within the red region indicate proteins downregulated with high-fat diet (**B**) Wild-type normal chow vs BACE1 knock-out high-fat where points within the green region indicate proteins upregulated with both BACE1 KO and HFD and points within the red region indicate proteins downregulated with both BACE1 KO and HFD (**C**) Wild-type high-fat vs BACE1 Knock-out high-fat where points within the green region indicate proteins upregulated with BACE1 KO and points within the red region indicate proteins downregulated with BACE1 KO. These hits were identified using quantitative analysis by CONSTANd normalisation. Volcano plots represents hits identified after one-way ANOVA with red points indicating hits significant after Bonferroni correction.

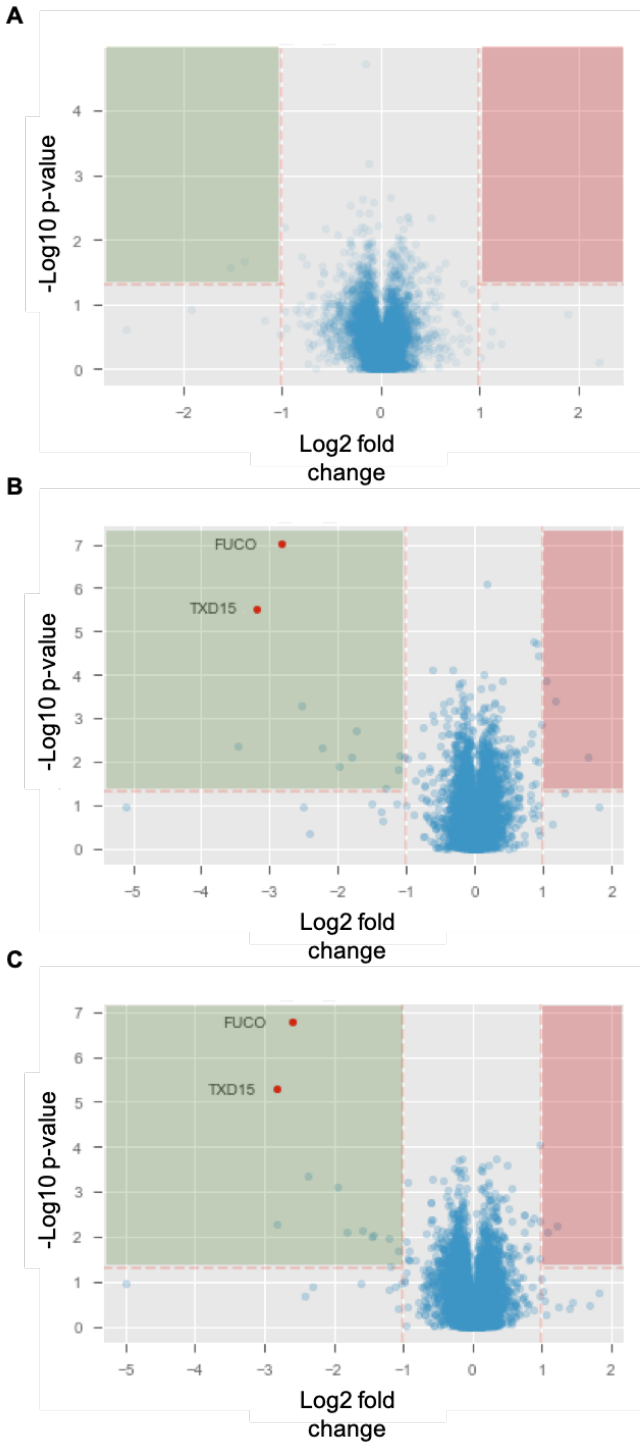

Figure 4.9 Volcano plots map protein reporter ion intensities within the hypothalamus between (**A**) Wild-type normal chow vs Wild-type high-fat where points within the green region indicate proteins upregulated with high-fat diet and points within the red region indicate proteins downregulated with high-fat diet (**B**) Wild-type normal chow vs BACE1 knock-out high-fat where points within the green region indicate proteins upregulated with both BACE1 KO and HFD and points within the red region indicate proteins downregulated with both BACE1 KO and HFD (**C**) Wild-type high-fat vs BACE1 Knock-out high-fat where points within the green region indicate proteins upregulated with BACE1 KO and points within the red region indicate proteins downregulated with BACE1 KO. These hits were identified using quantitative analysis by CONSTANd normalisation. Volcano plots represents hits identified after one-way ANOVA with red points indicating hits significant after Bonferroni correction.

4.2.6 BACE1 expression across models and comparison to preliminary data

Seven peptides were identified across the BACE1 protein sequence in the hippocampus with a peptide coverage of 11%; whilst in the hypothalamus, only three peptides were identified resulting in a peptide coverage of just 6% (Figure 4.10) The first identified peptide began at the first amino acid of the mature BACE1 protein as opposed to the signal or pro-peptides indicating that it is unlikely that immature BACE1 peptides were included. Unexpectedly, BACE1 was identified in both the hippocampus and hypothalamus of the BACE1 KO mice across both methods of analysis (Figure 4.11). Whilst method 1 suggests an approximate. 50% reduction of BACE1 in the KO line in both brain regions, method 2 only identified an approximate 50% reduction in BACE1 in the hippocampus. Normalised reporter ion intensities for each peptide (analysed by method 2) suggest that the 50% reduction is consistent across all identified peptides in both brain regions and the data to not suggest an over-representation of a specific region of the BACE1 protein (Figure 4.12). This confirms that the presence of these peptides is not due to the production of truncated native BACE1. Upon inspection it was noted that the quality of the MS spectra identifying the BACE1 peptides were very poor and the evidence for allocating these ion peaks to BACE1 peptides was tenuous. This suggested that the identification of BACE1 within the KO tissues was erroneous and may be due to contamination within the mass spectrometer between samples.

Western blot analysis of hippocampal, hypothalamic and cortical tissues support the BACE1 KO mice are indeed KOs as no BACE1 protein was identified in brain samples from this group (Figure 4.13). No change was observed in BACE1 expression with HFD compared to NC in WT mice across either method of analysis or brain region. This was reflected in the normalised peptide reporter ion intensities (Figures 4.11).

Figure 4.10 Map of MS/MS identified BACE1 peptides within the mouse hippocampus and hypothalamus. The blue sequence represents the BACE1 signal and propeptide region that is removed with protein maturation. Sequences underlined in green represent hypothalamic peptides and sequences underlines in black represent hippocampal peptides. Regions with underlined twice represent multiple peptides spanning the same section as a result of missed cleavages.

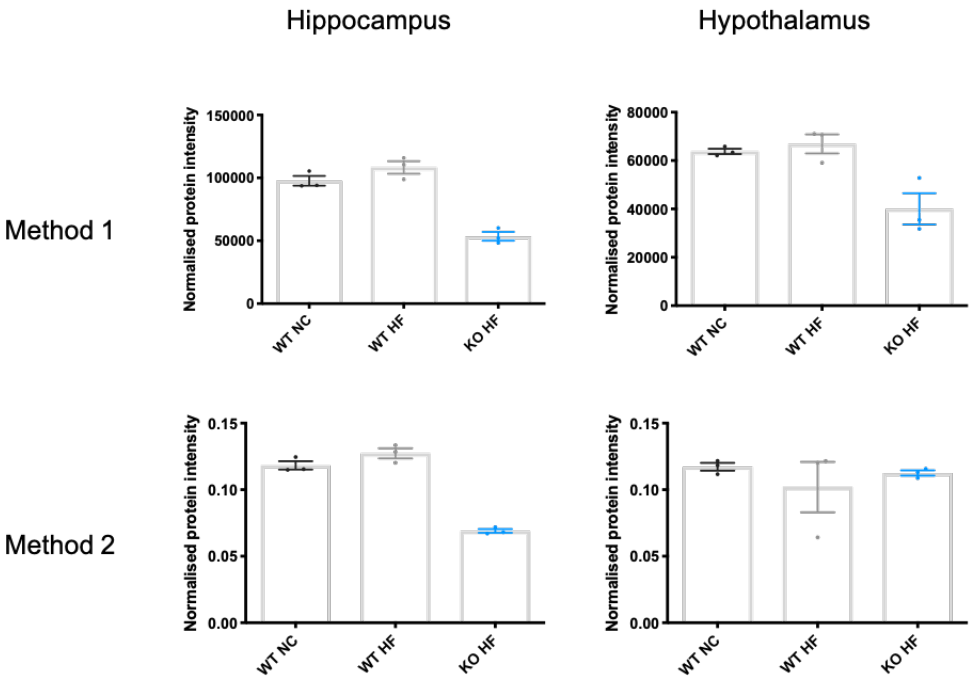

Figure 4.11 BACE1 protein intensities in the hippocampus and hypothalamus normalised by method 1 and method 2. Method 1 utilised a median sweet method of normalisation and identified an approximate 50% reduction in BACE1 expression within the hippocampus and hypothalamus of BACE1 KO mice. Method 2 utilised the CONSTANd method of normalisation and found an approximate 50% reduction of BACE1 expression within the hippocampus but no change in BACE1 expression in the hypothalamus. n=3 per group. Individual data points indicate the range of data. Standard error indicated by error bars.

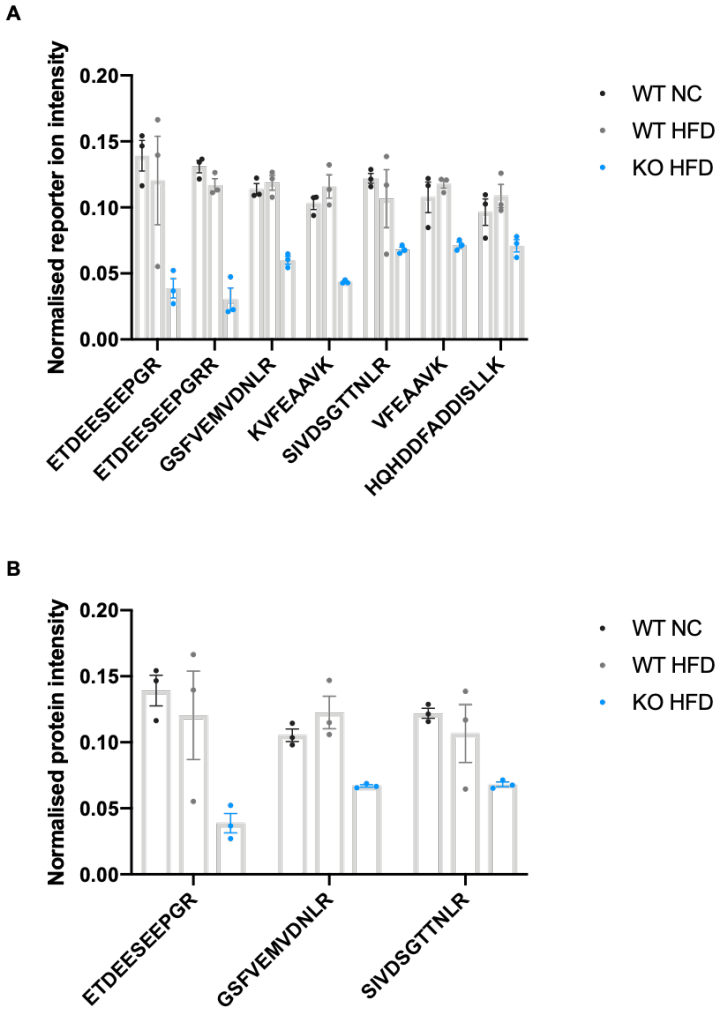

Figure 4.12 Normalised reporter ion intensities for each BACE1 peptides identified within the hippocampus (A) and the hypothalamus (B). Peptides were normalised using method 2- the CONSATNd method of normalisation. This revealed an approximate 50% reduction in each of the BACE1 peptides identified in both brain regions and does not suggest an over-representation of a specific region of the BACE1 protein. n=3 per group. Individual data points indicate the range of data. Standard error indicated by error bars.

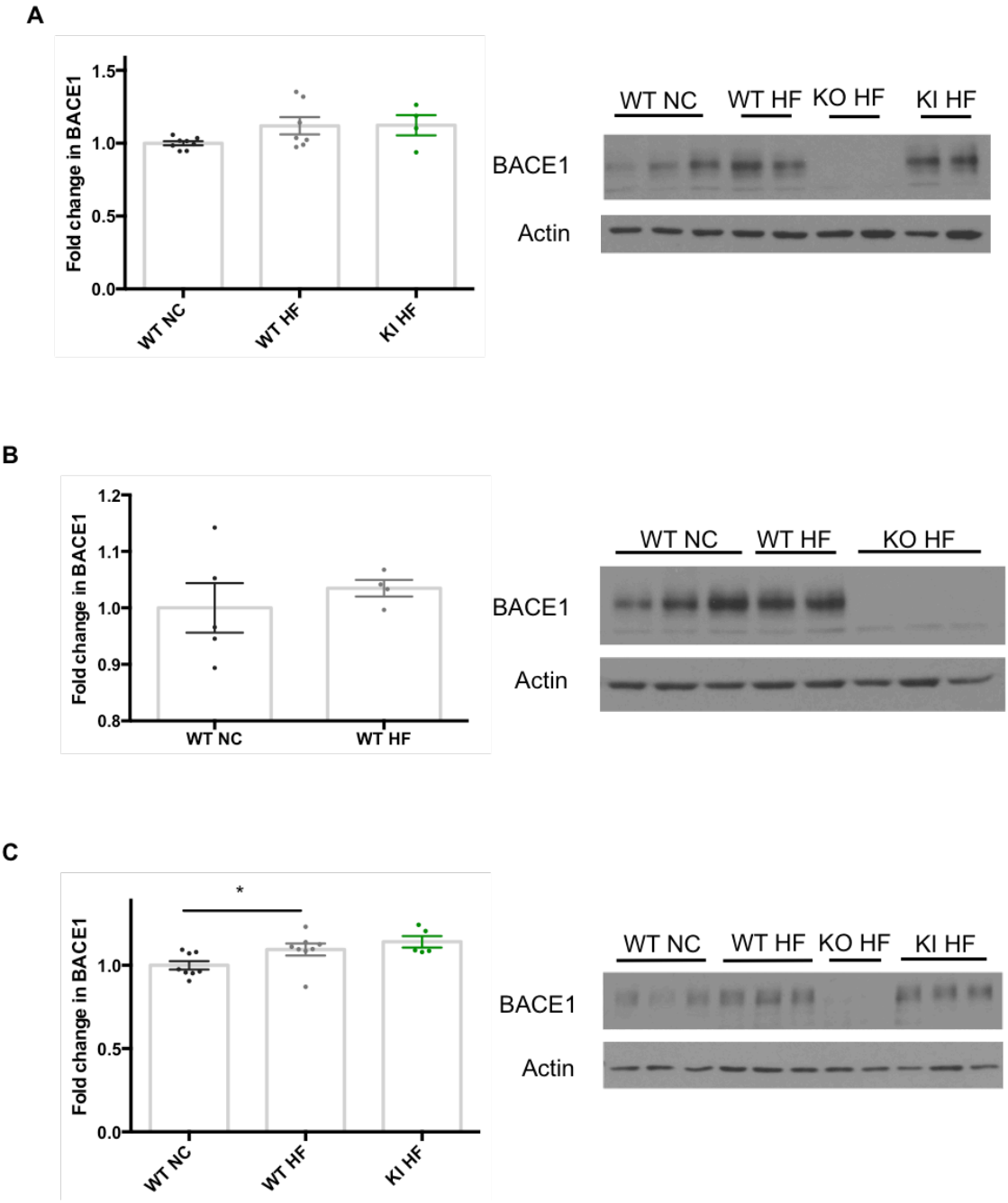

Figure 4.13 Western blot and densitometric analysis of BACE1 expression within the hippocampus (A), hypothalamus (B) and cortex (C). Immunoblots suggest complete absence of BACE1 within all brain regions in the BACE1 KO mouse model compared to WT and KI models. WT HF mice exhibit a trend towards increased BACE1 within the hypothalamus and cortex whilst this was not apparent in the hippocampus. BACE1 KI mice exhibit increased BACE1 expression within the hippocampus but not the cortex. n=5-9 per group. Individual data points indicate the range of data. Standard error indicated by error bars, * = $p<0.05$

4.2.7 Peptide coverage of proteomic hits

Three peptides were identified within the protein sequence for TXNDC15 representing a peptide coverage of 16% in both the hippocampus and hypothalamus (Figure 4.14). Two peptides were identified within the FUCA1 protein sequence representing a peptide coverage of approximately 6% in both brain regions (Figure 4.15).

The greatest peptide coverage was within protein 4.1N whereby 46 peptides were identified within the hippocampus and 44 within the hypothalamus. These peptides represent peptide coverage of 54% and 55% of the full-length protein in the hippocampus and hypothalamus respectively (Figures 4.16 & 4.17).

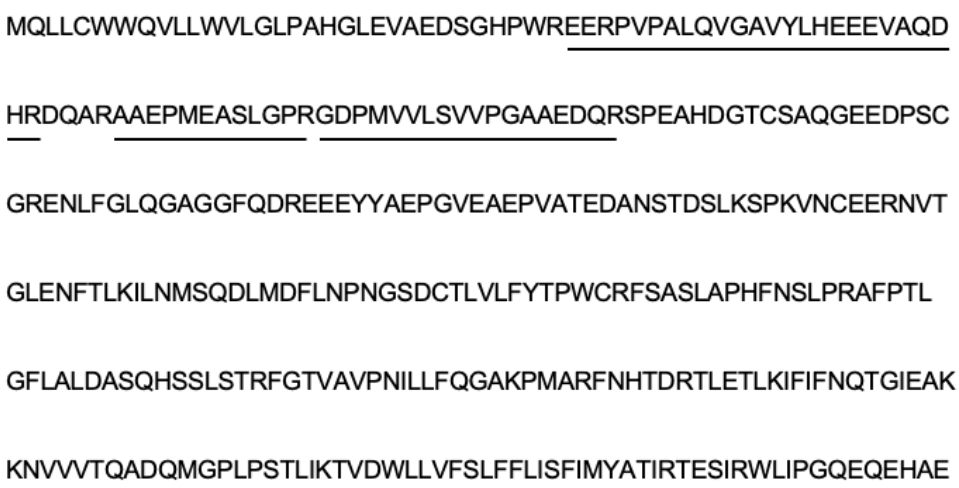

Figure 4.14 Map of MS/MS identified TXNDC15 peptides within the mouse hippocampus and hypothalamus. Sequences underlined represent peptides identified in proteomic analysis of both hippocampal and hypothalamic tissues.

Figure 4.15 Map of MS/MS identified FUCA1 peptides within the mouse hippocampus and hypothalamus. Sequences underlined represent peptides identified in proteomic analysis of both hippocampal and hypothalamic tissues.

Figure 4.16 Map of MS/MS identified protein 4.1N peptides within the mouse hippocampus. Sequences underlined represent peptides identified by MS/MS. Black and red sequences indicate alternating exons and highlighted residues indicate single amino acid changes. 46 peptides were identified representing a peptide coverage of 54%. Arrow indicates the absence of a peptide corresponding to exon 5 that is present in the hypothalamus. Regions with underlined twice represent multiple peptides spanning the same section as a result of missed cleavages.

Figure 4.17 Map of MS/MS identified protein 4.1N peptides within the mouse hypothalamus. Sequences underlined represent peptides identified by MS/MS. Black and red sequences indicate alternating exons and highlighted residues indicate single amino acid changes. 44 peptides were identified representing a peptide coverage of 55%. Arrow indicates the presence of a peptide corresponding to exon 5 that is absent in the hippocampus. Regions with underlined twice represent multiple peptides spanning the same section as a result of missed cleavages.

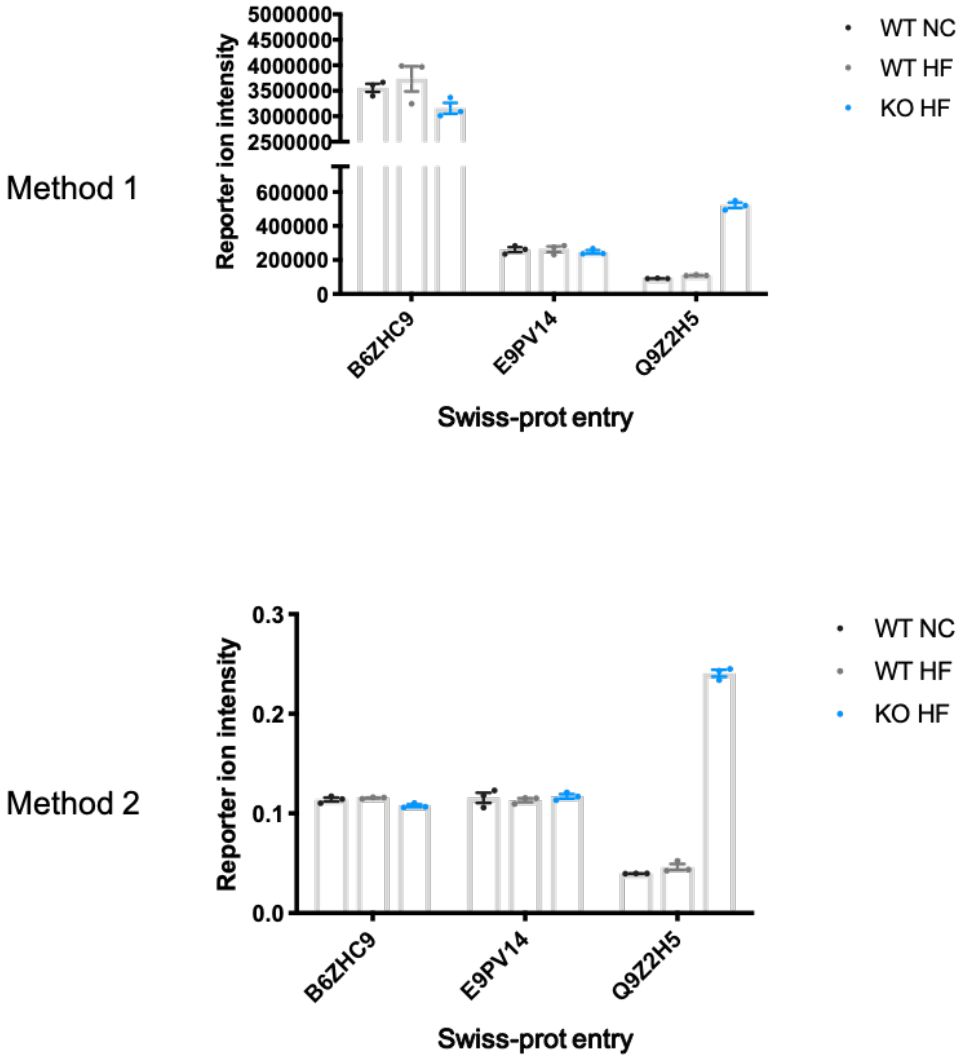

Figure 4.18 Normalised protein expression of the 4.1N Uniprot entries based on unique peptides. Three 4.1N entries within the Swiss-prot database were identified in proteomics, each with unique peptides. Normalisation and quantification of the unique peptides indicates that only 4.1N protein with sequence corresponding to entry Q9Z2H5 was altered with BACE1 KO in the hippocampus. This trend was consistent across both methods of analysis. n=3 per group. Individual data points indicate the range of data. Standard error indicated by error bars.

During proteomic analysis, it was noted that multiple entries exist within the Swiss-Prot and TrEMBL databases for protein 4.1N. These entries predominantly differ by single amino acid changes and splice variation (Figure 5.12). However, two entries (E9PV14 and B6ZHC9) exhibit substantial sequence variation from the others. As these entries were not reviewed within the database and were not significantly altered by BACE1 expression (Figure 4.18), they were not considered for further study. Interestingly, MS identified peptides containing

nucleotide polymorphisms from 3 different 4.1N sequences within each replicate corresponding to database entries A2AUK5, B6ZHC9 and Q9Z2H5. Entry A2AUK8 represents an alternatively spliced form of the A2AUK5 sequence and Q9Z2H52 & 3 represent splice variants of the Q9Z2H5 sequence (Figure 4.19). Due to concerns raised by MS spectra allocation in BACE1 identification, the spectra of these peptides were quality checked. It was determined that the spectra provided clear evidence for the presence of peptides from all forms of 4.1N therefore these sequence differences may suggest an accumulation of mutations in the EPB41L1 gene in these mice or the presence of a pseudogene or gene duplication of protein 4.1N; The ramifications of either are yet to be established. However, only the Q9Z2H5 variant was significantly increased with BACE1 expression as identified by both methods of analysis. This sequence is also the main entry within the Swiss-Prot database and the only one to have been reviewed.

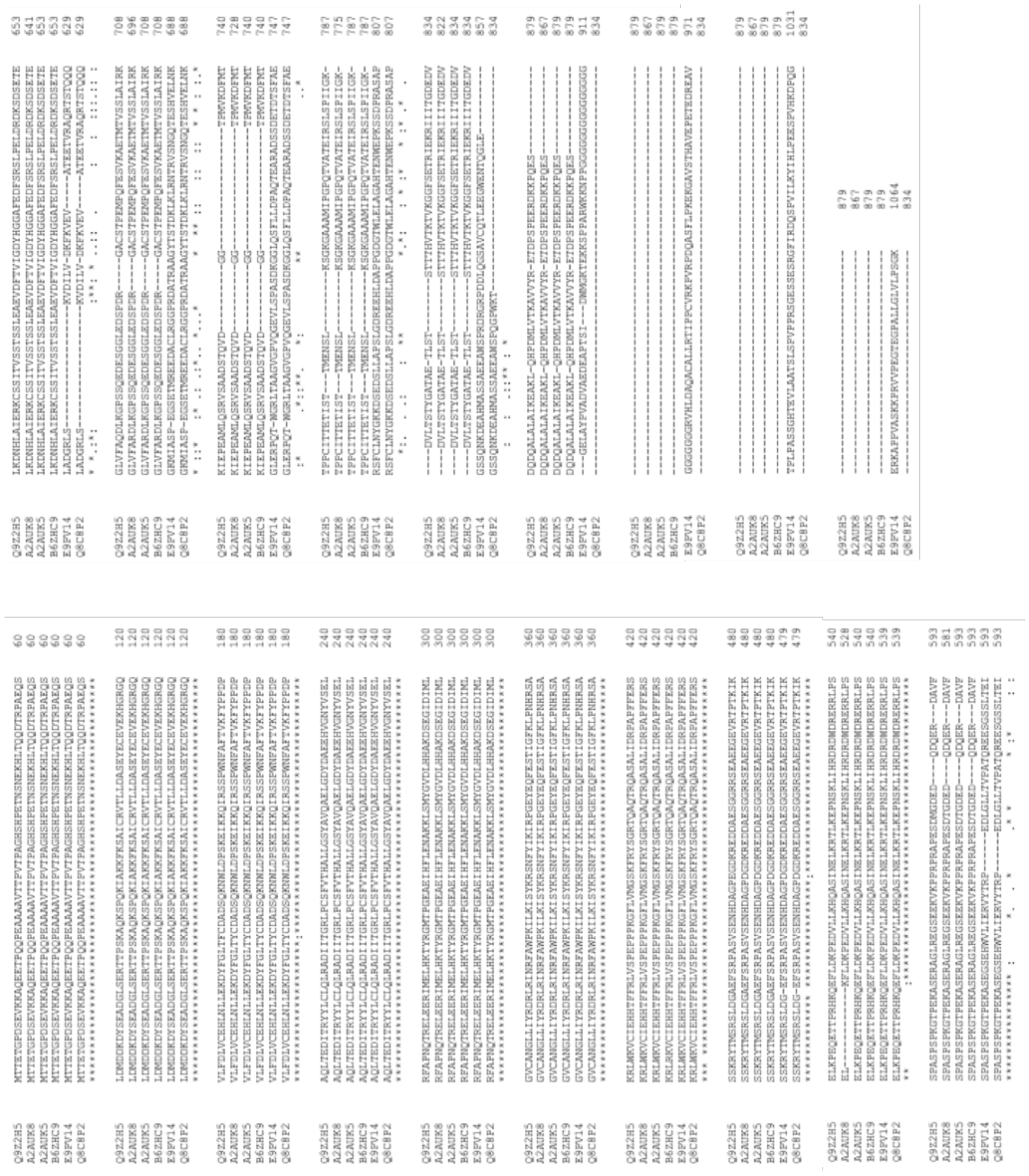

Figure 4.19 Multiple sequence alignment of UniProt database entries for protein 4.1N. All 6 entry sequences were identified as determined by the presence of peptides containing unique sequence variations for each entry. Sequences Q9Z2H5, A2AUK8, A2AUK5 and B6ZHC9 are distinguished by a small number of single amino acid changess. Entries E9PV14 and B6ZHC9 contain significantly different C-terminal regions to other sequences.

Many identified peptides within the proteomic screen covered exon junctions, allowing some interpretation of splice differences within the brain. A key difference between the 4.1N peptides between brain regions is the presence of a peptide spanning the N-terminal region of exon 4 in the hypothalamus that is absent within the hippocampus (Figure 4.16 and 4.17 respectively). This, in conjunction with an N-terminal exon 5 peptide in the hippocampus that is not in the hypothalamus, suggest an absence of exon 4 in the hippocampus. This would lead to the loss of a trypsin cleavage site at R163. Loss of this exon represents loss of 5% of the FERM domain corresponding to a region in a ubiquitin-like roll domain in the domain superfamily CATH 3.10.20.90 in protein 4.1R. However, this domain (3binA01) exhibits great diversity between members of the superfamily, so the potential functional relevance of exon 4 could not be determined. However, this region has been shown to be involved in the binding of glycophorin proteins to protein 4.1R so it is therefore feasible that this exon contributes to protein binding or specificity (Mohandas, Jap, Han, Nunomura, & Takakuwa, 2000).

4.3 Discussion

4.3.1 Comparison of WT mice between BACE1 KO and BACE1 KI transgenic lines

As described in section 3.3.1, the BACE1 KO and BACE1 KI mouse lines are different in their levels of breeding onto the C57bl/7J mouse line with the BACE1 KI being approximately >99% C57bl/6J. The BACE1 KO is genetically 97-99% C57bl/6J and 1-3% 129P having been repeatedly crossed onto this mouse line and back-crossed onto C57bl/6J in order to overcome breeding difficulties. This brings a degree of genetic variability into the study before considering the effects of BACE1 expression. Due to exposure to a metabolic stress within the study design and the use of BACE1 KI mice for validation attempts, it was decided that WT animals from the BACE1 KI (WT[KI]) line should be compared to WT animals from the BACE1 KO (WT[KO]) line in their body weight response to HFD. Since no other tests were performed on the mice to test their metabolic phenotype (eg. insulin/glucose tolerance) this was the only method that could be used to compare the metabolic function of the two mouse lines. Data here showed that whilst the WT[KI] animals were consistently heavier than those from the WT[KO] line, their weight gain in response to HFD was comparable and therefore their

response to metabolic stress may be comparable also. The starting weight (at 8wks age) of both WT[KO] mice were heavier than previously observed. Indeed, their starting weight was greater than the weights of mice from both genotypes after 12 weeks of HFD in previous studies (Meakin et al., 2012). However, the weight gain observed throughout the 12-week dietary intervention was consistently greater than seen previously, suggesting that their metabolic response to HFD has not changed. The body weights of WT[KI] mice were comparable to those previously reported in this mouse line (Plucinska et al., 2014; Plucińska et al., 2016). As no data were collected on the lean mass of these models and the body length of WT[KI] mice is not published, it cannot be determined whether the WT[KI] line are heavier due to increased size compared to WT[KO] or increased lean/fat mass but these data suggest the metabolic response to HFD is comparable between WT[KI] and WT[KO] groups.

4.3.2 Body weight gain in response to HFD and BACE1 expression

Body weight analysis revealed that HFD in WT mice led to DIO after 12 weeks of dietary stress. Unless otherwise stated, from here on 'WT' refers to WT mice from the BACE1 KO line. Obesity was defined in this study as the change in body weight over 12 weeks greater than three standard deviations of the mean weight gain of WT NC fed mice. Mice with weight gain less than this were considered DIO resistant and were not included in the study. By this definition, BACE1 KO mice were DIO resistant whereas BACE1 KI mice were considered obese. BACE1 KI mice were not heavier than WT DIO mice indicating that increases in BACE1 expression did not lead to increased weight gain; BACE1 KO however did offer some, but not total, protection against DIO. Both BACE1 KO and WT mice on HFD exhibited greater body weight gain in response to HFD than previously published with weight changes observed after 12 weeks in this study comparable to the weight change observed after 20 weeks of dietary intervention in previous studies (Meakin et al., 2012). This suggests that the current BACE1 KO mouse line have a greater propensity to fat accumulation than previously observed. As the diet composition and supplier remains unchanged, this effect is may be due to genetic drift within the BACE1 KO line since it was first obtained or environmental factors causing changes in stress response. Metabolic phenotyping in current BACE1 KO mice could provide further insight into whether

this line still demonstrate protection from metabolic dysfunction with dietary challenge.

It was also noted that WT NC mice were consistently heavier throughout the study compared to previous data. As no other measurements were taken regarding lean mass or body length, it cannot be determined whether this difference is due to increased fat mass, lean mass or difference in body size in current mice compared to previous animals.

4.3.3 Comparison of proteomic samples indicate good replicates within groups

Pearson's correlation coefficients revealed very strong correlation between replicates with each condition indicating good replicates within groups. Replicate 2 within the WT HFD group exhibited less correlation to others within the group but with a coefficient over 0.96, however this result still represents very high correlation between replicates. This pattern was observed in both methods of analysis.

PCA indicated little variability between the samples; therefore, this indicates few differences between the proteomes of all samples. This was an early indicator to suggest few proteomic hits between these groups.

4.3.4 Identification of possible BACE1 regulated proteins

As predicted by PCA, few proteins were identified as significantly changing with BACE1 expression, with neither analysis finding any significant differences with diet in either hippocampus or hypothalamus.

The data acquired through the 'binning' of reporter ion ratios, whilst increasing the number of hits, does not provide strong statistical evidence for those identified. This is due to a lack of bias correction and use of median sweep normalisation. Whilst this type of proteomic analysis was a good way of providing indicators of proteomic variability between samples and enabled pathway analysis to be conducted, these data are not as statistically reliable. In order to determine the most likely BACE1 regulated proteins from these data, only data

collected from volcano plots between mice on the BACE1 KO mouse line were continued for analysis.

Volcano plots produced from method 2 analysis identified 19 protein hits between the WT NC and KO HFD groups in the hippocampus and 15 in the hypothalamus. Comparison of WT HFD and BACE1 KO HFD produced fewer hits with 12 and 9 in the hippocampus and hypothalamus respectively. As the comparison between WT NC and WT HFD produced no hits, it was determined that hits in both of these comparisons are the result of changes in BACE1 expression and that, in this instance, genotype appears to have a greater effect on the hippocampal and hypothalamic proteome than HFD. However, as the WT NC vs KO HFD incorporated two variables, this comparison was not considered on its own, but rather, in combination with WT HFD vs KO HFD comparisons. Hits from WT HFD vs KO HFD were cross-referenced with WT NC vs KO HFD hits and proteins identified in both comparisons were considered to be the most significant. This analysis was conducted in each tissue and was followed by comparison between tissues. 10 proteins were therefore identified in the hippocampus (BACE1, Calcium transporting ATP-ase 2, Caskin 1, Microtubule-associated protein 1B, Protein 4.1N, PTPNS1, Serine protease inhibitor A3K, Uncharacterised aarF domain containing protein kinase 5 and thymosin β) and 7 in the hypothalamus (Microtubule-associated protein 1B, Calcium transporting ATP-ase 2, Protein 4.1N, Coiled-coil domain-containing protein 93, PTPNS1, Serine protease inhibitor A3K and Uncharacterised aarF domain containing protein kinase 5). Of these, all were upregulated with BACE1 KO except BACE1. Interestingly, 6 of the 7 of the proteins identified as changing with BACE1 in the hypothalamus were also detected in the hippocampus; thereby adding credibility to these proteins as being regulated by BACE1. Furthermore, upregulation of Aldo-keto reductase family 1 member B10 was identified only under WT NC Vs KO HFD conditions suggesting that this protein is under the dual control of BACE1 and diet. Due to the absence of a KO NC group, this hit would require further dietary studies to determine whether diet alone regulates expression and, in the absence of BACE1, is rescued.

Aldo-keto reductase family 1 member B10 reduces carbonyls to alcohols with cofactor NADPH (Cao, Fan, & Chung, 1998). The aldo-ketoreductases are more

commonly associated with cancers both centrally and within peripheral tissues (Laffin & Petrash, 2012). Originally identified in the GI tract, AKR1B10 has been shown by Ma et al. (2008) to be a potential regulator of fatty acid synthesis by association with acetyl-CoA carboxylase-α. In addition, AKR1B10 has been shown to reduce toxic aldehydes produced from the reduction of fatty acids in lipid membranes by reactive oxygen species (Martin & Maser, 2009) including 4-hydroxynonenal- a reactive aldehyde increased in the plasma of AD patients that may contribute to Aβ protofibril formation (McGrath et al., 2001; Siegel et al., 2007).

Also detected in the hippocampus was the brain specific scaffold protein caskin-1. Caskin-1 binds to CASK, a multi-domain scaffold protein known to interact with neurexins (Hata, Butz, & Südhof, 1996). Amongst the many functions of CASK, including synaptic ion channel targeting and synaptic adhesion, CASK binds transcription factor TBR1, a protein implicated with autism, a neurological disability which itself, has been linked with increased non-amyloidogenic APP processing and decreased amyloid secretion (Sokol et al., 2006). Functional knockout of TBR1-CASK interaction leads to memory deficits in mice (T.-N. Huang & Hsueh, 2017; A. Nagy et al., 1993). Caskin-1 KO mice exhibit deficits in both chronic pain transmission, anxiety and fear conditioning behaviours suggesting a role for this protein in synaptic transmission (Katano et al., 2018). Interestingly, the Caskin-1 binding partner CASK is also known to bind to protein 4.1R. A family member of another hit found in this study- protein 4.1N (Biederer & Südhof, 2001; Cohen et al., 1998). Surprisingly, BACE1 was only identified as a hit within the hippocampus and not the hypothalamus. This and validation of BACE1 expression will be discussed further in chapter 5.

The 6 proteins identified as hits in both brain regions include calcium transporting ATPase 2, a plasma membrane protein integral in the process of ATP-dependent calcium export out of the cell. Calcium signalling is an important messenger in eukaryotic cells mediating important functions such as cell proliferation, steroid synthesis and differentiation (Berridge, Lipp, & Bootman, 2000). It is of particular importance to neurons where it initiates synaptic neurotransmitter release in response to action potential. It is therefore essential for neuronal function to maintain the calcium gradient across the plasma membrane. Studies have

indicated that calcium transport may be dysfunctional in AD and amyloid peptides have been shown to inhibit Atp2B proteins, thereby inhibiting calcium efflux. However, this was not found to be the case with Atp2b2 (Berrocal et al., 2009).
Microtubule-associated protein 1B (MAP1B) is a stabilising protein for microtubule and possibly actin filaments (Tögel, Wiche, & Propst, 1998). This protein is a member of the MAP1 family of microtubule binding proteins, closely associated with MAP2 proteins of which Tau is a member. Neuronal deficiencies in MAP1B have been shown to lead to reduced excitatory synaptic density and increased inhibitory or immature synapses (Bodaleo, Montenegro-Venegas, Henríquez, Court, & Gonzalez-Billault, 2016).
Protein 4.1N was significantly upregulated with BACE1 KO in both brain regions. This protein will be discussed later in this section.

PTPNS1- also known as SIRPα- is a type I transmembrane immunoglobulin and receptor for CD47. Within the brain it contributes to synaptogenesis by promoting presynaptic maturation in hippocampal neurons. Interestingly, PTPNS1 has also been shown to shed its extracellular domain as part of the synaptic maturation process (Toth et al., 2013). Furthermore, both ADAM10 and the γ-secretase complex have been identified as proteases of PTPNS1 lending support towards the idea of PTPNS1 as a putative BACE1 substrate. Furthermore, PTPNS1 expression was found to be enriched in lysates of BACE1 -/- primary pancreatic islets but not identified as a hit in the brain in BACE1 secretome studies (Stützer et al., 2013). In metabolism, PTPNS1 is known to activate both SH2-domain-containing protein tyrosine phosphatases SHP-1 and SHP-2 (Fujioka et al., 1996). SHP-2 specifically is a known regulator of both insulin and leptin signalling through IRS-1 binding and inhibition of the JAK-STAT pathway as well as activating MAP kinase signalling downstream of both of insulin and leptin receptor activation (Banks et al., 2000; Myers et al., 1998).

Whilst little published evidence exists as to the specificity and function of Serine protease inhibitor A3K, some studies have suggested a role for this protein in anti-inflammatory effects with decreased expression leading to increased TNFα as well as preventing oxidative stress in diabetic retinopathy (Zhang, Hu, & Ma, 2009; B. Zhang & Ma, 2008).

No published evidence currently exists for the function of uncharacterised aarF domain containing protein kinase 5. Gene ontology suggests kinase activity for this protein through the presence of a kinase-like domain within the protein sequence and transmembrane- like helical domain.

Thymosin β 15 is an actin binding protein known to contribute to cancer metastasis and expression attenuated by transforming growth factor beta 1 (TGFB1) (Banyard, Barrows, & Zetter, 2009; Bao et al., 1996). Currently, little is known about the function of this protein, particularly within the brain.

Coiled-coil domain-containing protein 93 is a component of the COMMD/CCDC22/CCDC93 (CCC) complex- a regulator of protein recycling between endosomes and the cell surface including the LDL receptor (Bartuzi et al., 2016; Phillips-Krawczak et al., 2015). However, the mechanism through which this is achieved has not yet been established.

Method 2 identified 3 proteins as possible BACE1 effectors. Within the hypothalamus, Thioredoxin-domain containing protein 15 (TXNDC15) and α-L-fucosidase (FUCA1) were identified. Interestingly, these hits were not identified by semi-quantitative analysis thereby indicating the importance of normalisation method in proteomic analysis.

TXNDC15 is another single pass transmembrane protein making it a candidate as a BACE1 substrate. Besides structural data, little is known about this protein and BLAST results reveal very little sequence similarity to any other protein using either mouse or human protein sequences. It is a member of the protein disulphide isomerase (PDI) family of proteins known to contribute to protein folding in the ER and redox homeostasis; the mechanisms by which PDIs contribute to these processes have been reviewed by Okumura et al. (2015). Early studies have suggested a role for TXNDC15 in repressing store-operated Ca2+ entry (SOCE) in HELA cells (Konrad, 2016). This method of Ca2+ homeostasis involves the calcium channels TRPC and ORAI as well as STIM- a calcium signal transducer that facilitate ORAI mediated calcium entry into the cell (Yandong Zhou et al., 2018). SOCE has been implicated in multiple neurodegenerative diseases including AD, a subject which has been reviewed by

Bollimuntha et al. (2017). TXNDC15 mutations are associated with Meckel-Gruber syndrome- a lethal autosomal recessive disorder characterised by polycystic kidneys, liver fibrosis and CNS malformations (Kheir et al., 2012; Shaheen et al., 2016). High-throughput interactome analysis in HEK293 cells indicate that TXNDC15 interacts with the E3 ligase MARCH6 and GPI anchor biosynthesis protein PIGN (Huttlin et al., 2015). PIGN mutation has been shown to cause significant reduction in GPI anchoring and results in epilepsy, developmental delay and cerebellar atrophy in humans (Ohba et al., 2014). However, the association between TXNDC15 and PIGN has not been further validated. Cell type specific labeling using amino acid precursors (CTAP) proteomics identified 368 interacting proteins with TXNDC15, however BACE1 was not identified (Shaheen et al., 2016). Beyond this, little is known about the function of this thioredoxin family protein.

FUCA1 is an enzyme within the endosomal system responsible for the removal of fucose sugars from glycoproteins. Fucose, a monosaccharide, is a subunit of N and O-linked glycans and glycolipids. It is often the terminal component of glycan branches but can exist within the polysaccharide chain. The most common form of fucosylation is with the addition of a ‘core fucose’ to the core structure of N-terminal glycans (Schneider, Al-Shareffi, & Haltiwanger, 2017). (Figure 4.20) This modification occurs within the golgi by the fucosyltransferase FUT8 and is a requirement for postnatal and lung development in new born mice. Most FUT8 KO mice die within days due to growth defects most likely as a result of increased TGF-β1 activation and reduced EGF and PDGF signalling (Xiangchun Wang, Gu, Miyoshi, Honke, & Taniguchi, 2006). Terminal fucosylation also occurs within the golgi on N-terminal glycans by a variety of fucosyltransferases (Schneider et al., 2017).

Fucose may also be directly attached to serine and threonine residues on proteins with EGF and TSR repeats through two different fucosyltransferases FUT12 and FUT13 respectively (Luo, Koles, Vorndam, Haltiwanger, & Panin, 2006; Luo, Nita-Lazar, & Haltiwanger, 2006; Shao, Moloney, & Haltiwanger, 2003).

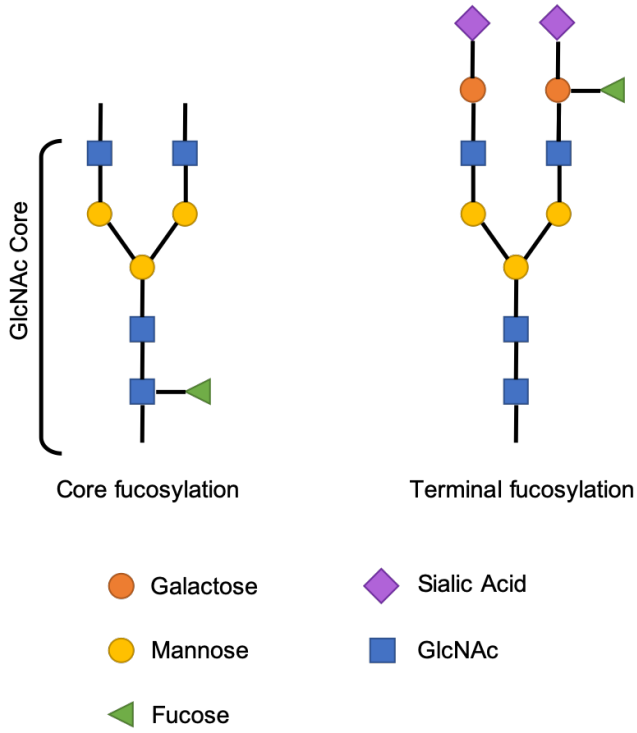

Figure 4.20 Structure of GlcNAc and types of fucosylation. Examples of N-linked fucose modification; Core and terminal fucosylation.

Fucose has been shown to be important in LTP with increased fucose uptake within the hippocampus having been shown to occur with LTP stimulation and brain fucose injections increasing LTP in rats (Krug, Wagner, Staak, & Smalla, 1994; Pohle, Acosta, Rüthrich, Krug, & Matthies, 1987).

Deficiencies in FUCA1 enzymatic function lead to fucosidosis: a lysosomal storage disorder whereby accumulations of undegraded fucosylated proteins and lipids in tissues lead to a variety of symptoms. It particularly affects the brain leading to seizures, motor deficits and motor and cognitive deficits which progress with age leading to premature death (Willems, Seo, Coucke, Tonlorenzi, & O'Brien, 1999). Demyelination and neuronal loss occurs within multiple brain regions in fucosidosis including the hypothalamus and cerebral cortex (Galluzzi, Rufa, Balestri, Cerase, & Federico, 2001). Symptoms in the periphery include angiokeratoma, muscle stiffness and visceromegaly, recurrent pulmonary infections, skeletal bone and cartilage abnormalities (dysostosis multiplex) and stunted growth (Turkia et al., 2008). Interestingly, proteomic analysis of lipid raft composition in 3xTgAD mice identified FUCA1 expression in healthy controls but not in the AD model (Chadwick, Brenneman, Martin, & Maudsley, 2010). This is contrary to previously published sub-cellular expression of FUCA1 leading to the idea of FUCA1 transport between the plasma membrane and lysosomal system. In addition, kinetic studies identified the optimal pH for FUCA1 activity as being normal physiological conditions (pH6.5-7) as opposed to the acidic conditions within the lysosome (Ezawa et al., 2016). The same study identified FUCA1 expression within the perinuclear region suggesting expression within the ER or golgi. This study also indicates that this expression profile is altered under AD conditions.FUCA1 is increased in cancers and has been identified as a target for the tumour suppressor and apoptosis inducer p53 (Cheng et al., 2015; Ezawa et al., 2016). Furthermore, p53 is upregulated in AD brains (Hooper et al., 2007).

Protein 4.1N was identified as being upregulated with BACE1 KO through both methods of analysis. The 4.1s are a little-characterised family of large cytoplasmic proteins of which protein 4.1N is a member. All family members are membrane targeted through a N-terminal 4.1 protein, Ezrin, Radixin and Moesin (FERM) domain, a central spectrin/actin binding domain and a C-terminal domain that allows substrate binding. (Figure 4.21) Encoded by the EPB41 genes, they

contain a large number of small exons that are differentially spliced in 3 regions between the known domains: U1, U2 and U3. Alternative splicing of the 4.1 proteins within the brain may be regulated by the RNA binding protein Nova1 (Ule et al., 2005). NOVA1 has been shown to increase in early Braak stages before the cognitive changes of AD appear, reducing to normal levels again in the later stages of the disease (Barbash et al., 2017). Little structural data has been collected on these proteins with only the FERM domain having been mapped to high resolution. Difficulties in gaining structural data suggests these proteins are largely unstructured. The 4.1 family has been extensively reviewed by Baines et al. (2014).

The best characterised of this family is protein 4.1R; first identified in erythrocytes, it is implicated in maintaining cell shape and plasma membrane organisation through interaction with the cytoskeleton and binding to integral membrane proteins (Gauthier, Guo, Mohandas, & An, 2011). A well-known interaction of 4.1R is that with the protein CASK (Biederer & Südhof, 2001). CASK is a ubiquitously expressed scaffold protein involved in protein anchoring and ion channel trafficking and contributes to gene expression through interaction with the transcription factor TBR1; a factor shown to be important in neuronal migration and axon formation in mature neurons and in developing embryos (Huang & Hsueh, 2017). Protein 4.1R also has suspected interactions with the neuroligins; cell adhesion proteins on the post-synaptic membrane that maintains synaptic connections within the brain through the association with neurexin (Biederer & Südhof, 2001). Additionally, cell surface expression of neuroligins 1,2 and 3 were recently identified as increasing with BACE1 inhibition (Herber et al., 2018).

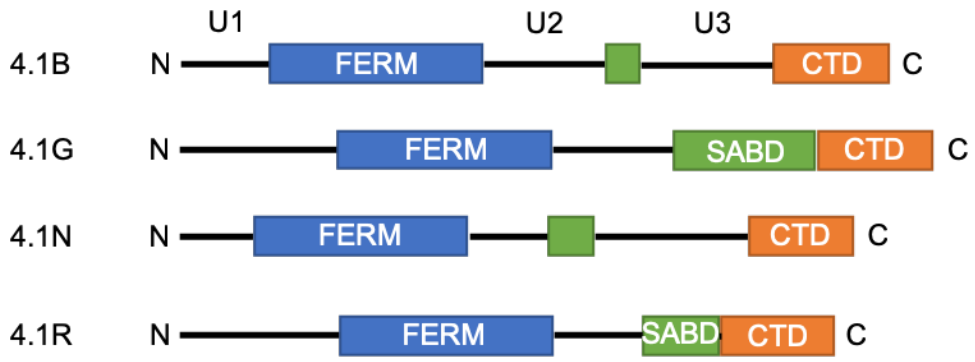

Figure 4.21 Domain profile of protein 4.1 family members B,G,N and R. Conserved FERM, Spectrin-actin binding (SABD) and C-terminal domains (CTD) are separated by alternatively spliced U1, U2 and U3 regions. These regions represent the majority of variability between these isoforms.

The vertebrate 4.1 family consists of 4 members: 4.1R, 4.1N, 4.1G and 4.1B all of which were first identified within the brain but are expressed in many tissues. 4.1N was first identified in neurons and expression within the brain is known to be higher than other tissues. In the brain it has been identified within the cerebellum in the granule cell layer and deep cerebellar nuclei. It is also expressed within all layers of the cortex, the striatum, the DG and CA1, 2 and 3 of the hippocampus (Walensky et al., 1999). 4.1N has been suggested to interact with D2 and D3 dopamine receptors (Binda, Kabbani, Lin, & Levenson, 2002) and AMPAR mGluR1 subunits (Lin et al., 2009; Shen, Liang, Walensky, & Huganir, 2000) at the plasma membrane and may be a requirement for synaptic expression of these receptors. 4.1N has also been associated with the synaptic calcium release channel inositol (1,4,5)-trisphosphate receptor 1 (Fukatsu, Bannai, Inoue, & Mikoshiba, 2006; Maximov, Tang, & Bezprozvanny, 2003).
4.1N has been shown to interact with cell adhesion molecules such as NECL1 (Yan Zhou et al., 2005) and acts as part of a neuronal complex to form actin filaments through interactions with CASK and neurexins (Biederer & Südhof, 2001).

4.1N has been shown to play a role in cell division through its interactions with the nuclear mitotic apparatus (NuMA) and regulates the proliferative effects of nerve growth factor (Ye, Compton, Lai, Walensky, & Snyder, 1999). PI3K- an activator of mTOR and a regulator of the cell cycle has also been shown to be regulated by 4.1N. 4.1N binding to an enhancer of PI3K named PIKE leads to

abolition of PI3K inhibition suggesting a role for 4.1N in core cellular processes such as protein/lipid synthesis, autophagy/mitophagy and cell growth (Ye et al., 2000).

These data hint at multiple functions for BACE1 through the upregulation of a variety of proteins in the BACE1 brain tissues. A recurring theme can be identified in BACE1's regulation of proteins involved in cell adhesion and synaptic function through the identification of hits Caskin-1, MAP1B, PTPNS1 and protein 4.1N. The effects of BACE1 on proteins such as FUCA1, TXNDC15 may be dependent on BACE1 sub-cellular localisation as these proteins are suspected to function in the endosomal system and endoplasmic reticulum respectively.

4.3.5 Pathway Analysis

In order to gain further insight into the physiological function of BACE1, the hits identified through 'binning' of reporter ion intensities analysis by method 1 were input into ingenuity pathway analysis software. These data were used as other methods of analysis did not produce hits in high enough quantity to conduct pathway analysis. By identifying pathways that are over-represented by WT NC vs WT HF and WT HF vs BACE1 KO vs HF comparisons, possible BACE1 regulating pathways were identified. Within the hippocampus both lipid metabolism and nervous system development pathways were over-represented in the protein hits. However, both lipid metabolism and nervous system development pathways identified were different between groups suggesting four independent pathways influenced by BACE1. Indeed, the pathway identified in the WT HF vs BACE1 KO group contained BACE1 as part of the pathway. The same was found of the hypothalamic nervous system development and function, cellular assembly and organisation, cellular movement, small molecule biochemistry and cancer pathways that were identified as changing with both diet and BACE1 expression. Overall, pathway analysis did not identify any common pathways influenced by diet and those influenced by BACE1 expression. This is unsurprising as data indicate that the HFD group did not exhibit significantly increased BACE1 expression and therefore dietary intervention in this instance is unlikely to have influenced BACE1 pathways. This also indicates that the absence of BACE1 with HFD does not result in down-regulatory effects on the same pathways as are upregulated with HFD but instead maintains metabolic

function through alternative pathway activation. However, this analysis was conducted using a method of analysis that was less statistically stringent than the others used and this must be considered when evaluating these results.

4.3.6 BACE1 expression in animal models

Proteomic and western blot analysis in both the rodent hippocampus and hypothalamus indicate that 12 weeks of HFD is not sufficient to increase expression of BACE1. This is unsurprising as previous studies have indicated that 10 weeks of dietary challenge is insufficient to raise BACE1 activity (Meakin, Jalicy, et al., 2018). However, it was surprising that no significant hits were identified within the brain with diet. This suggests that, at this dietary timepoint, either changes predominantly occur at the PTM level (as seen with phosphorylation changes in chapter 3 between BACE1 models) and not identifiable with this type of proteomics or that the study was underpowered and that a greater number of replicates are required to obtain significant effects.

Of main concern is the presence of BACE1 peptides within the BACE1 KO mouse model identified by proteomics. Upon further analysis, it was discovered that the MS spectra identifying the BACE1 peptides were of very poor quality making this result unreliable whilst the spectra identifying other protein hits were robust. In combination with poor peptide coverage and western blot analysis indicating an absence of BACE1 within all brain regions in the global BACE1 KO; it was determined that the proteomic identification of BACE1 within this model was unreliable and likely erroneous. This result does bring into question the reliability of the dietary data as poor BACE1 spectra were observed in all groups. Particularly as western blot analysis suggests an increase of BACE1 within the hypothalamus with dietary intervention, despite this trend not being significant upon quantification.

As a method of comparison between the cohort used in proteomic analysis and those used for preliminary study (as shown in chapter 3), GSK3 expression and phosphorylation were determined. As described in chapter 3, serine phosphorylation of both GSK3α and β were substantially increased with BACE1 KI in the cortex. This result was not replicated within the second cohort and may be due to a variety of factors. Whilst the first cohort were female, non-fasted mice with no dietary challenge, the second were male, fasted and placed on a 12-week

HFD. The loss of GSK3 serine phosphorylation may therefore be due to sex differences between the models, the introduction of a dietary intervention or, most likely, the fasted status of the mice (Clodfelder-Miller, De Sarno, Zmijewska, Song, & Jope, 2005; Kothari et al., 2017).

Due to the length of fast, it may be that protein synthesis was reduced for energy conservation which may have affected the overall proteome of the mice. Future studies would be better adopting a fast-refeed method whereby a shorter fasting period of 6 hours would be followed by a short period of food reintroduction prior to tissue harvest. This would enable interpretation of metabolically important pathways such as insulin and leptin responses that are also influenced by BACE1 expression (Dinely, Jahrling, Denner, 2014; Folch et al., 2015; Meakin et al., 2012; Meakin, Jalicy, et al., 2018; Plucińska et al., 2016). Furthermore, the type of proteomic analysis conducted may not have been appropriate. As preliminary data did not indicate changes in total protein with diet, it may have been more informative to identify changes in the proteome phosphorylation status. Furthermore, the complexity of multiple comparisons reduces the statistical strength of the proteomic analysis. Before looking into the effects of BACE1 expression in combination with dietary stress, it would be beneficial to look for changes in each variable individually to simplify the study.

4.3.7 Conclusions

Large differences in protein hits were achieved by using different methods of normalisation prior to analysis. This led to uncertainty with regard to which hits were significant enough for further study. Whilst many hits were observed by binning the reporter ion ratios in semi-quantitative analysis, pathway analysis of these hits did not reveal any pathways by which BACE1 may regulate metabolism. As this method did not include stringent statistical analysis, there were concerns regarding the significance of these hits and for this reason, these hits were not considered for validation. The analysis most likely to have produced statistically significant results and therefore most likely to be reproducible, was method 2. For this reason, TXNDC15, FUCA1 and Protein 4.1N were carried forward for validation studies and further study whilst the hits produced from qualitative analysis were not carried forward. However, protein 4.1N was identified as a hit with BACE1 KO in both volcano analyses of method 1 as well

as method 2, making this the hit most likely to be influenced by BACE1 expression.

Chapter 5

Testing validity of brain proteomic changes with BACE1 expression and diet

5.1 Introduction

As described in chapter 4, proteomic analysis of hippocampal and hypothalamic tissues of BACE1 KO HFD mice with WTNC and HFD controls identified 3 proteins that significantly changed with BACE1 expression. In the hypothalamus, both FUCA1 and TXNDC15 were significantly increased in the BACE1 KO HFD compared to WT HFD and NC controls. Within the hippocampus, expression of the protein 4.1N was identified as significantly increasing in the BACE1 KO mice when compared to WT controls. Identification of a relationship between BACE1 expression and 4.1N was considered to be highly relevant to AD and neurodegeneration. In part, due to the known relationship between 4.1N expression within the brain and cell surface AMPA receptor (AMPAR) expression. As described in chapter 1, AMPARs are key modulators of action potential and increased cell surface expression as a result of NMDA receptor (NMDAR) activation is one mechanism through which LTP and LTD occur. Therefore, increased 4.1N expression with BACE1 KO may indicate increased NMDAR and AMPAR stability at synapses and better cognitive function. It is therefore important to determine whether BACE1 influences excitatory signalling within the hippocampus and LTP.

Membrane anchoring is an essential part of maintaining neurotransmitter (NT) function, ensuring that the fluidity of the plasma membrane does not result in mis-localisation and therefore loss of function of ion channels and NT receptors. Dendritic spines on excitatory neurons have been shown both *in vitro* and *in vivo* to contain a high level of F-actin (Allison, Gelfand, Spector, & Craig, 1998; Matus, Ackermann, Pehling, Byers, & Fujiwara, 1982). 4.1N is a member of the 4.1 family, membrane targeted proteins that stabilise transmembrane targets by anchoring to the cytoskeleton. 4.1N has been shown to stabilise cell surface expression of AMPARs GluR1 and GluR4- both of which localise to post-synaptic densities and require cytoskeletal anchoring as an integral part of their function (Coleman, Cai, Mottershead, Haapalahti, & Keinänen, 2003; Lin et al., 2009; Scott, Keating, Bellamy, & Baines, 2001; Shen et al., 2000). Additionally, stable actin filaments have been shown to be important in the expression and distribution of synaptic NMDARs but not GABARs indicating the importance of the cytoskeleton in excitatory, but not inhibitory signalling (Allison et al., 1998). Furthermore, studies have indicated that dynamic actin is essential to LTP

(Krucker, Siggins, & Halpain, 2000). However, somewhat contradictory is a study (Gimm *et al,.* 2002) that suggests that the 4.1N spectrin actin binding domain is functionally incapable of binding to spectrin and actin. This, therefore, raises questions as to how 4.1N stabilises glutamate receptors as another study (Wozny *et al,.* 2009) revealed that the 4.1N/4.1G double knockout mice exhibited no alteration in hippocampal excitatory connectivity. However, it must be noted that these animals did not exhibit complete knockout of a smaller variant of 4.1N. Expression of 4.1B was unaltered but 4.1R expression was not reported so it is also possible that compensation can occur through upregulation of 4.1R. Protein 4.1N and its family members 4.1G and 4.1B have been shown to be upregulated in both amyloid and tau aggregates in the AD hippocampus but few studies have explored a connection between 4.1 proteins and AD (Ayyadevara et al., 2016).

There are multiple ways in which neurons can be classified. Often, they are described based on NT release such as excitatory or inhibitory if they release glutamate or GABA respectively. Neurons can also be defined by cell type. This is typically descriptive of cell morphology and gives a generalised idea of function. Two key neuron types within the brain are granule cells and pyramidal neurons. Granule cells are the most common and the term is used to describe neurons with small cell bodies. Typically, they are found within the DG of the hippocampus, the granular layers of the cerebral cortex, the granule layer of the cerebellum, the olfactory bulb and the dorsal cochlear nucleus. Atypical of neurons, DG granule cells actively undergo neurogenesis. These cells are excitatory and extend glutamatergic axons into the CA3 region of the hippocampus known as mossy fibers. Mossy fibers are distinct unmyelinated axons that connect granule cells of the DG to pyramidal cells of the CA3 and mossy cells of the DG polymorphic layer (Figure 5.1). Within the polymorphic layer, the mossy fibers become heavily branched leading to a large number of synapses from DG granule cells (Claiborne, Amaral, & Cowan, 1986).

Despite nomenclature, granule cells are not present within the granule layers of the cerebral cortex. These layers are predominantly small pyramidal cells and stellate cells (Figure 5.2). Pyramidal cells are highly expressed throughout the cortex and forebrain regions such as hippocampus. These cells receive both glutamatergic and GABAergic signals. The main suggested function of these

neurons is the perpetuation of action potentials (Reviewed by (Spruston, 2008)). It has also been suggested that the extent of pyramidal cell branching within the temporal lobe is an indicator of IQ (Goriounova et al., 2018). Pyramidal cell loss is associated with early stages of AD (Davies, Horwood, Isaacs, & Mann, 1992). AD mouse models suggest altered glucose metabolism and reduced synaptic density within mossy fibers of the DG with indications that loss of connectivity may be overcome with mimetics of NCAM- a neural cell adhesion protein (Corbett et al., 2013; Piquet et al., 2018; Silva et al., 2019).

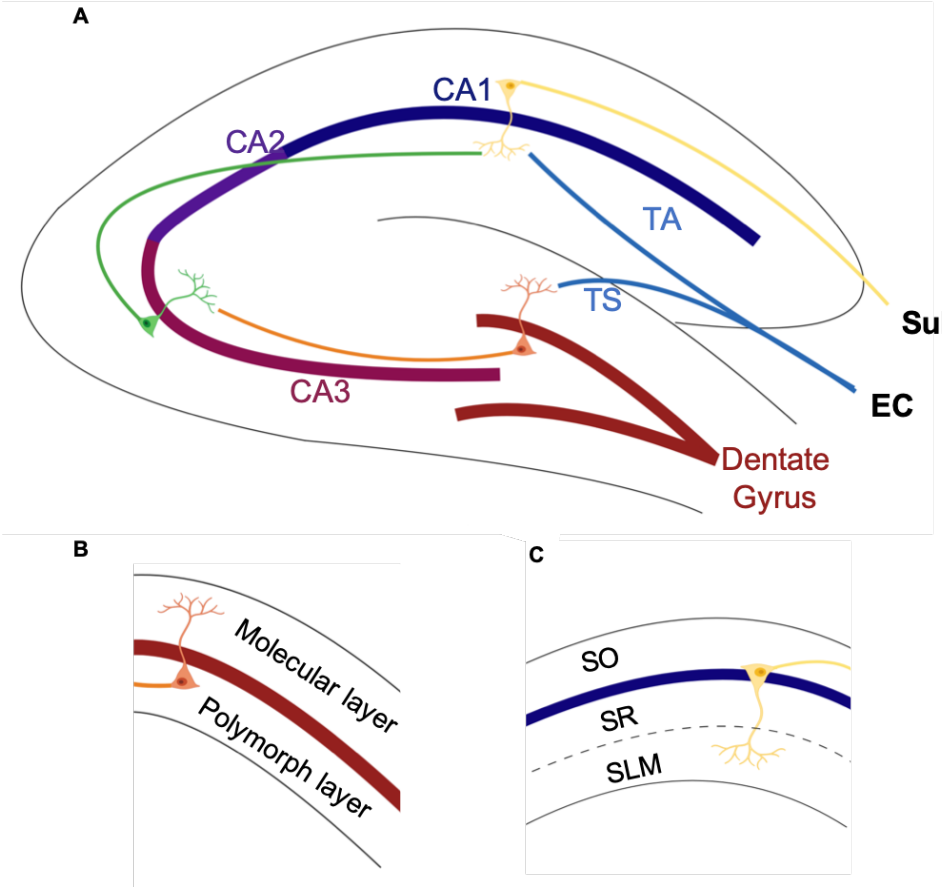

Figure 5.1 Schematic of the key regions of the hippocampus and neuronal pathways (A) and layers of the dentate gyrus (B) and CA1 (C). Signals entering the hippocampus along the performant pathway (light blue) from the entorhinal cortex (EC) can either travel directly to the CA1 via the temporoammonic pathway (TA) or enter the trisynaptic circuit (TS). Axons from the EC terminate at granule cells of the dentate gyrus. The potential travels along the mossy fibers (orange) to the pyramidal cells of the CA3. It then travels along Schaffer collaterals (green) to the CA1 pyramidal neurons. The potential then travels out of the hippocampus via the subiculum (sub). The DG can be defined by three layers. The central granule layer (red) contains the granular cell bodies with axons and dendrites projecting into the molecular layer towards the CA3. Afferent terminals constitute the polymorph layer receiving potentials from the EC. Within the cortex afferent potentials from the EC along the temporoammonic pathway connect with synapses within the stratum lacunosum moleculare (SLM) whilst signals from the trisynaptic pathway along Schaffer collaterals connect in the stratum radiatum (SR). Pyramidal cell bodies form the stratum pyrimidale (blue) and efferent branches towards the subiculum form the stratum oriens (SO). Figure was created using BioRender.com.

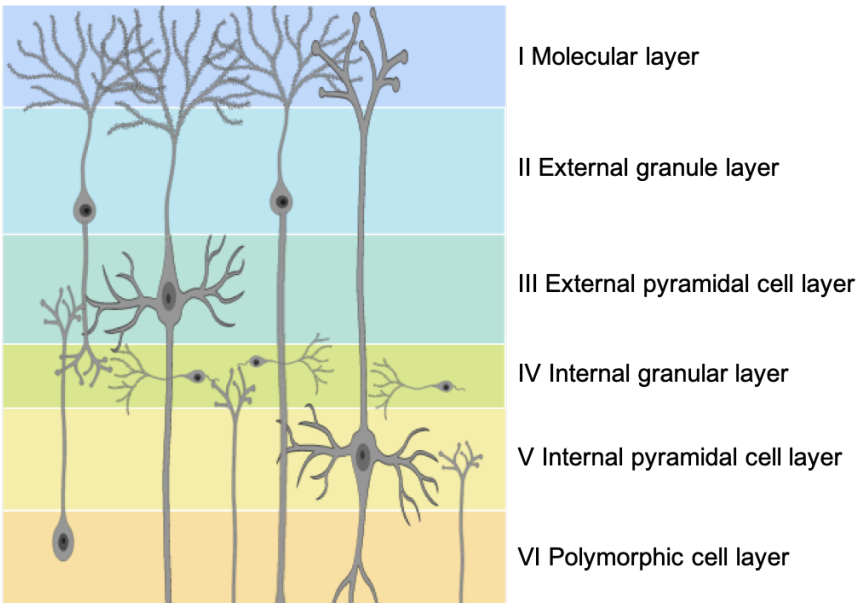

Figure 5.2 Schematic of the layers within the cerebral neocortex with representations of neuronal populations. The molecular layer (I) is largely populated by dendrites and terminal branches of neurons within layers II-VI. The external granule (II) and internal granule (IV) layers are populated by small pyramidal and stellate neurons. The external pyramidal (III) and Internal pyramidal (V) are predominantly pyramidal cells and the polymorphic layer (VI) contains axons and projections from neurons entering and leaving the cortex. Figure was created using BioRender.com.

This chapter aims to validate these proteomic hits in stored, frozen hippocampal, hypothalamic and cortical tissues from the proteomic mouse cohort. Cortical tissues were included for validation due to the degenerative effects of AD on this brain region. Expression within the cortex was included in the validation studies as this brain region, along with the hippocampus, undergoes severe atrophy in AD patients and sees some of the largest pathological changes.

5.2 Results

5.2.1 Comparing the proteomic cohort to previous data

To compare this cohort with those of the preliminary study, GSK3 expression and phosphorylation was analysed by western blot in the hippocampus, hypothalamus and cortex. No difference in either total, or serine phosphorylated GSK3α or β across any of the groups was observed (Figure 5.3).

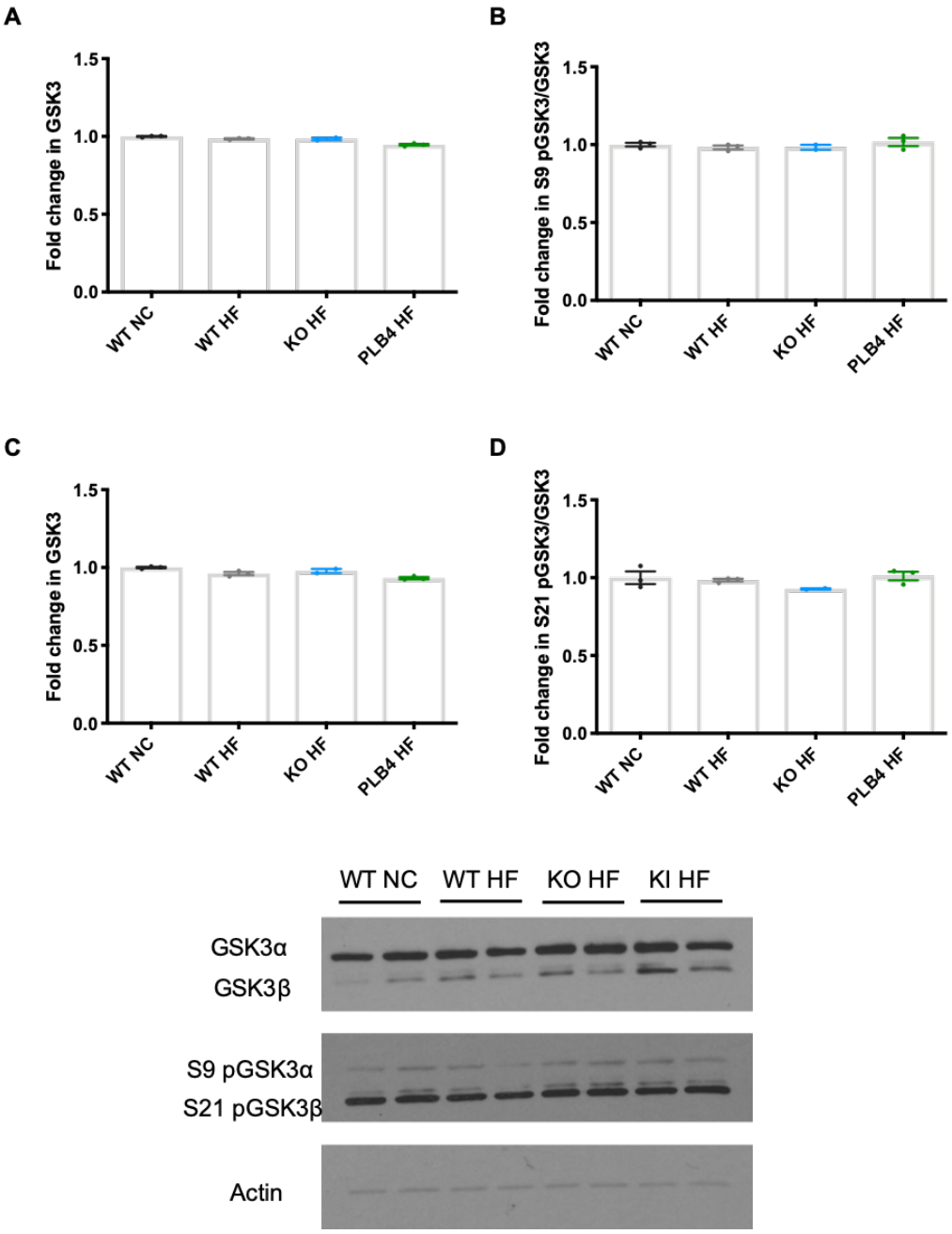

Figure 5.3 GSK3α and β expression and inhibitory phosphorylation state within the cortex. (A) GSK3α expression and **(B)** serine 9 phosphorylation. **(C)** GSK3β expression and **(D)** serine 21 phosphorylation. Total GSK3 expression of neither α or β isoform was altered with diet or BACE1 expression. No change was seen in serine phosphorylation with either diet or BACE1 genotype. n=3 per group. Individual data points indicate the range of data. Standard error indicated by error bars.

5.2.2 Testing the validity of Hypothalamic hits

Western blot analysis of WT NC, WT HF and BACE1 KO HF hypothalamic tissues was conducted in order to validate the proteomic result. However, immunoblot revealed no change in TXNDC15 expression with either diet or BACE1 expression (Figure 5.4A). Further analysis in cortical tissues was conducted as the cerebral cortex is also affected in the early stages of AD. However, no difference was observed in cortical tissues with either diet or BACE1 expression (Figure 5.4B).

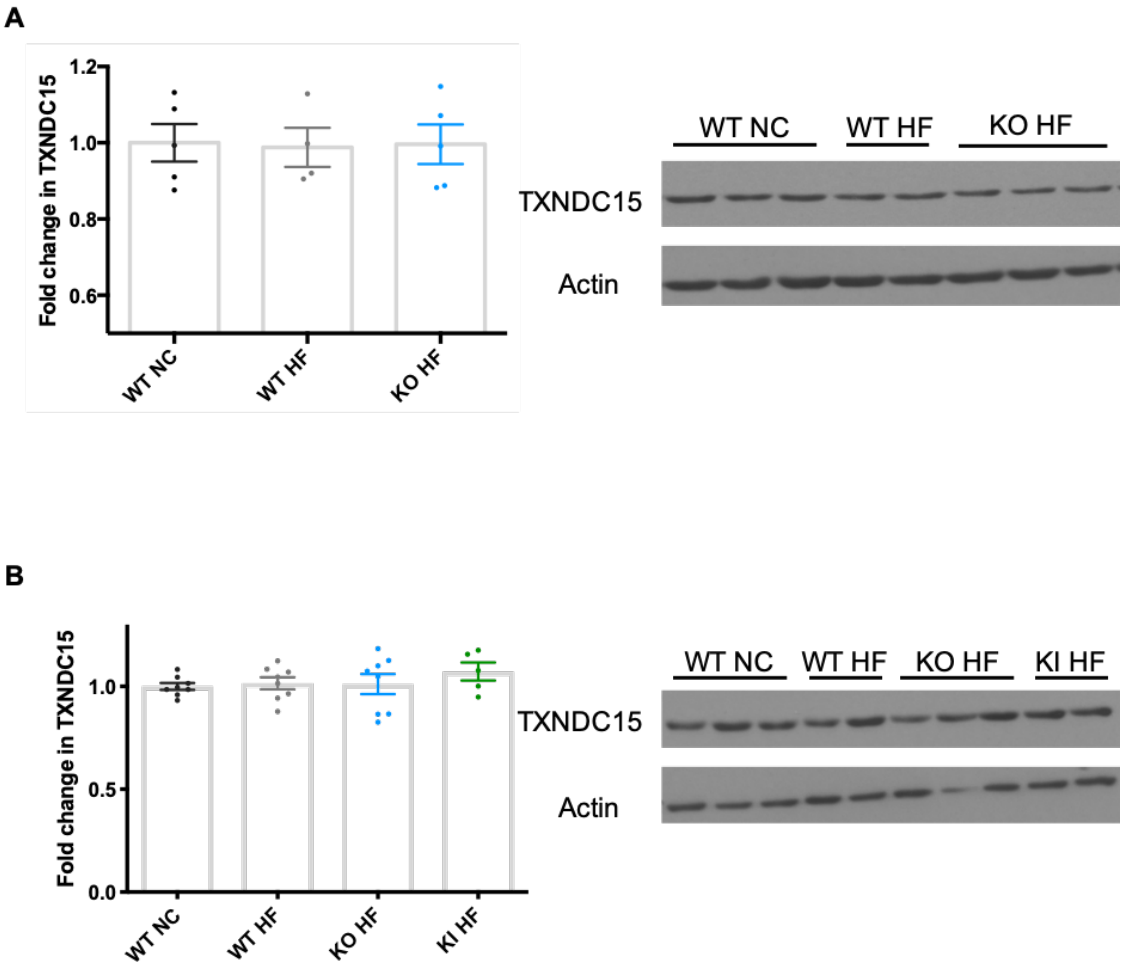

Figure 5.4 Western blot and densitometry analysis of TXNDC15 expression within the hypothalamus and the cortex. Western blot analysis did not identify any change in TXNDC15 expression in either the hypothalamus **(A)** or cortex **(B)** with diet of BACE1 genotype. n=4-8 per group. Individual data points indicate the range of data. Standard error indicated by error bars.

FUCA1 testing was also conducted on both hypothalamic and cortical tissues. The immunoblots for this were not of sufficient quality to quantify and the presence of multiple bands suggested either non-specific binding of the antibody or modification of this protein. The anticipated molecular mass for FUCA1 is approximately 54kDa and three bands were present within this region with further bands at approximately 43 and 24kDa (Figure 5.5). This pattern was observed in both the hypothalamic and cortical samples. Furthermore, whilst the proteomic data indicated that FUCA1 expression increased with BACE1 KO compared to both WT NC and WT HF groups, immunoblots of both brain regions suggest that FUCA1 expression decreases with HFD in WT mice and reduced further in BACE1 KO HFD mice compared to WT HF. These apparent expression changes were present across all bands however the significance of these changes could not be established without quantification.

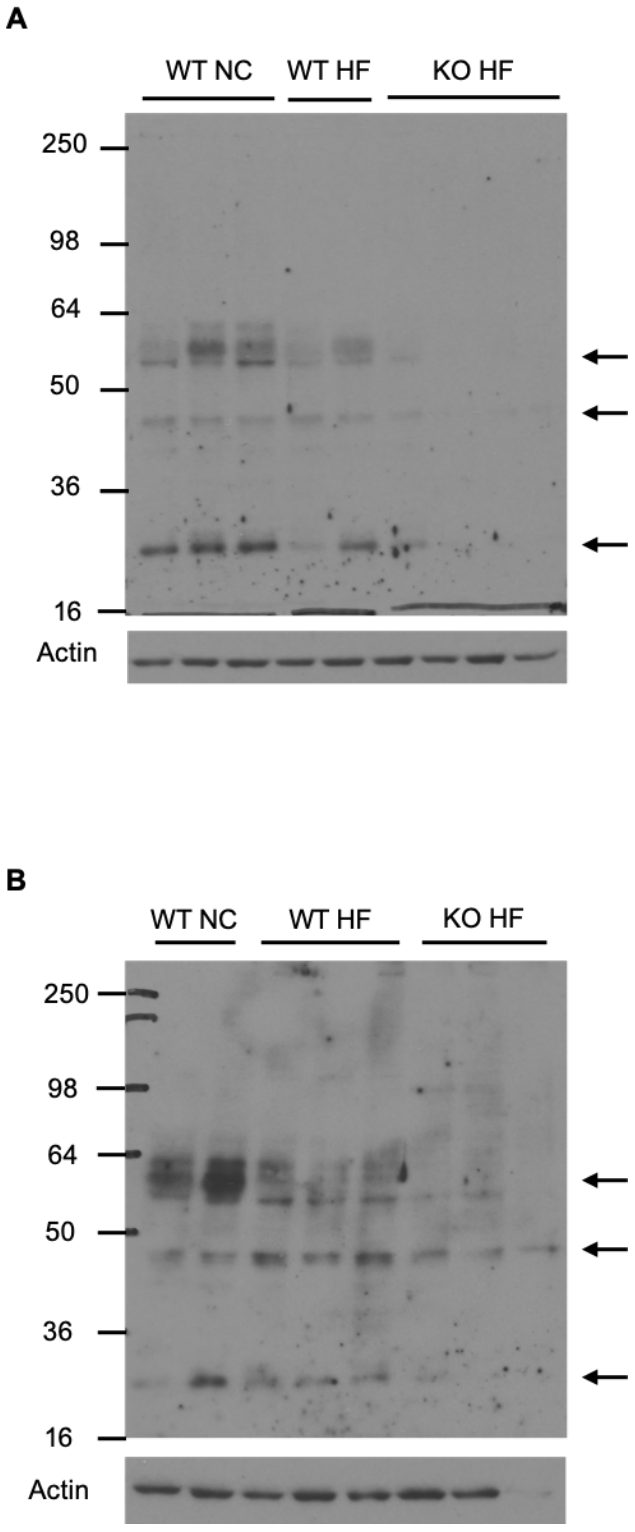

Figure 5.5 Western blot analysis of FUCA1 expression in the hypothalamus and cortex. Western blot revealed a possible decrease in FUCA1 expression in BACE1 KO hypothalamic **(A)** and cortical **(B)** tissues. However, due to the presence of multiple bands at approximately 54-64, 43 and 24kDa it could not be determined whether this blot represents FUCA1 expression. (n=4-8 per group)

5.2.3 Testing validity of Protein 4.1N

Protein 4.1N testing was conducted on hippocampal tissues from WT NC, WT HF, BACE1 KO HF and BACE1 KI HF mice. Initial analysis was conducted using an N-terminal antibody with an epitope corresponding to a region present in all of the 4.1N variants identified by proteomics. Immunoblots using this antibody did not identify any change in 4.1N expression with either diet or BACE1 genotype in either the hippocampus or cortex (Figures 5.6A and 5.6B respectively). An alternative protein 4.1N antibody was found that was compatible with IHC. Using this antibody, 3 bands were identified; likely corresponding to 3 splice variants at 130, 110 and 75kDa. Within the hippocampus, expression was variable, and no significant differences were observed in total 4.1N expression (Figure 5.7A) of any presumed splice variants with either diet or BACE1 genotype (Figure 5.7B-D). Protein 4.1N expression was equally variable in the cortex and no significant changes were observed within this brain region wither either diet or BACE1 genotype in either total 4.1N (Figure 5.8A) or any of the presumed 4.1N splice variants (Figure 5.8B-D).

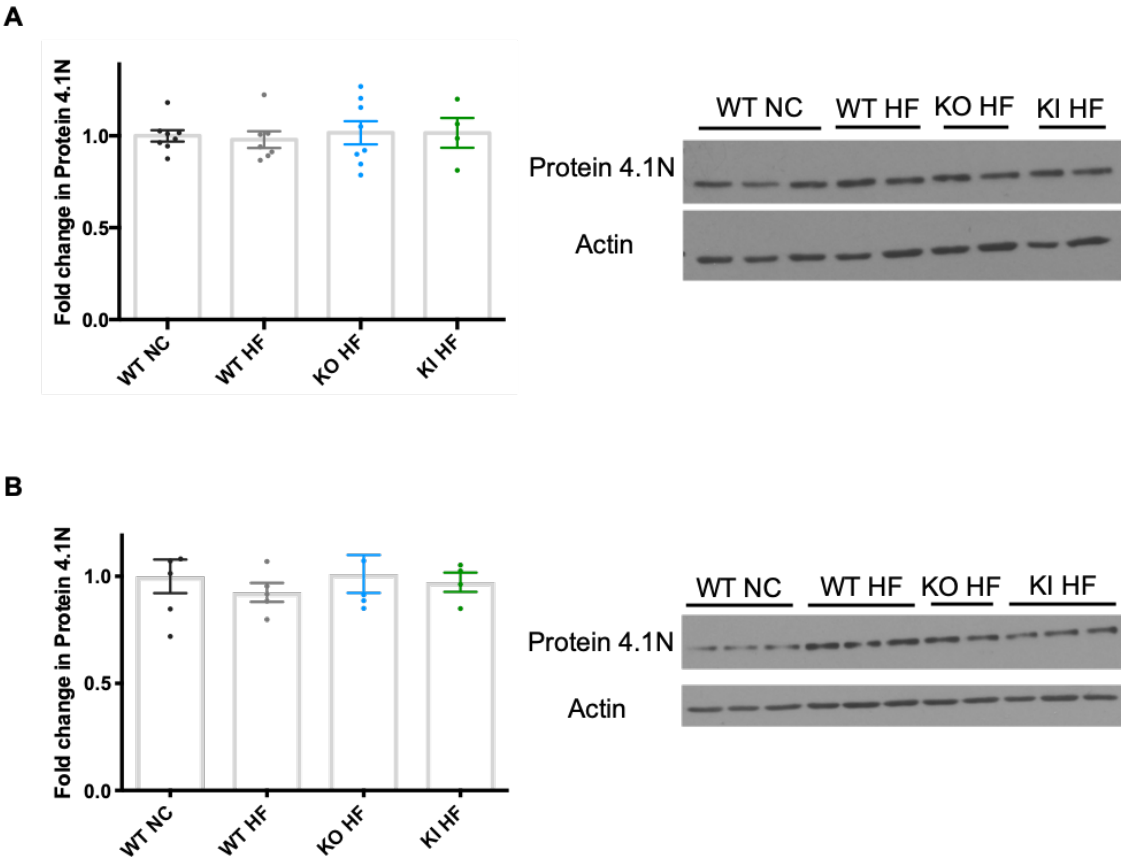

Figure 5.6 Western blot and densitometry analysis of protein 4.1N expression within the hippocampus and cortex. Western blot analysis revealed no change in protein 4.1N expression in either the hippocampus **(A)** or cortex **(B)** with diet or BACE1 genotype using an antibody specific to aa 1-100. n=4-8 per group. Individual data points indicate the range of data. Standard error indicated by error bars.

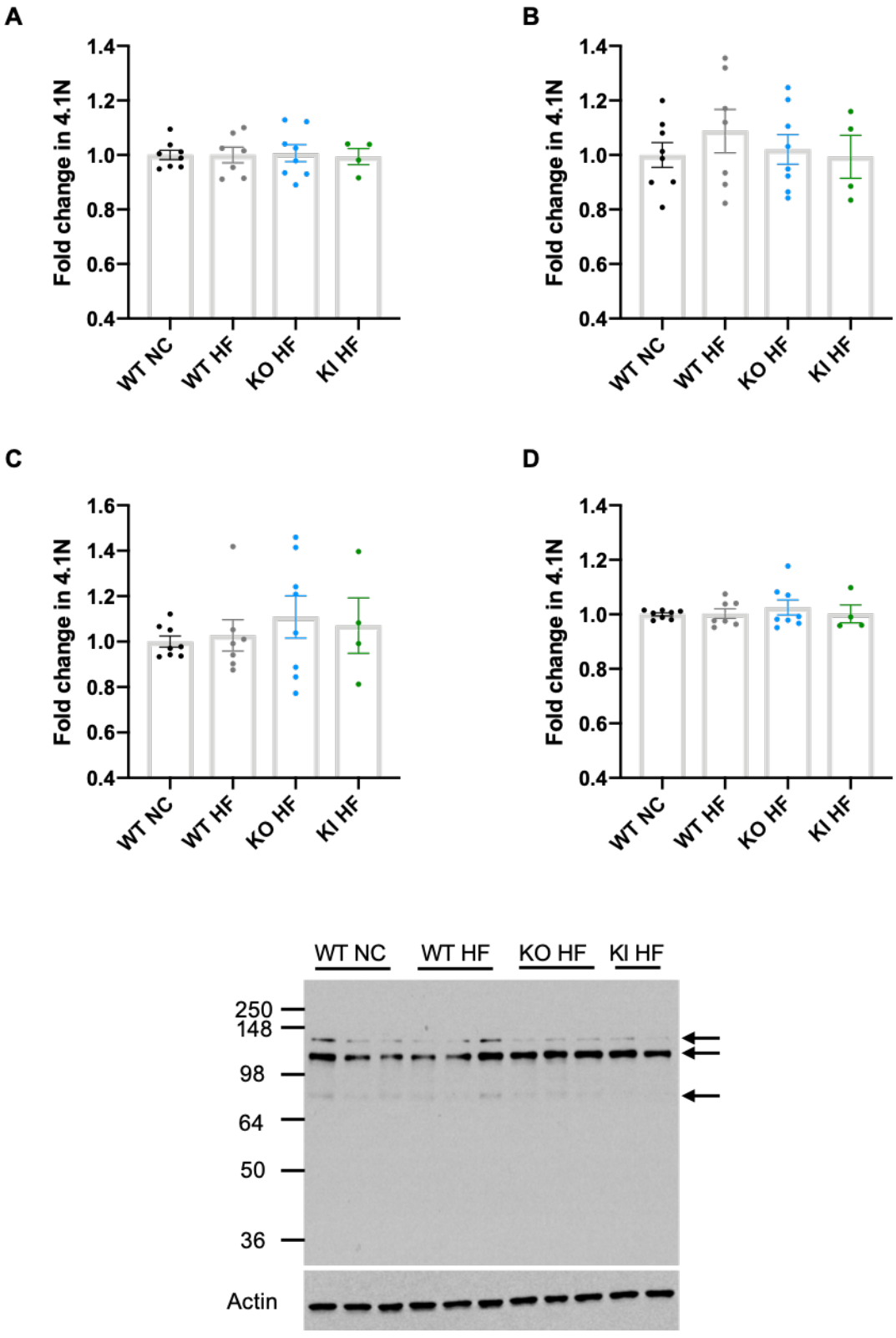

Figure 5.7 Western blot and densitometry analysis of 4.1N expression within the hippocampus. Western blot analysis did not reveal any change in 4.1N expression within the hippocampus using an antibody specific to aa 12-92. Multiple bands were identified using this antibody that represent probable splice variants of 4.1N. Total 4.1N expression was quantified (A) as well as bands at 130kDa (B),110kDa (C) and 75kDa (D). n=4-8 per group. Individual data points indicate the range of data. Standard error indicated by error bars.

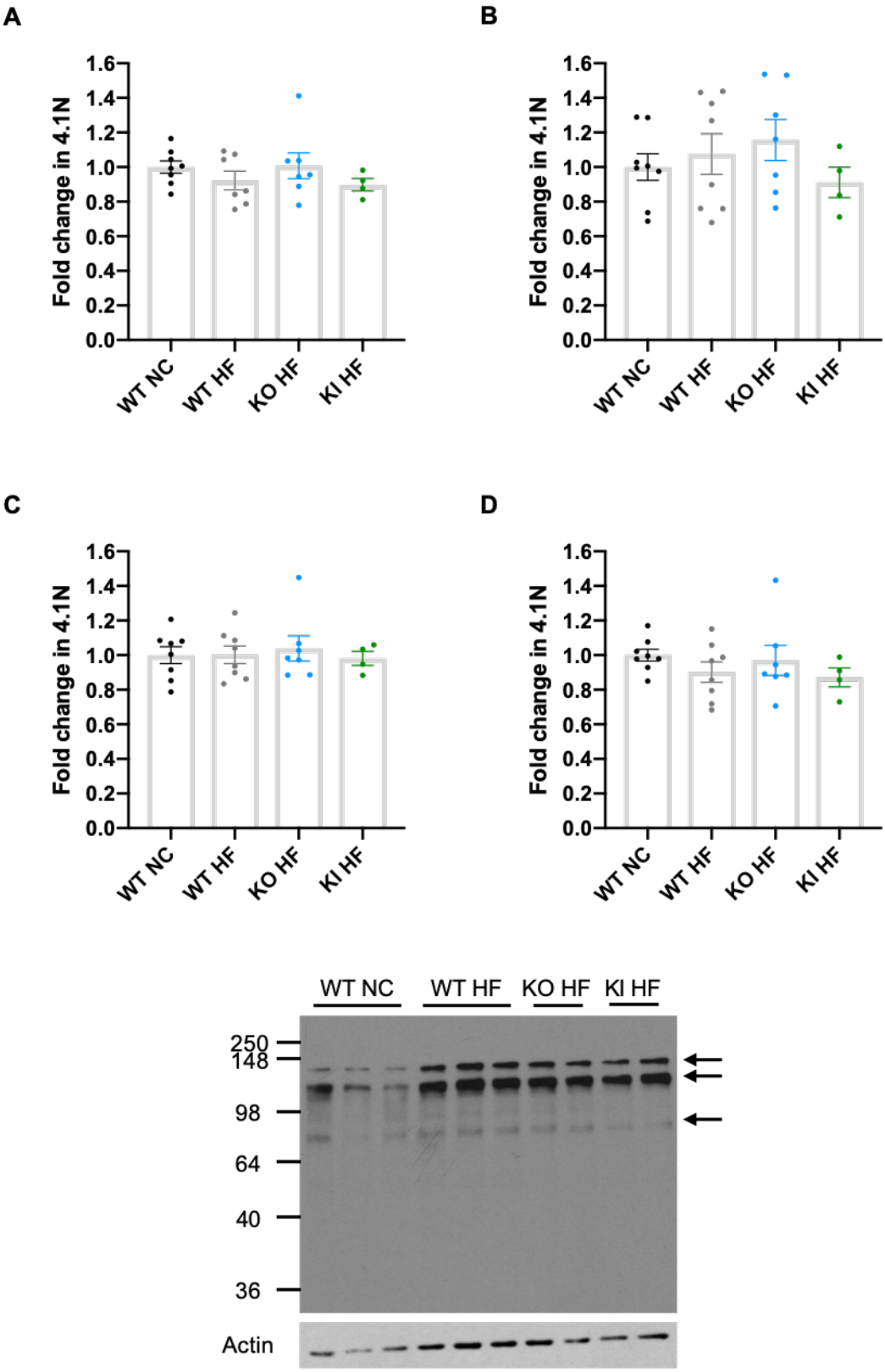

Figure 5.8 Western blot and densitometry analysis of 4.1N expression within the cortex. Western blot analysis did not reveal any change in 4.1N expression within the hippocampus using an antibody specific to aa 12-92. Multiple bands were identified using this antibody that represent probable splice variants of 4.1N. Total 4.1N expression was quantified (A) as well as bands at 130kDa (B),110kDa (C) and 75kDa (D). n=4-8 per group. Individual data points indicate the range of data. Standard error indicated by error bars.

5.2.4 Protein 4.1N expression with 20wk dietary stress in BACE1 KO hippocampus

Due to the absence of a BACE1 KO group fed a NC diet in the proteomic study design, archived frozen tissues were utilised to look for changes in protein 4.1N expression with diet in the BACE1 KO mice. Hippocampal tissues were utilised from 20-week HF fed mice with WT controls. Immunoblot revealed that with HFD, protein 4.1N expression increases 2-fold, thereby suggesting that 4.1N expression may be under dietary, as well as BACE1 control (Figure 5.9).

5.2.5 Protein 4.1N expression with chronic dietary excess in WT hippocampus

Further analysis into the effects of diet was performed on aged (>12 month) DIO WT mice with age-matched WT NC controls. IHC was performed to identify changes in protein 4.1N localisation and expression within the hippocampus, hypothalamus and cortex under chronic dietary stress. Staining for NeuN identified no change in the hippocampus with diet (Figure 5.10). This stain acted upon neuronal cell bodies and clearly identified the CA1-3 and DG regions of the hippocampus allowing for distinction between cell bodies and projections.

BACE1 expression within the hippocampus appeared to be isolated to the stratum radiatum and polymorph layer of the DG (Figure 5.10, arrows 1). BACE1 expression appears to be notably absent in stratum lacunosum moleculare with NC fed animals but this pattern is not present under HF conditions suggesting that HFD leads to increased BACE1 expression within this region (Figure 5.10, arrow 2). Slight staining can be seen in the stratum oriens and stratum radiatum of the hippocampus (Figure 5.10, arrows 3)

Protein 4.1N exhibited distinct expression within the molecular layer of the DG (Figure 5.10, arrow 6) but showed a similar expression pattern as BACE1 throughout the stratum radiatum of the CA3 region (Figure 5.10, arrow 4). This expression appeared reduced in the hippocampi of HFD mice. Interestingly, a band of staining appears following the stratum lacunosum moleculare with visibly increased staining with HFD. This suggests that co-localisation could occur with BACE1 under HF conditions (Figure 5.10, arrow 5). These staining patterns were observed consistently between replicates in each group.

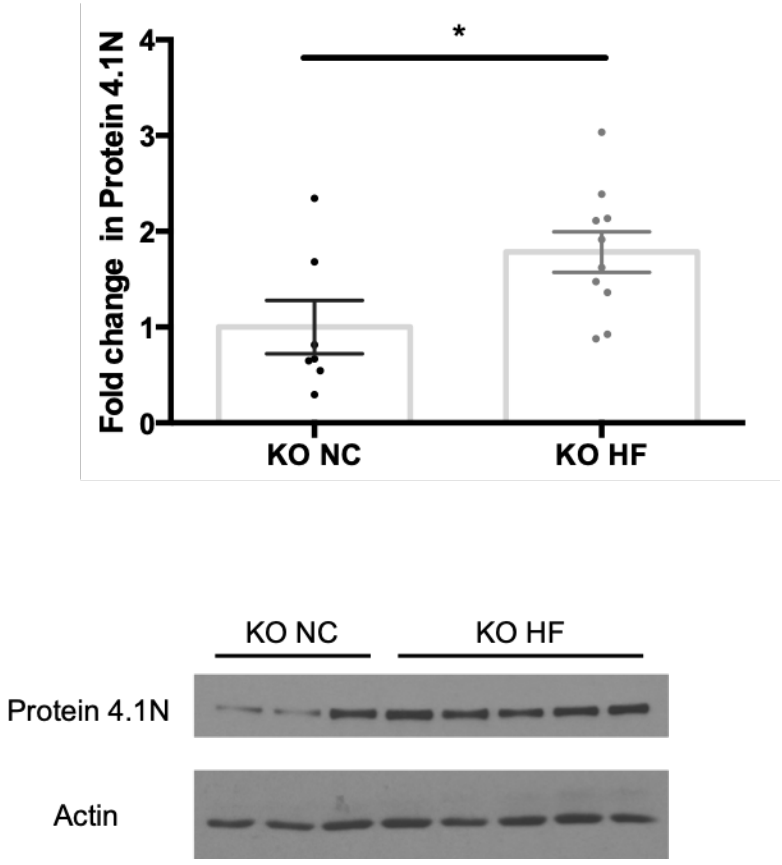

Figure 5.9 Western blot and densitometry analysis of protein 4.1N expression in the hippocampus of BACE1 KO mice with 20wk HFD. Non-parametric Mann-Whitney test revealed BACE1 KO mice challenged with HFD for 20 weeks revealed an approximately 2-fold increase in hippocampal 4.1N expression. n=6-10. Individual data points indicate the range of data. Standard error indicated by error bars, * = $p<0.05$.

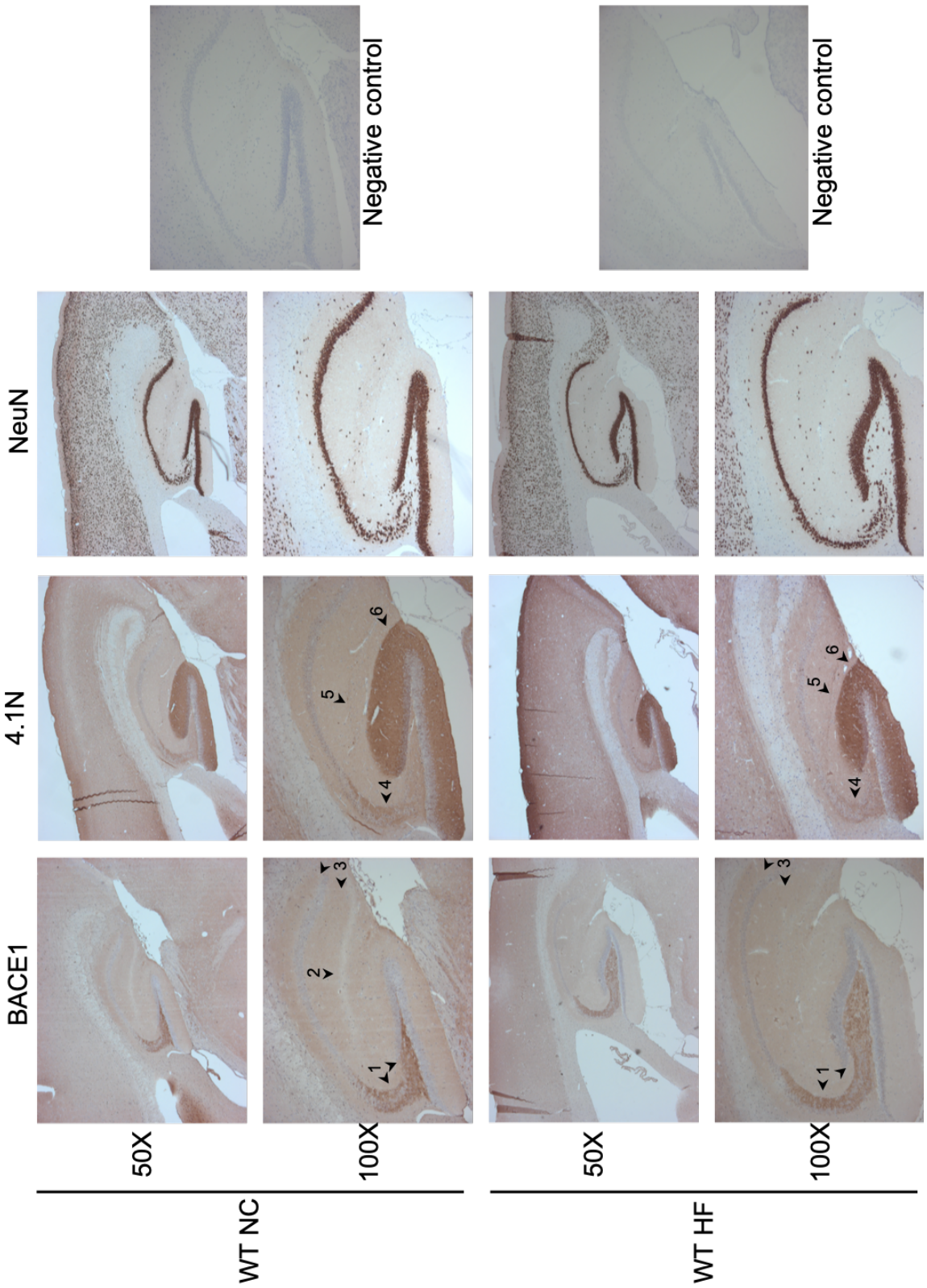

Figure 5.10 Hippocampal immunostaining of WT mice challenged with HFD or NC for 12 months. Sagittal brain sections stained for BACE1, 4.1N and NeuN expression. Immunohistochemical staining revealed that BACE1 expression is greatest within the stratum radiatum of the CA3 hippocampal region and the polymorph layer of the dentate gyrus (arrow 1) as well as some expression within stratum oriens and stratum radiatum regions of CA1 (arrow 3). BACE1 was notably absent in the stratum lacunosum moleculare in animals on NC diet (arrow 2) with expression increasing with HFD so that this structure is no longer visible. 4.1N expression was also present in the stratum radiatum of CA3 and the stratum lacunosum moleculare (arrows 4 and 5 respectively). However, 4.1N expression was greatest within the molecular layer of the dentate gyrus (arrow 6). NeuN expression clearly defined the hippocampal CA1-CA3 cell bodies as well as those within the dentate gyrus.

Within the cortex, NeuN clearly defined the molecular layer and external granule/pyramidial layers I-III (Figure 5.11) The expression of NeuN within the cortex did not appear to change with diet. BACE1 expression did not appear to be high within the cortex but patterns were identified that showed higher BACE1 expression within the molecular layer (I) and the internal granule layer (IV) (Figure 5.11, arrows 1 and 3 respectively). These darker bands were separated by a region of reduced expression within the external granule/pyramidial layers (II/III) (Figure 5.11, arrow 2). The same pattern was observed in HF mice. Protein 4.1N was expressed highly within the molecular layer of the cortex (I) (Figure 5.11, arrow 4) but exhibited a similar expression pattern to BACE1 with higher expression in the internal granule layer (IV) than the external granule/pyramidial layers (II/III) (Figure 5.11, arrows 6 and 5 respectively). This staining pattern was also observed in HF fed mice but the depth of staining in the internal granule layer was less apparent with HFD.

In the hypothalamus of aged mice, both BACE1 and 4.1N were absent from the medial mammillary nucleus (Figure 5.12, arrows 1 & 3 respectively). Whilst 4.1N expression was uniform across the hypothalamic area, expression did not change with diet. BACE1 expression was not isolated to a particular hypothalamic region but rather spanned the ventral edge. Hypothalamic expression of BACE1 appeared to increase with high-fat diet but again, expression was not isolated to a particular region (Figure 5.12, arrow 2).

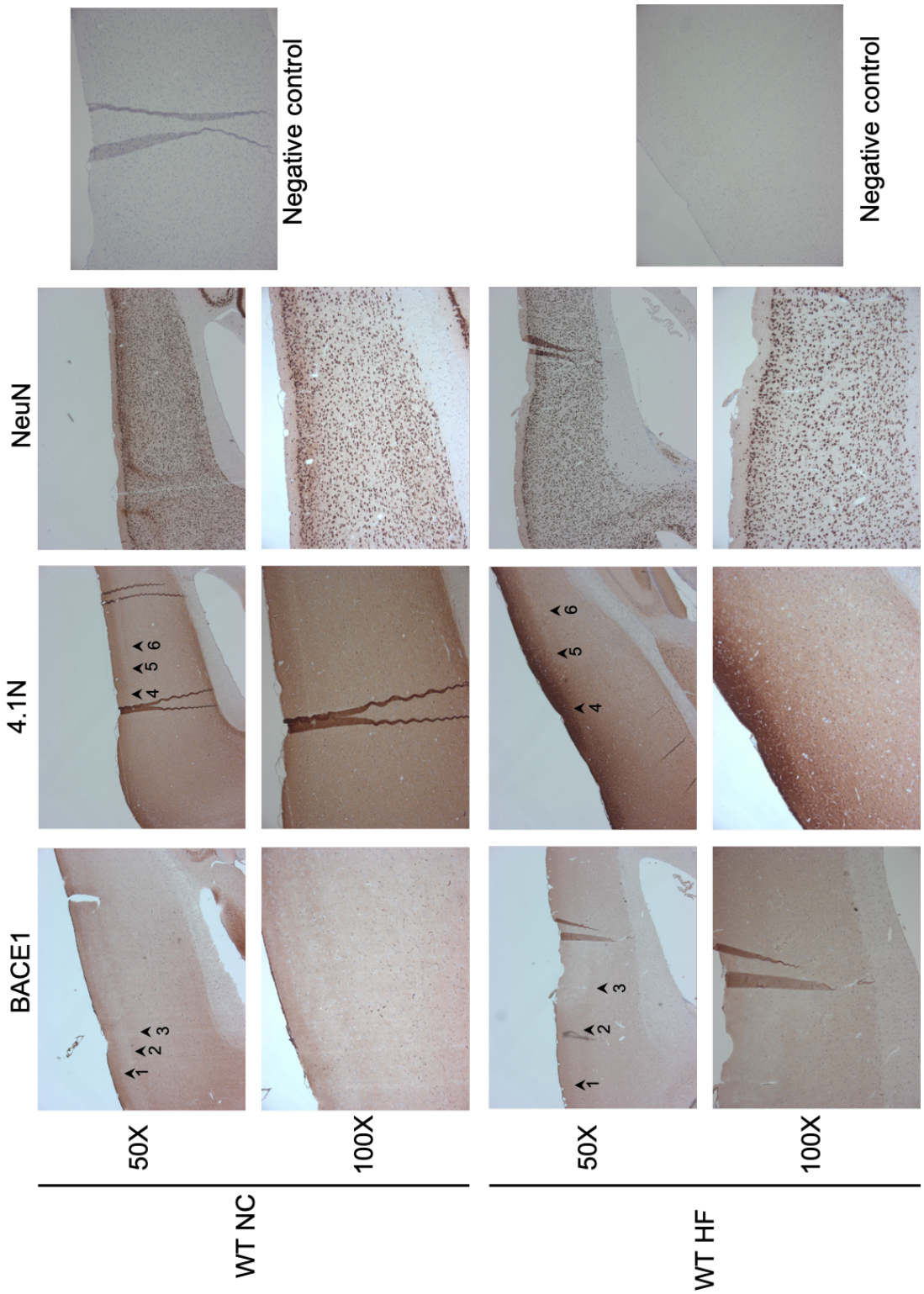

Figure 5.11 Cortical immunostaining of WT mice challenged with HFD or NC for 12 months. Saggital brain sections stained for BACE1, 4.1N and NeuN expression. Immunohistochemical staining revealed that BACE1 expression is greatest within the molecular layer (I) of the cortex (arrow 1) with some expression within the internal granule layer (IV) (arrow 3). These were separated by a band of low BACE1 expression in the external granule/pyramidal layers (II/III) (arrow 2). 4.1N expression followed a similar pattern of expression which was greatest in the molecular layer (I) (arrow 4), absent in the external granule/pyramidal layers (II/III) (arrow 5) and present in the internal granule layer (IV) (arrow 6). NeuN expression clearly defined layers I-IV through staining of cell bodies.

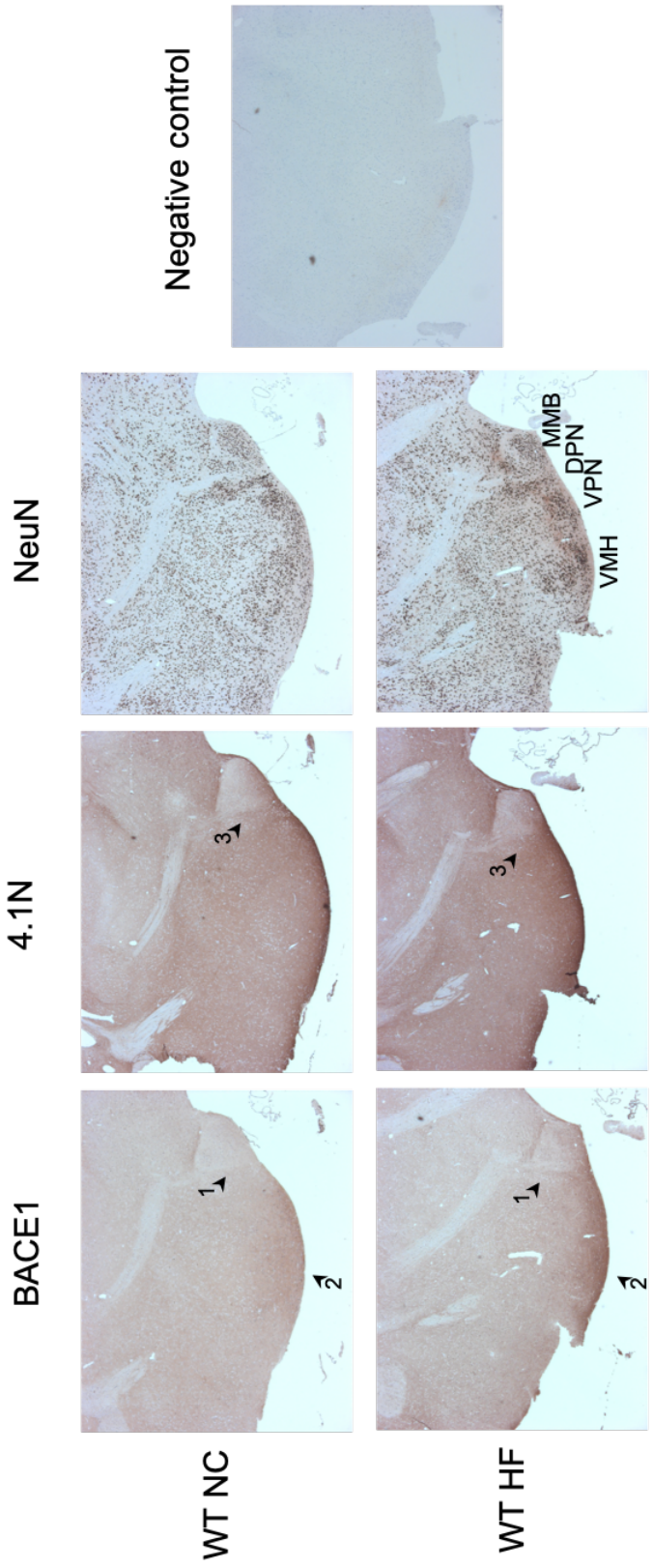

Figure 5.12 Hypothalamic immunostaining of WT mice challenged with HFD or NC for 12 months. Sagittal brain sections stained for BACE1, 4.1N and NeuN expression and visualised at x50 magnification. BACE1 staining within the hypothalamus could not be easily identified to a specific region however it was notable absent in the medial mammillary nucleus (arrow 1). Staining was predominantly along the ventral edge of the hypothalamus which increased with HFD (arrow 2). 4.1N expression was also absent within the medial mamillary nucleus (arrow 3). NeuN staining was clearly absent in the fiber tracts and show high neuronal body density within the medial mammillary body (MMB), ventral premammillary nucleus (VPN), dorsal premammillary nucleus (DPN) and ventromedial hypothalamus (VMH).

5.2.6 Human 4.1N expression with obesity and AD in the cortex and hippocampus

Paraffin embedded human cortical sections were obtained from Edinburgh brain bank for the purpose of IHC analysis of 4.1N and BACE1 expression in both obese and AD cases with age-matched controls (n=4 per group). Obese cases had a BMI of 36 ± 3.3, age 50 ± 8.4 and were 75% female. Controls for this group had a BMI of 22.5 ± 0.7, age 49 ± 10.4 and were 75% female. All AD cases were from patients at Braak stage VI and died due to complications associated with the disease. The average age for this group was 79 ± 3.8 whilst controls were 75 ± 7.8 years of age. The AD group was 25% female whilst the control was 50% female. The BMI of the AD cases were unknown however it is commonly understood that most individuals in late stages of AD have undergone severe weight loss (Johnson, Wilkins, & Morris, 2006a; White, Pieper, & Schmader, 1998). Despite this, epidemiological studies suggest that AD patients are still classified as overweight due to a high pre-AD BMI (Cronin-Stubbs et al., 1997). The BMI of AD controls were known for 3 of the 4 cases. One was had a BMI within a healthy range at 21.5; whilst two were obese or borderline obese with BMIs of 30.9 and 29 respectively.

Within the cortex, BACE1 expression appeared to be predominantly within the molecular layer (Layer I) and within some cell bodies throughout the cortex. Molecular layer expression of BACE1 appeared greatest in non-aged controls and was reduced with both obesity, age and AD (Figure 5.13, arrow 1). Aged non-obese controls exhibited a particularly low expression of BACE1 within the molecular layer of the cortex when compared to expression within the external granule and pyramidal layers. Cell body staining did not appear to change with age, obesity or AD (Figure 5.13, arrow 2).

Protein 4.1N expression also appears largely isolated to the molecular layer (layer I) of the cortex and cell bodies. Expression of 4.1N in the molecular layer (layer I) of the cortex varies with diet, age and AD. Whilst obese individuals exhibit reduced 4.1N expression in this region compared to healthy controls, this relationship appears to reverse with age as older individuals exhibit increased molecular layer expression of 4.1N in obesity and less with healthy BMI. AD cortices also exhibit staining of the molecular layer of the cortex (Figure 5.13,

arrow 3). 4.1N expression within cell bodies is present in both control and obese cortices and lost in both AD and aged obese individuals. Expression in cell bodies is retained in aged controls of a healthy body weight (Figure 5.13, arrow 4). This pattern of staining was similar to that seen with BACE1 suggesting there may be a level of co-localisation of these two proteins. Both BACE1 and 4.1N were increased in AD Cortex molecular layers compared to aged controls however aged obese cases exhibited no noticeable change in BACE1 expression. In non-aged cases, BACE1 too is increased within the molecular layer of the cortex in healthy controls and reduced with obesity.

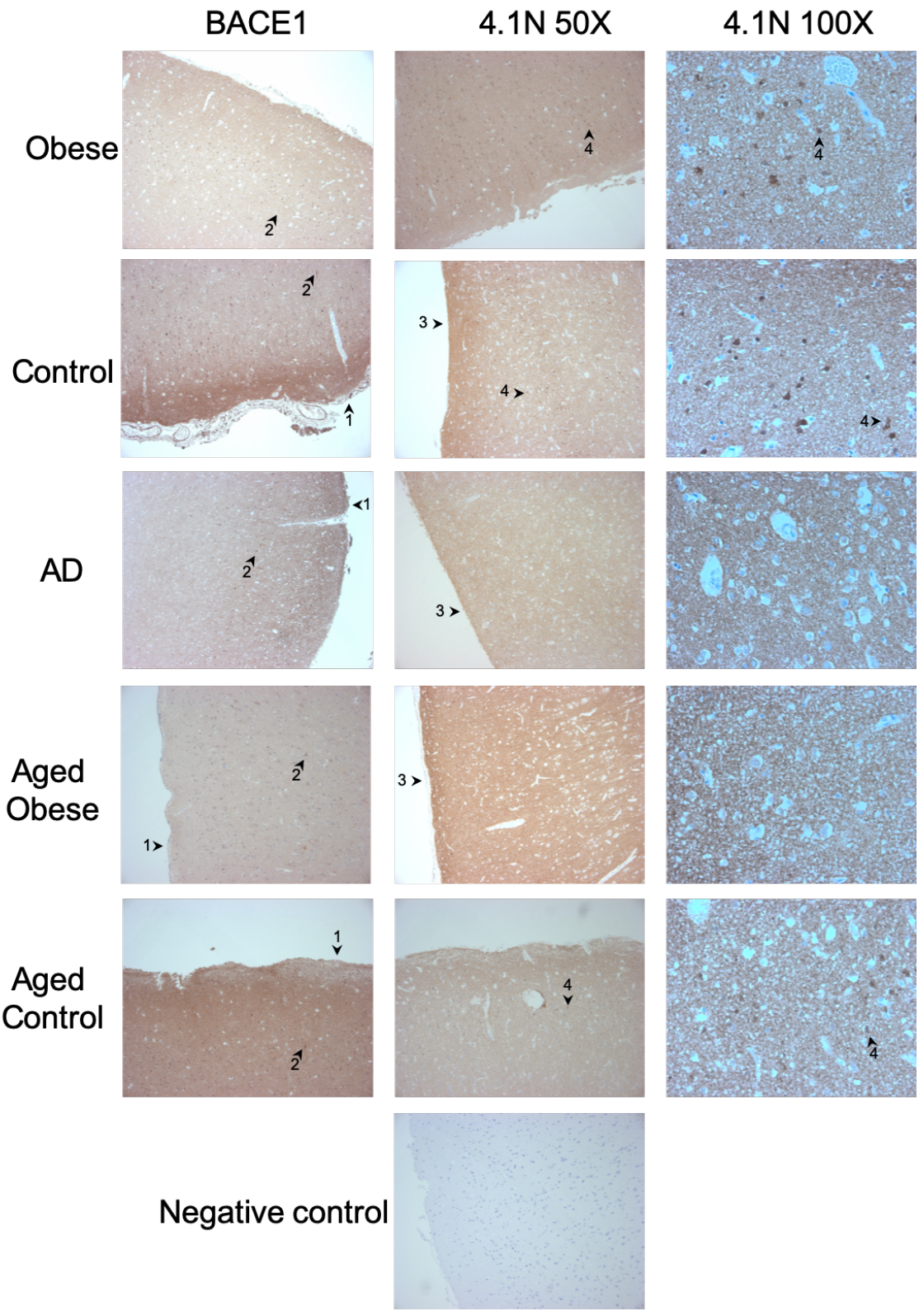

Figure 5.13 Cortical immunostaining of human cortical sections from controls, obese, AD, aged obese and aged control groups. Stained for BACE1 and 4.1N at both 50X and 100X magnification. BACE1 expression was predominantly within the molecular layer of the neocortex (arrow 1) with some expression within cell bodies in all groups (arrow 2). Expression within the molecular layer was reduced in aged controls and aged obese cases whilst retained in AD. 4.1N expression too was predominantly within the molecular layer of the neocortex in control, AD and aged obese cases (arrow 3). Cell body expression was not present in aged obese and AD cases but was present in aged controls (arrow 4).

Hippocampal AD sections were obtained from cases at late stages that died from complications associated with the disease whilst controls died from causes not related to the brain. The average age of AD cases was 82 ± 6.2 and controls 82 ± 7.5. 50% of each group was female and a total of 8 cases were obtained per group. BACE1 exhibited staining within the stratum pyramidale of rostral CA1 region of the hippocampus exhibiting expression in both projections and cell bodies within this region (Figures 5.14 and 5.25, arrow 1). This pattern of staining followed the stratum pyramidale from CA1 through CA3 (Figure 5.14, arrow 2) and into rostral pyramidal cells of the CA4 (Figure 5.14, arrow 3). BACE1 expression in cell projections was less pronounced within the CA4 region but maintained within cell bodies. Cell body staining was also apparent within the polyform layer of the rostral DG (Figure 5.14, arrow 4) staining of the molecular layer of the rostral DG was also observed (Figures 5.14 and 5.15, arrow 5) but not the subgranular zone of the rostral DG (Figures 5.14 and 5.15, arrow 6). This staining pattern was comparable between control and AD cases except for localisation within the DG. In AD cases, BACE1 appeared more localised to the subgranular zone (Figures 5.14 and 5.15, arrow 6) than the molecular layer of the rostral DG (Figures 5.14 and 5.15 arrow 5).

Interestingly, expression of 4.1N within the human hippocampus follows a very similar expression profile to BACE1. 4.1N can be found within stratum pyramidale from CA1 through to CA3 and CA4 (Figure 5.14, arrows 7-9 respectively) as well as polyform and molecular layers of the DG where diffuse staining suggests expression in neuronal projections rather than cell bodies as with BACE1 (Figure 5.14, arrows 10 and 11 respectively). 4.1N expression was not discernibly different between the subgranular zone and the molecular layer of the DG. 4.1N expression appeared to increase within the hippocampus in all mentioned areas in AD cases compared to controls (Figure 5.14).

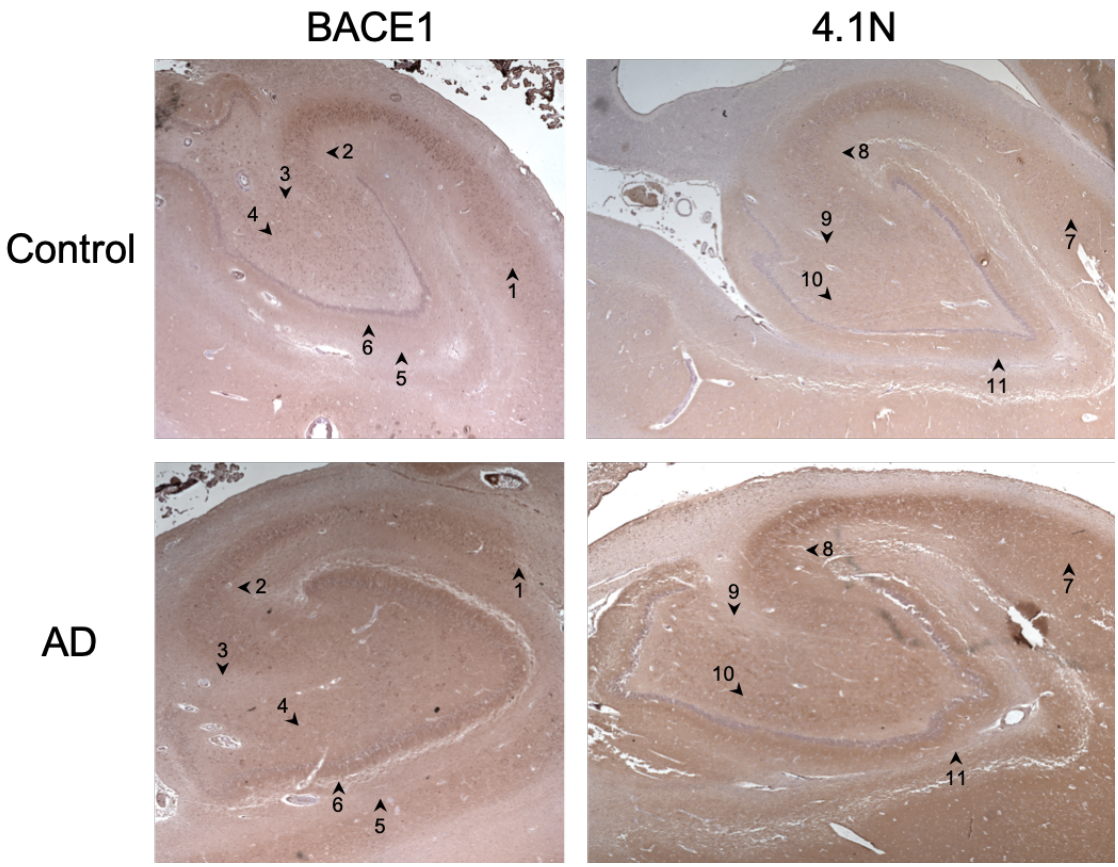

Figure 5.14 Hippocampal immunostaining of human sections from controls and AD cases stained for BACE1 and 4.1N expression. BACE1 expression was observed within the stratum pyramidale of rostral CA1 region of the hippocampus (arrow 1) through to CA3 (arrow 2) and into rostral pyramidal cells (arrow 3). BACE1 expression was also observed in the polyform layer of the rostral dentate gyrus and the and molecular layer of the dentate gyrus (arrows 4 and 5 respectively). BACE1 expression was notably absent in subgranular zone of the dentate gyrus (arrow 6). 4.1N expression followed a similar pattern with expression in CA1, CA3 and CA4 (arrows 7,8 and 9 respectively). As well as the polyform and molecular layers of the dentate gyrus (arrows 10 and 11). Whilst BACE1 expression did not appear to change with AD compared to controls, 4.1N expression increased in AD in all regions.

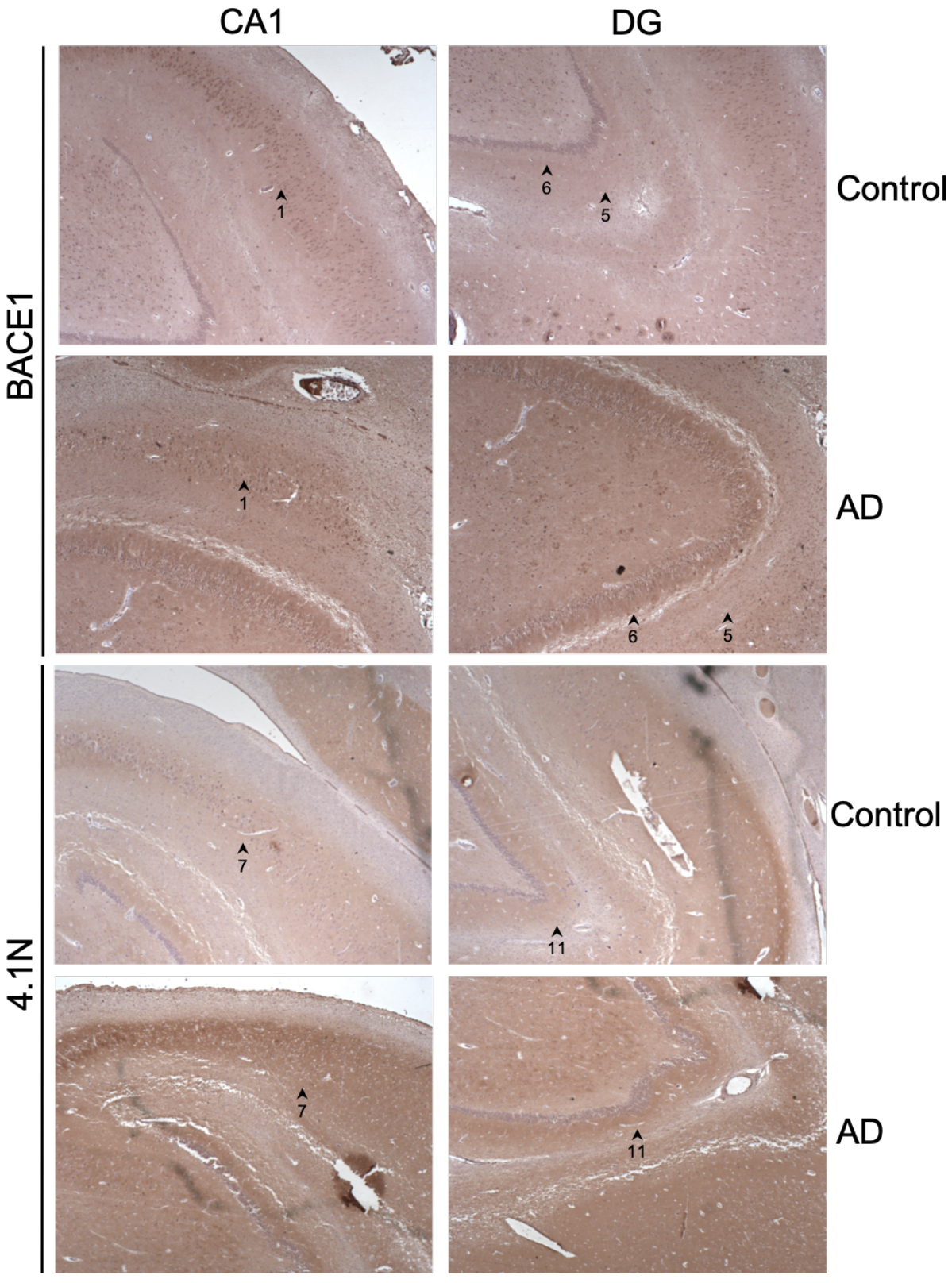

Figure 5.15 Hippocampal staining of human sections from controls and AD cases stained for BACE1 and 4.1N expression at 50X magnification. BACE1 expression was observed within the stratum pyramidale of rostral CA1 region of the hippocampus within cell bodies (arrow 1). BACE1 expression was also observed in the polyform layer of the molecular layer of the dentate gyrus where more diffuse staining implies expression in synapses (arrow 5). BACE1 expression was notably absent in subgranular zone of the dentate gyrus (arrow 6). 4.1N expression followed a similar pattern with expression in CA1 but confined to cell projections (arrow 7). As well as the molecular layer of the dentate gyrus (arrow 11).

5.3 Discussion

5.3.1 Brain expression of TXNDC15 and FUCA1

Peptide coverage of both TXNDC and FUCA1 within the hypothalamus was very low, leading to early doubts as to the validity of these proteins as real hits. Western blot analysis was conducted in the hypothalamus to test the validity of these proteomic results and the cortex to identify whether changes may also occur within this brain region. TXNDC15 was unaltered in either brain region therefore it remains unclear as to whether TXNSC15 is differentially regulated by BACE1. FUCA1, contrary to proteomic data, appeared reduced in BACE1 KO tissues. However, due to poor quality blots this result was not quantifiable. Multiple bands were also present within the FUCA1 immunoblot. This may be a result of alternative splicing or of unspecific binding of the FUCA1 antibody. Isolation of protein from these bands and MS analysis would provide further details of antibody accuracy and possible splice variation of this protein. As the main band identified by this antibody is larger than the anticipated FUCA1 size, it seems likely that lack of antibody specificity is the cause of this outcome and this proteomic hit could not be confidently validated.

These western blot data do not support the proteomic analysis, which may be due to multiple factors. As previously mentioned, the peptide coverage of both TXNDC15 and FUCA1 in the proteomic analysis was poor. It may be that mis-identification of these few peptides has occurred and these proteins have been falsely identified as hits. Alternatively, the western blot method may not be sensitive enough to identify small, but significant changes in the protein expression of these hits. Finally, due to the number of bands present on this blot it would be reasonable to suggest that many of these represent non-specific binding of the antibody and only validation of the antibody against a positive control would allow these data to be utilised appropriately.

5.3.2 Brain expression of protein 4.1N in mice

Validation testing of protein 4.1N expression was initially conducted using an antibody specific to aa 1-100 of full length 4.1N. Western blot analysis of hippocampal and cortical lysates revealed a single band at approximately 130kDa that was unchanged with either diet or BACE1 expression. An additional antibody was used as a requirement for immunohistochemical analysis of brain

sections which revealed multiple bands corresponding to suspected splice variants of 4.1N (Rangel, Lospitao, Ruiz-Sáenz, Alonso, & Correas, 2017; Scott et al., 2001; Wang et al., 2010). However, none changed with diet or BACE1 genotype.

Multiple Uniprot IDs were identified during the proteomic analysis that were expressed in all mice leading to some confusion about 4.1N as a true hit.

As a BACE1 KO NC group was not included in the proteomic analysis, stored hippocampal samples were utilised to identify whether 4.1N expression changes with diet in BACE1 KO mice however, for this study a 20-week dietary intervention had been utilised. This analysis revealed an approximate 2-fold increase in 4.1N expression in the hippocampus with HF compared to NC indicating that 4.1N expression may be influenced by both diet and BACE1. Due to limitations brought about by splice variation and antibody specificity with western blot, further analysis was conducted on brain sections using IHC to identify whether possible co-localisation of BACE1 and 4.1N may occur and whether this changes with diet.

One of the key outcomes of staining in mouse sections was the confirmation of previous published findings that 4.1N expression occurs predominantly within the DG (Walensky et al., 1999). This result had implications for the western blot analysis and may explain the large variability observed for 4.1N expression within groups. Due to human error in hippocampal dissection, the samples harvested are predominantly CA1-CA3. Extraction of the DG often varies with the speed and accuracy of dissection and inconsistencies in the amount of DG present in each sample may explain the inconsistencies of the western blot data. The inconsistency between western blot and proteomic data may also be explained by inaccuracies in the immunoblot methodology. Neither 4.1N antibody had been validated for specificity to this protein 4.1 isoform. It may be that the antibody is not specific enough to identify 4.1N specifically and therefore the presence of 4.1B, G and R are masking changes in 4.1N expression. Alternatively, as only one variant of 4.1N identified in the proteomic analysis was significantly changed with BACE1 KO, it may be that the antibody is not specific to a region that is unique to this variant; therefore the presence of other 4.1N variants are masking the effect of BACE1 KO on Q9Z2H5.

Consistent with published findings, both BACE1 and 4.1N were identified within the stratum radiatum of the hippocampal CA3 region and the polymorph layer of

the DG. This neuronal pathway represents mossy fibre axons of the granule cells of the DG to form synapses with predominantly inhibitory cells of the CA3 but also excitatory pyramidal cells (Acsády, Kamondi, Sík, Freund, & Buzsáki, 1998). High expression of 4.1N within granule cells is consistent with published findings showing high levels of 4.1N mRNA in granular regions of the hippocampus (Parra et al., 2000). Interestingly, in mice, expression of D1 and D2 dopaminergic receptors- known interactors of 4.1N- are also high within the molecular layer of the DG (Binda et al., 2002; Gangarossa et al., 2012). Therefore, it may be that within mouse granule cells, 4.1N is a key regulator of synaptic dopaminergic receptor expression. One possible explanation for the high expression of 4.1N within this area is that granule cells experience high levels of plasticity and indeed, are one of the few resident brain cells known to undergo cell turnover into adulthood and actin assembly is critical within this process (Altman & Das, 1965). Furthermore, exposure to stress hormones (glucocorticoids) has been shown to reduce plasticity within this region (Reviewed in (McEwen, 1999)). This is perhaps consistent with an apparent reduction in 4.1N expression within this region with dietary stress in BACE1 KO mice and studying the role of glucocorticoids in 4.1N and BACE1 expression within this region could be an avenue of further study. Electrophysiology and synaptic integrity experiments would be required to identify whether the apparent reduction in 4.1N expression is representative of altered excitatory connectivity between the DG and CA3.

Another possible area for co-localisation of BACE1 with 4.1N is within the stratum lacunosum moleculare (SLM)- a layer of the hippocampal CA1 region made from the dendrites of pyramidal cells that receives input from layer III of the entorhinal cortex via the temporoammonic pathway and heterogeneous interneurons (Figure 5.1). This includes the highest density of noradrenergic fibres from the locus coeruleus in the hippocampus (Oleskevich, Descarries, & Lacaille, 1989). Furthermore, activation of α-adrenergic receptor α_{2A}AR has been shown to increase amyloidogenesis by increased co-localisation of BACE1 with APP, a receptor associated with the SLM (Chen et al., 2014; Milner, Lee, Aicher, & Rosin, 1998). Whilst increased noradrenaline within the hippocampus has not yet been associated with obesity, increased noradrenaline and increased binding to both α and β adrenergic receptors in the hypothalamus has been associated with genetic mouse models of obesity (Boundy & Cincotta, 2000).

The region of cortex taken during brain dissection is parietal and corresponds to the retrosplenial, visual and somatosensory areas. These regions of cortex can be associated with cognitive functions such as memory, processing of visual information and somatic sensory processing such as touch, temperature and pain respectively. Due to tissue sectioning, the regions of cortex represented in the staining are retrosplenial. This region of the cortex has reciprocal connections with the subicular regions of the hippocampus as well as the entorhinal cortex and the anterior nuclei of the thalamus, all of which can be connected to memory function (Vann, Aggleton, & Maguire, 2009). Within the cortex the retrosplenial area forms connections with the dorsolateral prefrontal cortex- involved in higher cognitive function such as emotion response and working memory (Mars & Grol, 2007). Furthermore, APPswe mice have exhibit APP accumulation within the retrosplenial area from 5 months of age accompanied by decreased c-Fos expression as a marker of reduced plasticity and neuronal dysfunction (Poirier, Amin, Good, & Aggleton, 2011). Animal studies inducing lesions within this cortical region have shown it to be important in spatial and episodic memory as well as utilisation of visual cues in determining direction (Pothuizen, Aggleton, & Vann, 2008; Vann & Aggleton, 2002). This supports evidence that 10% of the retrosplenial area neurons are head direction cells that are important in directional learning and spatial cognition, even in total darkness (Chen, Lin, Green, Barnes, & McNaughton, 1994). Furthermore, the neurons within the cortical region are glutamatergic and responsive to non-competitive NMDAR antagonism in layers II & III and V & VI of the cortex (Fox, Li, Zhao, & Tsien, 2017). It is therefore possible that the staining observed in layer I are represent terminal projections from these excitatory neurons. However, the effect of HFD and subsequent increase in 4.1N expression on directional learning and memory within these animals was not established so the effect of 4.1N expression on the function of this cortical region can only be speculated.

Staining within the hypothalamus was sub-optimal as a result of the sectioning method utilised. Whilst sagittal sections are best to monitor changes in the hippocampus, they do not allow for visualisation of all hypothalamic regions such as the lateral hypothalamic area and arcuate nucleus. Despite this, many key hypothalamic areas were included in the sections however neither BACE1 nor 4.1N staining could be identified within a particular region. Whilst surprising that

BACE1 staining could not be identified within energy regulatory regions of the hypothalamus, we have previously identified the arcuate nucleus as an area of high BACE1 expression and this region was not within the sections used (Meakin, Jalicy, et al., 2018). However, we have also previously described high BACE1 expression within the VMH that was not observed in this study (Meakin, Jalicy, et al., 2018). It may be that the aged mice in this study exhibit increased hypothalamic BACE1 expression thereby reducing the dietary effect, however age-dependent BACE1 increase in WT mice has not been published. Despite not specific hypothalamic BACE1 localisation, there is a general increase in BACE1 staining with HFD which was expected based on previous studies (Meakin et al., 2012; Meakin, Jalicy, et al., 2018). Consistent with proteomic analysis, 4.1N expression appeared unchanged with diet.

5.3.3 Brain expression of protein 4.1N in humans

4.1N expression within human sections differed from mouse sections in the extent of staining. In human sections staining was predominantly within the CA1 region whilst mice expressed most highly within the DG. 4.1N was present in both regions of humans but mice did not appear to express 4.1N greatly within the CA1 region. Both species expressed 4.1N within the CA3 region suggesting that in humans too, the mossy fibre connections between the DG and CA3 are high in 4.1N. Interestingly, whilst mice expressed 4.1N within neuronal projections, humans sections showed staining with cell bodies as well as projections both within the CA regions and the DG.

BACE1 expression also varied between the species. In humans, BACE1 expression showed much greater overlap with 4.1N expression indicating possibly greater co-localisation in humans than mice. BACE1 was expressed to the greatest extent in humans in the CA1-CA3 regions of the hippocampus whilst mice exhibited great expression in the mossy fibers of the stratum radiatum. Similar to 4.1N, BACE1 expression within cell bodies was noted throughout all stained regions for human BACE1 whilst mice exhibited staining only within the neuronal projections of the hippocampus. However, as no information is available on 4.1N expression and function within the human brain, this is speculative. Of greatest interest is the apparent increase in 4.1N expression in all CA and DG regions in AD cases. Whilst excitotoxicity (cell death by over-stimulation by

glutamate) has been associated with AD, it is unlikely that increased expression of 4.1N in this instance is representative of increased excitatory signalling and therefore indicative of aberrant glutamatergic signalling (Reviewed (Wang and Reddy, 2017)). This is due to published data indicating decreased NMDAR expression following progression of AD and the suggestion that 4.1N expression does not influence glutamatergic signalling (Kravitz, Gaisler-Salomon, & Biegon, 2013; Wozny et al., 2009). An alternative mechanism through which 4.1N may regulate plasticity is via a known connection with inositol (1,4,5)-trisphosphate receptor 1 (Maximov et al., 2003). This intracellular calcium channel, when activated leads to an efflux of Ca^{2+} from the ER to the cytosol that has been shown to initiate action potential within pyramidal neurons of the CA1 (Fedorenko et al., 2014; Nakamura et al., 2000). It is therefore feasible that expression of 4.1N, particularly within the cell bodies, may reflect regulation of intracellular Ca^{2+} oscillations that mediate action potential propagation. Alternatively, the increase in 4.1N may indicative of an increase in BACE1 expression. As 4.1N stabilises transmembrane proteins it is plausible that it directly binds to BACE1. Binding studies would be required to determine whether the increase in 4.1N may represent increased BACE1- or other transmembrane protein- stabilisation within the plasma membrane.

Human cortical samples were parietal and represent a brain region involved in visuomotor activities. Samples were obtained from both AD and obese individuals for this brain region with age matched controls for both. This allowed for analysis of 4.1N and BACE1 expression with age, BMI and AD. As with mouse sections, both BACE1 and 4.1N expression was predominantly within layer I of the cortex indicating expression within neuronal termini and some staining within the cell bodies in all layers. BACE1 expression within cell bodies was consistent throughout the groups but expression within layer I appeared to vary with both age and diet. In aged control cases, layer I expression of BACE1 appeared greater in obese individuals suggesting that increased BMI with age leads to increased synaptic expression of BACE1. This result differed from mice whereby HFD did not appear to influence the cortical expression of BACE1. Cortical expression of BACE1 did not appear to change with AD when compared to aged controls leading to the conclusion that BMI is the predominant factor in regulating cortical BACE1 expression. Interestingly, the presence of cell body 4.1N

appeared dependent on age and BMI. All non-aged cases exhibited cell body 4.1N expression whilst both AD and aged obese cases had none. Only aged controls retained cell body 4.1N expression. These findings are in keeping with previous reports suggesting that the RNA binding protein and regulator of 4.1N alternative splicing NOVA1 is increased in AD. However, they also found that expression of NOVA1 in advanced AD returned to pre-clinical levels (Barbash et al., 2017). Expression analysis of NOVA1 would be required to determine whether this 4.1N regulator is influenced by age and diet. As too little is known about the functions of 4.1N outside membrane protein stabilisation it is too early to speculate at the physiological significance of this result. However, this result is likely to be a product of alternative splicing of 4.1N. As described in chapter 4, the 4.1N proteins consist of 22 exons and have been document in their variability (Discher et al., 1995; Walensky et al., 1999). As the FERM domain of 4.1N is integral to its targeting to the plasma membrane, it may be that 4.1N within the cell bodies represents a splice variant whereby the FERM domain is missing (Baines et al., 2014). Determination of 4.1N domain expression could be determined using In-situ hybridisation staining whereby probes are generated to stain for specific mRNA regions. This could be performed to identify the cortical and cellular localisation of the FERM, SAB and C-terminal domains as an indicator of function with disease and age (Wang et al., 2012).

5.3.4 Conclusions

Whilst the proteomic data indicated a relationship between BACE1 and TXNDC15, FUCA1 and protein 4.1N, western blot analysis was not able to validate any of these results. This may be be due to shortcomings in the proteomic analysis or that the tools and methods used to validate lacked the accuracy and sensitivity required. α-L-Fucosidase may still be a significant hit with both diet and BACE1 genotype based on visual inspection of western blots but further analysis is required to establish this.

Western blot analysis of protein 4.1N revealed multiple splice variants that appeared to change in expression to varying degrees and samples exhibited a high degree of variability within groups. It was concluded that this high variability is likely due to the dissection methods used when harvesting brain tissue and the

expression within the blot is more representative of the amount of DG harvested in the hippocampal sample.

Staining in mouse and human sections revealed localisation differences between the species that may indicate difficulties in further studies. Whilst mouse expression of 4.1N was predominantly confined to the DG, humans express this protein to a greater extent in the CA1, CA2 and CA3 regions of the hippocampus. Both of which are involved in memory and LTP. Expression within the CA regions represents a greater likelihood of expression in pyramidal neurons whereas neurons of the DG are more likely to be granular and contain mossy fibers (Wheeler et al., 2015). It may therefore be that differences in DG expression are actually reflective of the granule cell population differences between species as it is known that humans have proportionally fewer granule cells in the DG than rodents (Reviewed by (Amaral, Scharfman, & Lavenex, 2007)). In humans, 4.1N expression appeared to be increased with AD in the hippocampus however, this was not quantified. Due to lack of published data on the role of 4.1N in learning and memory, the implications of this change cannot be interpreted. Within the cortex, opposing effects were observed within the mouse and human with increased 4.1N expression within the molecular layer of the cortex in HF fed mice and reduced expression with obesity in humans. It is plausible that this is a result of the type of diet leading to obesity. Whilst the typical western diet is high in fats, it is also high in sugar, cholesterol and low in fibre and protein. The difference between a simple increase in dietary fat used in this study and the more complex nutrition representative western diet may be the reason behind the opposing effects. Of great interest is the effect of diet and age on the cell body localisation of 4.1N within the cortex. Data here suggest that sub-cellular localisation of 4.1N is regulated by both age and diet and increased membrane targeting in aged obese and AD cases may be a result of alternative splicing. As 4.1N has been implicated in glutamatergic signalling, a process known to be dysregulated in AD, the changes observed in this study may provide a mechanism through which age and AD alter hippocampal function and memory formation. If localisation and domain structure of 4.1N is altered with diet, age and AD, 4.1N may provide a novel mechanism through which both age and HFD increase the risk of developing this dementia. Furthermore, changes in 4.1N may be a way through which AD affects neuronal structure, connectivity and signalling through actin

binding and glutamate receptor stabilisation. Therefore, targeting this protein pharmaceutically may improve hippocampal function and memory in those affected by AD. However, further studies into splice variation with both diet and AD as well as analysis of glutamatergic signalling within these groups could provide valuable insight into how 4.1N may influence hippocampal function.

Chapter 6

Determining the BACE1 interactome

6.1 Introduction

BACE1 is the protease responsible for the production of amyloid peptides from APP. This transmembrane aspartyl protease cleaves APP at two sites: the β site, located between residues Met671 and Asp672 producing full length amyloid peptides (1-X) and the β' site at residues Tyr681 and Gln682 producing truncated amyloid species' (11-X) (Liu, Doms, & Lee, 2002; Vassar et al., 1999). Cleavage of APP by BACE1 leads to the release of sAPPβ and subsequent cleavage by a γ-secretase complex results in the formation of the amyloid-β as described in Chapter 1.

Despite its well-characterised role in amyloid production and thus pathogenicity, little is known about the physiological role of BACE1. The gene for BACE1 is highly conserved throughout evolution and variants have been traced back to Cnidaria with BACE1 orthologues existing in basal chordates. Whilst BACE1 has been highly conserved, the APP protein evolved more recently in lobe finned fish indicating the importance of BACE1 outside of APP cleavage and an estimated evolutionary separation of BACE1 from amyloid-β of 360 million years. Crucially, conservation of function has been determined as expression of *Branchiostoma* (Lancelets) BACE1 with human APP in cells led to increased amyloid production compared to GFP controls (Moore et al., 2014a).

Upon maturation, BACE1 is transported to the plasma membrane whereby palmitoylation leads to targeting to lipid rafts. From the plasma membrane, BACE1 is cycled into endosomes from which it can be targeted to lysosomes for degradation, cycled back to the plasma membrane or undergo retrograde transport to the TGN; from which the whole cycle is repeated (Araki, 2016). It has been hypothesised that BACE1 localisation within the cell may be responsible for off-target effects leading to disease. Changes in BACE1 compartmentalisation may alter the substrate profile due to differences in the proteins expressed between organelles. Accumulation of BACE1 in these compartments may allow access to proteins which are known to be poor BACE1 substrates (such as APP) but due to BACE1 surplus, become targets for proteolysis (Grüninger-Leitch, Schlatter, Küng, Nelböck, & Döbeli, 2002).

Many studies have been conducted into possible interactors of BACE1. Advancing proteomic techniques have allowed interactomic studies to become more diverse leading to identification and validation of BACE1 substrates such as APLP1, APLP2, CHL1, NRG1, NRG3, Sez6, Sez6L1 and PSGL1. Many putative substrates have been identified through quantitative proteomics and secretome studies, most of which are type I transmembrane proteins. (Dislich et al., 2015; Hemming et al., 2009; Kuhn et al., 2012). However, these substrates have only offered further insight into the pathogenicity of BACE1 and not the physiological function.

As described in chapter 1, BACE1 has been implicated in many physiological processes. Most studies have focussed on nervous system functions for BACE1 and have suggested roles including muscle spindle formation, myelination, synaptogenesis and axon guidance, all of which have been extensively reviewed (Vassar et al., 2014; Yan, 2017). Evidence also associates BACE1 with metabolic homeostasis through changes in insulin/leptin sensitivity, glucose uptake and thermogenesis (Hamilton et al., 2014; Meakin et al., 2012; Meakin, Jalicy, et al., 2018; Meakin, Mezzapesa, et al., 2018; Plucińska et al., 2016; Wang et al., 2013a). BACE1 has also been suggested as a modulator of inflammatory signalling and microglial activation (Heneka et al., 2005; Thakker et al., 2015). However, whilst these associations have been suggested through human and animal studies, the molecular mechanisms behind these suggested functions have yet to be determined.

A novel technique for the identification of interacting proteins was developed by Roux *et al*. (2012). They describe a proximity assay based on the DamID methodology used to map DNA binding sites of a protein of interest by creating a fusion protein with a DNA methyltransferase (Vogel, Peric-Hupkes, & van Steensel, 2007). The BioID method utilises an *E.coli* BirA protein with a R118G point mutation within a disordered loop of active site (Choi-Rhee, Schulman, & Cronan, 2008; Cronan, 2005). This point mutation confers substrate promiscuity and enables the protein to biotinylate proteins based on proximity rather than substrate specificity by altering biotin binding and catalytic properties of BirA (Kwon & Beckett, 2000). The BirA protein is a biotin ligase that, upon creation of a fusion protein, biotinylates proteins within 10nm of BirA (Kim et al., 2014).

Streptavidin pulldown and MS/MS then enables identification of the biotinylated proteins and allows insight into binding partners of the protein of interest.

In order to better understand the physiological role of BACE1 in non-diseased conditions, a BioID assay was developed for BACE1 creating both BACE1-BirA and BirA-BACE1 constructs. It was hypothesised that the N-terminal BirA-BACE1 fusion protein would provide information about possible substrates of BACE1 as this region contains the active site and is extracellular. However, the presence of the large BirA tag could interfere with BACE1 activity or transport if the signal and pro-peptides could not be processed. The C-terminal fusion protein BACE1-BirA would identify the greatest number of hits and provide information about the BACE1 environment as this tag would be cytoplasmic and would be less likely to interfere with BACE1 protease activity. The BACE1-BirA construct was expressed in the HT-22 and GT1-7 cell lines. Both are murine cell lines of hippocampal and hypothalamic origin respectively and by their use we hoped to identify the BACE1 interactome in cell types physiologically relevant to both AD and metabolic diseases. Biotin incubations were conducted at 24 and 48 hours as both timepoints had been previously optimised using another construct (personal communication, Dr William Fuller, University of Glasgow) and would provide information regarding BACE1 production and degradation pathways. The experiment was repeated 3 times and proteins were considered hits if they were identified in more than one of these replicates within each timepoint. Identification of proximal proteins was achieved, and hits analysed for likely substrates as well as pathway analysis. The known trafficking and previously identified substrates were used as identifiers for cycling of the BACE1-BirA construct and were used as indicators of correct BACE1 processing within the cell.

6.2 Results

6.2.1 Cloning BACE1 BirA fusion proteins

Cloning an N-terminal BirA BACE1 fusion protein (BirA-BACE1) required addition of both the signal and propeptides upstream of the BirA gene. These peptides are required for BACE1 targeting into the membrane and correct folding of the BACE1 protein; meaning that these peptides are a requirement of BACE1 function. As these peptides are cleaved upon BACE1 maturation, including them *in situ* within the BACE1 gene would result in removal of the N-terminal BirA tag.

Therefore, the signal and propeptides were inserted 5' of the BirA gene with the sequence for mature BACE1 being cloned into the multiple cloning site (MCS). In order to do this, site directed mutagenesis was conducted on the empty vector to insert the peptides and a 5' Kozak consensus sequence to initiate translation of translated mRNA. The reverse primer was designed in order to remove the Kozak sequence upstream of the MCS. Mutagenesis was achieved with the Kozak sequence signal peptide sequence thus a vector was created that would target to the membrane. Insertion of the propeptide proved difficult and multiple cloning efforts were unsuccessful. Due to the limitations in the insertion site to keep the peptide both in-frame and abutting the signal peptide, few options were available in primer design. Due to high GC content of the available primers and moderate-high secondary structure of the primers, the propeptide was not able to be added to the vector. Variations in PCR conditions such as the addition of DMSO and increasing $MgSO_4$ were unsuccessful as well as increasing the number of cycles and varying the annealing temperature. Due to this, further attempts at creating the BirA-BACE1 fusion protein were halted and it was decided that the construct would be synthesised commercially.

The C-terminal BACE1 BirA fusion protein (BACE1-BirA) was attempted using restriction cloning. The BACE1 gene was amplified using primers designed to create compatible restriction sites to the empty vector. The amplified insert was purified and insertion into both a shuttle vector and directly into the empty vector was attempted. Neither proved to be successful with multiple primer designs and varying ligation conditions. Restriction cloning was unsuccessful leading to attempts to clone using the InFusion method. This method also proved unsuccessful even with multiple primer designs and upon consideration, it was decided that this construct, would be made synthetically.

6.2.2 Expression of BACE1-BirA in neuronal cell lines

Transfection of the BACE1-BirA construct was successful in both GT1-7 and HT-22 cell lines (Figure 6.1A) giving rise to bands at approximately 98 and 110kDa when immunoblotted for the HA-tag. The estimated molecular weight of the fusion protein was 92kDa. Immunoblot of the BACE1 protein leads to characteristic double banding with a lower molecular weight representing the immature, unprocessed BACE1 protein. Upon BACE1 maturation extensive post-

translational modifications through glycation, phosphorylation and palmitoylation lead to a mature BACE1 band at a higher molecular weight. This characteristic banding pattern was evident in the BACE1-BirA fusion protein in both the GT1-7 and HT-22 cell lines when immunoblotted against the HA-tag. It was also noted that construct expression was reduced at the 48 hour timepoint when compared to 24 hour timepoint across both cell lines. Expression of BACE1-BirA was substantially lower in GT1-7 cells compared to the HT-22s and experiments in this hypothalamic cell line did not successfully produce biotinylated proteins in concentrations high enough to be visualised by western blot. Consequently, HT-22 cells were used in this experiment due to their high-expression of BACE1-BirA (Figure 6.1B). Proximity assay in the HT-22 cell line revealed many biotinylated proteins in the soluble lysate in transfected cells after 24 hour and 48 hour biotin load (Figure 6.1C). Untransfected cells exhibited no biotinylation after 48 hour biotin load. Biotinylated proteins were absent in the unbound fraction after streptavidin pulldown indicating successful purification of BACE1 proximal proteins (Figure 6.1C)

Trypsinised, biotinylated proteins were sent to the Fingerprints proteomics facility for identification. The samples were purified and MALDI-TOF MS/MS was conducted to identify the peptide fragments of purified proteins. Peptides were scored using Mascot probability-based scoring to determine whether results were significant or not. The score represented the probability of a peptide being assigned by chance and a high score indicated a high probability of that result being real. The score in this instance was set to ≥36 with $p<0.05$ indicating that the peptides assigned to the protein show extensive sequence similarity to the hit protein. This ion score was used as a cut-off (as opposed to ≥68 used in human protein databases) as the protein database for *Mus musculus* is smaller than the database for *Homo sapiens*. As the mouse database contains fewer proteins the theoretical peptides used to create the ion score are fewer. This leads to a skewing of the data and therefore requires the ion score cut-off to be lower. Once a protein list was created, each replicate was compared to its control and proteins identified within the control were removed as hits. Protein lists between replicates were then compared in order to identify proteins that occurred in more than one replicate at each timepoint.

6.2.3 BACE1 interactors in HT-22 cells

Proximity assay with 24 hour biotin load identified 291, 409 and 216 proteins in replicates 1,2 and 3 respectively; 182 proteins were identified in more than one replicate (Table 6.1). At 48 hour biotin load 272, 256 and 190 proteins were identified in replicates 1,2 and 3 respectively; 133 proteins were identified in more than one replicate (Table 6.2). 77 proteins were identified at both 24 hour and 48 hour timepoints, 14 of which appeared in every replicate at both timepoints (Afdn, Bace1, Bsg, Cav1, Cavin2, Ddr2, Dlg1, Slc1a5, Slc6a9, Snap23, Sptbn1, Steap3, Vamp3 and Zdhhc20). 12 proteins were identified in every replicate at 24 hours that did not appear in more than 1 replicate at 48 hours (Abcf2, Arhgap1, Axl, Efr3a, Gart, Ifitm3, Kars, Krt10, Mettl16, Myof, Sh3pxd2a and Vang1) 3 proteins appeared in every replicate at 48 hours without being identified in more than one replicate at 24hours (Gigyf1, Mprip, Vps13c). 5 previously identified BACE1 interactors were identified (Bsg, Epha2, Flot2, Gga2, Zdhhc20), these include proteins involved in BACE1 sorting and membrane targeting as well as putative substrates.

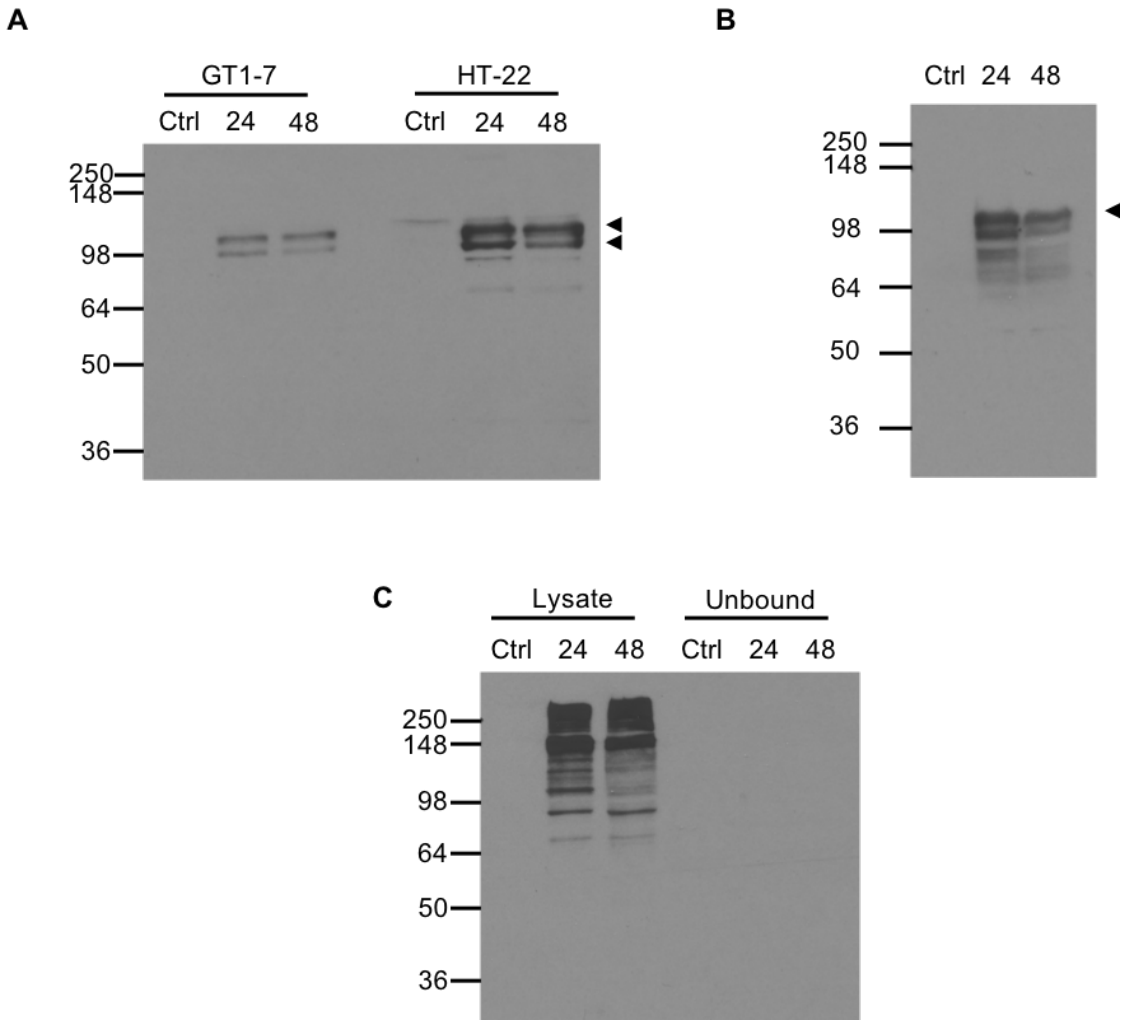

Figure 6.1 BACE1 expression and biotinylation profile of transfected GT1-7 and HT-22 cell lines. BACE1-BirA fusion protein expression in GT1-7 and HT-22 neuronal cell lines (A) Western blot of GT1-7 and HT-22 cell lysates revealed expression of the BACE1-BirA fusion protein as identified by the presence of the HA-tag. The presence of two bands is reminiscent of native BACE1 whereby immature and mature BACE1 can be seen at 64 and 70kDa respectively. (**B**) Western blot of HT-22 cell lysate reveals BACE1 expression at a comparable molecular weight to that seen using HA antibody. (**C**) HT-22 cell lysate and unbound fraction after streptavidin pull-down reveal biotinylated proteins as a product of the proximity assay and their removal from solution post purification.

24 hr		
1 & 2	2 & 3	1 & 3
	Abcb1b	
Abcc1		
Abcf1		
Abcf2	Abcf2	Abcf2
Acta2		
Adrm1		
Afdn	***Afdn***	***Afdn***
Ano6	**Ano6**	**Ano6**
		Anxa7
		ApoB
Arhgap1	Arhgap1	Arhgap1
		Arl6ip5
Asns		
		Atp2b1
	Aurkb	
Axl	Axl	Axl
Bace1	***Bace1***	***Bace1***
Bsg	***Bsg***	***Bsg***
		Bub1
Canx		
Cav1	***Cav1***	***Cav1***
	Cavin1	
Cavin2	***Cavin2***	***Cavin2***
Cct7		
Cd44		
	Cdc27	
Cdc42bpb		
Ckap4		
Clic1		
		Ctgf
	Cttn	
Ddr2	***Ddr2***	***Ddr2***
	Ddx39a	
Dlg1	***Dlg1***	***Dlg1***
		Dnajc11
		Dnttip1
		Dpy19l1
Dync1li2		
Eef1b		
Efr3a	Efr3a	Efr3a
Ehd1		
Eif2s1		
Eif3c		
	Eif3h	
Eif3i	**Eif3i**	**Eif3i**
Eif3l		
Eif4g1		
Eif5a2		
		Elp1
Emc1		
Epb41l2		
Epb41l3		
Epha2	**Epha2**	**Epha2**
Ephb3		
Erbin		
Esd		
Fam98a		
Fermt2	**Fermt2**	**Fermt2**
Flot2		
G6pdx		
Ganab		

24 hr		
1 & 2	2 & 3	1 & 3
Gart	Gart	Gart
	Gga2	
Gja1	**Gja1**	**Gja1**
	Gk	
Gmps		
Gorasp2		
Hba	**Hba**	**Hba**
Hmox2		
Ifitm3	Ifitm3	Ifitm3
Itgb1		
	Jak1	
Kars	Kars	Kars
	Khdrbs1	
		Kif22
Kif5b		
Klc1		
Krt10	Krt10	Krt10
Krt14		
Ktn1		
Lrrc8c		
Ltbp1		
	Ltbp3	
Mettl16	Mettl16	Mettl16
Mtatp6		
Myadm		
Myh9		
Myof	Myof	Myof
Naca		
Nckap1		
	Nfic	
	Nob1	
Nomo1	**Nomo1**	**Nomo1**
Notch2		
Pacsin2		
	Paics	
Palm		
	Patl1	
	Pcdhga4	
Pgk1		
Pgrmc2	**Pgrmc2**	**Pgrmc2**
Phactr4		
Piezo1		
Plod3		
Plp2		
Plxnb2		
Pnn		
		Polr2h
Psma5		
Psmc1		
Psmc6		
	Ptk2	
	Ptprd	
Ptprf		
Rab10		
Rab11fip5		
Rab14		
	Rab1A	
	Rab1B	
		Rab21
Rab32	**Rab32**	**Rab32**
Rab5C	**Rab5C**	**Rab5C**

24 hr		
1 & 2	2 & 3	1 & 3
Rab7A	**Rab7A**	**Rab7A**
	Rad51	
		Rai14
	Rbm17	
	Rbmx	
Ralgapb		
Reps1		
Rheb		
	Rnp219	
Rpl22		
Rpl5		
Rplp1		
	Rps2	
Rps10		
Rps13		
	Rras2	
Rrbp1	**Rrbp1**	**Rrbp1**
	Sec23a	
		Sept11
Sept7	***Sept7***	***Sept7***
Serpinb6		
Sh3pxd2a	Sh3pxd2a	Sh3pxd2a
Slc12a2	**Slc12a2**	**Slc12a2**
Slc1a5	***Slc1a5***	***Slc1a5***
Slc20a2		
	Slc38a1	
Slc6a9	***Slc6a9***	***Slc6a9***
	Slco2a1	
Slk		
Snap23	***Snap23***	***Snap23***
Sptan1		
Sptbn1	***Sptbn1***	***Sptbn1***
	Sqle	
	Stat5a	
Steap3	***Steap3***	***Steap3***
Tars		
Tfrc		
Tjap1		
	Tmed9	
	Tmem41b	
Tmx1		
	Top2a	
Ttc23		
	Tuba1c	
		Tulp4
	Ubr2	
		Utp4
Vamp3	***Vamp3***	***Vamp3***
Vamp5		
		Vamp7
Vang1	Vang1	Vang1
	Wdr77	
Wipi2		
	Wwox	
		Ykt6
		Ywhae
Ywhag		
Zdhhc20	***Zdhhc20***	***Zdhhc20***
Zdhhc5		
		Zmiz2

Table 6.1 BACE1 proximal proteins after 24 hour biotin load. Columns indicate which technical replicates each hit was identified in, 1&2, 2&3 or 1&3. Highlighted- Gene names of proteins identified in all replicates, Red- known BACE1 interactors, Bold- appear in at least 4 of 6 replicates across both timepoints, Italics- appear in every replicate.

48hr		
1 & 2	2 & 3	1 & 3
Abcc1		
	Acin1	
Afdn	***Afdn***	***Afdn***
Agfg1		
	Agps	
		Alg10b
Ano6		
		Asns
Bace1	***Bace1***	***Bace1***
		Basp1
Bsg	***Bsg***	***Bsg***
Canx		
Cav1	***Cav1***	***Cav1***
	Cavin1	
Cavin2	***Cavin2***	***Cavin2***
Cavin3		
Ccdc115		
Cd44		
Cdc42bpb	***Cdc42bpb***	***Cdc42bpb***
Cdc42se2		
	Cfl1	
	Chchd2	
Ckap4		
	Clic1	
		Cltc
Cobll1		
Ddr2	***Ddr2***	***Ddr2***
		Dhrs1
Dlg1	***Dlg1***	***Dlg1***
Dock8		
Dync1li2		
		Eef1d
Ehd1		
Eif3i		
Endod1		
Epb41l2		
Epb41l3		
	Epha2	
Esd		
Ezr		
Fermt2		
	Fkbp1a	
Gigyf1	Gigyf1	Gigyf1
Gja1		
		Gnai2

48hr		
1 & 2	2 & 3	1 & 3
Gorasp2		
		Hba
Hist1h1c		
	Hist1h2bc	
Hsd17b7		
Ifitm3		
Itgb1		
		Khdrbs1
Kif5b	**Kif5b**	**Kif5b**
Lin7a		
Lnpk		
Lrrc8c		
	Mfsd1	
Mprip	Mprip	Mprip
Mtatp6		
Myadm		
	Myh9	
Nckap1		
		Nf1
		Nomo1
	Pacs1	
Pacsin2		
Palm		
Pank4		
	Pcgf5	
Pgrmc2	***Pgrmc2***	***Pgrmc2***
Piezo1		
Plod3		
Plp2		
Pnn		
Pole		
		Polr2h
Rab10		
Rab32		
Rab5c		
Rab7a		
		Rai14
Ralgapa1		
Ralgapb		
		Rasl2-9
Rheb		
	Rras2	
Rrbp1		
		S100a6
	Scrib	

48hr		
1 & 2	2 & 3	1 & 3
Sept7	***Sept7***	***Sept7***
Sept8		
		Sept11
Slc12a2		
Slc12a4		
Slc1a5	***Slc1a5***	***Slc1a5***
Slc20a2		
Slc30a4		
	Slc35a1	
	Slc35f6	
Slc39a7		
Slc6a9	***Slc6a9***	***Slc6a9***
Slc7a11		
Slk		
Snap23	***Snap23***	***Snap23***
		Sptan1
Sptbn1	***Sptbn1***	***Sptbn1***
		Srd5a3
		Srsf3
	Srsf7	
	Steap1	
Steap3	***Steap3***	***Steap3***
Tfrc		
	Tmed2	
Tmem176b		
	Tmem41b	
Tmem59		
Tmx1		
	Top2a	
Triobp		
Ttc23		
	Tuba1c	
	Ubr2	
		Usp30
Vamp3	***Vamp3***	***Vamp3***
Vamp7		
Vangl1		
Vps13c	Vps13c	Vps13c
		Wdr59
Wwox		
Ykt6	**Ykt6**	**Ykt6**
Ywhag		
Zdhhc20	***Zdhhc20***	***Zdhhc20***

Table 6.2 BACE1 proximal proteins after 48 hour biotin load. Columns indicate which technical replicates each hit was identified in, 1&2, 2&3 or 1&3. Highlighted- Gene name of proteins identified in all replicates, Red- known BACE1 interactors, Bold- appear in at least 4 of 6 replicates across both timepoints, Italics- appear in every replicate.

6.2.4 Functional analysis of BACE1 interactors

Only hits that appeared in every replicate at each time point were further studied for function and mapped based on known cellular localisation. Protein functions and subcellular localisations were identified by the Reactome pathway analysis program which utilises the Uniprot database. BACE1 was removed from this analysis as it could not be determined whether this hit was due to self-biotinylation of the fusion protein or a product of BACE1 dimerisation. Proteins with multiple locations were mapped to all known organelles. With 24 hour biotin load, 5 main functions can be identified from the protein hits; cell signalling (3 hits), cytoskeletal organisation (5 hits), ion homeostasis (4 hits), protein synthesis (3 hits) and protein trafficking (7 hits) (Table 6.3). When mapped by known localisation of these proteins, only protein trafficking proteins appear to be in high abundance in a single location, with 4 of the 7 hits known to localise to the plasma membrane. (Figure 6.2) With 48 hour biotin load, 2 main functions can be identified from the protein hits; cytoskeletal organisation (5 hits) and protein trafficking (5 hits). (Table 6.4) When mapped by known localisation of these proteins, 3 protein trafficking proteins were identified that localise to the plasma membrane. No other cellular function was identified as enriched in a specific cellular locale. (Figure 6.3)

24 hour			
Gene	**Protein**	**Expression**	**Function**
Slc1a5	Neutral amino acid transporter B(0)	plasma membrane	amino acid transport
Afdn	Afadin	Nuclear, plasma membrane, cell junctions	cell adhesion
Gja1	Gap junction alpha-1 protein	Nuclear, Vesicles, cell junctions, plasma membrane	cell adhesion
Myof	Myoferlin	vesicles, plasma membrane	cell repair
Epha2	Ephrin type-A receptor 2	nuclear, golgi, plasma membrane, cell junctions	cell signalling
Arhgap1	Rho GTPase-activating protein 1	vesicles	cell signalling
Axl	Tyrosine-protein kinase receptor UFO	plasma membrane	cell signalling
Ddr2	Discoidin domain-containing receptor 2	cytoskeletal, plasma membrane	cell surface receptor
Pgrmc2	Membrane-associated progesterone receptor component 2	Nucleus, plasma membrane, cytosol	cell surface receptor
Sptbn1	Spectrin beta chain, non-erythrocytic 1	golgi, plasma membrane	cytoskeletal organisation
Krt10	Keratin, type I cytoskeletal 10	cytoskeleton	cytoskeletal organisation
Dlg1	Disks large homolog 1	vesicles, plasma membrane	cytoskeleton organisation
Fermt2	Fermitin family homolog 2	nuclear, focal adhesion sites	cytoskeleton organisation
Sep7	Septin-7	Cytoskeleton, Nuclear	cytoskeleton organisation
Nomo1	Nodal modulator 1	ER	development
Vang1	Vang-like protein 1	plasma membrane	development
Sh3pxd2a	SH3 and PX domain-containing protein 2A	Cytosol	ECM organisation
Ifitm3	Interferon-induced transmembrane protein 3	Plasma membrane, endosome, lysosome	Immune response
Ano6	Anoctamin-6	Cytosol, plasma membrane	ion homeostasis
Abcf2	ATP-binding cassette sub-family F member 2	cytosol	ion homeostasis
Steap3	Metalloreductase STEAP3	cytosol, nuclear	ion homeostasis
Slc12a2	Solute carrier family 12 member 2	vesicles, plasma membrane	ion homesostasis
Bsg	Basigin	Vesicles, secreted, plasma membrane	membrane targeting
Efr3a	Protein EFR3 homolog A	plasma membrane, cytosol	membrane targeting
Slc6a9	Sodium- and chloride-dependent glycine transporter 1	Nuclear, golgi	neurotransmitter-related
Hba	Hemoglobin subunit alpha	Cytosol	Oxygen transport
Zdhhc20	Palmitoyltransferase ZDHHC20	Vesicles, plasma membrane, mitochondria	Palmitoylation
Eif3i	Eukaryotic translation initiation factor 3 subunit I	nuclear, cytosol	protein synthesis
Kars	Lysine--tRNA ligase	cytosol	protein synthesis
Rrbp1	Ribosome-binding protein 1	ER	protein synthesis
Cavin2	Caveolae-associated protein 2	Cytosol	protein trafficking
Cav1	Caveolin-1	golgi, plasma membrane	protein trafficking
Rab32	Ras-related protein Rab-32	cytosol	protein trafficking
Rab5c	Ras-related protein Rab-5C	Endosomes, plasma membrane	protein trafficking
Rab7a	Ras-related protein Rab-7a	lysosomes, endosome	protein trafficking
Snap23	Synaptosomal-associated protein 23	plasma membrane	protein trafficking
Vamp3	Vesicle-associated membrane protein 3	plasma membrane	protein trafficking
Gart	Trifunctional purine biosynthetic protein adenosine-3	Nuclear, cytosol, mitochondria	purine metabolism
Mettl6	U6 small nuclear RNA (adenine-(43)-N(6))-methyltransferase	Nuclear, cytosol	RNA nethylation

Table 6.3 Protein functions and cellular localisations of BioID hits after 24 hour biotin load

48hr			
Gene	**Protein**	**Expression**	**Function**
Slc1a5	Neutral amino acid transporter B(0)	plasma membrane	amino acid transport
Afdn	Afadin	Nuclear, plasma membrane, cell junctions	cell adhesion
Gigyf1	GRB10-interacting GYF protein 1	vesicles, cytoskeleton	cell signalling
Ddr2	Discoidin domain-containing receptor 2	cytoskeletal, plasma membrane	cell surface receptor
Pgrmc2	Membrane-associated progesterone receptor component 2	Nucleus, plasma membrane, cytosol	cell surface receptor
Sptbn1	Spectrin beta chain, non-erythrocytic 1	golgi, plasma membrane	cytoskeletal organisation
Sept7	Septin-7	Cytoskeleton, Nuclear	cytoskeleton organisation
Mprip	Myosin phosphatase Rho-interacting protein	cytoskeleton, cytosol	cytoskeleton organisation
Cdc42bpb	Serine/threonine-protein kinase MRCK beta	plasma membrane, cell junctions,	cytoskeleton organisation
Dlg1	Disks large homolog 1	vesicles, plasma membrane	cytoskeleton organisation
Steap3	Metalloreductase STEAP3	cytosol, nuclear	ion homeostasis
Bsg	Basigin	Vesicles, secreted, plasma membrane	membrane targeting
Vps13c	Vacuolar protein sorting-associated protein 13C	mitochondria, cytoskeleton	Mitochondrial function
Slc6a9	Sodium- and chloride-dependent glycine transporter 1	Nuclear, golgi	neurotransmitter-related
Kif5b	Kinesin-1 heavy chain	cytoskeleton, cytosol	Organelle transport
Zdhhc20	Palmitoyltransferase ZDHHC20	Vesicles, plasma membrane, mitochondria	Palmitoylation
Snap23	Synaptosomal-associated protein 23	plasma membrane	protein trafficking
Cav1	Caveolin-1	golgi, plasma membrane	protein trafficking
Vamp3	Vesicle-associated membrane protein 3	plasma membrane	protein trafficking
Cavin2	Caveolae-associated protein 2	Cytosol	protein trafficking
Ykt6	Synaptobrevin homolog YKT6	Cytocol, golgi, mitochondria	protein trafficking

Table 6.4 Protein functions and cellular localisations of BioID hits after 48 hour biotin load

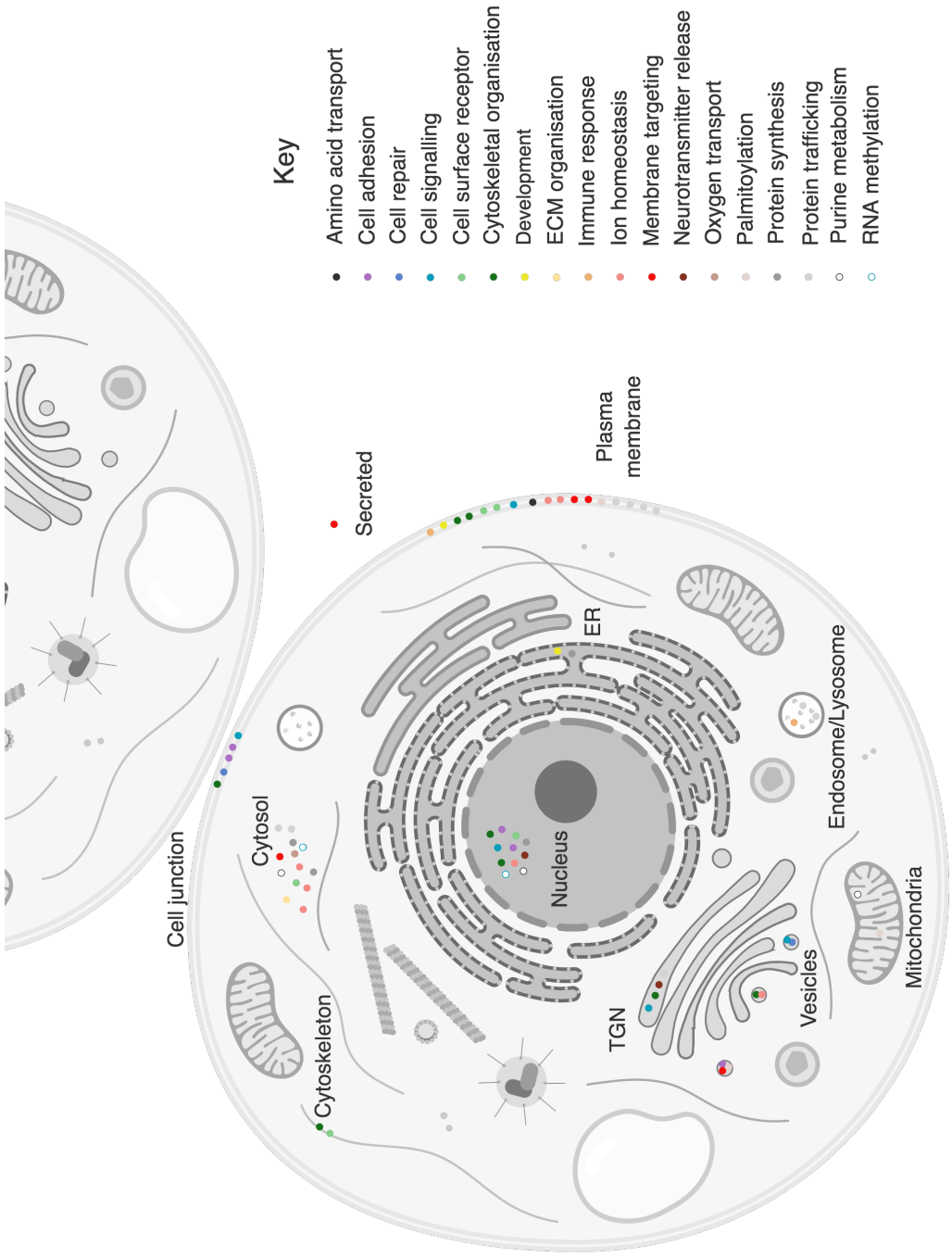

Figure 6.2 Mapping of BACE1 interactor function by cell localisation with 24 hour biotin load. Protein trafficking proteins were more highly represented at the plasma membrane after 24 hours biotin load but no other cellular function was highly represented in another organelle. This suggests BACE1 does not target specific functions at different cellular localisations. Figure was made using BioRender.com.

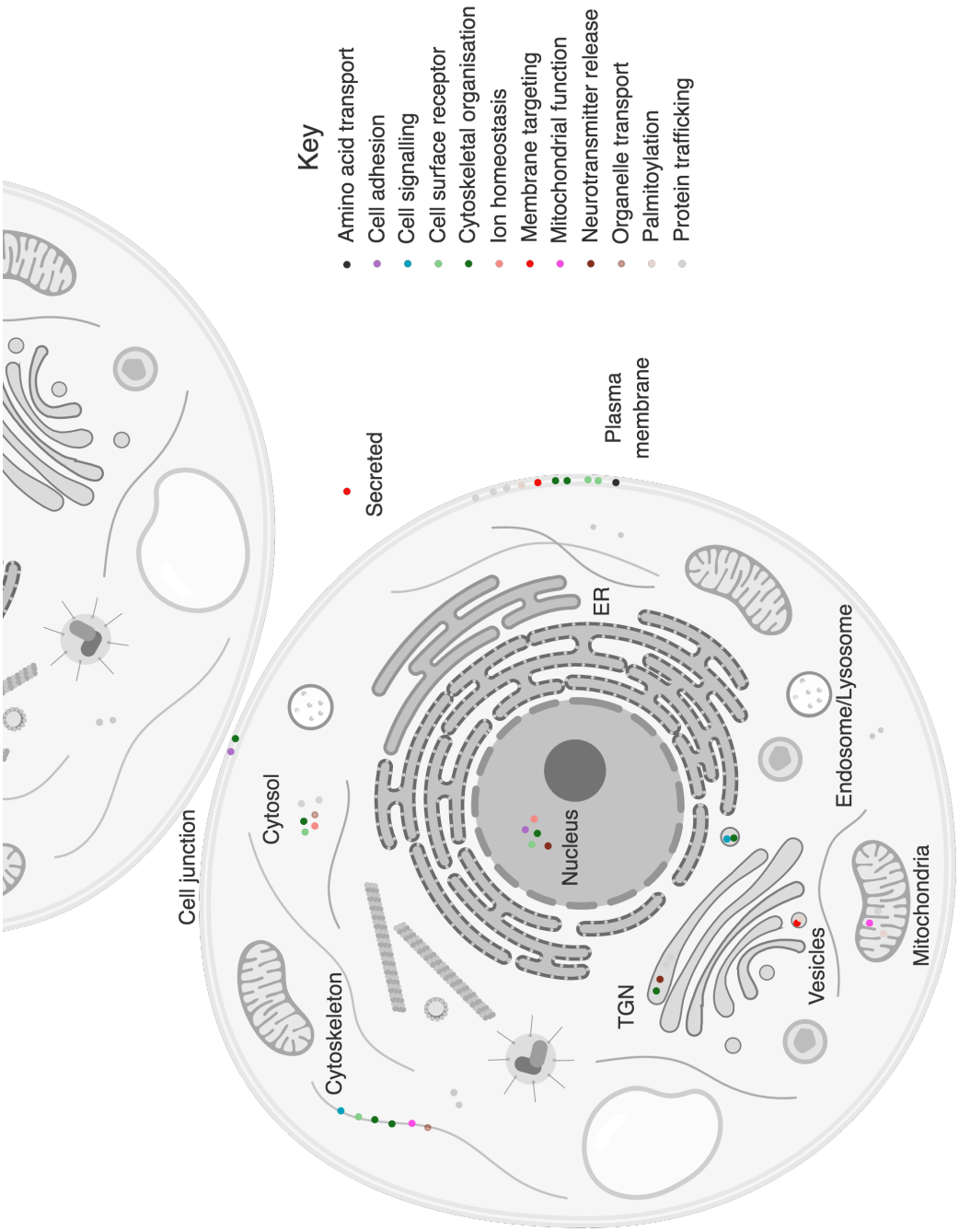

Figure 6.3 Mapping of BACE1 interactor function by cell localisation with 48 hour biotin load. Protein trafficking proteins were more highly represented at the plasma membrane after 48 hours biotin load as with 24 hours. No other cellular function was highly represented in another organelle. This provides further evidence that BACE1 does not target specific functions at different cellular localisations. Figure was made using BioRender.com.

6.2.5 Pathway analysis of BACE1 interactors

Pathway analysis was conducted using hits from >2 replicates to improve the input data. Hits in all 3 replicates identified no enriched pathways, possibly as a result of too few hits (38 hits at 24 hours and 40 hits at 48 hours). Pathway analysis was conducted using the reactome pathway database to allow visualisation of enriched pathways identified through the BioID assay. Pathways were filtered by species to identify those within *Mus musculus* as HT-22 cells are of murine origin. The 25 most significant pathways were identified by FDR corrected over-representation analysis and any pathway with a single protein identified within it was discounted. This led to an indicator of pathways that interact with BACE1.

Of the protein hits input, 37 hits were not identified at 24 hours. (Table 6.5) Using the remaining 145 hits, 5015 pathways were identified. At 48 hours, 40 hits were not identified. (Table 6.5) Using the remaining 93 hits, 3661 pathways were identified. The top 25 pathways at each timepoint were identified, pathways with the same FDR were ranked by the p-value. Pathways identified at 24 hour and 48 hour timepoints are represented in tables 6.6 and 6.7 respectively. Only RHO GTPase activation of kinectin 1 (KTN1) with 24 hour biotin load had $p<0.05$ of all the pathways identified at 24 hours biotin load. (Figure 6.4)

24 hours			48 hours		
Abcf2	Naca	Rab11fip5	Basp1	Palm	Slk
Anxa7	Nomo1	Sept11	Cavin2	Pgrmc2	Steap1
Clic1	Palm	Slk	Cavin3	Piezo1	Tmem176b
Cavin2	Plxnb2	Tjap1	Ccdc115	Pnn	Tmem41b
Cdc42bpb	Pcdhga4	Tmx1	Cdc42bpb	Rail4	Tmem59
Dnttipl	Pgrmc2	Ttc23	Cdc42se2	Ralgapa1	Tmx1
Dpy19l1	Phactr4	Tmem41b	Clic1	Rasl2-9	Triobp
Efr3a	Piezo1	Vamp5	Cobll1	Rras2	Ttc23
Emc1	Pnn	Vang1	Dhrs1	Rrbp1	Vangl1
Fam98a	Rai14	Zdhhc20	Gigyfl1	S100a6	Vps13c
Mettl16	Rnf219	Zmiz2	Lnpk	Sept11	Wdr59
Myadm	Rras2		Mfsd1	Sept8	Zdhhc20
Myof	Rrbp1		Myadm	Slc30a4	
			Nomo1	Slc35f6	

Table 6.5 BioID hits not recognised during pathway analysis Gene names of proteins that were not recognised by the pathway analysis software and therefore not included in pathway analysis.

	24 hours					
	Entities				Reactions	
Pathway name	found	ratio	p-value	FDR	found	ratio
RHO GTPases activate KTN1	25/36	0.003	9.57E-12	5.26E-09	2/2	2.65e-04
Hyaluronan uptake and degradation	8/24	0.002	0.01	0.997	3/7	9.29e-04
Hyaluronan metabolism	8/28	0.002	0.023	0.997	1/4	5.31e-04
TP53 regulates transcription of gene involved in cytochrome C release	3/12	8.62e-04	0.182	0.997	1/4	5.31e-04
Golgi cisternae pericentriolar stack reorganisation	3/13	9.34e-04	0.212	0.997	2/2	2.65e-04
Interleukin-12 signalling	3/13	9.34e-04	0.212	0.997	4/15	0.002
Localisation of the PINCH-ILK-PARVIN complex to focal adhesions	1/2	1.44e-04	0.216	0.997	1/1	1.33e-04
Sigalling by Leptin	1/2	1.44e-04	0.216	0.997	1/1	1.33e-04
Formation of the ternary complex and subsequently, the 43S complex	8/49	0.004	0.251	0.997	3/3	3.98e-04
Translation initiation complex formation	9/58	0.004	0.279	0.997	2/2	2.65e-04
Ribosomal scanning and start codon recognition	9/59	0.004	0.295	0.997	2/2	2.65e-04
Activation of the mRNA upon binding of the cap-binding complex and eIFs, and subsequent binding to 43s	9/59	0.004	0.295	0.997	3/4	5.31e-04
Notch 2 activation and transmission of signalling to the nucleus	1/3	2.16e-04	0.306	0.997	2/2	2.65e-04
Interleukin-2 signalling	3/16	0.001	0.309	0.997	13/17	0.002
Formation of a pool of free 40S subunits	7/45	0.003	0.311	0.997	1/1	1.33e-04
L13a-mediated translational silencing of ceruloplasmin expression	9/60	0.004	0.312	0.997	1/1	1.33e-04
Interleukin-15 sigalling	3/17	0.001	0.342	0.997	10/11	0.001
Post-translational protein phosphorylation	22/166	0.012	0.375	0.997	1/1	1.33e-04
Interleukin-9 signalling	3/18	0.001	0.375	0.997	8/12	0.002
Translocation of SLC2A4 (GLUT4) to the plasma membrane	2/11	7.90e-04	0.387	0.997	1/2	2.65e-04
Synaptic adhesion-like molecules	4/26	0.002	0.39	0.997	3/8	0.001
Interleukin-21 signalling	3/19	0.001	0.408	0.997	5/5	6.63e-04
Interleukin-27 signalling	3/19	0.001	0.408	0.997	10/16	0.002
MAPK1 (ERK2) activation	2/12	8.62e-04	0.429	0997	1/3	3.98e-04
Interleukin-35 signalling	3/20	0.001	0.44	0.997	17/24	0.003

Table 6.6 Top 25 pathways identified from over-representation analysis of BACE1 proximal proteins at 24 hour biotin load. Under entities, the columns indicate the number of proteins found within a pathway are identified (found) and the ratio of total Reactome molecules covered by this pathway (ratio), the p-value and the FDR corrected p-value (FDR). Under reactions the columns indicate the number of reactions in a given pathway represented by the input data (found) and the ratio of Reactome pathways covered by this pathway.

	48 hours					
	Entities				Reactions	
Pathway name	found	ratio	p-value	FDR	found	ratio
Hyaluronan uptake and degradation	8/24	0.002	5.89e-04	0.256	3/7	9.29e-04
Hyaluronan metabolism	8/28	0.002	0.002	0.338	3/9	0.001
Plasmalogen biosynthesis	5/14	0.001	0.005	0.669	2/2	2.65e-04
TP53 regulates transcription of gene involved in cytochrome C release	3/12	8.62e-04	0064	0.992	1/4	5.31e-04
Localisation of the PINCH-ILK-PARVIN complex to focal adhesions	1/2	1.44e-04	0.141	0.992	1/1	1.33e-04
Basigin interactions	4/30	0.002	0214	0.992	9/9	0.001
TP53 regulates transcription of cell death genes	3/21	0.002	0.214	0.992	2/3	3.98e-04
Cation-coupled chloride cotransporters	2/13	9.34e-04	0.259	0.992	2/3	3.98e-04
c-src mediated regulation of Cx43 function and closure of gap junctions	1/5	3.59e-04	0.315	0.992	3/3	3.98e-04
Regulation of gap junction activity	1/5	3.59e-04	0.315	0.992	3/3	3.98e-04
Integrin cell surface interactions	10/112	0.008	0.345	0.992	23/44	0.006
Microtubule-dependent trafficking of connexons from golgi to the plasma membrane	2/17	0.001	0369	0.992	2/2	2.65e-04
Transport of connexons to the plasma membrane	2/18	0.001	0.396	0.992	2/3	3.98e-04
PTK6 regulates proteins involved in RNA processing	1/7	5.03e-04	0.412	0.992	3/7	9.29e-04
Pre-NOTCH processing in golgi	1/8	5.75e-04	0.455	0.992	2/4	5.31e-04
MET interacts with TNS proteins	1/8	5.75e-04	0.455	0.992	1/2	2.65e-04
Transferrin endocytosis and recycling	4/46	0.003	0.46	0.992	7/11	0.001
Fibronectin matrix formation	1/9	6.47e-04	0.494	0.992	2/3	3.98e-04
Sodium-coupled phosphate cotransporters	1/9	6.47e-04	0.949	0.992	1/3	3.98e-04
Zinc influx into cells by the SLC39 gene family	1/9	6.47e-04	0.494	0.992	1/4	5.31e-04
Interaction between L1 and Ankyrins	2/22	0.002	0.496	0.992	1/1	1.33e-04
Formation of annular gap junctions	2/23	0.002	0.520	0.992	2/2	2.65e-04
NOSTRIN mediated eNOS trafficking	1/10	7.19e-04	0.531	0.992	4/4	5.31e-04
Cell-extracellular matrix interactions	2/24	0.002	0.543	0.992	2/7	9.29e-04
Translocation of SLC2A4 (GLUT4) to the plasma membrane	1/11	7.90e-04	0.565	0.992	1/2	2.65e-04

Table 6.7 Top 25 pathways identified from over-representation analysis of BACE1 proximal proteins at 48 hour biotin load. Under entities, the columns indicate the number of proteins found within a pathway are identified (found) and the ratio of total Reactome molecules covered by this pathway (ratio), the p-value and the FDR corrected p-value (FDR). Under reactions the columns indicate the number of reactions in a given pathway represented by the input data (found) and the ratio of Reactome pathways covered by this pathway.

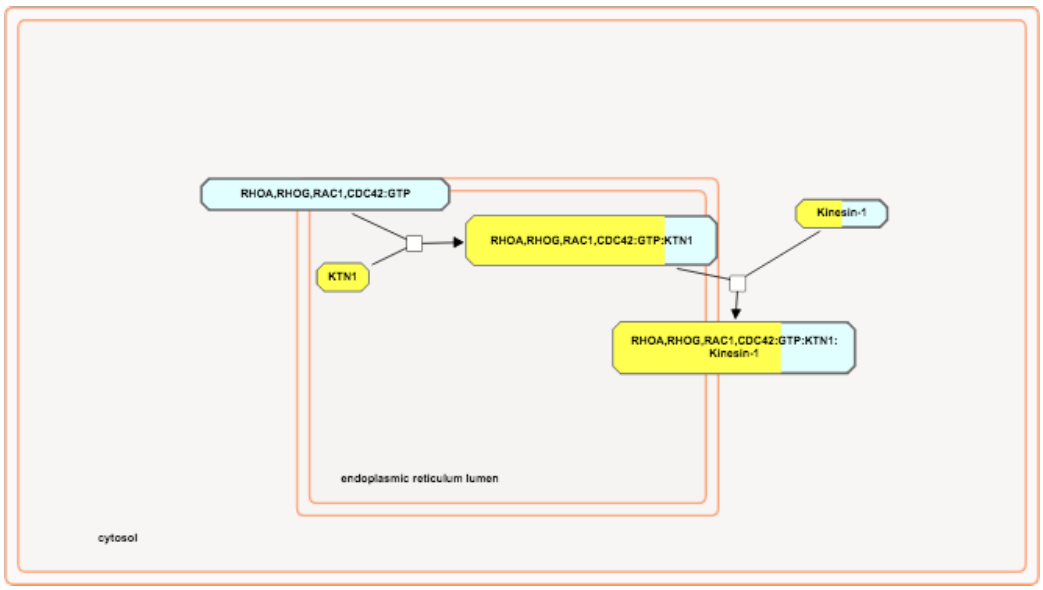

Figure 6.4 Rho GTPase activation of KTN1 pathway. This pathway was significantly over-represented by BACE1 proximal proteins at 24 hour biotin load. Shading of boxes represents the extent to which that complex is represented within the input data. Ie. the number of proteins within the complex that have been identified as proximal BACE1 proteins. Proteins from this pathway that were identified are KTN1, kinesin heavy and light chains as well as a kinesin receptor.

6.3 Discussion

6.3.1 Determining BACE1 interacting proteins

The GT1-7 cell line was produced using gonadotropin-releasing hormone (GnRH) hypothalamic neurons at the SALK institute. The SV40 T-antigen oncogene coupled to the promoter region of GnRH was introduced into transgenic mice carrying the hybrid GnRH-Tag gene. The resultant tumours were removed and dissociated to produce an immortalised cell line. (Mellon et al., 1990) The metabolic phenotype of hypothalamic neurons made them a good model for determining the BACE1 interactome as it is known that animal metabolic homeostasis is altered in BACE1 KO mice via signalling changes in POMC/CART, AgrP/NPY and likely other hypothalamic neurons (Meakin, Jalicy, et al., 2018).

6.3.2 Evidence supporting known BACE1 interactors

Interestingly, whilst 5 known BACE1 interacting proteins were identified in the BioID assay, APP and the APLP proteins were not identified. This may be indicative of the differences in BACE1 substrate specificity between healthy and diseased cells. This provides evidence that the HT-22 cell model may be useful in identifying stimuli that change the BACE1 interactome from non-diseased conditions into a more disease-like state. Alternatively, the interaction time between BACE1 and substrate may be too short for biotinylation to occur. It may be that a catalytically inactive mutant such as that used by Meakin, Mezzapesa, *et al.* (2018) may increase the interaction time and therefore increase the likelihood of biotin labelling. They found increased immunoprecipitation of the insulin receptor with a $D_{289}A$ BACE1 mutant that they suggested was due to increased residency of the substrate within the active site. However, this could also be explained by an inability of the substrate to leave the binding pocket without proteolysis- a mechanism that would prevent BACE1 recycling and use within BioID would be limited. Activity assay of IR-BACE1 co-IP would provide further information about the strength and duration of substrate binding with this mutation. The BACE1 interacting proteins that were identified are putative substrates and known processors of BACE1. A qualitative proteomic study (Hemming et al., 2009) identified both Basigin (Bsg) and Ephrin type-A receptors including A2 (Epha2) as possible substrates. This study provides evidence for this with Bsg appearing in each replicate at 24 and 48 hour biotin load and Epha2

appearing in 5 of the 6 replicates at both timepoints. The strength of this assay lies in its ability to detect not only BACE1 substrates but any interacting protein. Flotillin-2 (Flot2) was identified with 24 hour biotin load in 2 of the 3 replicates. This protein has been identified as a co-regulator of BACE1 endosomal sorting along with flotillin-1 however it was identified as a non-direct interactor in HeLa cells (John et al., 2014). Flotillin KO cells exhibited accumulation of BACE1 in lysosomal compartments but not early endosomes. Furthermore, flotillins have been shown to compete with GGA proteins such as ADP-ribosylation factor-binding protein (GGA2) which was also identified in 2 of 3 replicates at 24 hours biotin load (John et al., 2014). GGA proteins also bind BACE and regulate trafficking between endosomes and the TGN (He, Chang, Koelsch, & Tang, 2002; Kang et al., 2012). Competition between flotillin and GGA may be responsible for BACE1 substrate specificity by regulation of BACE1 sub-cellular localisation. These results support this model as a tool to only identify the BACE1 proteome but also BACE1 localisation and trafficking events in both healthy and diseased conditions. BACE1 regulation may also occur through post-translational modifications. Palmitoylation of BACE1 has been shown to increase APP processing in lipid rafts and may contribute to amyloidogenesis (Vetrivel et al., 2009). Identification of the palmitoyl transferase DHHC20 (Zdhhc20)- a known palmitoyltransferase for BACE1- indicates that the BACE1 fusion protein is being palmitoylated. These hits provide evidence that the fusion protein is being processed in ways known to occur to native BACE1 and that the presence of the BirA tag is not likely to be affecting BACE1 targeting, processing and activity. It must also be noted that many suggested BACE1 substrates were not identified in this assay. This may be due to the nature of the assay compared to those used in previous BACE1 substrate experiments. Previous studies have utilised BACE1 protease activity to look for enrichment of cleaved fragments within the extracellular space to identify substrates for BACE1 and often utilise AD models such as APP over-expressors to mimic AD conditions or use non-neuronal cells for cell-based assays (Dislich et al., 2015; Hemming et al., 2009; Herber et al., 2018; Kuhn et al., 2012). This experiment was designed to mimic physiologically healthy conditions in a model of hippocampal neurons to identify BACE1 interactors under non-diseased conditions in a disease-relevant cell type. Furthermore, this study did not rely upon the proteolytic activity of BACE1 so was not limited to possible substrates as were previous studies. These differences are

likely to be the cause of variations in protein hits between this and published data on the BACE1 interactome.

6.3.3 BACE1 interacting protein families

The data indicate that some protein families appear to interact with BACE1. Cavin 1,2 and 3 were all identified in at least 2 replicates after 48 hours of biotin loading. Septins 7 and 11 were all identified interacting with BACE1 after 24 hours of biotin treatment with Sept8 also identified after 48 hours. Vesicle-associated membrane proteins 3,5 and 7 were identified at 24 hours with 3 and 7 remaining after 48 hour biotin load. Other protein families identified include: Eukaryotic translation initiation factor 3 subunits (Eif3), Ras-related proteins (Rab) proteins and Solute carrier family proteins (Slc).

Cavin proteins are part of the cavin-complex involved in plasma membrane invagination and the formation of caveolae. These proteins, along with caveolins, form the protein coat of caveolae (Hansen, Bright, Howard, & Nichols, 2009). The expression of Caveolin 1 (Cav1) alongside these proteins hint at the microdomain localisation of BACE1 to caveolae at the cell surface. This is consistent with the presence of DHHC20, a palmitoyltransferase known to act upon BACE1 thereby targeting it to lipid rafts- of which caveolae are a subset. It is widely believed that neurons do not express caveolin proteins and therefore do not form caveolae leading to the questioning of the HT-22 as a suitable cellular model for neurons. (Head & Insel, 2007) However, immature neurons in culture have been shown to express caveolin proteins and, indeed, differentiation of the progenitor cells leads to reductions in their expression (D'Orlando et al., 2008). In their study, retinoic acid and phorbol ester were used as differentiation factors that led to reduced caveolin expression. Interestingly, both of these compounds have been implicated in BACE1 regulation; retinoic acid by downregulating BACE1 expression and phorbol esters by increasing BACE1 ectodomain shedding (Hussain et al., 2003; Wang et al., 2015). Whilst their presence and function in neurons are debated, the function of caveolae and associated proteins are still unknown.

Eif proteins are members of the eukaryotic translation initiation process. Within the BioID assay 7 members of this pathway were identified as interactors of

BACE1 (Eif2s1, Eif3c, Eif3h, Eif3i, Eif3l, Eif4g1, Eif5a2) at 24 hours biotin load however only Eif3i was identified at 48 hours. It is therefore probably that these proteins constitute the translation complex that created the BACE1-BirA fusion protein. After 24 hours of biotin the cells will have been transfected for 48 hours, therefore it would be expected that the cells would still be actively producing the protein. However, at 48 hours biotin load, the cells will have been transfected for 72 hours making it plausible that by this stage, much less of the fusion protein is being actively produced and therefore less of the translation machinery is being labelled. This complements the western blots of both BACE1 and HA at the 48 hour biotin load timepoint that indicate less of the construct at this time.

Eif3 is a component of the Eif-3 initiation factor complex. This complex binds to the 40S ribosome and facilitates the binding of other initiation cofactors such as Eif1, Eif2 and Eif5. This forms the 43S pre-initiation complex and only then, may the 43S subunit join the 60S ribosomal subunit and permit translation. This study identified Eif3c, h, i and l as interacting with BACE1 with Eif3i being more consistently biotinylated suggesting a closer proximity to this Eif3 than the other subunits.

Other Eif proteins identified such as Eif2s1 are also involved in translation initiation. It regulates the binding of Met-tRNA to the 40S ribosomal subunit. Eif4g1 is part of a protein complex involved in recognition of the mRNA cap and recruitment of mRNA to the ribosome. Eif5a2 is an mRNA binding protein and facilitates elongation of translating proteins. The biotinylation of these proteins offers a detailed view into the translation of the BACE1 protein.

Rab GTPases are heavily implicated in protein trafficking. The identification of 8 Rab proteins (Rab10, 14, 1a, 1b, 21, 32, 5c and 7a) by the BioID assay gives confirmation of BACE1 transport within the cells. It is known that BACE1 undergoes cycling within the cell with current knowledge suggesting transport to the plasma membrane upon activation in the TGN. BACE1 is then internalised into endosomes where it can be cycled back to the cell surface, trafficked to the TGN or retained for lysosomal degradation. The transport of BACE1 has been heavily implicated in its function with studies indicating that the low pH of endosomes increases BACE1 activity and suggesting that targeting both APP

and BACE1 to endosomes may be responsible for the majority of Aβ production (Haass, Koo, Mellon, Hung, & Selkoe, 1992; Koo & Squazzo, 1994; Pasternak et al., 2003). Rab 10 is involved in vesicular transport from the TGN to the plasma membrane. Rab 14 is implicated in transport from the TGN to endosomes. Rab1a facilitates transport from the ER to both the endosome and the cell surface whilst Rab1b regulates transport from the ER to the TGN. Rab 32, has not been implicated in protein trafficking but may be important in the internalisation of membrane proteins for recycling. Rab5c has been identified in early endosomes and may be part of the process of the endocytic pathway for protein recycling. Additionally, Rab7a is a classic late endosomal marker and is implicated in endosome maturation and lysosome formation. The BACE1 cycling is completed by the identification of a Rab interacting protein Rab11fip5 which assists Rab11 in the movement of recycling endosomes back to the plasma membrane (Sugawara, Shibasaki, Mizoguchi, Saito, & Seino, 2009). (Figure 6.5) Rab expression between the two timepoints support earlier hypotheses that 72 hours after transfection, production of the fusion protein is substantially reduced. At the 48 hours timepoint expression of early Rab proteins involved in membrane trafficking from the ER and TGN are not identified thus suggesting substantially reduced protein synthesis.

The septins are also GTPases, they are highly associated with the cytoskeleton and vesicle trafficking (Mavrakis et al., 2014; Wang et al., 2018). Septins 11, 8 and 7 were identified. It is therefore likely that these proteins become biotinylated whilst the BACE1 fusion protein is being transported throughout the cell. Due to the BirA tag being localised to the C-terminus, upon vesicular transport, the tag is on the cytoplasmic side of the membrane. This leads to biotinylation of cytoplasmic proteins and filaments along which the vesicle travels. Indeed kinesin-1 heavy chain, kinesin light chain 1 and the kinesin receptor kinectin were also biotinylated- most likely as a result of anterograde transport of BACE1. Interestingly, kinesin subunits were not identified in the later 48 hour timepoint but the Dynein 1 light intermediate chain 2 was, suggesting retrograde transport of BACE1 at this later timepoint. However, a study by Kurkinen *et al.* (2016) suggested that septin 8 (SEPT8) expression modulates BACE1 cellular localisation and that downregulation of this protein reduces BACE1 expression and APP β-cleavage. They suggested that SEPT8 achieved this by increasing

BACE1 stability as well as increasing targeting to the early and recycling endosomes. Furthermore, expression of a SEPT8 variant was shown to correlate with NFT pathology in AD temporal cortical tissue.

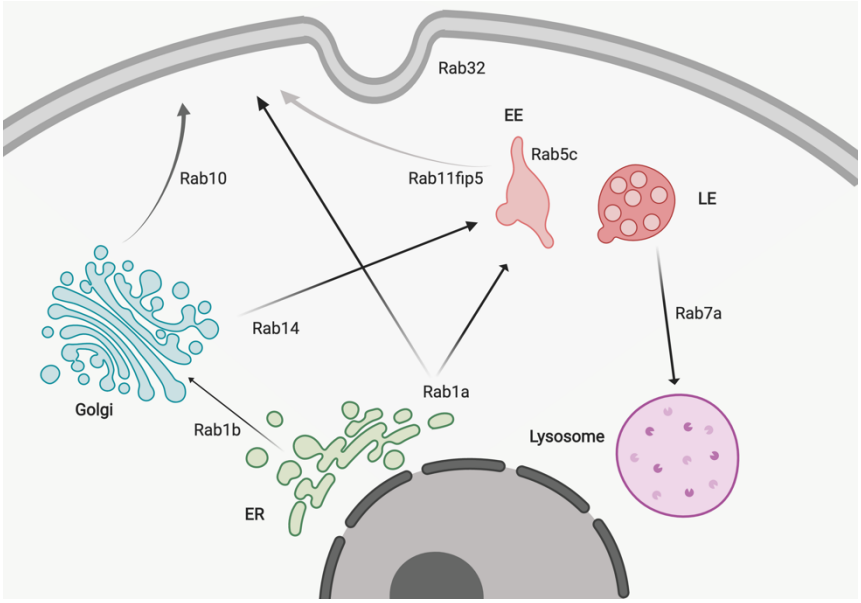

Figure 6.5 Mapped movement of BACE1-BirA throughout the cell from identified proximal Rab proteins. Rabs 10, 14, 1a, 1b, 21, 32, 5c and 7a were identified after 24 hour biotin load suggesting transport from the Golgi to the ER (endoplasmic reticulum) and on to the PM (plasma membrane). From the PM BACE1 is trafficked to early endosomes which mature to LE (late endosomes) and lysosomes. From EE (early endosomes) BACE1 may be trafficked back to the PM. BACE1 may also be trafficked directly to the endosomes from both the golgi and ER. After 48 hour biotin load only Rabs 10, 32, 5c and 7a were detected suggesting that movement to the membrane from the ER and trafficking back into the endosomal/lysosomal compartments occur later in the BACE1 trafficking process and by this timepoint, BACE1-BirA is not being transported from the endosomal system, back to the plasma membrane. Figure was made using BioRender.com.

BACE1 was identified as localising proximal to 12 solute carrier proteins (Slcs12a2, 12a4, 1a5, 20a2, 30a4, 35a1, 35f6, 38a1, 39a7, 6a9, 7a11 and Slc02a1). These large proteins are multi-pass transmembrane proteins containing 10 or more membrane spanning domains. They are transporters of small molecules and often confer ion gradients across the membrane or mediate uptake of amino acids or neurotransmitters.

Slc12a2, Slc1a5, Slc20a2 and Slc6a9 were all identified at both timepoints. Slc12a2 is responsible for sodium and chloride transport across membranes. Whilst the sodium gradient across the PM is a key aspect of action potential transmission, the chloride gradient is a regulator of neurotransmitters such as promotion of inhibitory GABAergic signalling by altering PM subunit expression

(Succol, Fiumelli, Benfenati, Cancedda, & Barberis, 2012). Slc1a5 is an amino acid transporter with broad specificity targeting all neutral amino acids. Slc20a2 is a sodium phosphate transporter and Slc6a9 a glycine transporter. It appears from these hits that transport of a specific ion or solute transporter set is not being targeted by BACE1, rather the family may be targeted due to localisation at a cell surface microdomain as multiple sequence alignment of these proteins identified very poor sequence identity.

Slc12a4 is a potassium chloride cotransporter, Slc30a4 and Slc39a7 are zinc transporters, Slc35a1 a cytidine monophosphate (CMP)-sialic acid transporter, Slc35f6 may be a mitochondrial protein of unknown function and Slc7a11 an anionic amino acid transporter were all identified at 24 but not 48 hours. Interestingly, these proteins have been identified in intracellular membranes such as Golgi and ER as opposed to the cell membrane. Presence of these proteins may be further indication of targeted interactions of BACE1 with solute carrier proteins due to interactions in multiple organelles.

Slc38a1, a glutamine transporter and a solute carrier organic anion transporter (Slco2a1) that transports prostaglandins were identified after 48 hour biotin load; both of which have been identified at the plasma membrane. The array of solute carrier proteins identified within this assay begs many questions about the role of BACE1 within the cells. These proteins, with multiple membrane passes, would not be immediately considered as BACE1 substrates as BACE1 is known to target single pass transmembrane proteins (such as APP, LRP1 and the Sez6). Association between BACE1 and these proteins occur in multiple cellular localisations thereby making the idea of BACE1 targeting to this type of protein more suggestable however the confirmation of this association and physiological function would need to be established experimentally. Interestingly, analysis of the cell surface proteome identified multiple Slc proteins significantly increasing with BACE1 inhibition but secretome analysis does not identify these proteins as potential BACE1 substrates (Herber et al., 2018; Kuhn et al., 2012). This opens the possibility of a non-enzymatic relationship between the Slc proteins and BACE1- a function that is not commonly studied but has been previously shown in sodium channel gating as BACE1 may functionally replace the β2 subunit of these channels (Huth et al., 2009). Furthermore, yeast-two hybrid studies using the intracellular c-terminal domain of BACE1 identified interactions with proteins

such as BRI_3 and RanBPM involved in TNFα induced cell death and microtubule nucleation respectively (Wickham, Benjannet, Marcinkiewicz, Chretien, & Seidah, 2005).

Vesicle associated membrane proteins (Vamps) are type IV transmembrane proteins containing a C-terminal single transmembrane domain. They are a family of SNARE proteins known to mediate vesicular transport throughout the cell. Vamp3 is a known synaptic protein that has been implicated in the reuptake of neurotransmitters into the presynaptic membrane. It has also been shown to mediate the transport of secretory vesicles through interactions with Ykt6, and Snap proteins. As both Ykt6 and Snap23 (a synaptosomal protein involved in vesicle docking and fusion) were identified within this screen, it may be suggested that BACE1 is playing a role in the secretory pathway in these cells (Gordon et al., 2017). Vamp5 is also expressed at the plasma membrane and the STRING database indicates that it too, interacts with Snap23 and Ykt6. Vamp 7 is implicated in the fusion of late endosomes to lysosomes as well as secretion of soluble factors in immune cells. (Chiaruttini et al., 2016; Ward, Pevsner, Scullion, Vaughn, & Kaplan, 2000) Whilst the nature of BACE1 transport throughout the cell dictates that these hits are likely to be due to co-transport with BACE1 or expression at the same membranes, it cannot be overlooked that these single pass transmembrane proteins are candidates for BACE1 substrates.

6.3.4 BACE1 interacting proteins

A number of proteins were identified as possible BACE1 interactors in every replicate at both timepoints (Afdn, Bsg, Cav1, Cavin2, Ddr2, Dlg1, Pgrmc2, Sept7, Slc1a5, Slc6a9, Snap23, Sptbn1, Steap3, Vamp3 and Zdhhc20). These proteins are therefore the strongest candidates for true BACE1 interacting proteins from this assay.

Afadin (Afdn) is a structural protein that binds to actin and maintains cell adhesion through interaction with nectin and ponsin (NAP) in NAP systems. NAP systems co-localise with the cadherin-catenin system at adherens junctions and may be linked through vinculin (Ikeda et al., 1999; Mandai et al., 1999). It has also been suggested that afadin interacts with clusters of Eph receptors, receptor tyrosine kinases that are putative BACE1 substrates (Hock et al., 1998). In neurons,

afadin assists in axonal branching and dendritic branching through R-ras GTPase mediated actin reorganisation (Iwasawa, Negishi, & Oinuma, 2012). It is therefore of note that BACE1 proximity assay also identified Rras2 at both 24 hour and 48 hour timepoints. In addition, the scaffolding protein and BioID hit Disks large homolog 1 (Dlg1) may localise to adherens junctions and mediate their formation (Bossinger, Klebes, Segbert, Theres, & Knust, 2001). As well as acting as in cell adherence, Dlg1 mediates the localisation of cell surface proteins to microdomains resulting in cell polarisation and, in neural cells, membrane formation (Bolis et al., 2009; Woods, Hough, Peel, Callaini, & Bryant, 1996). Interestingly, afadin has been shown to be phosphorylated by AKT through activation of the PI3K signalling cascade. This results in translocation of afadin from adherens junctions to the nucleus and increases cell permeability and migration in endothelial cells (Elloul, Kedrin, Knoblauch, Beck, & Toker, 2014; Zhai et al., 2018). The suggestion of a role for BACE1 in regulation of cell adhesion is growing with evidence that APP-like proteins may be adhesion molecules themselves or accessory proteins at focal adhesion points (Chen & Dou, 2012; Dunsing, Mayer, Liebsch, Multhaup, & Chiantia, 2017).

Discoidin domain-containing receptor 2 (Ddr2) is a type I transmembrane tyrosine kinase expressed at the cell surface. As this protein is a type I transmembrane protein, this suggests that this hit may be a substrate for BACE1. Ddr2 also regulates remodelling of the extracellular matrix through collagen binding as well as activation of signalling cascades such as ERK and PI3K as reviewed by Fu, Valiathan, *et al.* (2013). Furthermore, reports of Ddr1 ectodomain shedding through a metalloproteinase method is somewhat similar to known methods of APP processing (Fu, Sohail, et al., 2013). Whilst there has been no confirmation of Ddr2 shedding, studies have found similar effects of the cleaved extracellular domain of Ddr2 to Ddr1 (Flynn, Blissett, Calomeni, & Agarwal, 2010). Whilst more studies would need to be conducted to establish whether Ddr2 is in fact cleaved and the role of BACE1 in this process; if true, interaction with Ddr2 would offer further evidence for the importance of BACE1 in maintaining cell morphology.

Membrane-associated progesterone receptor component 2 (Pgrmc2) is another type I transmembrane protein identified from this assay. However, this protein is not implicated in cell junctions and morphology but steroid binding. The precise

role of this protein within the nervous system has not been determined as it has been shown that this receptor does not bind progesterone but may still play a role in progesterone signalling (Liu et al., 2009; Petersen et al., 2013). A recent Bio-ID study into the interactome of fatty acid 2-hydroxylase (FA2H) (a ceramide processing enzyme important in myelination) found an association between FA2H and Pgmrc proteins 1 and 2 (Hardt, Winter, Gieselmann, & Eckhardt, 2018). Whilst Pgmrc2 was not validated in this study, they found that inhibition of Pgmrc1 reduced the production of 2-hydroxylated sphingolipids (such as ceramide). Mice deficient in FA2H show axon degeneration and deficit in learning and memory. The implications of this protein as a possible BACE1 substrate stretch beyond AD as progesterone signalling has many effects throughout the brain; particularly within the hypothalamus in the regulation of sex hormones (Wen He et al., 2017).

Spectrin beta chain non-erythrocytic 1 (Sptbn1) is an actin binding cytoskeletal protein. This hit is likely to be due to its proximity during vesicle transport of BACE1. However due to the high number of cytoskeletal proteins identified during this study, it cannot be ruled out that BACE1 interacts with a spectrin binding complex. This is particularly noteable due to the appearance of the spectrin/actin binding proteins 4.1G and 4.1B. The 4.1 family of proteins are membrane targeted and, similar to Dlg1, modulate protein microdomain targeting and maintain cell morphology (Discher et al., 1995; Gimm et al., 2002). This evidence, combined with *in vivo* proteomic evidence that protein 4.1N expression changes with BACE1 expression within the hippocampus as shown in chapter 4 highly implicates BACE1 in membrane sorting and cellular structure.

Metalloreductase STEAP3 (Steap3) is an endosomal multi-pass transmembrane protein that is involved in Fe3+ reduction (Lambe et al., 2009). As little evidence exists with regard to BACE1's direct role in iron homeostasis within neurons this was most likely due to proximity after endosomal targeting of the BACE1. As both Rab 5c and Rab7a were biotinylated at both timepoints indicating endosomal targeting, it is feasible that this hit, despite its consistency across replicates, was not a true interactor of BACE1.

These proteins strongly hint towards a role for BACE1 cellular connectivity. In healthy cells BACE1 was identified as localising to the plasma membrane with many structural, adhesion and ECM proteins and these were the predominant function of the most reliable hits. The nature of the interactions between BACE1 and cell adhesion requires further investigation but a study by Deng et al. (2017) has suggested a role for increased BACE1 in disrupting the vascular endothelial layer as a result of TNFα treatment. Increased BACE1 within EA.hy926 endothelial cells led to significant disruption of tight-junctions suggesting a role for BACE1 in maintaining the BBB.

Whilst many cell adhesion and cytoskeletal proteins are highly represented in the Bio-ID hits, it cannot be overlooked that these proteins were labelled purely as part of BACE1 transport. Further co-localisation studies and cellular fractionation would determine the location of these interactions and suggest the function of these associations. Additionally, as many are transmembrane proteins, enzyme assays could determine which, if any, are substrates of BACE1.

6.3.5 BACE1 interaction differ between timepoints

A number of proteins were identified in every replicate at 24 hours but appeared in none after 48 hours. At first it was supposed that this was a result of changes in cellular localisation of the BACE1 construct and that the hits at 24 hours would be localised to cellular compartments early in the BACE1 trafficking stages such at the ER or TGN. However further research suggested that this was not the case as many of the hits are cytosolic or membrane targeted. There also appears to be no common function or pathway between these proteins so it seems unlikely that the higher BACE1 expression at the earlier timepoint was leading to activation of different pathways. It may be, however, that high expression of BACE1 at the 24 hour timepoint is leading to off-target effects of BACE1 or interactions with less abundant substrates as the usual substrates became saturated. ATP-binding cassette sub-family F member 2 (Abcf2) is an ABC transporter (Lindner et al., 2012). RHO GTPase-activating protein 1 (Arhgap1) is a family member of RhoGAPs, activators of Rho and Rac proteins (Amin et al., 2016). Tyrosine protein kinase receptor UFO (Axl) is a member of the TAM family of receptor tyrosine kinases. The many functions of TAM receptors including Axl were extensively reviewed by Linger et al. (2008) as well as their roles in cancers;

a field in which they have been extensively studied. Protein EFR3 homolog A (Efr3a) is a member of the localisation complex of PI4-kinase that targets to the plasma membrane (Nakatsu et al., 2012). Trifunctional purine biosynthetic protein adenosine-3 (Gart) plays a role in purine biosynthesis (Ng, Uribe, Yieh, Nuckels, & Gross, 2009). Interferon induced transmembrane protein 3 (Ifitm3) is an antiviral protein that may disrupt cholesterol homeostasis and transport (Amini-Bavil-Olyaee et al., 2013). Lysine tRNA ligase (Kars) is an amino acyl tRNA synthetase required for the combining of Lysine to its corresponding tRNA. Keratin (type I cytoskeletal 10) (Krt10) is a filamentous intermediate filament protein. RNA N6-adenosine methyltransferase (Mettl16) methylates adenosine residues on mRNA (Shima et al., 2017). Myoferlin (Myof) is localised to caveolae and lipid rafts. Here, it may play a role in maintaining the plasma membrane and endocytosis within these microdomains (Bernatchez et al., 2007; Bernatchez, Sharma, Kodaman, & Sessa, 2009). SH3 and PX domain-containing protein 2A (Sh3pxd2a) are adaptor proteins involved in the structure of podosomes and invadopodia and has been implicated in AD susceptibility through its stabilising effects of ADAM proteins (Harold et al., 2007; Laumet et al., 2010). Vang-like protein 1 (Vang1) is a multi-pass membrane protein implicated in neurite formation and cell polarisation (Sanchez-Alvarez et al., 2011).

At 48 hours, the proteins GRB10 interacting GYF protein 1 (Gigyf1), myosin phosphatase rho-interacting protein (Mprip) and vacuolar protein sorting associated protein 13c (Vps13c) were identified that were not present at 24 hours. These hits are most likely to be present at this timepoint due to limitations in the MS/MS identification process. High abundance peptides may mask the presence of lower abundance proteins. As the 24 hour timepoint contained high protein abundance, many low abundance proteins may have been lost in the detection method. These proteins may have become detectable at the lower protein concentrations at 48 hours. As these proteins are not localised to later BACE1 cycling locations, detection errors seem the most likely cause for the lack of these proteins at the earlier timepoint. These proteins are a regulator of insulin-like growth factor signalling, a RhoA binding protein and activator and an outer leaflet mitochondrial protein that regulates mitochondrial susceptibility to stress implicated in Parkinson's disease respectively. (Giovannone et al., 2003; Koga & Ikebe, 2005; Lesage et al., 2016)

6.3.6 Pathway analysis

The only pathway identified as being significantly over-represented from the proximity assay hits was RHO GTPase activation of Kinectin (Ktn1); Ktn1 itself being a protein identified in the assay. This pathway describes the activation of vesicular transport from the endoplasmic reticulum upon binding of RHO GTPases to kinectin (Hotta, Tanaka, Mino, Kohno, & Takai, 1996; Vignal, Blangy, Martin, Gauthier-Rouviere, & Fort, 2001). Consequently, enrichment is likely to be due to BACE1 trafficking as opposed to direct BACE1 interaction. As this pathway is no longer enriched at 48 hours, a timepoint previously described as exhibiting less fusion protein production, it may be determined that this pathway became biotinylated purely by proximity to the fusion protein, rather than a product of BACE1 interaction.

6.3.7 Conclusions

This study offers proof of principle that the Bio-ID method offers an accurate representation of the BACE1 interactome as data collected are supported by known BACE1 interactors and transport pathways. In this assay the presence of C-terminal BirA does not appear to interfere with BACE1 function or processing making it a good model for studying BACE1 interactions. This means that this assay can be used to determine BACE1 interacting proteins; not only offering suggestions for new substrates and binding partners, but also to track the cycling of BACE1 throughout the cell. The data lend themselves to the suggestion that BACE1 may play a role in cell adhesion and cytoskeletal maintenance under normal physiological conditions. Further studies into the nature of these associations- whether they be enzyme-substrate, non-enzymatic binding partners or merely a product of BACE1 transport will determine how these hits tie in to BACE1 physiological function. With further optimisation, the method may be used as a quantifiable proteomic method of identifying BACE1 interactors. This could be achieved through measurement of protein and peptide concentrations throughout sample preparation to ensure that an equal amount of peptide product is analysed per sample. Quantifiable proteomics would offer further information on the extent of interaction between BACE1 and each hit and may shed light on which hits are products of co-transport or indirect interactions. This would also

enable future studies to calculate the change in interaction between BACE1 and Bio-ID hits under different conditions.

Further experiments in the HT-22 hippocampal cell line would enable the identification of BACE1 interactome changes with cellular stresses that are known to increase the risk of AD. The incubation of cells with free-fatty acids (such as palmitate) and high glucose can be used to mimic western diet within cell culture and in doing so, identify targets that may explain the association between metabolic dysfunction with AD. With the identification of known BACE1 modifiers such as DHHC20, these experiments would also offer insight into whether stressors modulate BACE1 PTMs as well as trafficking.

As cell adhesion molecules play a vital role in maintenance of the BBB, it would be of interest to conduct the BioID study within endothelial cells. Again, conditions such as high-glucose – a known influencer of BBB permeability- can be utilised to determine whether BACE1 plays a role in metabolic BBB dysfunction.

Chapter 7

Effects of β-amyloid on leptin sensitivity

7.1 Introduction

Leptin is most commonly considered a modulator of appetite and energy homeostasis with reduced leptin signalling alongside hyperleptinemia (termed 'leptin resistance') being associated with obesity. In recent years it has been shown that leptin exerts neuroprotective effects within the brain (Amantea et al., 2011; Malekizadeh et al., 2017). First indicators of the neuroprotective actions of leptin came from behavioural and biochemical analysis of leptin and leptin receptor deficient mice. Ahima *et al.* (1999) identified locomotor deficits in *ob/ob* mice that could be overcome with leptin treatment. They showed that the absence of leptin signalling led to reduced brain weight, decreased synaptic protein expression and reduced myelination- indicators of neurodegeneration. Leptin is now being investigated as a potential therapeutic for AD as it has been shown that leptin administration improves cognitive function in both AD mouse models and leptin deficient humans (Greco et al., 2010; Paz-Filho et al., 2008). In addition to decreased circulating leptin, it has been suggested by Maioli *et al.* (2015) that AD patients exhibit reduced leptin signalling within the hippocampus and that leptin targeting switches from neurons to astrocytes irrespective of leptin concentration. A recent study indicated that central chronic infusion of the AD peptide $A\beta_{1-42}$ induces leptin resistance in DIO mice, however the mechanism behind this process was not determined (Meakin, Jalicy, et al., 2018).

CSF $A\beta_{1-42}$ decreases with AD progression with reductions seen in MCI compared to cognitively normal controls and a further reduction seen in AD patients (Bonda et al., 2014; Johnston et al., 2014). In contrast, hippocampal tissue exhibits increased amyloid deposition with disease progression and lower CSF amyloid that could be explained by reduced amyloid clearance from the brain (Hsu et al., 2015). Furthermore, animal studies indicate that amyloid burden within the cortex is greatly increased with chronic high-fat diet and both BACE1 expression and activity is increased under nutrient excess (Meakin et al., 2012; Vandal et al., 2014). Studies into circulating amyloid concentrations with chronic dietary stress revealed that a high-fat diet for 20 weeks led to mean plasma $A\beta_{1-42}$ at ~20pg/ml and $A\beta_{1-40}$ at ~80pg/ml whilst NC controls at the same age exhibited plasma $A\beta_{1-42}$ at ~10pg/ml and $A\beta_{1-40}$ ~100pg/ml (Supplemental figure S5, Ashford group, University of Dundee). This helped determine the initial amyloid concentration used in this study and it is within the physiological range

observed in CSF of cognitively healthy individuals and those with MCI. (Forlenza et al., 2015; Haapalinna et al., 2016) Circulating $A\beta_{1-40}$ was approximately 4 times higher than that of $A\beta_{1-42}$ in animals on HFD and human data indicate that plasma and CSF $A\beta_{1-40}$ concentrations are greater than the corresponding $A\beta_{1-42}$ in both control and diseased tissues (Dorey, Perret-Liaudet, Tholance, Fourier, & Quadrio, 2015). Follow up studies exposing mice to intracerebroventricular (ICV) $A\beta_{1-42}$ identified hypothalamic leptin resistance within these animals as a result of mouse amyloid exposure and dietary stress (Meakin, Jalicy, et al., 2018). For these reasons, 400pM mouse $A\beta_{1-40}$ was applied in this study alongside 100pM mouse $A\beta_{1-42}$ (hereafter referred to as $A\beta_{40}$ and $A\beta_{42}$ respectively) to determine whether these peptides induce differing effects on leptin sensitivity. The higher amyloid concentrations for both Aβ species concentrations used, whilst above those identified within both amyloid infused and HFD fed mice, is within the range observed in the CSF of humans (Bertens, Tijms, Scheltens, Teunissen, & Visser, 2017; Maruyama et al., 2001; Schoonenboom et al., 2005).

This study aimed to identify the mechanism behind amyloid mediated leptin resistance through monitoring the effects of chronic $A\beta_{42}$ and $A\beta_{40}$ on leptin receptor activation. Phosphorylation of STAT3 Y705 was utilised as the indicator of leptin receptor activation due to difficulties in time response and western blot analysis of JAK2. Expression of key modulators in leptin signalling SOCS3, PTP1B and Y580 and Y542 pSHP-2 were determined in order to establish whether amyloid peptides result in leptin resistance within this model. This study could also help determine the mechanism behind the amyloid dependent reduction in pSTAT3 observed *in vivo*.

Experiments were initially conducted in the immortallised mouse hypothalamic neuronal cell line GT1-7. This was due to their neuronal phenotype without need for differentiation as the differentiation process of neuronal cell lines leads to increased endogenous amyloidogenesis. (Wang et al., 2015). Furthermore GT1-7 cells show characteristics of hypothalamic neurons such as glucose sensing making them an good model for central metabolic signalling experiments (Beall et al., 2012; Watterson et al., 2013). Their expression profile of the leptin signalling pathway components made them favourable over other hypothalamic cell lines such as the mHypoA cells. However, due to loss of leptin sensitivity, a

substitute was made for HEK 293 cells expressing the leptin receptor isoform b (ObRb).

7.2 Results

7.2.1 Leptin signalling in GT1-7 cells

A leptin dose response performed in GT1-7 stably transfected (but not clonally selected) with mObRb indicated that they were not leptin sensitive (Figure 7.1A) so they were transfected with the b isoform of the mouse leptin receptor (mObRb) and once again subjected to a leptin dose response at 5, 15 and 30 minute stimulation times. With expression of mObRb, the GT1-7s became leptin responsive and exhibited a dose response effect at all time points. (Figure 7.1B). The 30 minute time point was chosen for further studies as it exhibited greater STAT3 phosphorylation at 1nM than shorter time points. This allowed experiments to utilise a lower (though, still supraphysiological) concentration of leptin to monitor changes in sensitivity (Nam et al., 2001; Schwartz, Peskind, Raskind, Boyko, & Porte, 1996). Further experiments monitored the effects of 5-day incubation with 11pM ScrP, $A\beta_{40}$ and $A\beta_{42}$ compared to vehicle treated controls on GT1-7 mObRb sensitivity to 1nM leptin. No change in leptin sensitivity was observed with any peptide treatment (Figure 7.1C) however, the effects of 1nM leptin in all treatments appears to be diminished when compared to the 1nM treatment in previous dose response experiments. It is likely that the cells were beginning to show reduced leptin sensitivity at this stage and soon after the cells lost their sensitivity to leptin halting further experiments. As a result, few replicates were achieved. Attempts were made to identify the ObRb construct expression within the cells as loss of transgene may have caused this loss of leptin sensitivity. Detection was attempted through pulldown with HA tag affinity resin and western blot using an ObR antibody and western blot of crude lysate with anti-HA antibody. However, neither method proved sufficient to detect the protein in GT1-7 mObRb cells.

7.2.2 Leptin signalling in HEK 293 cells

In order to create a leptin sensitive cell line that could be used consistently, HEK 293 cells were employed. HEK 293 cells are human embryonic kidney cells immortalised through transformation with adenovirus 5 DNA which resulted in incorporation of viral DNA into the genome of this cell line. (Graham, Smiley,

Russell, & Nairn, 1977) HEK 293 cells were not leptin sensitive but became responsive upon stable transfection with mObRb as observed by increased STAT3 phosphorylation with 1nM leptin treatment. (Figure 7.2)

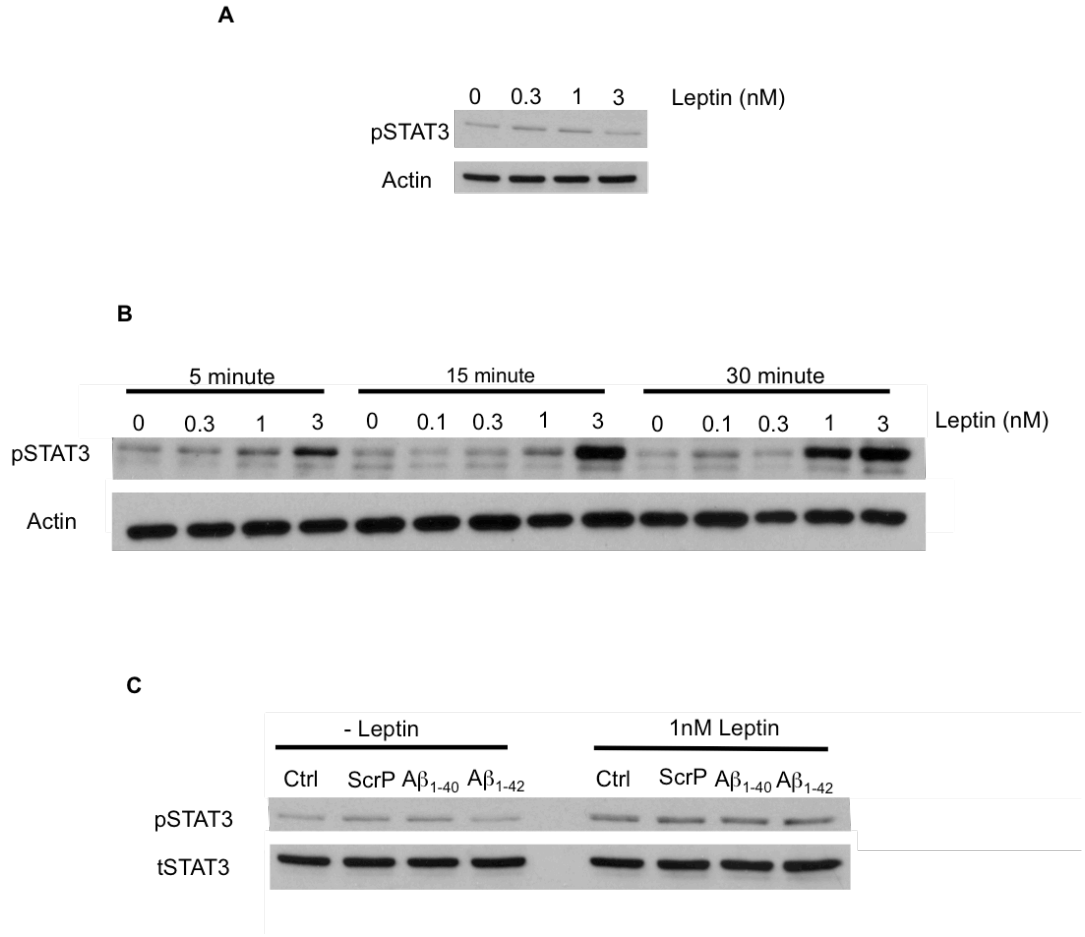

Figure 7.1 Phosphorylation of STAT3 with leptin stimulation in transfected GT1-7 cells. The neuronal cell line GT1-7 is not responsive to leptin until transfected with the b isoform of the leptin receptor. Western blots showing the phosphorylation of STAT3 in response to leptin stimulation in A) Untransfected GT1-7 cells show no change in STAT3 phosphorylation with increasing leptin concentration B) mObRb GT1-7 cells show increasing STAT3 activation with leptin concentration at 5, 15 and 30 minute stimulation times C) STAT3 activation in mObRb GT1-7 cells does not change with exposure to 11pM scrambled peptide (ScrP) $A\beta_{1-42}$ or $A\beta_{1-40}$.

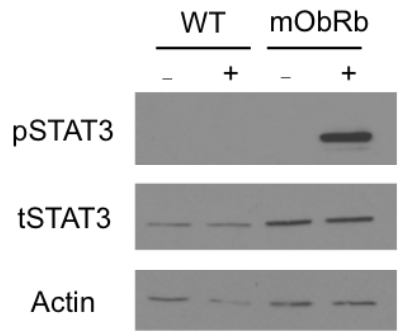

Figure 7.2 Phosphorylation of STAT3 with leptin stimulation in transfected HEK293 cells. HEK293 cells transfected with mObRb exhibit STAT3 activation in response to leptin. Western blot exhibiting no STAT3 activation of untransfected HEK293 cells either with or without leptin stimulation. mObRb exhibit STAT3 activation when stimulated with 1nM leptin for 30 minutes.

7.2.3 Leptin sensitivity with chronic exposure to 11pM amyloid

Cell lysates were collected after 5-day exposure to amyloid peptides and following a 30-minute leptin stimulation. Western blot indicated no change in the expression of total STAT3 (tSTAT3) with leptin dose. (Figure 7.3A) STAT3 expression was also unchanged between ScrP and $A\beta_{42}$. (Figure 7.3B) Phosphorylation of STAT3 was unchanged with $A\beta_{42}$ compared to ScrP controls across all leptin doses observed. (Figure 7.3C). Bands were not identified at 0 and 0.5nM leptin stimulations meaning a baseline phosphorylation state could not be determined in this study. Due to this, the dose response change in pSTAT3 was not quantified.

No change was observed in STAT3 regulating protein PTP1B (Figure 7.4). A trend towards increased PTP1B expression with $A\beta_{1\text{-}42}$ was observed however this was due to a single replicate exhibiting greater PTP1B expression with $A\beta_{42}$ that was not observed in other replicates.

Total SHP-2 (tSHP-2) expression was unaltered with $A\beta_{42}$ exposure or leptin concentration. (Figure 7.5). Phosphorylation of SHP-2 at Y580 was unchanged with leptin concentration and $A\beta_{42}$ exposure (Figure 7.6A-B). A trend towards increased pSHP-2 Y542 with leptin in a concentration dependent manner was seen with $A\beta_{42}$ but not with scrambled peptide (ScrP) (Figure 7.6C). $A\beta_{42}$ appeared to reduce SHP-2 Y452 phosphorylation at basal leptin levels. 0 and 0.5nM leptin led to approximately 20% reduced SHP-2 Y452 although this result was not significant (Figure 7.6D).

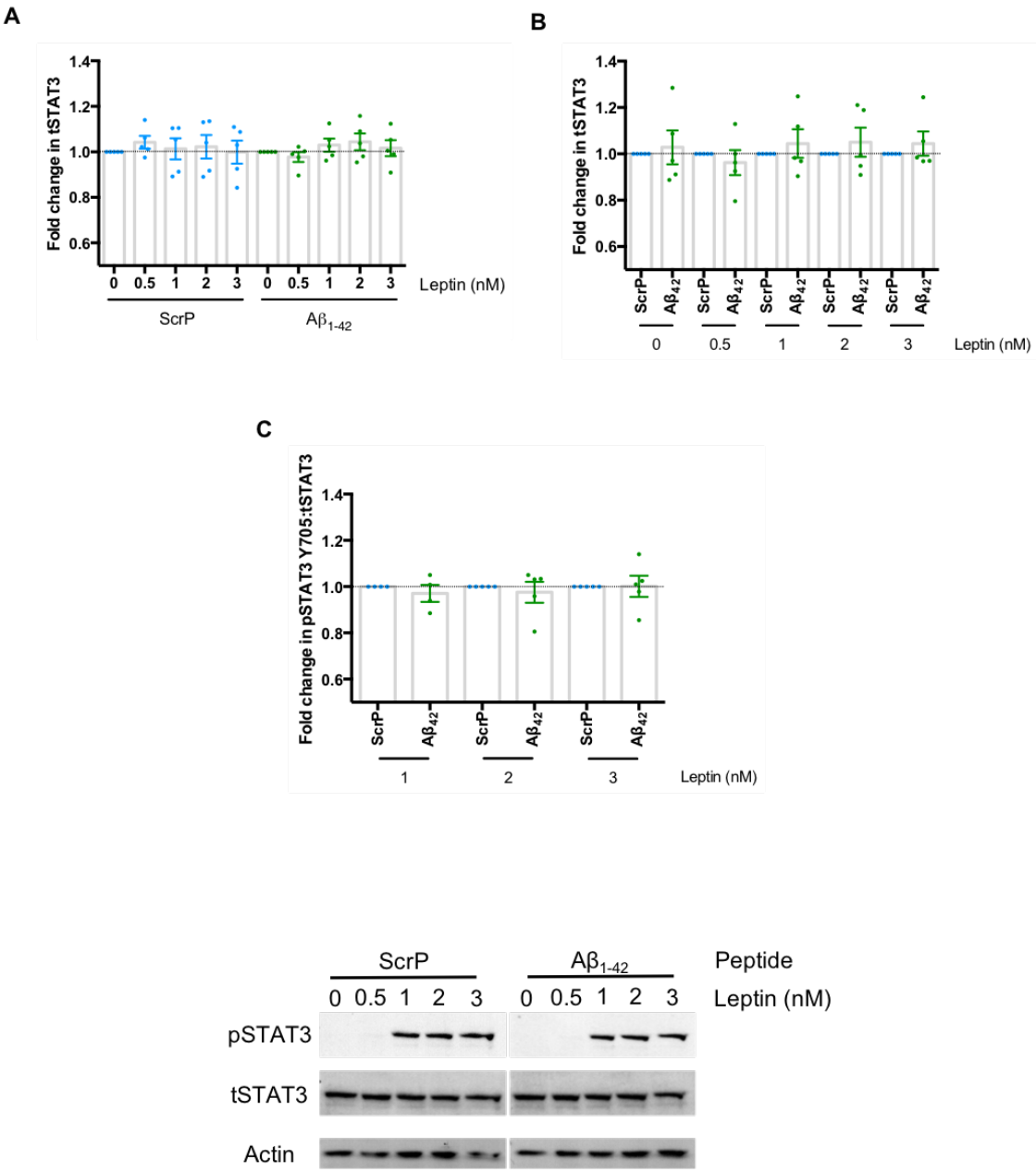

Figure 7.3 STAT3 expression and phosphorylation with 11pM amyloid exposure and leptin stimulation Total STAT3 (tSTAT3) protein expression and pSTAT3 in response to leptin concentration are unchanged with 5-day exposure to 11pM $A\beta_{1-42}$. Histograms showing relative tSTAT3 expression with leptin concentration with representative western blots (normalised to 0nM leptin) **(A)** and 11pM $A\beta_{1-42}$ exposure (normalised to ScrP) **(B)**. **A)** tSTAT3 expression does not change with leptin concentration (n=5) **B)** tSTAT3 expression does not change with exposure to 11pM $A\beta_{1-42}$ **C)** STAT3 activation (as denoted by p-STAT:tSTAT3 levels) does not change with 11pM $A\beta_{1-42}$ exposure. n=5 per group. Individual data points indicate the range of data. Standard error indicated by error bars.

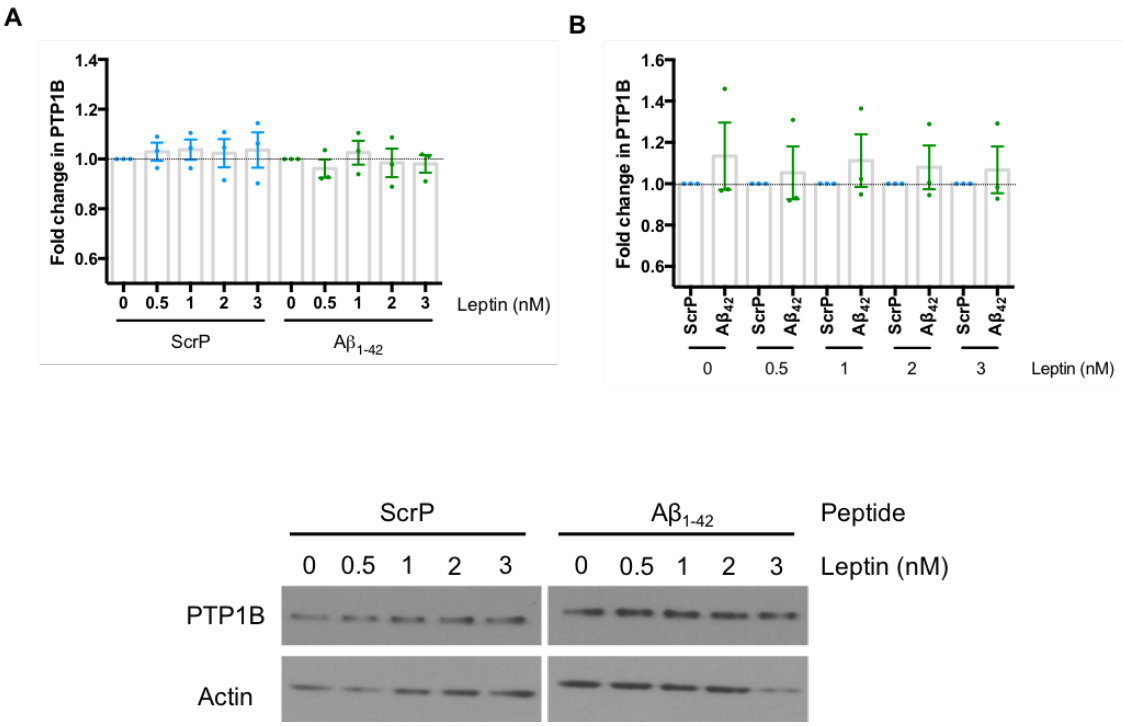

Figure 7.4 PTP1B with 11pM amyloid exposure and leptin stimulation. PTP1B expression does not change with leptin concentration or 5-day exposure to 11pM $A\beta_{1\text{-}42}$. Histograms representing relative PTP1B expression with leptin concentration (normalised to 0nM leptin) **A)** and 11pM $A\beta_{1\text{-}42}$ exposure (normalised to ScrP) **(B)** and representative western blots. **A)** PTP1B expression is unaltered with leptin concentration **B)** PTP1B expression does not change with 11pM $A\beta_{1\text{-}42}$. n=3 per group. Individual data points indicate the range of data. Standard error indicated by error bars.

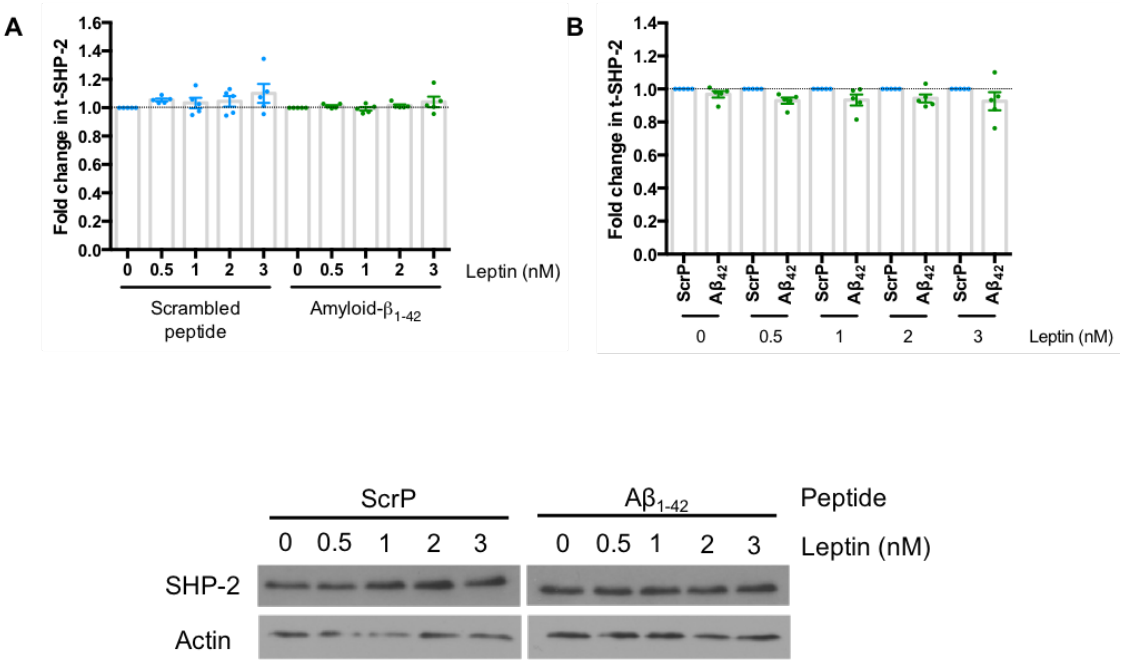

Figure 7.5 SHP-2 expression with 11pM amyloid exposure and leptin stimulation. SHP-2 expression does not change with leptin concentration or 5-day exposure to 11pM $A\beta_{1-42}$. Histograms representing relative total SHP-2 expression with leptin concentration (normalised to 0nM leptin) **A)** and 11pM $A\beta_{1-42}$ exposure (normalised to ScrP) **(B)** with representative western blots. **A)** SHP2 expression is unaltered with leptin concentration **B)** Total SHP-2 expression does not change with 11pM $A\beta_{1-42}$. n=5 per group. Individual data points indicate the range of data. Standard error indicated by error bars.

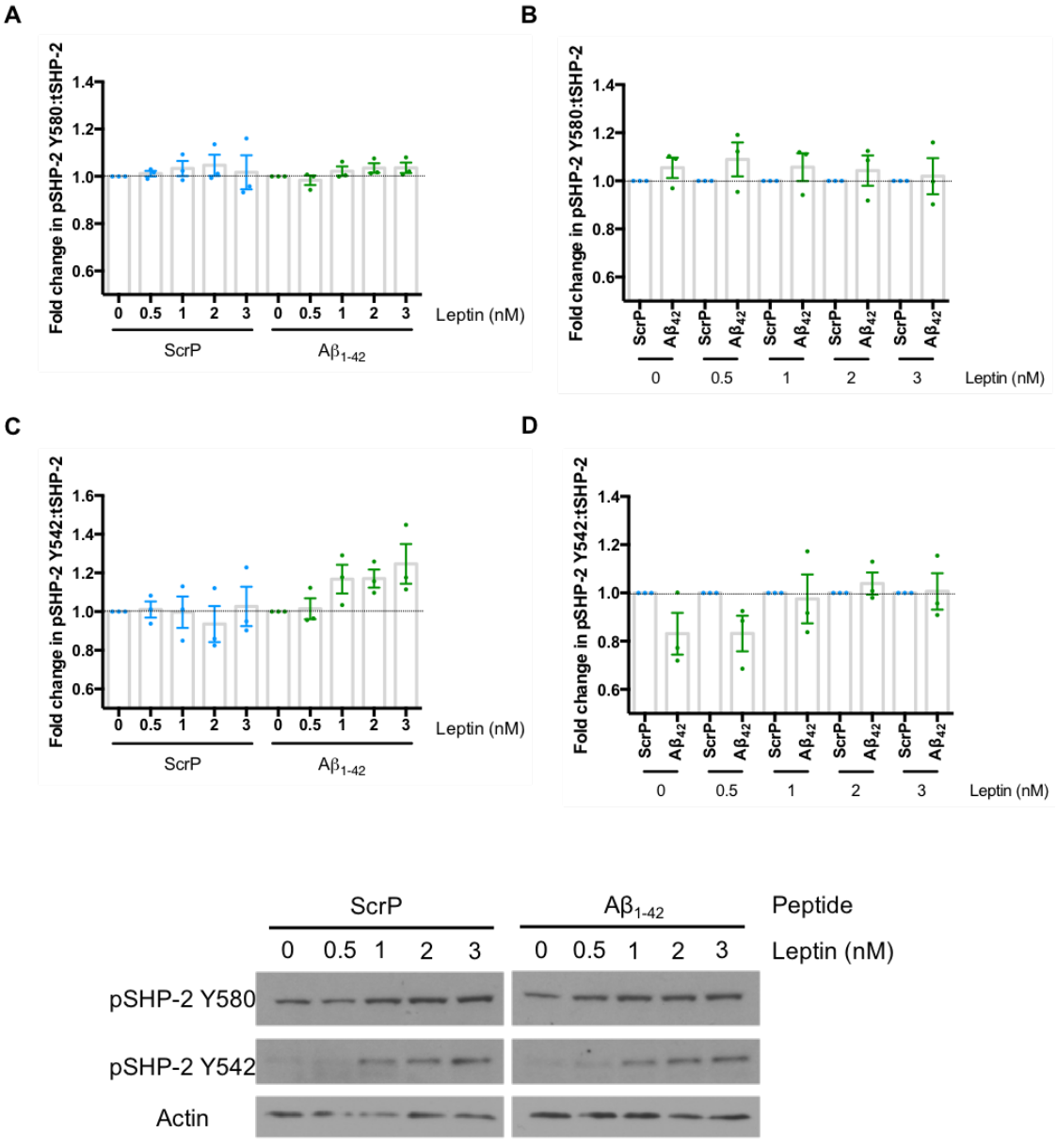

Figure 7.6 SHP-2 phosphorylation with 11pM amyloid exposure and leptin stimulation. SHP-2 phosphorylation at Y541 does not change with leptin concentration but basal phosphorylation is reduced with exposure to 11pM $A\beta_{1-42}$. Histograms representing relative Y580 and Y542 SHP-2 phosphorylation with leptin concentration (**A)(C)** (normalised to 0nM leptin) and 11pM $A\beta_{1-42}$ exposure **(B)(D)** (normalised to ScrP**)** with representative western blots. **A)** Y580 pSHP-2 does not change with leptin concentration **B)** Y580 pSHP-2 does not change with 11pM $A\beta_{1-42}$ exposure. **(C)** Y542 SHP-2 does not increase with leptin when exposed ScrP but increases in a leptin concentration dependent manner with 11pM $A\beta_{1-42}$ although this trend is not significant. **(D)** Basal Y542 SHP-2 is decreased with 11pM $A\beta_{1-42}$ but this is overcome with higher concentrations of leptin. However, this trend is not significant. n=3 per group. Individual data points indicate the range of data. Standard error indicated by error bars.

7.2.4 Leptin sensitivity with chronic exposure to 100pM/400pM $A\beta_{42/40}$

Experimental design remained consistent but with approximately 10-fold higher amyloid concentrations. Additionally, in an effort to see a basal pSTAT3 level, the cells were starved for 2 hours. Cell lysates were collected after 5-day exposure to amyloid and a 30-minute leptin stimulation. Despite this, pSTAT3 was still not detectable at 0 and 0.5nM leptin (Figure 7.7). No significant change in pSTAT3 was observed with 100pM $A\beta_{42}$ or 400pM $A\beta_{40}$ when compared to ScrP at basal or either dose of leptin (Figure 7.7C). No difference was observed in tSTAT3 expression with either leptin dose (Figure 7.7A) or $A\beta_{42}$ or $A\beta_{40}$ exposure (Figure 7.7B).

Expression of SOCS3 (Figure 7.8) and PTP1B (Figure 7.9) were unchanged with both exposure to $A\beta_{42}$ and with leptin concentration. A trend towards increased PTP1B expression with $A\beta_{40}$ exposure was observed. However, this change is likely due to a single replicate with increased PTP1B expression. Increased replicates would likely negate this trend.

Total SHP-2 expression did not change with $A\beta_{40}$ and $A\beta_{42}$ or leptin concentration. (Figure 7.10A-B). Phosphorylation of SHP-2 at Y542 was highly variable and not significant with either $A\beta_{42}$ exposure or leptin dose. Increasing SHP-2 Y542 phosphorylation followed a dose dependent trend with both ScrP and $A\beta_{42}$ however these changes were not significant due to high variability of the data. No leptin dependent effects were noted with $A\beta_{40}$ (Figure 7.10C) SHP-2 Y542 phosphorylation did not change with $A\beta_{40}$ or $A\beta_{42}$ exposure.

7.2.5 β-Amyloid1-42 oligomerisation

The oligomerisation state of $A\beta_{42}$ was determined by western blot (Figure 7.11). Serum and cell-free culture medium containing 1nM $A\beta_{42}$ and incubated at 37°C for 5 days was shown to predominantly contain dimeric structures as indicated by a band at approximately 8kDa. However oligomeric forms of $A\beta_{42}$ were observed with bands appearing at approximately 30, 63 and 90kDa. No bands were present in amyloid-free medium.

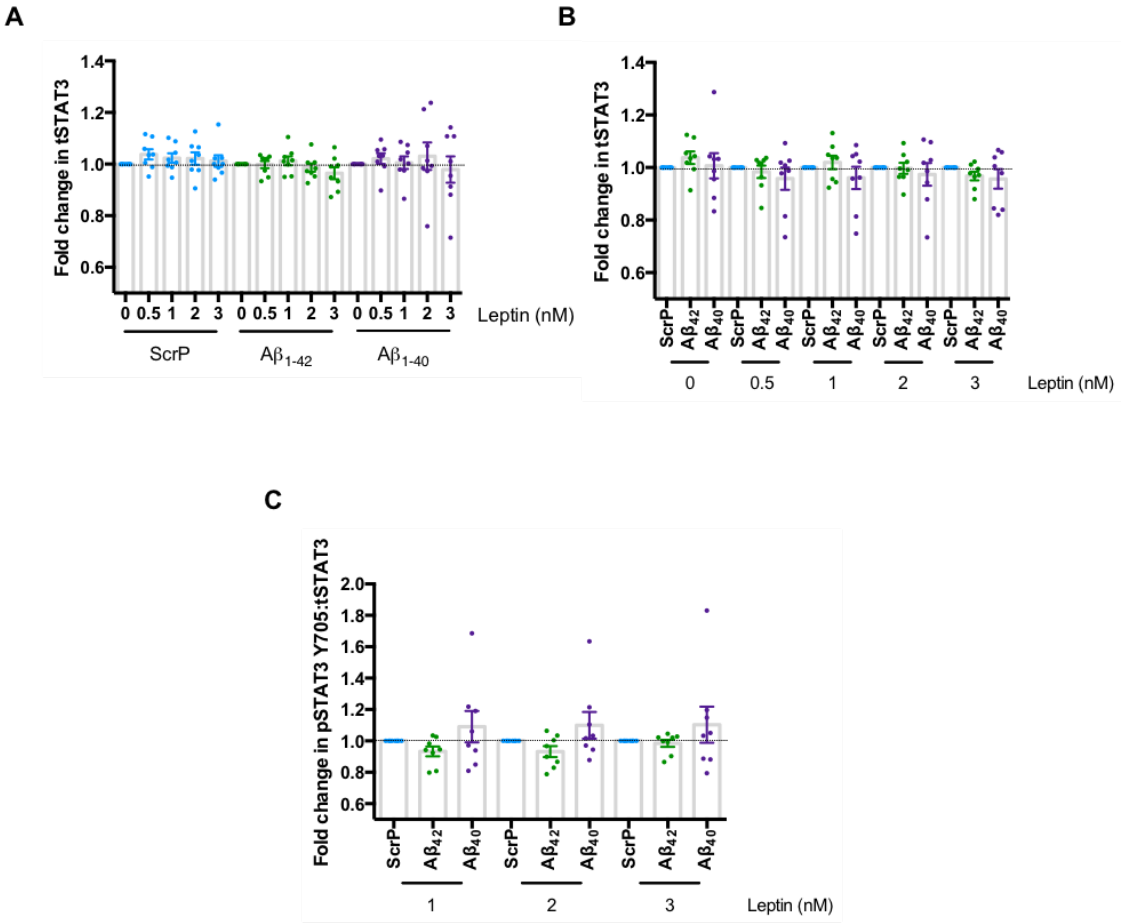

Figure 7.7 STAT3 expression and phosphorylation with amyloid exposure and leptin stimulation. STAT3 expression and activation is unaltered in HEK293 mObRb cells exposed to 100pM $A\beta_{1-42}$ or 400pM $A\beta_{1-40}$ when stimulated with leptin. Histograms represent the effect of amyloid peptides on leptin dose response (normalised to 0nM leptin) (**A)** the effect of amyloid peptides on STAT3 expression at each leptin concentration (normalised to ScrP) **(B)** as well as STAT3 phosphorylation with 100pM $A\beta_{1-42}$ /400pM $A\beta_{1-40}$ exposure (normalised to ScrP) **(C)** with representative western blots.
A) STAT3 expression does not change with leptin concentration. **B)** STAT3 expression does not change with $A\beta_{1-42}$ or $A\beta_{1-40}$ exposure. **C)** pSTAT3 does not change with $A\beta_{1-40}$ or $A\beta_{1-42}$ exposure at basal or with leptin stimulation. n=8 per group. Individual data points indicate the range of data. Standard error indicated by error bars.

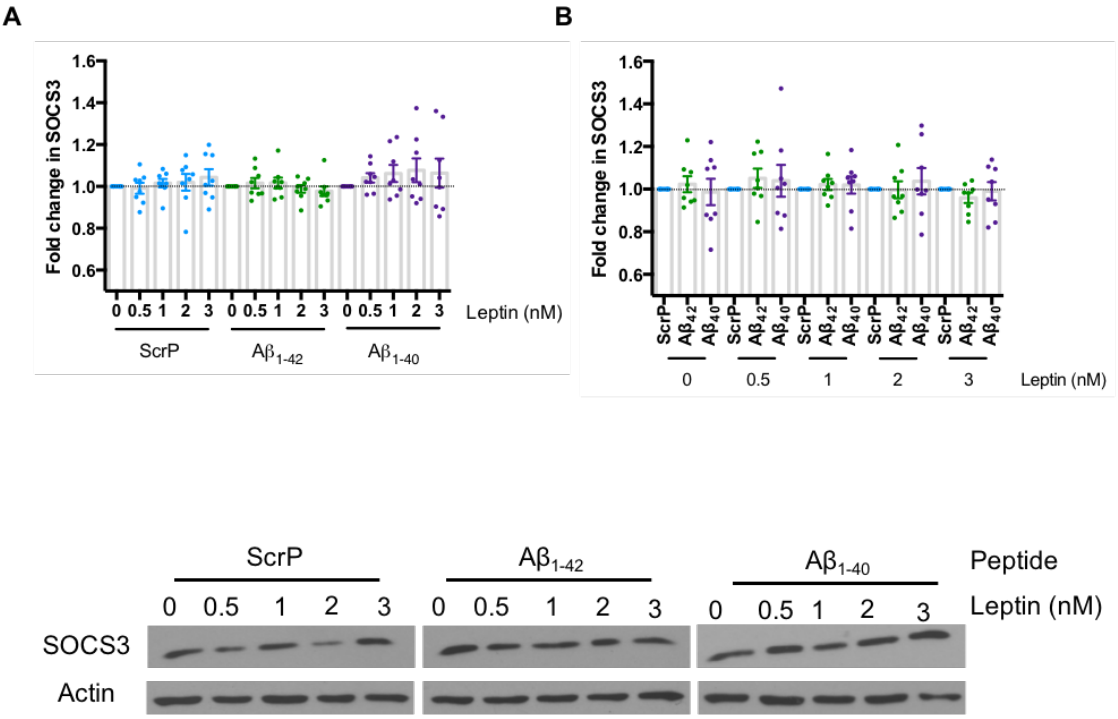

Figure 7.8 SOCS3 expression with amyloid exposure and leptin stimulation. SOCS3 expression is unchanged in HEK293 mObRb cells exposed to 100pM $A\beta_{1-42}$ and 400pM $A\beta_{1-40}$. Histograms representing SOCS3 expression with 0.5-3nM leptin (normalised to 0nM leptin) (**A)** and 100pM $A\beta_{1-42}$ /400pM $A\beta_{1-40}$ exposure (normalised to ScrP) **(B)** with representative western blots. SOCS3 expression does not change with leptin concentration. **(A)** SOCS3 expression does not change with ScrP, $A\beta_{1-42}$ or $A\beta_{1-40}$ exposure **(B)** n=8 per group. Individual data points indicate the range of data. Standard error indicated by error bars.

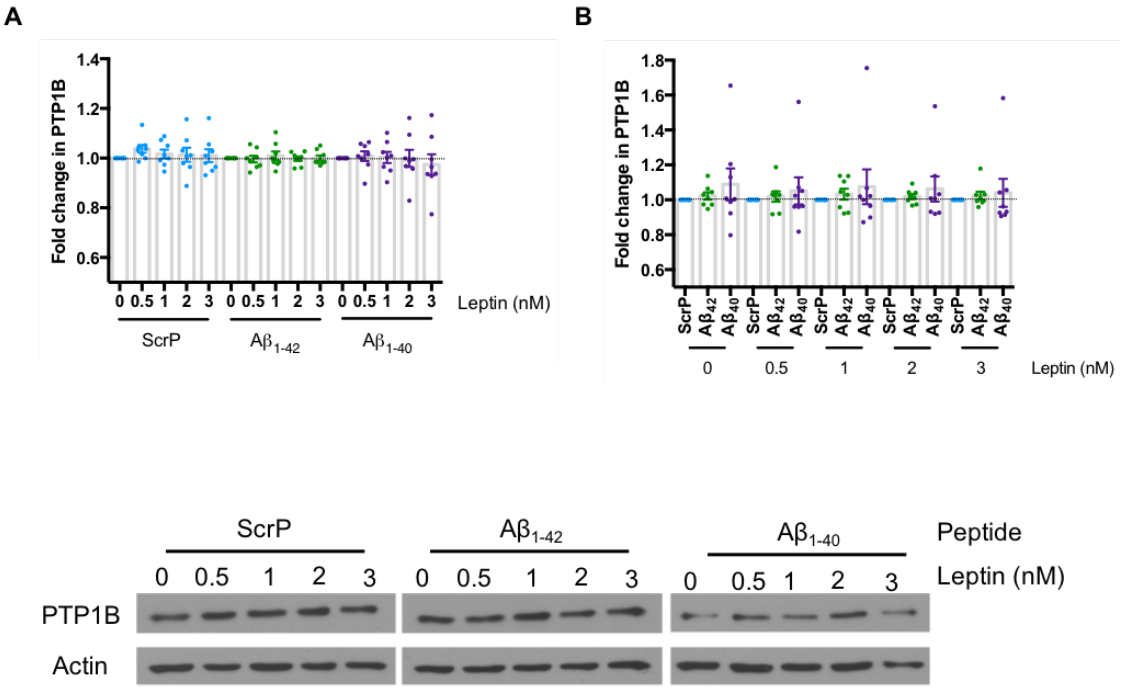

Figure 7.9 PTP1B expression with amyloid exposure and leptin stimulation. PTP1B expression is unchanged in HEK293 mObRb cells exposed to 100pM $A\beta_{1-42}$ and 400pM $A\beta_{1-40}$. Histograms representing PTP1B expression with 0.5-3nM leptin (normalised to 0nM leptin) **(A)** and 100pM $A\beta_{1-42}$ /400pM $A\beta_{1-40}$ exposure (normalised to ScrP) **(B)** with representative western blots. PTP1B expression does not change with leptin concentration (n=8) **(A)** PTP1B expression does not change with ScrP, $A\beta_{1-42}$ or $A\beta_{1-40}$ exposure **(B)** n=8 per group. Individual data points indicate the range of data. Standard error indicated by error bars.

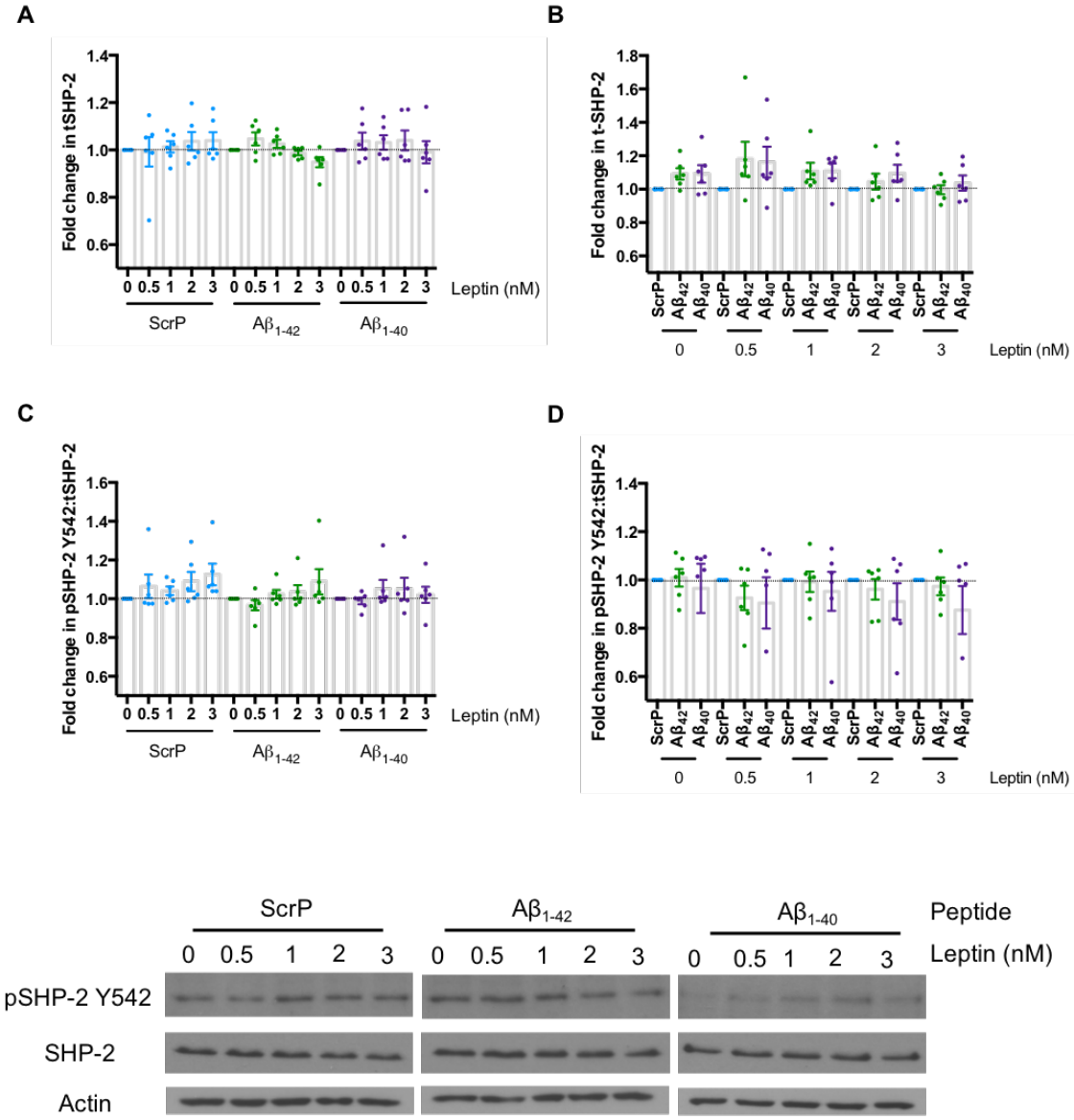

Figure 7.10 SHP-2 expression and phosphorylation with amyloid exposure and leptin stimulation. SHP-2 expression is increased in HEK293 mObRb cells exposed to 100pM $A\beta_{1-42}$ and 400pM $A\beta_{1-40}$ whilst Y542 phosphorylation is reduced in $A\beta_{1-40}$ treated cells**.** Histograms representing total and Y542 phosphorylated SHP-2 expression with 0.5-3nM leptin (normalised to 0nM leptin) (**A)(C)** and 100pM $A\beta_{1-42}$ /400pM $A\beta_{1-40}$ exposure (normalised to ScrP) **(B)(D)** with representative western blots. **A)** SHP-2 expression does not change with leptin concentration. **B)** SHP-2 shows a trend towards increasing with both $A\beta_{1-42}$ and $A\beta_{1-40}$ exposure however this is not significant. **C)** Y542 SHP-2 shows a trend towards leptin concentration dependent increases under all conditions with a dampened response upon exposure to $A\beta_{1-40}$. This trend is not significant. **(D)** Y542 SHP-2 does not change with ScrP or $A\beta_{1-40}$ or $A\beta_{1-42}$ exposure. n=6 per group. Individual data points indicate the range of data. Standard error indicated by error bars.

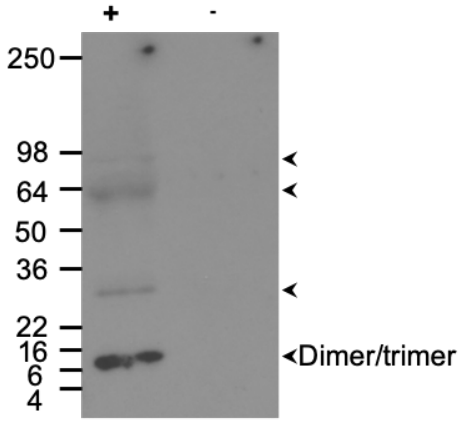

Figure 7.11 Oligomerisation state of Amyloid-β_{1-42} after 5-day incubation in culture medium. Amyloid-β_{1-42} exists primarily as dimers after 5-day incubation in culture medium. Western blot indicating the oligomerization state of $A\beta_{1-42}$ when incubated in cell culture medium for 5 days under cell-culture conditions compared to amyloid-free medium.

7.3 Discussion

7.3.1 Effect of chronic 11pM amyloid on leptin signalling

Previous data indicate that after 20-weeks on a HFD, circulating $A\beta_{42}$ peptide concentration in wild-type mice increases to 11pM. These mice also exhibit signs of metabolic dysfunction such as obesity, reduced glucose tolerance, insulin resistance, and reduced sensitivity to leptin. (Meakin et al., 2012; Meakin, Jalicy, et al., 2018). This study used these physiological concentrations of amyloid to determine whether amyloid concentrations associated with obesity and metabolic dysfunction are sufficient *per se* to lead to changes in leptin signalling. Reduced leptin sensitivity was also observed in mice exposed to ICV $A\beta_{1-42}$ (3.36 µg/kg) for 28 days following 10 weeks on a HF diet (Meakin, Jalicy, et al., 2018). Indeed, this study found that ICV $A\beta_{42}$ exacerbated the obese phenotype and led to the hypothesis that amyloid exposure causes leptin signalling dysregulation within the brain.

The present study utilised a leptin sensitive cell model to test this hypothesis and aimed to determine the mechanism behind amyloid mediated leptin resistance. Despite this, the GT1-7 cells proved to be unresponsive to leptin stimulation and

even when transfected with the leptin receptor mObRb, quickly lost leptin sensitivity. It is likely that this represents low transfection efficiency within these cells and ineffective plasmid retention. As the leptin receptor and its HA tag was never identified via western blot, the effectiveness of the transfection was never fully established and future studies would need to address this issue. The loss of leptin sensitivity may also be due to the methods of transfection. As expression of full length ObRb was never determined, the cells were not selected for clonal growth. Therefore, the cells used in this experiment were mixed and may grow at different rates leading to a gradual decline in full ObRb expression over passages. Subsequently, the HEK 293 cell line was chosen and stable cells expressing the mObRb leptin receptor were created to make them leptin responsive. Whilst these cells were not representative of central leptin resistance or indeed, central metabolic signalling, due to their responsiveness to leptin they may have provided mechanistic insights into amyloid induced leptin resistance. The HEK 293 mObRb cells were shown to be sensitive to 1nM leptin making them a useable model for this study. Unlike the GT1-7 cell line, the HEKs maintained leptin responsiveness beyond passage 30 and with freezing.

There was no observed difference in pSTAT3 with 11pM exposure indicating that HEK 293 mObRb cells do not replicate the results seen *in vivo*. This may be due to the differences in cell type and therefore protein expression between brain cells and HEK 293s or that cells in culture may generally be less responsive to amyloid than cells *in vivo*. In order to determine whether the amyloid concentration was too low for *in vitro* experiments, further experiments were conducted using higher physiological concentrations of amyloid. The cell starvation period prior to stimulation was also reduced to 2 hours to improve the likelihood of getting detectable pSTAT3 without leptin stimulation and determine baseline activation of the JAK-STAT pathway.

Interestingly a dose-dependent effect was noted in Y542 pSHP-2 with $A\beta_{42}$ but not with ScrP or at Y580 pSHP-2 with either $A\beta_{42}$ or ScrP. This suggests that JAK2 regulation of this pathway occurs through only Y542 SHP-2 phosphorylation. This, in combination with reduced Y542 phosphorylation at low concentrations of leptin with $A\beta_{42}$ suggest lower basal SHP-2 activation with exposure to amyloid- possibly through inhibition of an alternative SHP-2

activation pathway. This may be the cause of leptin concentration dependent phosphorylation at this site with amyloid exposure but not ScrP as maximum phosphorylation had been achieved with ScrP but not $A\beta_{42}$ exposure. Phosphorylation at the Y580 was unaltered with $A\beta_{42}$ implying that Y542 as the primary regulatory site through this pathway. These data bring into question whether selective phosphorylation of SHP-2 by different growth factor pathways is a regulatory factor in SHP-2 activity. As yet, studies have not identified the role of these phosphorylation sites in leptin signalling and their relevance in ERK pathway activation by leptin is unclear.

7.3.2 Effect of chronic 100pM $A\beta_{42}$ or 400pM $A\beta_{40}$ on leptin signalling

To determine if the amyloid concentration used previously was too low to induce amyloid dependent leptin resistance, $A\beta_{42}$ concentration was increased to 100pM and a 400pM $A\beta_{40}$ group was added. The higher concentration of $A\beta_{40}$ was consistent with plasma amyloid concentrations found in *in* vivo HFD studies (Meakin, Jalicy, et al., 2018). This concentration is comparable with CSF amyloid levels in cognitively normal individuals and patients with MCI. (Forlenza et al., 2015) Despite shortening of the serum-free conditions to 2 hours, no Y705 pSTAT3 was detected in the unstimulated control and the presence of a band at 0.5nM was inconsistent between replicates. This made quantification at low leptin concentrations impossible and therefore no basal pSTAT3 could be used for comparison.

No significant changes in pSTAT3 were observed at this higher $A\beta_{42}$ concentration or with $A\beta_{40}$ exposure indicating that neither amyloid species induces leptin resistance in HEK 293 mObRb cells after 5 day exposure. It is likely that the model used in these experiments was insufficient to replicate the *in vivo* data due to a variety of factors. The HEK 293 cell line is not representative of cells within the brain and may therefore not exhibit the leptin sensitivity observed with neurons. These cells are also limited in that downstream effectors such as POMC and AgRP mRNA cannot be utilised as a functional output of JAK-STAT pathway activation and metabolic dysfunction. Despite the effects of differentiation on amyloid production in neuronal cell lines, comparisons may still be made between treated and untreated cells making them much more

representative of brain physiology. Furthermore, 5-day amyloid exposure may not be long enough to result in leptin resistance; particularly as the cells are actively dividing so the proportion of cells exposed to amyloid for 5 days may be low. *In vivo*, animals were exposed to amyloid for 4 weeks so the length of exposure may be important. The length of exposure may also affect oligomerisation state so longer incubations may result in larger aggregates that could exude a greater influence on leptin signalling. Due to low concentrations of plasma amyloid, oligomerisation state could not be determined *in vitro* so the amyloid species between the two experiments could not be compared.

No change was observed in the negative regulators of STAT3 signalling SOCS3 and PTP1B with either amyloid exposure or leptin concentration. Data on SOCS3 expression was highly variable making significant results difficult to achieve. An alternative such as mRNA expression may be a more reliable measure in future studies and may be a better representative of JAK-STAT pathway activation at this time point as a 30 minute stimulation has previously been shown to be insufficient to see changes in protein, whilst the transcriptional changes occur after 30 minutes of stimulation (Bjørbaek, El-Haschimi, Frantz, & Flier, 1999). In order to determine effects in protein expression of both of these regulators it may be that a longer stimulation time is required, and a time course may reveal further information regarding the regulatory effects of these proteins on leptin signalling in this system.

Total SHP-2 expression was highly variable thereby preventing conclusive results but both $A\beta_{40}$ and $A\beta_{42}$ exhibited a trend towards increased SHP-2 expression. At 100pM amyloid, a concentration dependent increase in Y542 pSHP-2 with leptin was observed in both the ScrP and $A\beta_{42}$ treated cells whereas the concentration dependent response was only observed in the amyloid treated cells at 11pM. However, these results were not significant at any amyloid concentration. The concentration dependent effect of leptin was not observed with $A\beta_{40}$ at 400pM but due to the variability in the data with each peptide it is difficult to form any conclusions. It may be that a greater number of replicates using a more sensitive, quantitative detection method, such as ELISA, would make this result more conclusive. The effect of lower basal Y542 SHP-2 with $A\beta_{42}$ exposure was not observed at this higher amyloid concentration leading to

questions regarding the reliability of the data at 11pM $A\beta_{1-42}$. Due to greater replicates at higher amyloid concentrations it is reasonable to suggest that these data are more reliable. Whilst no changes in Y542 SHP-2 phosphorylation were observed with either $A\beta_{40}$ or $A\beta_{42}$, the trend towards increased total SHP-2 expression suggests that both total and Y542 phosphorylated SHP-2 are increased with both $A\beta_{40}$ and $A\beta_{42}$. However, as all other indicators of leptin signalling within these cells were unchanged, it is likely that this effect is due to changes in an alternative SHP-2 activating pathway. qPCR analysis of SHP-2 would determine whether increased transcription of SHP-2 follows amyloid exposure. Most receptor tyrosine kinases cause activation of the Ras-ERK pathway through SHP-2; including the insulin receptor which, upon binding to IRS-1 causing dephosphorylation of PI3K binding sites and regulating downstream protein synthesis (Backer et al., 1992; Lima et al., 2002; Müssig et al., 2005; Myers et al., 1998). As discussed in section 1.2.2 the leptin receptor shares structural similarity to cytokine receptors such as the IL-6 receptor subunit gp-130. It could therefore be feasible that amyloid peptides activate alternative cytokine signalling pathways which in turn, phosphorylate SHP-2 (Schaper et al., 1998). However, no evidence has been published to date to suggest an interaction between amyloid peptides and this family of RTKs.

This study ties in with published data indicating that amyloid exposure leads to increases in Ras-ERK signalling (Kirouac et al., 2017), a downstream effect of SHP-2 activation. Indeed, Ras-ERK activation has been implicated in the hyperphosphorylation of Tau both *in* vitro and *in* vivo leading to the hypothesis that amyloid mediated effects on SHP-2 activity may be a missing link between these two AD pathologies. (Lambourne et al., 2005; Qi et al., 2016). Activation requirements of SHP-2 protein are uncertain with some showing that tyrosine phosphorylation is not required for GRB2 association but necessary for ERK activation (Araki, Nawa, & Neel, 2003); others indicate that phosphorylation of SHP-2 is not necessary for Ras-ERK pathway activation (Bennett, Hausdorff, O'reilly, Freeman, & Neel, 1996); indeed, even in pathways where SHP-2 phosphorylation is identified, removal of phosphorylated SHP-2 does not result in abolition of ERK signalling (Araki et al., 2003). If this is the case, increases in SHP-2 expression alone may confer increases in ERK activation within our model. Analysis of ERK phosphorylation state would offer insights into the effects

of increased SHP-2 on Ras-ERK activation in this model. Further experiments utilising SHP-2 phospho-site mutants would allow the determination of the importance of phosphorylation in leptin-mediated ERK activation. Further Amyloid incubations with these mutants would allow confirmation of the importance of SHP-2 in ERK signalling and offer further insight into the role of amyloid.

7.3.3 Oligomerisation of mouse $A\beta_{42}$

The amyloid oligomerisation state was determined as many studies have indicated that some oligomeric species may contribute more to the AD phenotype than plaques. Until recently, it was supposed that fibrillar amyloid in the form of amyloid plaques were the most neurotoxic species due to their accruement in AD however more recent data suggest that smaller, oligomeric forms may contribute more to disease than amyloid plaques. (Cleary et al., 2005). During this *in vitro* study we showed that 5 days incubation at 37°C and 5% CO_2 leads to slight aggregation of mouse $A\beta_{42}$ whilst the predominant form is either monomeric or dimeric. This is consistent with recent published data that shows only aged C57BL/6J mice show signs of native $A\beta_{42}$ aggregation (Ahlemeyer, Halupczok, Rodenberg-Frank, Valerius, & Baumgart-Vogt, 2018).

7.3.4 Conclusions

This study was designed to better understand the mechanism behind amyloid mediated leptin resistance observed in obese mice subjected to ICV $A\beta_{42}$. These mice exhibited increased basal Y705 STAT3 phosphorylation compared to ScrP infused controls which did not increase further when stimulated with leptin within the hypothalamus (Meakin, Jalicy, et al., 2018). This study was therefore designed to explore the prospect of direct inhibition of $A\beta_{42}$ on the leptin signalling pathway. No significant changes were identified in STAT3 activation therefore the mechanism behind leptin resistance in $A\beta_{42}$ treated mice could not be determined. However, there were suggestions towards increased SHP-2 expression and activation with amyloid peptides which likely originate from alternative pathways such as insulin- which amyloid is known to activate. Further studies, such as colocalization experiments, could identify which pathway leads to this observed change in SHP-2.

Interestingly, plasma leptin was increased in $A\beta_{42}$ treated mice and decreased circulating leptin with BACE1 inhibition suggesting that central amyloid regulates leptin expression (Meakin, Jalicy, et al., 2018). This supports previously published data suggesting that amyloid increases leptin within the hippocampus (Marwarha et al., 2010). This study (Meakin, Jalicy, et al., 2018) did not look for changes in leptin within tissues so whilst plasma leptin concentration was high, it was not determined whether the leptin was able to cross the BBB and enter either hippocampal or hypothalamic tissues. Therefore, BBB integrity and tissue leptin concentrations within this model would be an essential step in determining how leptin resistance is induced. If BBB integrity remains in-tact, it may be that amyloid directly inhibits the leptin receptor leading to accumulation of free leptin. There are known variants of leptin within the human population which have been studied in their relationship to obesity but not dementia (Dasgupta et al., 2015). Whilst no evidence exists to suggest that leptin variants are associated with an increased risk of developing AD, these studies would not identify variants of leptin that would confer protective effects against this dementia. An interesting study would be to compare competitive binding of both amyloid species and leptin variants to the long form of the leptin receptor to identify whether specific leptin species have greater binding affinity to the receptor and whether amyloid interferes with this process. As leptin has been suggested to induce BACE1 expression current evidence on this association is inconclusive (Sastre et al., 2006). However, as leptin is not thought to be expressed within the brain, this vicious cycle could be of greater relevance in leptin secreting tissues such as adipocytes. Studies into the effects of amyloid on leptin secretion in adipocytes could offer insight into this relationship as it has been shown that they express APP and produce amyloid peptides (Lee et al., 2008). This could be of significance in AD as both circulating $A\beta_{42}$ and leptin concentrations are reduced, it could therefore be plausible that this leads to a reduction in leptin secretion and a loss of the neuroprotective effects that it offers (Koyama et al., 2012).

Alternatively, leptin resistance may be induced through a multi-organ system that requires multiple cell types and cannot be simply replicated in *in vitro*. The glucocorticoid (GC) system, for example is a known regulator the leptin sensitivity with both *in vivo* and *in vitro* studies indicating that GCs increase leptin mRNA

and secretion from adipocytes and adrenalectomy leads to increased central leptin sensitivity (Slieker et al., 1996; Zakrzewska, Cusin, Sainsbury, Rohner-Jeanrenaud, & Jeanrenaud, 1997). However, GCs were shown to inhibit leptin signalling in in a human hepatoma cell line suggesting that the effects of GCs on leptin sensitivity may be organ-specific or not replicable *in vitro*. Hepatic cell leptin resistance was shown to be ameliorated by inhibition of MAP-kinase signalling through inhibition of MEK (Ishida-Takahashi et al., 2004). Initial studies into the BACE1 KO mouse identified increased plasma corticosterone in these mice compared to WT controls when challenged with a HFD (Meakin et al., 2012). However, the data do not complement other published studies indicating that HFD increases circulating GCs (Champy et al., 2004). Indeed, no dietary effect was observed in either WT or BACE1 animals. Further confounding factors include the duration of fasting as published data indicate that plasma corticosterone increases with length of fast prior to blood being taken, reaching maximal concentrations after approximately 6hrs in males (Champy et al., 2004). As these blood samples were taken after 16hr fast, it may be that these data represent maximal corticosterone rather than concentrations within the normal physiological range of these mice. Whilst this could explain the lack of change seen in plasma corticosterone with diet, it is important to note that the maximal corticosterone concentration is increased with BACE1 KO and further study could reveal whether this result represents a general increase in plasma corticosterone or a greater response with HPA axis stimuli.

Amyloid peptides have also been shown to increase hypothalamic corticotropin-releasing hormone (CRH) and plasma adrenocorticotropin hormone (ACTH) 3 weeks after ICV amyloid injection in rats. Plasma corticosterone was increased from 1 week after ICV amyloid injection and remained elevated for 6 weeks. This indicates prolonged activation of the HPA axis with a single amyloid exposure. Furthermore, amyloid increased hippocampal, hypothalamic and amygdala expression of the glucocorticoid receptor with elevations lasting upwards of 6 weeks in the hippocampus (Brureau et al., 2013). High GCs have been identified in the CSF of AD patients and correlated to more rapid cognitive decline making this a feasible hypothesis for the mechanism of amyloid mediated leptin resistance (Csernansky et al., 2006). Further *in vivo* analysis to determine plasma cortisol and the expression of cortisol producing cyp11b1 protein within the

adrenal gland as well as CRH mRNA within the hypothalamus with amyloid exposure could provide evidence towards this hypothesis.

Chapter 8

Conclusions

8.1 Physiological function of BACE1

Dementias, including Alzheimer's disease (AD) are fast becoming the leading cause of death in the western population with cases expected to rise to 2 million in the UK alone by 2050 (Prince et al., 2007). This has largely been attributed to an increased life expectancy due to better treatments for previous leading causes of death such as cancers. However, an alternative hypothesis is that increased metabolic dysfunction within higher-income populations as a result of western diet and sedentary lifestyle leads to increased incidence of AD. As both mid-life obesity and diabetes increase the risk of developing AD, it may be that diets high in fat and sugar induce changes within the CNS that contribute to the onset of dementia. HFD has been shown to increase the expression of a key AD protein BACE1 (Meakin et al., 2012). BACE1 activity is the rate limiting step in the production of the neurotoxic β-amyloid peptides characteristic of AD and is therefore a key target when studying the relationship between obesity and AD.
The neurological effects of obesity have been well documented with overweight and obese individuals consistently exhibiting decreased executive functions ,such as planning and decision making, and poorer short-term memory (Reviewed by Nguyen, Killcross and Jenkins, (2014)). Neuroimaging of obese individuals has revealed brain atrophy and animal studies have shown decreased pyramidal cell dentritic spine density from the early stages of obesity. This suggests altered brain connectivity in association high BMI (Bocarsly et al., 2015; Ward, Carlsson, Trivedi, Sager, & Johnson, 2005). An animal study by Niedowicz *et al.* (2014) indicates that the effects of metabolic diseases on cognitive function occur irrespective of amyloid deposition and synapse loss; this suggests an alternative mechanism is at play.

Current findings show that BACE1 activity is an early step in the development of AD and many factors contribute to increased amyloid production. Inflammation is just one example of suspected amyloidogenesis whereby chronic inflammation leads to increased BACE1 expression; BACE1 then increases the production of reactive oxygen species and contributes to further inflammation which, in turn, increases BACE1 expression. What is currently unknown is why this vicious cycle of increased BACE1 expression and inflammation is not ubiquitous amongst those with chronic inflammation. The initiating factor has yet to be identified.

Previous studies to determine BACE1 physiological function have focussed on two key features of BACE1; its function as a protease and its interaction with APP. Efforts to establish the substrate profile of this enzyme have studied changes in secreted protein ectodomains with altered BACE1 expression (Dislich et al., 2015; Hemming et al., 2009; Herber et al., 2018; Kuhn et al., 2012). However this does not account for known functions for BACE1 outside of proteolysis (Huth et al., 2009). Whilst many others have looked for physiological functions of the APP peptide products of BACE1 activity (Reviewed by Brothers, Gosztyla and Robinson. (2018)). This study was designed to investigate the physiological function of BACE1 by proteomics and interactomics as a method of studying BACE1 physiology without the limitation of assuming proteolytic activity and APP association.

Studies using a BACE1 KO mouse whereby exon 1 of BACE1 was replaced with the LacZ gene (Harrison et al., 2003) found that BACE1 KO led to protection from diet-induced obesity, improved glucose and insulin tolerance when challenged with chronic over-nutrition and protection from leptin resistance commonly associated with obesity. Furthermore, DIO led to increased hypothalamic BACE1 expression that was recovered with pharmacological inhibition (Meakin et al., 2012; Meakin, Jalicy, et al., 2018). In addition, increased neuronal BACE1 expression has been shown to induce insulin resistance without the need for dietary or chemical induction of diabetes (Plucińska et al., 2016).

Behavioural and neurological studies have suggested an increased seizure phenotype in another BACE1 KO model as well as hyperactivity, hypomyelination and schizophrenia. (Dominguez et al., 2005; Harrison et al., 2003; Hitt et al., 2010; Hu et al., 2006; Roberds et al., 2001). However, these phenotypes have not been consistently identified across all BACE1 KO models and are therefore inconclusive.

Despite the limited effects of BACE1 KO on mouse survival or phenotype, the mutation rate of this protein throughout evolution is very low and conservation of catalytic activity is very high. Indeed, BACE1 proteins from marine lancelets are capable of cleaving human APP (Moore et al., 2014b). This begs the question as to why BACE1 is so evolutionarily important.

8.2 BACE1 as a regulator of neurotransmission

The main outcome of the proteomic study was the suggestion that BACE1 may influence the expression of hippocampal protein 4.1N. By association, this connection could implicate BACE1 in post-synaptic neurotransmitter binding through stabilisation of receptors such as NMDAR, AMPAR and the dopamine receptors D2 and D3.

Co-expression studies would be required to determine whether there is indeed a direct interaction between BACE1 and protein 4.1N. This would be achieved through co-immunoprecipitation. This could be performed in the HT-22 hippocampal cell line utilised in the Bio-ID proximity assay. As HT-22 cells do not express endogenous protein 4.1N they may be stably transfected with 4.1N constructs of different splice variants. As HT-22s express endogenous BACE1, co-IP would allow for mass spectrometry identification of protein 4.1N interactors within these cells and identification of BACE1 if it is a true binding partner. In addition, co-staining experiments in BACE1 KO and WT control mice would reveal whether the presence of 4.1N and BACE1 within the cortical molecular layer, the stratum radiatum of the hippocampus and SLM under NC and HF conditions leads to changes in glutamatergic, GABAergic or dopaminergic receptor expression at synpases.

Co-expression within the synapses may also be a key regulator of glutamatergic signalling and stabilisation of both AMPA and NMDA receptors. To test this, synaptosomal fractions from hippocampal tissues could be analysed for expression of BACE1 and 4.1N as well as NMDARs and AMPARs. It would also be of benefit to transfect HT-22 cells with APP and conduct imaging studies and quantification of synapses to ascertain whether the BACE1/4.1N relationship is a product of APP/4.1N association. Following this, patch clamp electrophysiological experiments on 4.1N or BACE1 overexpressing HT-22 cells would help determine whether increased expression of these proteins influences excitatory signalling within these neurons.

Long-term *in vivo* experiments would be required to determine the effects of protein 4.1N on cognition. Cognitive testing of a 4.1N-null mouse would include

spatial working memory analysis by way of morris water maze, long and short term memory by the novel object recognition task and hippocampal dependent memory with the Y-maze spontaneous alternation tasks. Furthermore, electrophysiological experiments on hippocampal sections could identify any changes in LTP and LTD within 4.1N null mice whilst staining for glutamatergic receptors may offer insight into the localisation of these receptors without 4.1N stabilisation.

8.3 BACE1 and membrane channels

BACE1 proximity assay suggested interaction of BACE1 with a large number of channel proteins, varying in function from ion to amino acid transport. This result builds upon previous findings (Reviewed by Lehnert et al. (2016)) suggesting non-enzymatic functions of BACE1 and showing that this protease may, in fact, act as a regulator of Na2+ and K+ channel function; both through proteolytic cleavage of α subunits and itself, acting as a β subunit. Two proteins involved in ion homeostasis were consistently identified as BACE1 interactors. Anoctamin-6, and Solute carrier family 12 member 2 (also known as NKCC1) involved in Ca2+, and Na2+/Cl- transport across biological membranes respectively. A process essential in neurons to maintain membrane polarisation and action potential transmission. Whilst co-localisation studies would be required to validate the direct interaction of BACE1 with these proteins, hyperexcitability of neurons in BACE1 KO mice has been previously documented. These results may provide insight into the mechanism behind this finding (Hu et al., 2010). Furthermore, the hippocampal proteomic hit protein 4.1N is known to bind to the intracellular Ca^{2+} channel InsP(3)R1, possibly regulating internal calcium concentration and cell membrane potential (Maximov et al., 2003).

8.4 BACE1 in neuronal junctions

Results from the proximity assay also strongly suggest a role for BACE1 in cell connectivity with multiple hits indicating an association with cell adhesion molecules. This is supported by published data that suggest a role for APP in synaptic adhesion. Evidence suggests that shedding of the APP ectodomain reduces synaptogenesis and expression of APP and induces synaptic formation with co-cultured primary neurons (Stahl et al., 2014; Wang et al., 2009). Furthermore, Wang *et al.* (2009) showed that APP forms a complex with Mint1

and CASK, the latter a known binding partner of protein 4.1N which, together, promote F-actin assembly (Biederer & Südhof, 2001). Dynamic actin has been shown to be essential in LTP (Krucker et al., 2000). It is reasonable, therefore, to hypothesise that protein 4.1N may be a member of the APP/CASK complex. This would cause increases in BACE1 activity to reduce the formation of F-actin by inhibiting the formation of APP/Mint1/CASK/4.1N complex and reduce the expression of protein 4.1N. Therefore, as seen in the proteomic study, BACE1 KO would increase cell surface APP expression allowing the formation of APP/Mint1/CASK/4.1N complex and increasing the expression of 4.1N within the hippocampus. This is supported by staining in the mouse hippocampus that indicates increased BACE1 expression in the stratum radiatum with high-fat feeding coincides with reduced 4.1N expression. However, this correlation does not necessarily confirm causation and possible co-expression in the polymorph layer of the DG did not influence 4.1N expression. It must be noted though, that the polymorph layer represents granular cell synapses whilst the stratum radiatum is predominantly pyramidal cell projections. Mouse data from this project suggest the high-fat feeding leads to increased 4.1N expression within the molecular layers of both the cortex and CA1 pyramidal cells suggesting increased synaptic density with HFD based on this hypothesis. However, as human staining did not replicate the expression pattern or changes with diet, it cannot be suggested that the changes seen with chronic HFD may induce changes similar to those in AD. Further evidence for the role of APP in actin formation comes from APP knockout mice. They have been shown to exhibit reduced dendritic length of CA1 pyramidal cells into the stratum radiatum suggesting a potential deficit in temporoammonic pathway activity. LTP was tested via trisynaptic pathway activation but potentiation was found to be lower in APP KO mice (Seabrook et al., 1999). Co-localisation studies using immunoprecipitation and mass spectrometry (IP/MS) as well as cell staining in HT-22 cells could help identify whether 4.1N does complex with these proteins. This study would also assist in identifying whether the 4.1N/BACE1 association is due to a direct interaction as suggested by identification of 4.1N family members 4.1G and 4.1B in the proximity assay. As HT-22s are an excitatory cell line, glutamate release, axon elongation and synaptic formation could all be studied through 4.1N, APP and BACE1 inhibition (or gene downregulation by

methods such as shRNA and CRISPR) on these differentiated neurons through culture in microfluidic chambers.

Proximity assay data support the hypothesis of a role for BACE1 in cell connectivity with identification of two cell adhesion molecules; afadin and gap junction α1 protein. Additionally, 5 cytoskeletal organisation proteins; spectrin β-chain, keratin, disks large homologue 1, fermitin family homolog 1 and septin 7 were identified as BACE1 proximal proteins. However, due to high levels of BACE1 trafficking throughout the cell, it must be considered that interaction with cytoskeletal proteins may well be due to cytosolic BirA of the fusion protein interacting with the vesicle trafficking machinery.

Afadin, like the 4.1 proteins, acts in the stabilisation of cell membrane proteins by binding them to the actin cytoskeleton. Afadin have been well characterised in its association with the adherens-junction protein nectin. Afadin is expressed highly within the mossy fibers of granule cells of the DG, particularly within punctate cell adhesions; non-signalling neuronal connections. Furthermore, Afadin is expressed within the stratum lucidum of CA3 and synaptic junctions of pyramidal cells throughout the stratum oriens and radiatum of CA1 to CA3 (Nishioka et al., 2000). This matches the hippocampal expression of BACE1 and 4.1N and providing further evidence for BACE1 physiological function within this hippocampal structure. gap junction α1 protein (also known as Connexin 43) is primarily associated with neurogenesis and migration during development (Cina et al., 2009; Duval et al., 2002; Rinaldi et al., 2014). This function corresponds strongly to observed BACE1 expression within the hippocampus as mice appeared to exhibit highest BACE1 within the granule cells of the GD- one of the few cells types of the brain known to undergo neurogenesis into adulthood.

In adults, expression of this protein is predominantly within astrocytes whereby it contributes to the formation of hemi-channels- areas where astrocytes can provide neurons with resources such as glucose, lactate, glutamate and glutamine through small molecule diffusion. Furthermore, connexin 43 expression is known to increase in neurons and astrocytes near amyloid plaques providing further evidence for co-localisation of this protein with amyloidogenic BACE1 (Reviewed by Mayorquin *et al.* (2018)). It would therefore be of interest to conduct the proximity assay in a cell model of astrocytes to observe whether BACE1 co-localises with connexin 43 in this cell type. Co-culture of astrocytes

with neurons may provide evidence of co-localisation at neuron/astrocyte hemichannels. Microfluidic chamber culture of neurons with astrocytes may enable analysis if hemichannel function. Using a microscopy adapted click chemistry method in which click-inducible glutamine-azide uptake can be quantified using an alkyne fluorophore; an assay in development by Prof. David Finlay (Trinity college, Dublin) in conjunction with the University of Dundee. This technique could allow for hemichannel function by loading astrocytes with glutamine-azide and monitoring fluorescence in the neuronal cells. monitoring If developed, this assay would enable the study of BACE1 inhibition in astrocytes and neurons individually on hemichannel function.

8.5 BACE1 in brain metabolism

Despite previous studies providing evidence to the contrary, this project revealed little evidence for a role for BACE1 in energy homeostasis. Whilst previous studies have revealed little effect of dietary excess on BACE1 expression after 10-12 weeks of HF feeding, it is somewhat surprising that no significant changes were seen in the hypothalamic proteome with this length of dietary intervention (Meakin, Jalicy, et al., 2018). Reasons for this may include that this length of HFD is not sufficient to induce permanent changes in basal protein expression or that the study was underpowered with only n=3 per group. A fast-refeed model whereby animals are subjected to a shorter, 4-hour fast followed by a period of *ad libitum* food access may be more enlightening as to the hypothalamic metabolism in BACE1 tg and HF-fed conditions. Also surprising was the lack of BACE1 increase within key hypothalamic structures with ~1 year HFD as increased BACE1 expression with obesity has been well documented (Meakin et al., 2012; Meakin, Jalicy, et al., 2018). Whilst this may be a product of sectioning methods or unverified increased BACE1 expression with age masking the effects of HFD, further investigation comparing young and aged mice with chronic HFD intervention will be required to determine whether age is the cause of this unexpected result. However, effects of HFD on 4.1N expression were visible within both the cortex and hippocampus which increased 4.1N expression in the molecular layer of the cortex with dietary excess and increased expression within the SLM of CA1. Both suggest that, in mice, HFD drives 4.1N expression in the synapses of pyramidal neurons. Human samples indicate that this effect may be age-dependent as molecular layer expression of 4.1N decreased with obesity in

non-aged cases and also in all aged cases, irrespective of BMI or AD. It may therefore be hypothesised that in humans, both obesity and age lead to decreased cortical connectivity. Further imaging studies may reveal whether this decrease in 4.1N expression represents loss of synaptic density or reduced expression of 4.1N within the synapses. Furthermore, it appears that in aged cases, 4.1N expression within cell bodies is reduced with obesity, the implications of this change will require further exploration and may represent a change in splice variation in 4.1N or altered vesicular trafficking.

In vitro methods were also unsuccessful in identifying an association between BACE1 and metabolism. Proximity assay failed to identify proximity of BACE1 to metabolic regulators. However, it must be noted that this assay was conducted in hippocampal neurons which have not been studied for nutrient sensing capabilities. It is also possible that BACE1 association with metabolic proteins is the product of metabolic stress and conditions such as increased free-fatty acids or increased glucose may be required to initiate these interactions. Both of these conditions can be easily simulated *in vitro* and this study could also provide valuable information as to the effects of nutrient excess on BACE1 cellular localisation.

Finally, the leptin desensitisation effect of amyloid peptides seen *in vitro* could not be replicated in cell models. This may have been due to multiple factors such as the physiological relevance of the cell line used, serum composition and culture conditions such as high glucose and low FFA/lipoprotein content or the requirement of peripheral factors such as corticosteroid exposure to replicate *in vivo* results.

8.6 Final comments

This project provided preliminary data for studying a role of BACE1 in modulating cell connectivity; Not only in the maintenance of neuronal structure, but in hippocampal excitability and possible nutrient availability through neuron/astrocyte synapse and hemichannel formation respectively.

Experimentally, the next steps would need to identify a role for 4.1N in cognition and identify the mechanism of interaction between BACE1 and protein 4.1N. As previously mentioned; these studies provide support for the idea that BACE1 may directly associate with 4.1N but this has yet to be established. Fluorescent co-

staining of hippocampal sections would provide an indication of physiological co-localisation. Use of the humanised BACE1 KI could provide evidence that any co-localisation is translational to the human form of BACE1. Imaging analysis of human sections could too provide evidence for a direct interaction between these proteins and further staining in AD tissues would offer insight into whether the association changes in this dementia. Further evidence of 4.1N localisation changes in humans, with age, obesity and AD in the cortex would be insightful. In addition, the production of antibodies specific to domains such as the FERM and spectrin/actin binding domain or *in situ* hybridisation techniques could identify whether splice variation in these conditions are responsible for this change in 4.1N localisation. Use of the 4.1N null mouse line can provide information as to the cognitive benefits of 4.1N expression but as AD patients appear to exhibit increased 4.1N within the hippocampus, a brain or excitatory neuron-specific 4.1N overexpressing mouse would be more physiologically relevant in the context of AD. Live cell imaging and co-IP in cell lines could identify the relationship between these two proteins and use of the BioID proximity assay in further neuronal cell lines known to express protein 4.1N could be utilised. As the 4.1N construct has been created under a tetracycline-inducible promoter, through the generation of a compatible neuronal FRT cell line this assay could explore the effects of chronic exposure to known AD risk factors such as prolonged inflammation, amyloid exposure and increased fatty acids on the BACE1/4.1N relationship and sub-cellular localisation of 4.1N. Whilst these studies may be more easily conducted in cell lines *in vitro*, many of the outcomes are not representative of physiological conditions as neuronal cells lines often vary greatly in expression profile and are rarely representative of more than one type of cell, if any. Further human studies will also be essential in carrying this study forward as the expression profile of 4.1N varied in mouse compared to human. Therefore, whilst mouse models may be informative as to the mechanisms of protein interactions, the human translational relevance of expression in specific neurons and brain regions is limited. If indeed, 4.1N splice variation or BACE1 interaction proves to be an indicator of cognitive decline and AD progression, it may signify a novel drug target in the prevention of synaptic loss or loss of function with this dementia. NOVA1 has already been identified as a regulator of 4.1N splice variation and reduced expression of this protein has been identified in AD cortical tissue (Tollervey et al., 2011). the effects of

disrupting this association may prove valuable in developing preventative AD treatments and potentially, in treating the cognitive effects of obesity. Alternatively, if compensation occurs in 4.1N KO by increasing the expression of other 4.1 family members- 4.1N specific inhibition may be a plausible treatment; assuming that increased 4.1 family expression within the brain does not contribute towards the disease but maintains physiological function.

This project has also provided proof-of principle that the Bio-ID proximity assay for BACE1 works. Follow up studies in alternative cell lines (hypothalamic neurons, astrocytes, endothelial cells) will provide substantial information as to the role of BACE1 in different neurons and different cell types. Use of a tetracycline inducible promoter in the BACE1-BirA plasmid would also allow for expressional control and enable future studies to expose cells to chronic stresses such as inflammation, amyloid, high glucose and FFAs prior to BACE1-BirA expression. The effects of these stressors may then be studied through changes in BACE1 interactors and cell localisation. This technique may prove valuable in identifying changes in the early stages of AD onset- a period that the scientific community know little about- and possibly identify conditions required to induce BACE1/APP interaction.

The current cost of dementia on the UK economy is estimated £26bn and expected to double by 2040 (Lewis, Karlsberg Schaffer, Sussex, O'Neill, & Cockcroft, 2014; Prince et al., 2007). With increasing prevalence of obesity and metabolic disease- as contributors to AD risk- in developed and developing countries, the economic burden of dementia is becoming a global concern. One of the main barriers in our understanding of AD is the time delay between disease onset and the appearance of clinical symptoms-currently thought to represent decades of physiological changes that we know little about and therefore cannot design targeted treatments to inhibit disease progression. By better understanding the role that BACE1 plays in healthy physiology, we can begin to understand how this process may be disrupted in the early stages of AD and use this to develop targeted, preventative treatments.

Chapter 9

References

Abraham, W. C., Logan, B., Greenwood, J. M., & Dragunow, M. (2002). Induction and experience-dependent consolidation of stable long-term potentiation lasting months in the hippocampus. *The Journal of Neuroscience : The Official Journal of the Society for Neuroscience*, *22*(21), 9626–9634. Retrieved from http://www.ncbi.nlm.nih.gov/pubmed/12417688

Acsády, L., Kamondi, A., Sík, A., Freund, T., & Buzsáki, G. (1998). GABAergic cells are the major postsynaptic targets of mossy fibers in the rat hippocampus. *The Journal of Neuroscience : The Official Journal of the Society for Neuroscience*, *18*(9), 3386–3403. https://doi.org/10.1523/JNEUROSCI.18-09-03386.1998

Adeyemi, E., & Abdulle, A. (2000). A comparison of plasma leptin levels in obese and lean individuals in the United Arab Emirates. *Nutrition Research*, *20*(2), 157–166. https://doi.org/10.1016/S0271-5317(99)00149-9

Adriaanse, S. M., van Dijk, K. R. A., Ossenkoppele, R., Reuter, M., Tolboom, N., Zwan, M. D., … van Berckel, B. N. M. (2014). The effect of amyloid pathology and glucose metabolism on cortical volume loss over time in Alzheimer's disease. *European Journal of Nuclear Medicine and Molecular Imaging*, *41*(6), 1190–1198. https://doi.org/10.1007/s00259-014-2704-z

Ahima, R. S., Bjorbaek, C., Osei, S., & Flier, J. S. (1999). Regulation of Neuronal and Glial Proteins by Leptin: Implications for Brain Development [1]. *Endocrinology*, *140*(6), 2755–2762. https://doi.org/10.1210/endo.140.6.6774

Ahlemeyer, B., Halupczok, S., Rodenberg-Frank, E., Valerius, K.-P., & Baumgart-Vogt, E. (2018). Endogenous Murine Amyloid-β Peptide Assembles into Aggregates in the Aged C57BL/6J Mouse Suggesting These Animals as a Model to Study Pathogenesis of Amyloid-β Plaque Formation. *Journal of Alzheimer's Disease*, *61*(4), 1425–1450. https://doi.org/10.3233/JAD-170923

Ahmed, M., Davis, J., Aucoin, D., Sato, T., Ahuja, S., Aimoto, S., … Smith, S. O. (2010). Structural conversion of neurotoxic amyloid-β1–42 oligomers to fibrils. *Nature Structural & Molecular Biology*, *17*(5), 561–567. https://doi.org/10.1038/nsmb.1799

Ahmed, R. R., Holler, C. J., Webb, R. L., Li, F., Beckett, T. L., & Murphy, M. P. (2010). BACE1 and BACE2 enzymatic activities in Alzheimer's disease. *Journal of Neurochemistry*, *112*(4), 1045–1053. https://doi.org/10.1111/j.1471-4159.2009.06528.x

Ahrens, K., Mumford, S. L., Schliep, K. C., Kissell, K. A., Perkins, N. J., Wactawski-Wende, J., & Schisterman, E. F. (2014). Serum leptin levels and reproductive function during the menstrual cycle. *American Journal of Obstetrics and Gynecology*, *210*(3), 248.e1-9. https://doi.org/10.1016/j.ajog.2013.11.009

Akasaka-Manya, K., Manya, H., Sakurai, Y., Wojczyk, B. S., Kozutsumi, Y., Saito, Y., … Endo, T. (2010). Protective effect of N-glycan bisecting GlcNAc residues on -amyloid production in Alzheimer's disease. *Glycobiology*, *20*(1), 99–106. https://doi.org/10.1093/glycob/cwp152

Akasaka-Manya, Keiko, Manya, H., Sakurai, Y., Wojczyk, B. S., Spitalnik, S. L., & Endo, T. (2008). Increased bisecting and core-fucosylated N-glycans on mutant human amyloid precursor proteins. *Glycoconjugate Journal*, *25*(8), 775–786. https://doi.org/10.1007/s10719-008-9140-x

Alhurani, R. E., Vassilaki, M., Aakre, J. A., Mielke, M. M., Kremers, W. K., Machulda, M. M., … Roberts, R. O. (2016). Decline in Weight and Incident Mild Cognitive Impairment: Mayo Clinic Study of Aging. *JAMA Neurology*,

73(4), 439–446. https://doi.org/10.1001/jamaneurol.2015.4756

Allison, D. W., Gelfand, V. I., Spector, I., & Craig, A. M. (1998). Role of actin in anchoring postsynaptic receptors in cultured hippocampal neurons: differential attachment of NMDA versus AMPA receptors. *The Journal of Neuroscience : The Official Journal of the Society for Neuroscience*, *18*(7), 2423–2436. https://doi.org/10.1523/JNEUROSCI.18-07-02423.1998

Allison, M. B., Myers, M. G., & Jr. (2014). 20 years of leptin: connecting leptin signaling to biological function. *The Journal of Endocrinology*, *223*(1), T25-35. https://doi.org/10.1530/JOE-14-0404

Altman, J., & Das, G. D. (1965). Autoradiographic and histological evidence of postnatal hippocampal neurogenesis in rats. *The Journal of Comparative Neurology*, *124*(3), 319–335. https://doi.org/10.1002/cne.901240303

Amantea, D., Tassorelli, C., Russo, R., Petrelli, F., Morrone, L. A., Bagetta, G., & Corasaniti, M. T. (2011). Neuroprotection by leptin in a rat model of permanent cerebral ischemia: effects on STAT3 phosphorylation in discrete cells of the brain. *Cell Death & Disease*, *2*(12), e238–e238. https://doi.org/10.1038/cddis.2011.125

Amaral, D. G., Scharfman, H. E., & Lavenex, P. (2007). The dentate gyrus: fundamental neuroanatomical organization (dentate gyrus for dummies). *Progress in Brain Research*, *163*, 3–22. https://doi.org/10.1016/S0079-6123(07)63001-5

American Diabetes Association. (n.d.). Diabetes Complications. Retrieved April 29, 2019, from http://www.diabetes.org/living-with-diabetes/complications/

Amin, E., Jaiswal, M., Derewenda, U., Reis, K., Nouri, K., Koessmeier, K. T., … Ahmadian, M. R. (2016). Deciphering the Molecular and Functional Basis of RHOGAP Family Proteins: A SYSTEMATIC APPROACH TOWARD SELECTIVE INACTIVATION OF RHO FAMILY PROTEINS. *The Journal of Biological Chemistry*, *291*(39), 20353–20371. https://doi.org/10.1074/jbc.M116.736967

Amini-Bavil-Olyaee, S., Choi, Y. J., Lee, J. H., Shi, M., Huang, I.-C., Farzan, M., & Jung, J. U. (2013). The Antiviral Effector IFITM3 Disrupts Intracellular Cholesterol Homeostasis to Block Viral Entry. *Cell Host & Microbe*, *13*(4), 452–464. https://doi.org/10.1016/j.chom.2013.03.006

Andrew, R. J., Fernandez, C. G., Stanley, M., Jiang, H., Nguyen, P., Rice, R. C., … Thinakaran, G. (2017). Lack of BACE1 S-palmitoylation reduces amyloid burden and mitigates memory deficits in transgenic mouse models of Alzheimer's disease. *Proceedings of the National Academy of Sciences of the United States of America*, *114*(45), E9665–E9674. https://doi.org/10.1073/pnas.1708568114

Araki, T., Nawa, H., & Neel, B. G. (2003). Tyrosyl phosphorylation of Shp2 is required for normal ERK activation in response to some, but not all, growth factors. *The Journal of Biological Chemistry*, *278*(43), 41677–41684. https://doi.org/10.1074/jbc.M306461200

Araki, W. (2016). Post-translational regulation of the β-secretase BACE1. *Brain Research Bulletin*, *126*, 170–177. https://doi.org/10.1016/J.BRAINRESBULL.2016.04.009

ARUK. (2017). Dementia statistics hub: Deaths due to dementia. Retrieved March 17, 2019, from https://www.dementiastatistics.org/statistics/deaths-due-to-dementia/

ARUK. (2018). Types of dementia: Alzheimer's disease. Retrieved March 17, 2019, from https://www.alzheimersresearchuk.org/about-dementia/types-of-dementia/alzheimers-disease/about/

Atwal, J. K., Chen, Y., Chiu, C., Mortensen, D. L., Meilandt, W. J., Liu, Y., … Watts, R. J. (2011). A therapeutic antibody targeting BACE1 inhibits amyloid-β production in vivo. *Science Translational Medicine*, *3*(84), 84ra43. https://doi.org/10.1126/scitranslmed.3002254

Avrahami, L., Farfara, D., Shaham-Kol, M., Vassar, R., Frenkel, D., & Eldar-Finkelman, H. (2013). Inhibition of glycogen synthase kinase-3 ameliorates β-amyloid pathology and restores lysosomal acidification and mammalian target of rapamycin activity in the Alzheimer disease mouse model: in vivo and in vitro studies. *The Journal of Biological Chemistry*, *288*(2), 1295–1306. https://doi.org/10.1074/jbc.M112.409250

Ayyadevara, S., Balasubramaniam, M., Parcon, P. A., Barger, S. W., Griffin, W. S. T., Alla, R., … Shmookler Reis, R. J. (2016). Proteins that mediate protein aggregation and cytotoxicity distinguish Alzheimer's hippocampus from normal controls. *Aging Cell*, *15*(5), 924–939. https://doi.org/10.1111/acel.12501

Backer, J. M., Myers, M. G., Shoelson, S. E., Chin, D. J., Sun, X.-J., Miralpeix, M., … White, M. F. (1992). *Phosphatidylinositol 3'-kinase is activated by association with IRS-1 during insulin stimulation*. *The EMBO Journal* (Vol. 1). Retrieved from https://www.ncbi.nlm.nih.gov/pmc/articles/PMC556882/pdf/emboj00094-0312.pdf

Baines, A. J., Lu, H.-C., & Bennett, P. M. (2014). The Protein 4.1 family: Hub proteins in animals for organizing membrane proteins. *Biochimica et Biophysica Acta (BBA) - Biomembranes*, *1838*(2), 605–619. https://doi.org/10.1016/J.BBAMEM.2013.05.030

Baker, C. (2018). Obesity statistics. *House of Commons Library*, (3336). Retrieved from file:///Users/jen/Downloads/SN03336.pdf

Balazs, Z., Panzenboeck, U., Hammer, A., Sovic, A., Quehenberger, O., Malle, E., & Sattler, W. (2004). Uptake and transport of high-density lipoprotein (HDL) and HDL-associated alpha-tocopherol by an in vitro blood-brain barrier model. *Journal of Neurochemistry*, *89*(4), 939–950. https://doi.org/10.1111/j.1471-4159.2004.02373.x

Banerjee, S. L., Dionne, U., Lambert, J. P., & Bisson, N. (2018). Targeted proteomics analyses of phosphorylation-dependent signalling networks. *Journal of Proteomics*, *189*, 39–47. https://doi.org/10.1016/j.jprot.2018.02.004

Banerji, M. A., Faridi, N., Atluri, R., Chaiken, R. L., & Lebovitz, H. E. (1999). Body Composition, Visceral Fat, Leptin, and Insulin Resistance in Asian Indian Men. *The Journal of Clinical Endocrinology & Metabolism*, *84*(1), 137–144. https://doi.org/10.1210/jcem.84.1.5371

Banks, A. S., Davis, S. M., Bates, S. H., & Myers, M. G. (2000). Activation of downstream signals by the long form of the leptin receptor. *The Journal of Biological Chemistry*, *275*(19), 14563–14572. https://doi.org/10.1074/JBC.275.19.14563

Banyard, J., Barrows, C., & Zetter, B. R. (2009). Differential regulation of human thymosin beta 15 isoforms by transforming growth factor beta 1. *Genes, Chromosomes & Cancer*, *48*(6), 502–509. https://doi.org/10.1002/gcc.20659

Bao, J., Qin, M., Mahaman, Y. A. R., Zhang, B., Huang, F., Zeng, K., … Wang, X. (2018). BACE1 SUMOylation increases its stability and escalates the protease activity in Alzheimer's disease. *Proceedings of the National Academy of Sciences of the United States of America*, *115*(15), 3954–

3959. https://doi.org/10.1073/pnas.1800498115
Bao, L., Loda, M., Janmey, P. A., Stewart, R., Anand-Apte, B., & Zetter, B. R. (1996). Thymosin beta 15: a novel regulator of tumor cell motility upregulated in metastatic prostate cancer. *Nature Medicine*, *2*(12), 1322–1328. Retrieved from http://www.ncbi.nlm.nih.gov/pubmed/8946830
Barbash, S., Garfinkel, B. P., Maoz, R., Simchovitz, A., Nadorp, B., Guffanti, A., … Soreq, H. (2017). Alzheimer's brains show inter-related changes in RNA and lipid metabolism. *Neurobiology of Disease*, *106*, 1–13. https://doi.org/10.1016/j.nbd.2017.06.008
Barger, S. W., & Harmon, A. D. (1997). Microglial activation by Alzheimer amyloid precursor protein and modulation by apolipoprotein E. *Nature*, *388*(6645), 878–881. https://doi.org/10.1038/42257
Barnes, N. Y., Li, L., Yoshikawa, K., Schwartz, L. M., Oppenheim, R. W., & Milligan, C. E. (1998). Increased production of amyloid precursor protein provides a substrate for caspase-3 in dying motoneurons. *The Journal of Neuroscience : The Official Journal of the Society for Neuroscience*, *18*(15), 5869–5880. https://doi.org/10.1523/JNEUROSCI.18-15-05869.1998
Barron, A. M., Tokunaga, M., Zhang, M.-R., Ji, B., Suhara, T., & Higuchi, M. (2016). Assessment of neuroinflammation in a mouse model of obesity and β-amyloidosis using PET. *Journal of Neuroinflammation*, *13*(1), 221. https://doi.org/10.1186/s12974-016-0700-x
Bartuzi, P., Billadeau, D. D., Favier, R., Rong, S., Dekker, D., Fedoseienko, A., … van de Sluis, B. (2016). CCC- and WASH-mediated endosomal sorting of LDLR is required for normal clearance of circulating LDL. *Nature Communications*, *7*(1), 10961. https://doi.org/10.1038/ncomms10961
Bateman, R. J., Xiong, C., Benzinger, T. L. S., Fagan, A. M., Goate, A., Fox, N. C., … Morris, J. C. (2012). Clinical and Biomarker Changes in Dominantly Inherited Alzheimer's Disease. *New England Journal of Medicine*, *367*(9), 795–804. https://doi.org/10.1056/NEJMoa1202753
Baumann, H., Morella, K. K., White, D. W., Dembski, M., Bailon, P. S., Kim, H., … Tartaglia, L. A. (1996). The full-length leptin receptor has signaling capabilities of interleukin 6-type cytokine receptors. *Proceedings of the National Academy of Sciences of the United States of America*, *93*(16), 8374–8378. https://doi.org/10.1073/PNAS.93.16.8374
Beall, C., Hamilton, D. L., Gallagher, J., Logie, L., Wright, K., Soutar, M. P., … Ashford, M. L. J. (2012). Mouse hypothalamic GT1-7 cells demonstrate AMPK-dependent intrinsic glucose-sensing behaviour. *Diabetologia*, *55*(9), 2432–2444. https://doi.org/10.1007/s00125-012-2617-y
Beckett, L. A., Donohue, M. C., Wang, C., Aisen, P., Harvey, D. J., Saito, N., & Alzheimer's Disease Neuroimaging Initiative. (2015). The Alzheimer's Disease Neuroimaging Initiative phase 2: Increasing the length, breadth, and depth of our understanding. *Alzheimer's & Dementia*, *11*(7), 823–831. https://doi.org/10.1016/j.jalz.2015.05.004
Bednarek-Tupikowska, G., Filus, A., Kuliczkowska-Płaksej, J., Tupikowski, K., Bohdanowicz-Pawlak, A., & Milewicz, A. (2006). Serum leptin concentrations in pre- and postmenopausal women on sex hormone therapy. *Gynecological Endocrinology*, *22*(4), 207–212. https://doi.org/10.1080/09513590600702774
Ben Halima, S., Mishra, S., Raja, K. M. P., Willem, M., Baici, A., Simons, K., … Rajendran, L. (2016). Specific Inhibition of β-Secretase Processing of the Alzheimer Disease Amyloid Precursor Protein. *Cell Reports*, *14*(9), 2127–2141. https://doi.org/10.1016/j.celrep.2016.01.076

Benjannet, S., Elagoz, A., Wickham, L., Mamarbachi, M., Munzer, J. S., Basak, A., … Seidah, N. G. (2001). Post-translational processing of beta-secretase (beta-amyloid-converting enzyme) and its ectodomain shedding. The pro- and transmembrane/cytosolic domains affect its cellular activity and amyloid-beta production. *The Journal of Biological Chemistry*, *276*(14), 10879–10887. https://doi.org/10.1074/jbc.M009899200

Bennett, A. M., Hausdorff, S. F., O'reilly, A. M., Freeman, R. M., & Neel, B. G. (1996). *Multiple Requirements for SHPTP2 in Epidermal Growth Factor-Mediated Cell Cycle Progression*. *MOLECULAR AND CELLULAR BIOLOGY* (Vol. 16). Retrieved from http://mcb.asm.org/

Bennett, B. D., Denis, P., Haniu, M., Teplow, D. B., Kahn, S., Louis, J. C., … Vassar, R. (2000). A furin-like convertase mediates propeptide cleavage of BACE, the Alzheimer's beta -secretase. *The Journal of Biological Chemistry*, *275*(48), 37712–37717. https://doi.org/10.1074/jbc.M005339200

Bernatchez, P. N., Acevedo, L., Fernandez-Hernando, C., Murata, T., Chalouni, C., Kim, J., … Sessa, W. C. (2007). Myoferlin regulates vascular endothelial growth factor receptor-2 stability and function. *The Journal of Biological Chemistry*, *282*(42), 30745–30753. https://doi.org/10.1074/jbc.M704798200

Bernatchez, P. N., Sharma, A., Kodaman, P., & Sessa, W. C. (2009). Myoferlin is critical for endocytosis in endothelial cells. *American Journal of Physiology. Cell Physiology*, *297*(3), C484-92. https://doi.org/10.1152/ajpcell.00498.2008

Berridge, M. J., Lipp, P., & Bootman, M. D. (2000). The versatility and universality of calcium signalling. *Nature Reviews Molecular Cell Biology*, *1*(1), 11–21. https://doi.org/10.1038/35036035

Berrocal, M., Marcos, D., Sepúlveda, M. R., Pérez, M., Ávila, J., & Mata, A. M. (2009). Altered Ca^{2+} dependence of synaptosomal plasma membrane Ca^{2+} -ATPase in human brain affected by Alzheimer's disease. *The FASEB Journal*, *23*(6), 1826–1834. https://doi.org/10.1096/fj.08-121459

Bertens, D., Tijms, B. M., Scheltens, P., Teunissen, C. E., & Visser, P. J. (2017). Unbiased estimates of cerebrospinal fluid β-amyloid 1–42 cutoffs in a large memory clinic population. *Alzheimer's Research & Therapy*, *9*(1), 8. https://doi.org/10.1186/s13195-016-0233-7

Biederer, T., & Südhof, T. C. (2001). CASK and Protein 4.1 Support F-actin Nucleation on Neurexins. *Journal of Biological Chemistry*, *276*(51), 47869–47876. https://doi.org/10.1074/JBC.M105287200

Binda, A. V, Kabbani, N., Lin, R., & Levenson, R. (2002). D2 and D3 dopamine receptor cell surface localization mediated by interaction with protein 4.1N. *Molecular Pharmacology*, *62*(3), 507–513. Retrieved from http://www.ncbi.nlm.nih.gov/pubmed/12181426

Bitan, G., Kirkitadze, M. D., Lomakin, A., Vollers, S. S., Benedek, G. B., & Teplow, D. B. (2003). Amyloid beta -protein (Abeta) assembly: Abeta 40 and Abeta 42 oligomerize through distinct pathways. *Proceedings of the National Academy of Sciences of the United States of America*, *100*(1), 330–335. https://doi.org/10.1073/pnas.222681699

Bjørbaek, C., El-Haschimi, K., Frantz, J. D., & Flier, J. S. (1999). The role of SOCS-3 in leptin signaling and leptin resistance. *The Journal of Biological Chemistry*, *274*(42), 30059–30065. https://doi.org/10.1074/JBC.274.42.30059

Bjorbak, C., Lavery, H. J., Bates, S. H., Olson, R. K., Davis, S. M., Flier, J. S., & Myers, M. G. (2000). SOCS3 mediates feedback inhibition of the leptin

receptor via Tyr985. *The Journal of Biological Chemistry*, *275*(51), 40649–40657. https://doi.org/10.1074/jbc.M007577200

Blalock, E. M., Geddes, J. W., Chen, K. C., Porter, N. M., Markesbery, W. R., & Landfield, P. W. (2004). Incipient Alzheimer's disease: microarray correlation analyses reveal major transcriptional and tumor suppressor responses. *Proceedings of the National Academy of Sciences of the United States of America*, *101*(7), 2173–2178. https://doi.org/10.1073/pnas.0308512100

Bliss, T. V. P., & Lømo, T. (1973). Long-lasting potentiation of synaptic transmission in the dentate area of the anaesthetized rabbit following stimulation of the perforant path. *The Journal of Physiology*, *232*(2), 331–356. https://doi.org/10.1113/jphysiol.1973.sp010273

Blouet, C., & Schwartz, G. J. (2012). Brainstem nutrient sensing in the nucleus of the solitary tract inhibits feeding. *Cell Metabolism*, *16*(5), 579–587. https://doi.org/10.1016/j.cmet.2012.10.003

Bocarsly, M. E., Fasolino, M., Kane, G. A., LaMarca, E. A., Kirschen, G. W., Karatsoreos, I. N., … Gould, E. (2015). Obesity diminishes synaptic markers, alters microglial morphology, and impairs cognitive function. *Proceedings of the National Academy of Sciences of the United States of America*, *112*(51), 15731–15736. https://doi.org/10.1073/pnas.1511593112

Bodaleo, F. J., Montenegro-Venegas, C., Henríquez, D. R., Court, F. A., & Gonzalez-Billault, C. (2016). Microtubule-associated protein 1B (MAP1B)-deficient neurons show structural presynaptic deficiencies in vitro and altered presynaptic physiology. *Scientific Reports*, *6*, 30069. https://doi.org/10.1038/srep30069

Bodendorf, U., Fischer, F., Bodian, D., Multhaup, G., & Paganetti, P. (2001). A Splice Variant of β-Secretase Deficient in the Amyloidogenic Processing of the Amyloid Precursor Protein. *Journal of Biological Chemistry*, *276*(15), 12019–12023. https://doi.org/10.1074/jbc.M008861200

Bolis, A., Coviello, S., Visigalli, I., Taveggia, C., Bachi, A., Chishti, A. H., … Bolino, A. (2009). Dlg1, Sec8, and Mtmr2 regulate membrane homeostasis in Schwann cell myelination. *The Journal of Neuroscience : The Official Journal of the Society for Neuroscience*, *29*(27), 8858–8870. https://doi.org/10.1523/JNEUROSCI.1423-09.2009

Bollimuntha, S., Pani, B., & Singh, B. B. (2017). Neurological and Motor Disorders: Neuronal Store-Operated Ca2+ Signaling: An Overview and Its Function. *Advances in Experimental Medicine and Biology*, *993*, 535–556. https://doi.org/10.1007/978-3-319-57732-6_27

Bonda, D. J., Stone, J. G., Torres, S. L., Siedlak, S. L., Perry, G., Kryscio, R., … Lee, H. (2014). Dysregulation of leptin signaling in Alzheimer disease: evidence for neuronal leptin resistance. *Journal of Neurochemistry*, *128*(1), 162–172. https://doi.org/10.1111/jnc.12380

Borg, M. L., Omran, S. F., Weir, J., Meikle, P. J., & Watt, M. J. (2012). Consumption of a high-fat diet, but not regular endurance exercise training, regulates hypothalamic lipid accumulation in mice. *The Journal of Physiology*, *590*(17), 4377–4389. https://doi.org/10.1113/jphysiol.2012.233288

Borst, S. E., & Conover, C. F. (2005). High-fat diet induces increased tissue expression of TNF-alpha. *Life Sciences*, *77*(17), 2156–2165. https://doi.org/10.1016/j.lfs.2005.03.021

Bossinger, O., Klebes, A., Segbert, C., Theres, C., & Knust, E. (2001). Zonula Adherens Formation in Caenorhabditis elegans Requires dlg-1, the

Homologue of the Drosophila Gene discs large. *Developmental Biology*, *230*(1), 29–42. https://doi.org/10.1006/dbio.2000.0113

Boundy, V. A., & Cincotta, A. H. (2000). Hypothalamic adrenergic receptor changes in the metabolic syndrome of genetically obese (ob / ob) mice. *American Journal of Physiology-Regulatory, Integrative and Comparative Physiology*, *279*(2), R505–R514. https://doi.org/10.1152/ajpregu.2000.279.2.R505

Braak, H., & Braak, E. (1995). Staging of alzheimer's disease-related neurofibrillary changes. *Neurobiology of Aging*, *16*(3), 271–278. https://doi.org/10.1016/0197-4580(95)00021-6

Bradford, M. M. (1976). A rapid and sensitive method for the quantitation of microgram quantities of protein utilizing the principle of protein-dye binding. *Analytical Biochemistry*, *72*(1–2), 248–254. https://doi.org/10.1016/0003-2697(76)90527-3

Brothers, H. M., Gosztyla, M. L., & Robinson, S. R. (2018). The Physiological Roles of Amyloid-β Peptide Hint at New Ways to Treat Alzheimer's Disease. *Frontiers in Aging Neuroscience*, *10*, 118. https://doi.org/10.3389/fnagi.2018.00118

Brureau, A., Zussy, C., Delair, B., Ogier, C., Ixart, G., Maurice, T., & Givalois, L. (2013). Deregulation of hypothalamic-pituitary-adrenal axis functions in an Alzheimer's disease rat model. *Neurobiology of Aging*, *34*(5), 1426–1439. https://doi.org/10.1016/J.NEUROBIOLAGING.2012.11.015

Burguera, B., Couce, M. E., Long, J., Lamsam, J., Laakso, K., Jensen, M. D., … Lloyd, R. V. (2000). The Long Form of the Leptin Receptor (OB-Rb) Is Widely Expressed in the Human Brain. *Neuroendocrinology*, *71*(3), 187–195. https://doi.org/10.1159/000054536

Cakir, I., Cyr, N. E., Perello, M., Litvinov, B. P., Romero, A., Stuart, R. C., & Nillni, E. A. (2013). Obesity induces hypothalamic endoplasmic reticulum stress and impairs proopiomelanocortin (POMC) post-translational processing. *The Journal of Biological Chemistry*, *288*(24), 17675–17688. https://doi.org/10.1074/jbc.M113.475343

Callen, D. J. A., Black, S. E., Gao, F., Caldwell, C. B., & Szalai, J. P. (2001). Beyond the hippocampus: MRI volumetry confirms widespread limbic atrophy in AD. *Neurology*, *57*(9), 1669–1674. https://doi.org/10.1212/WNL.57.9.1669

Cancello, R., Zingaretti, M. C., Sarzani, R., Ricquier, D., & Cinti, S. (1998). Leptin and UCP1 Genes are Reciprocally Regulated in Brown Adipose Tissue. *Endocrinology*, *139*(11), 4747–4747. https://doi.org/10.1210/endo.139.11.6434

Cao, D., Fan, S. T., & Chung, S. S. (1998). Identification and characterization of a novel human aldose reductase-like gene. *The Journal of Biological Chemistry*, *273*(19), 11429–11435. https://doi.org/10.1074/JBC.273.19.11429

Capell, A., Steiner, H., Willem, M., Kaiser, H., Meyer, C., Walter, J., … Haass, C. (2000). Maturation and pro-peptide cleavage of beta-secretase. *The Journal of Biological Chemistry*, *275*(40), 30849–30854. https://doi.org/10.1074/jbc.M003202200

Caporaso, G. L., Takei, K., Gandy, S. E., Matteoli, M., Mundigl, O., Greengard, P., & De Camilli, P. (1994). Morphologic and biochemical analysis of the intracellular trafficking of the Alzheimer beta/A4 amyloid precursor protein. *The Journal of Neuroscience : The Official Journal of the Society for Neuroscience*, *14*(5 Pt 2), 3122–3138. Retrieved from

http://www.ncbi.nlm.nih.gov/pubmed/8182461

Carbonell, F., Zijdenbos, A. P., McLaren, D. G., Iturria-Medina, Y., Bedell, B. J., & Alzheimer's Disease Neuroimaging Initiative, for the A. D. N. (2016). Modulation of glucose metabolism and metabolic connectivity by β-amyloid. *Journal of Cerebral Blood Flow and Metabolism : Official Journal of the International Society of Cerebral Blood Flow and Metabolism*, *36*(12), 2058–2071. https://doi.org/10.1177/0271678X16654492

Caro, J. F., Kolaczynski, J. W., Nyce, M. R., Ohannesian, J. P., Opentanova, I., Goldman, W. H., … Considine, R. V. (1996). Decreased cerebrospinal-fluid/serum leptin ratio in obesity: a possible mechanism for leptin resistance. *Lancet (London, England)*, *348*(9021), 159–161. https://doi.org/10.1016/S0140-6736(96)03173-X

Carpenter, L. R., Farruggella, T. J., Symes, A., Karow, M. L., Yancopoulos, G. D., & Stahl, N. (1998). Enhancing leptin response by preventing SH2-containing phosphatase 2 interaction with Ob receptor. *Proceedings of the National Academy of Sciences of the United States of America*, *95*(11), 6061–6066. https://doi.org/10.1073/PNAS.95.11.6061

Cawley, N. X., Li, Z., & Loh, Y. P. (2016). 60 YEARS OF POMC: Biosynthesis, trafficking, and secretion of pro-opiomelanocortin-derived peptides, 77–97.

Chadwick, W., Brenneman, R., Martin, B., & Maudsley, S. (2010). Complex and multidimensional lipid raft alterations in a murine model of Alzheimer's disease. *International Journal of Alzheimer's Disease*, *2010*, 604792. https://doi.org/10.4061/2010/604792

Chai, Y. L., Chong, J. R., Weng, J., Howlett, D., Halsey, A., Lee, J. H., … Lai, M. K. P. (2019). Lysosomal cathepsin D is upregulated in Alzheimer's disease neocortex and may be a marker for neurofibrillary degeneration. *Brain Pathology*, *29*(1), 63–74. https://doi.org/10.1111/bpa.12631

Chambers, J. K., Tokuda, T., Uchida, K., Ishii, R., Tatebe, H., Takahashi, E., … Nakayama, H. (2015). The domestic cat as a natural animal model of Alzheimer's disease. *Acta Neuropathologica Communications*, *3*(1), 78. https://doi.org/10.1186/s40478-015-0258-3

Champy, M., Selloum, M., Piard, L., Zeitler, V., Caradec, C., Chambon, P., & Auwerx, J. (2004). Mouse functional genomics requires standardization of mouse handling and housing conditions. *Mammalian Genome*, *15*(10), 768–783. https://doi.org/10.1007/s00335-004-2393-1

Charlwood, J., Dingwall, C., Matico, R., Hussain, I., Johanson, K., Moore, S., … Camilleri, P. (2001). Characterization of the glycosylation profiles of Alzheimer's beta -secretase protein Asp-2 expressed in a variety of cell lines. *The Journal of Biological Chemistry*, *276*(20), 16739–16748. https://doi.org/10.1074/jbc.M009361200

Chasseigneaux, S., Dinc, L., Rose, C., Chabret, C., Coulpier, F., Topilko, P., … Allinquant, B. (2011). Secreted Amyloid Precursor Protein β and Secreted Amyloid Precursor Protein α Induce Axon Outgrowth In Vitro through Egr1 Signaling Pathway. *PLoS ONE*, *6*(1), e16301. https://doi.org/10.1371/journal.pone.0016301

Chehab, F. F., Lim, M. E., & Lu, R. (1996). Correction of the sterility defect in homozygous obese female mice by treatment with the human recombinant leptin. *Nature Genetics*, *12*(3), 318–320. https://doi.org/10.1038/ng0396-318

Chen, C.-H., Zhou, W., Liu, S., Deng, Y., Cai, F., Tone, M., … Song, W. (2012). Increased NF-κB signalling up-regulates BACE1 expression and its therapeutic potential in Alzheimer's disease. *The International Journal of*

Neuropsychopharmacology, *15*(01), 77–90. https://doi.org/10.1017/S1461145711000149

Chen, C., Gu, J., Basurto-Islas, G., Jin, N., Wu, F., Gong, C.-X., … Liu, F. (2017). Up-regulation of casein kinase 1ε is involved in tau pathogenesis in Alzheimer's disease. *Scientific Reports*, *7*(1), 13478. https://doi.org/10.1038/s41598-017-13791-5

Chen, K., & Dou, F. (2012). Selective Interaction of Amyloid Precursor Protein with Different Isoforms of Neural Cell Adhesion Molecule. *Journal of Molecular Neuroscience*, *46*(1), 203–209. https://doi.org/10.1007/s12031-011-9578-3

Chen, L. L., Lin, L. H., Green, E. J., Barnes, C. A., & McNaughton, B. L. (1994). Head-direction cells in the rat posterior cortex. *Experimental Brain Research*, *101*(1), 8–23. https://doi.org/10.1007/BF00243212

Chen, Y.-R., & Glabe, C. G. (2006). Distinct early folding and aggregation properties of Alzheimer amyloid-beta peptides Abeta40 and Abeta42: stable trimer or tetramer formation by Abeta42. *The Journal of Biological Chemistry*, *281*(34), 24414–24422. https://doi.org/10.1074/jbc.M602363200

Chen, Y., Peng, Y., Che, P., Gannon, M., Liu, Y., Li, L., … Wang, Q. (2014). α2A adrenergic receptor promotes amyloidogenesis through disrupting APP-SorLA interaction. *Proceedings of the National Academy of Sciences of the United States of America*, *111*(48), 17296. https://doi.org/10.1073/PNAS.1409513111

Cheng, T.-C., Tu, S.-H., Chen, L.-C., Chen, M.-Y., Chen, W.-Y., Lin, Y.-K., … Ho, Y.-S. (2015). Down-regulation of α-L-fucosidase 1 expression confers inferior survival for triple-negative breast cancer patients by modulating the glycosylation status of the tumor cell surface. *Oncotarget*, *6*(25), 21283–21300. https://doi.org/10.18632/oncotarget.4238

Chiaruttini, G., Piperno, G. M., Jouve, M., Valitutti, S., Galli, T., & Benvenuti, F. (2016). The SNARE VAMP7 Regulates Exocytic Trafficking of Interleukin-12 in Dendritic Cells. *CellReports*, *14*, 2624–2636. https://doi.org/10.1016/j.celrep.2016.02.055

Cho, E., & Park, M. (2016). Palmitoylation in Alzheimer's disease and other neurodegenerative diseases. *Pharmacological Research*, *111*, 133–151. https://doi.org/10.1016/j.phrs.2016.06.008

Choi-Rhee, E., Schulman, H., & Cronan, J. E. (2008). Promiscuous protein biotinylation by Escherichia coli biotin protein ligase. *Protein Science*, *13*(11), 3043–3050. https://doi.org/10.1110/ps.04911804

Chouraki, V., Lee, S. J. van der, Grenier-Boley, B., Simino, J., Adams, H., Tosto, G., … Duijn, C. van. (2017). Genome-wide Association Study Links APOEє4 and BACE1 Variants with Plasma Amyloid β Levels. *BioRxiv*, 194266. https://doi.org/10.1101/194266

Cina, C., Maass, K., Theis, M., Willecke, K., Bechberger, J. F., & Naus, C. C. (2009). Involvement of the cytoplasmic C-terminal domain of connexin43 in neuronal migration. *The Journal of Neuroscience : The Official Journal of the Society for Neuroscience*, *29*(7), 2009–2021. https://doi.org/10.1523/JNEUROSCI.5025-08.2009

Cizas, P., Budvytyte, R., Morkuniene, R., Moldovan, R., Broccio, M., Lösche, M., … Borutaite, V. (2010). Size-dependent neurotoxicity of beta-amyloid oligomers. *Archives of Biochemistry and Biophysics*, *496*(2), 84–92. https://doi.org/10.1016/j.abb.2010.02.001

Claiborne, B. J., Amaral, D. G., & Cowan, W. M. (1986). A light and electron microscopic analysis of the mossy fibers of the rat dentate gyrus. *The*

Journal of Comparative Neurology, *246*(4), 435–458. https://doi.org/10.1002/cne.902460403

Clarimon, J., Bertranpetit, J., Calafell, F., Boada, M., Tarraga, L., & Comas, D. (2003). Association study between Alzheimer?s disease and genes involved in A? biosynthesis, aggregation and degradation: suggestive results with BACE1. *Journal of Neurology*, *250*(8), 956–961. https://doi.org/10.1007/s00415-003-1127-8

Clarke, J. R., Lyra E Silva, N. M., Figueiredo, C. P., Frozza, R. L., Ledo, J. H., Beckman, D., … De Felice, F. G. (2015). Alzheimer-associated Aβ oligomers impact the central nervous system to induce peripheral metabolic deregulation. *EMBO Molecular Medicine*, *7*(2), 190–210. https://doi.org/10.15252/emmm.201404183

Cleary, J. P., Walsh, D. M., Hofmeister, J. J., Shankar, G. M., Kuskowski, M. A., Selkoe, D. J., & Ashe, K. H. (2005). Natural oligomers of the amyloid-β protein specifically disrupt cognitive function. *Nature Neuroscience*, *8*(1), 79–84. https://doi.org/10.1038/nn1372

Clodfelder-Miller, B., De Sarno, P., Zmijewska, A. A., Song, L., & Jope, R. S. (2005). Physiological and Pathological Changes in Glucose Regulate Brain Akt and Glycogen Synthase Kinase-3. *Journal of Biological Chemistry*, *280*(48), 39723–39731. https://doi.org/10.1074/jbc.M508824200

Cohen, A. R., Wood, D. F., Marfatia, S. M., Walther, Z., Chishti, A. H., & Anderson, J. M. (1998). Human CASK/LIN-2 Binds Syndecan-2 and Protein 4.1 and Localizes to the Basolateral Membrane of Epithelial Cells. *The Journal of Cell Biology*, *142*(1), 129–138. https://doi.org/10.1083/JCB.142.1.129

Coimbra, J. R. M., Marques, D. F. F., Baptista, S. J., Pereira, C. M. F., Moreira, P. I., Dinis, T. C. P., … Salvador, J. A. R. (2018). Highlights in BACE1 Inhibitors for Alzheimer's Disease Treatment. *Frontiers in Chemistry*, *6*, 178. https://doi.org/10.3389/fchem.2018.00178

Coleman, S. K., Cai, C., Mottershead, D. G., Haapalahti, J.-P., & Keinänen, K. (2003). Surface expression of GluR-D AMPA receptor is dependent on an interaction between its C-terminal domain and a 4.1 protein. *The Journal of Neuroscience : The Official Journal of the Society for Neuroscience*, *23*(3), 798–806. https://doi.org/10.1523/JNEUROSCI.23-03-00798.2003

Commins, S. P., Watson, P. M., Levin, N., Beiler, R. J., & Gettys, T. W. (2000). Central leptin regulates the UCP1 and ob genes in brown and white adipose tissue via different beta-adrenoceptor subtypes. *The Journal of Biological Chemistry*, *275*(42), 33059–33067. https://doi.org/10.1074/jbc.M006328200

Corbett, N. J., Gabbott, P. L., Klementiev, B., Davies, H. A., Colyer, F. M., Novikova, T., & Stewart, M. G. (2013). Amyloid-Beta Induced CA1 Pyramidal Cell Loss in Young Adult Rats Is Alleviated by Systemic Treatment with FGL, a Neural Cell Adhesion Molecule-Derived Mimetic Peptide. *PLoS ONE*, *8*(8), e71479. https://doi.org/10.1371/journal.pone.0071479

Costantini, C., Ko, M. H., Jonas, M. C., & Puglielli, L. (2007). A reversible form of lysine acetylation in the ER and Golgi lumen controls the molecular stabilization of BACE1. *The Biochemical Journal*, *407*(3), 383–395. https://doi.org/10.1042/BJ20070040

Cova, I., Clerici, F., Rossi, A., Cucumo, V., Ghiretti, R., Maggiore, L., … Caracciolo, B. (2016). Weight Loss Predicts Progression of Mild Cognitive Impairment to Alzheimer's Disease. *PloS One*, *11*(3), e0151710.

https://doi.org/10.1371/journal.pone.0151710
Cronan, J. E. (2005). Targeted and proximity-dependent promiscuous protein biotinylation by a mutant Escherichia coli biotin protein ligase. *The Journal of Nutritional Biochemistry*, *16*(7), 416–418. https://doi.org/10.1016/j.jnutbio.2005.03.017
Cronin-Stubbs, D., Beckett, L. A., Scherr, P. A., Field, T. S., Chown, M. J., Pilgrim, D. M., … Evans, D. A. (1997). Weight loss in people with Alzheimer's disease: a prospective population based analysis. *BMJ (Clinical Research Ed.)*, *314*(7075), 178–179. https://doi.org/10.1136/bmj.314.7075.178
Csernansky, J. G., Dong, H., Fagan, A. M., Wang, L., Xiong, C., Holtzman, D. M., & Morris, J. C. (2006). Plasma Cortisol and Progression of Dementia in Subjects With Alzheimer-Type Dementia. *American Journal of Psychiatry*, *163*(12), 2164–2169. https://doi.org/10.1176/ajp.2006.163.12.2164
D'Orlando, C., Guzzi, F., Gravati, M., Biella, G., Toselli, M., Meneveri, R., … Parenti, M. (2008). Retinoic acid- and phorbol ester-induced neuronal differentiation down-regulates caveolin expression in GnRH neurons. *Journal of Neurochemistry*, *104*(6), 1577–1587. https://doi.org/10.1111/j.1471-4159.2007.05109.x
DaRocha-Souto, B., Coma, M., Pérez-Nievas, B. G., Scotton, T. C., Siao, M., Sánchez-Ferrer, P., … Gómez-Isla, T. (2012). Activation of glycogen synthase kinase-3 beta mediates β-amyloid induced neuritic damage in Alzheimer's disease. *Neurobiology of Disease*, *45*(1), 425–437. https://doi.org/10.1016/J.NBD.2011.09.002
Dasgupta, S., Salman, M., Siddalingaiah, L. B., Lakshmi, G. L., Xaviour, D., & Sreenath, J. (2015). Genetic variants in leptin: Determinants of obesity and leptin levels in south Indian population. *Adipocyte*, *4*(2), 135–140. https://doi.org/10.4161/21623945.2014.975538
Davies, D. C., Horwood, N., Isaacs, S. L., & Mann, D. M. A. (1992). The effect of age and Alzheimer's disease on pyramidal neuron density in the individual fields of the hippocampal formation. *Acta Neuropathologica*, *83*(5), 510–517. https://doi.org/10.1007/BF00310028
De Felice, F. G., & Ferreira, S. T. (2014). Inflammation, defective insulin signaling, and mitochondrial dysfunction as common molecular denominators connecting type 2 diabetes to Alzheimer disease. *Diabetes*, *63*(7), 2262–2272. https://doi.org/10.2337/db13-1954
De Pietri Tonelli, D., Mihailovich, M., Di Cesare, A., Codazzi, F., Grohovaz, F., & Zacchetti, D. (2004). Translational regulation of BACE-1 expression in neuronal and non-neuronal cells. *Nucleic Acids Research*, *32*(5), 1808–1817. https://doi.org/10.1093/nar/gkh348
Deng, X., Zhang, J., Liu, Y., Chen, L., & Yu, C. (2017). TNF-α regulates the proteolytic degradation of ST6Gal-1 and endothelial cell-cell junctions through upregulating expression of BACE1. *Scientific Reports*, *7*(1), 40256. https://doi.org/10.1038/srep40256
Di Paolo, G., & Kim, T.-W. (2011). Linking lipids to Alzheimer's disease: cholesterol and beyond. *Nature Reviews. Neuroscience*, *12*(5), 284–296. https://doi.org/10.1038/nrn3012
Dinely, K.T. Jahrling, J.B. Denner, L. (2014). Insulin resistance in Alzheimer's disease. *Neurobiology of Disease*, *72*, 92–103.
Discher, D. E., Winardi, R., Schischmanoff, P. O., Parra, M., Conboy, J. G., & Mohandas, N. (1995). *Mechanochemistry of Protein 4.1's Spectrin-Actin-Binding Domain: Ternary Complex Interactions, Membrane Binding,*

Network Integration, Structural Strengthening. Retrieved from http://images.biomedsearch.com/7642705/jc1304897.pdf?AWSAccessKeyId=AKIAIBOKHYOLP4MBMRGQ&Expires=1544227200&Signature=WI3j0IvNKUXCHRc4kqEWVgfXKf0%3D

Dislich, B., Wohlrab, F., Bachhuber, T., Müller, S. A., Kuhn, P.-H., Hogl, S., … Lichtenthaler, S. F. (2015). Label-free Quantitative Proteomics of Mouse Cerebrospinal Fluid Detects β-Site APP Cleaving Enzyme (BACE1) Protease Substrates In Vivo. *Molecular & Cellular Proteomics : MCP*, *14*(10), 2550–2563. https://doi.org/10.1074/mcp.M114.041533

Dominguez, D., Tournoy, J., Hartmann, D., Huth, T., Cryns, K., Deforce, S., … De Strooper, B. (2005). Phenotypic and biochemical analyses of BACE1- and BACE2-deficient mice. *The Journal of Biological Chemistry*, *280*(35), 30797–30806. https://doi.org/10.1074/jbc.M505249200

Dorey, A., Perret-Liaudet, A., Tholance, Y., Fourier, A., & Quadrio, I. (2015). Cerebrospinal Fluid Aβ40 Improves the Interpretation of Aβ42 Concentration for Diagnosing Alzheimer's Disease. *Frontiers in Neurology*, *6*, 247. https://doi.org/10.3389/fneur.2015.00247

Duffy, K. R., & Pardridge, W. M. (1987). Blood-brain barrier transcytosis of insulin in developing rabbits. *Brain Research*, *420*(1), 32–38. Retrieved from http://www.ncbi.nlm.nih.gov/pubmed/3315116

Dunsing, V., Mayer, M., Liebsch, F., Multhaup, G., & Chiantia, S. (2017). Direct evidence of amyloid precursor-like protein 1 trans interactions in cell-cell adhesion platforms investigated via fluorescence fluctuation spectroscopy. *Molecular Biology of the Cell*, *28*(25), 3609–3620. https://doi.org/10.1091/mbc.E17-07-0459

Duval, N., Gomès, D., Calaora, V., Calabrese, A., Meda, P., & Bruzzone, R. (2002). Cell coupling and Cx43 expression in embryonic mouse neural progenitor cells. *Journal of Cell Science*, *115*(Pt 16), 3241–3251. Retrieved from http://www.ncbi.nlm.nih.gov/pubmed/12140256

Eggert, S., Gonzalez, A. C., Thomas, C., Schilling, S., Schwarz, S. M., Tischer, C., … Kins, S. (2018). Dimerization leads to changes in APP (amyloid precursor protein) trafficking mediated by LRP1 and SorLA. *Cellular and Molecular Life Sciences*, *75*(2), 301–322. https://doi.org/10.1007/s00018-017-2625-7

Ehehalt, R., Keller, P., Haass, C., Thiele, C., & Simons, K. (2003). Amyloidogenic processing of the Alzheimer-amyloid precursor protein depends on lipid rafts. *The Journal of Cell Biology*, *160*(1), 113–123. https://doi.org/10.1083/jcb.200207113

Ehehalt, R., Michel, B., De Pietri Tonelli, D., Zacchetti, D., Simons, K., & Keller, P. (2002). Splice variants of the β-site APP-cleaving enzyme BACE1 in human brain and pancreas. *Biochemical and Biophysical Research Communications*, *293*(1), 30–37. https://doi.org/10.1016/S0006-291X(02)00169-9

El-Haschimi, K., Pierroz, D. D., Hileman, S. M., Bjørbaek, C., & Flier, J. S. (2000). Two defects contribute to hypothalamic leptin resistance in mice with diet-induced obesity. *The Journal of Clinical Investigation*, *105*(12), 1827–1832. https://doi.org/10.1172/JCI9842

Ellis, C. R., & Shen, J. (2015). pH-Dependent Population Shift Regulates BACE1 Activity and Inhibition. *Journal of the American Chemical Society*, *137*(30), 9543–9546. https://doi.org/10.1021/jacs.5b05891

Elloul, S., Kedrin, D., Knoblauch, N. W., Beck, A. H., & Toker, A. (2014). The Adherens Junction Protein Afadin Is an AKT Substrate that Regulates

Breast Cancer Cell Migration. *Molecular Cancer Research*, *12*(3), 464–476. https://doi.org/10.1158/1541-7786.MCR-13-0398

Enriori, P. J., Evans, A. E., Sinnayah, P., Jobst, E. E., Tonelli-Lemos, L., Billes, S. K., … Cowley, M. A. (2007). Diet-induced obesity causes severe but reversible leptin resistance in arcuate melanocortin neurons. *Cell Metabolism*, *5*(3), 181–194. https://doi.org/10.1016/j.cmet.2007.02.004

Ezawa, I., Sawai, Y., Kawase, T., Okabe, A., Tsutsumi, S., Ichikawa, H., … Ohki, R. (2016). Novel p53 target gene *FUCA1* encodes a fucosidase and regulates growth and survival of cancer cells. *Cancer Science*, *107*(6), 734–745. https://doi.org/10.1111/cas.12933

Fang, X., Yu, S. X., Lu, Y., Bast, R. C., Woodgett, J. R., & Mills, G. B. (2000). Phosphorylation and inactivation of glycogen synthase kinase 3 by protein kinase A. *Proceedings of the National Academy of Sciences*, *97*(22), 11960–11965. https://doi.org/10.1073/pnas.220413597

Farr, S. A., Yamada, K. A., Butterfield, D. A., Abdul, H. M., Xu, L., Miller, N. E., … Morley, J. E. (2008). Obesity and Hypertriglyceridemia Produce Cognitive Impairment. *Endocrinology*, *149*(5), 2628–2636. https://doi.org/10.1210/en.2007-1722

Farzan, M., Schnitzler, C. E., Vasilieva, N., Leung, D., & Choe, H. (2000). BACE2, a beta -secretase homolog, cleaves at the beta site and within the amyloid-beta region of the amyloid-beta precursor protein. *Proceedings of the National Academy of Sciences*, *97*(17), 9712–9717. https://doi.org/10.1073/pnas.160115697

Fedorenko, O. A., Popugaeva, E., Enomoto, M., Stathopulos, P. B., Ikura, M., & Bezprozvanny, I. (2014). Intracellular calcium channels: inositol-1,4,5-trisphosphate receptors. *European Journal of Pharmacology*, *739*, 39–48. https://doi.org/10.1016/j.ejphar.2013.10.074

Fewlass, D. C., NOBOA, K., PI-SUNYER, F. X., JOHNSTON, J. M., YAN, S. D., & TEZAPSIDIS, N. (2004). Obesity-related leptin regulates Alzheimer's Aβ. *The FASEB Journal*, *18*(15), 1870–1878. https://doi.org/10.1096/fj.04-2572com

Finan, G. M., Okada, H., & Kim, T.-W. (2011). BACE1 retrograde trafficking is uniquely regulated by the cytoplasmic domain of sortilin. *The Journal of Biological Chemistry*, *286*(14), 12602–12616. https://doi.org/10.1074/jbc.M110.170217

Flajolet, M., He, G., Heiman, M., Lin, A., Nairn, A. C., & Greengard, P. (2007). Regulation of Alzheimer's disease amyloid-beta formation by casein kinase I. *Proceedings of the National Academy of Sciences*, *104*(10), 4159–4164. https://doi.org/10.1073/pnas.0611236104

Flynn, L. A., Blissett, A. R., Calomeni, E. P., & Agarwal, G. (2010). Inhibition of collagen fibrillogenesis by cells expressing soluble extracellular domains of DDR1 and DDR2. *Journal of Molecular Biology*, *395*(3), 533–543. https://doi.org/10.1016/j.jmb.2009.10.073

Folch, J., Patraca, I., Martínez, N., Pedrós, I., Petrov, D., Ettcheto, M., … Camins, A. (2015). The role of leptin in the sporadic form of Alzheimer's disease. Interactions with the adipokines amylin, ghrelin and the pituitary hormone prolactin. *Life Sciences*, *140*, 19–28. https://doi.org/10.1016/j.lfs.2015.05.002

Foley, P. (2010). Lipids in Alzheimer's disease: A century-old story. *Biochimica et Biophysica Acta (BBA) - Molecular and Cell Biology of Lipids*, *1801*(8), 750–753. https://doi.org/10.1016/j.bbalip.2010.05.004

Forlenza, O. V., Radanovic, M., Talib, L. L., Aprahamian, I., Diniz, B. S.,

Zetterberg, H., & Gattaz, W. F. (2015). Cerebrospinal fluid biomarkers in Alzheimer's disease: Diagnostic accuracy and prediction of dementia. *Alzheimer's & Dementia: Diagnosis, Assessment & Disease Monitoring*, *1*(4), 455–463. https://doi.org/10.1016/j.dadm.2015.09.003

Fox, G. E., Li, M., Zhao, F., & Tsien, J. Z. (2017). Distinct retrosplenial cortex cell populations and their spike dynamics during ketamine-induced unconscious state. *PLOS ONE*, *12*(10), e0187198. https://doi.org/10.1371/journal.pone.0187198

Frederich, R. C., Hamann, A., Anderson, S., Löllmann, B., Lowell, B. B., & Flier, J. S. (1995). Leptin levels reflect body lipid content in mice: Evidence for diet-induced resistance to leptin action. *Nature Medicine*, *1*(12), 1311–1314. https://doi.org/10.1038/nm1295-1311

Fu, H.-L., Sohail, A., Valiathan, R. R., Wasinski, B. D., Kumarasiri, M., Mahasenan, K. V., … Fridman, R. (2013). Shedding of Discoidin Domain Receptor 1 by Membrane-type Matrix Metalloproteinases. *Journal of Biological Chemistry*, *288*(17), 12114–12129. https://doi.org/10.1074/jbc.M112.409599

Fu, H.-L., Valiathan, R. R., Arkwright, R., Sohail, A., Mihai, C., Kumarasiri, M., … Fridman, R. (2013). Discoidin Domain Receptors: Unique Receptor Tyrosine Kinases in Collagen-mediated Signaling. *Journal of Biological Chemistry*, *288*(11), 7430–7437. https://doi.org/10.1074/JBC.R112.444158

Fujioka, Y., Matozaki, T., Noguchi, T., Iwamatsu, A., Yamao, T., Takahashi, N., … Kasuga, M. (1996). A novel membrane glycoprotein, SHPS-1, that binds the SH2-domain-containing protein tyrosine phosphatase SHP-2 in response to mitogens and cell adhesion. *Molecular and Cellular Biology*, *16*(12), 6887–6899. Retrieved from http://www.ncbi.nlm.nih.gov/pubmed/8943344

Fukatsu, K., Bannai, H., Inoue, T., & Mikoshiba, K. (2006). 4.1N binding regions of inositol 1,4,5-trisphosphate receptor type 1. *Biochemical and Biophysical Research Communications*, *342*(2), 573–576. https://doi.org/10.1016/J.BBRC.2006.02.010

Fukumoto, H., Cheung, B. S., Hyman, B. T., & Irizarry, M. C. (2002). β-Secretase Protein and Activity Are Increased in the Neocortex in Alzheimer Disease. *Archives of Neurology*, *59*(9), 1381. https://doi.org/10.1001/archneur.59.9.1381

Galluzzi, P., Rufa, A., Balestri, P., Cerase, A., & Federico, A. (2001). MR brain imaging of fucosidosis type I. *AJNR. American Journal of Neuroradiology*, *22*(4), 777–780. Retrieved from http://www.ncbi.nlm.nih.gov/pubmed/11290499

Gangarossa, G., Longueville, S., De Bundel, D., Perroy, J., Hervé, D., Girault, J., & Valjent, E. (2012). Characterization of dopamine D1 and D2 receptor-expressing neurons in the mouse hippocampus. *Hippocampus*, *22*(12), 2199–2207. https://doi.org/10.1002/hipo.22044

Garcia-Osta, A., & Alberini, C. M. (2009). Amyloid beta mediates memory formation. *Learning & Memory (Cold Spring Harbor, N.Y.)*, *16*(4), 267–272. https://doi.org/10.1101/lm.1310209

Gauthier, E., Guo, X., Mohandas, N., & An, X. (2011). Phosphorylation-dependent perturbations of the 4.1R-associated multiprotein complex of the erythrocyte membrane. *Biochemistry*, *50*(21), 4561–4567. https://doi.org/10.1021/bi200154g

Gervais, F. G., Xu, D., Robertson, G. S., Vaillancourt, J. P., Zhu, Y., Huang, J., … Nicholson, D. W. (1999). Involvement of caspases in proteolytic

cleavage of Alzheimer's amyloid-beta precursor protein and amyloidogenic A beta peptide formation. *Cell*, *97*(3), 395–406. https://doi.org/10.1016/S0092-8674(00)80748-5

Ghamari-Langroudi, M., Srisai, D., & Cone, R. D. (2011). Multinodal regulation of the arcuate/paraventricular nucleus circuit by leptin. *Proceedings of the National Academy of Sciences of the United States of America*, *108*(1), 355–360. https://doi.org/10.1073/pnas.1016785108

Giovannone, B., Lee, E., Laviola, L., Giorgino, F., Cleveland, K. A., & Smith, R. J. (2003). Two Novel Proteins That Are Linked to Insulin-like Growth Factor (IGF-I) Receptors by the Grb10 Adapter and Modulate IGF-I Signaling. *Journal of Biological Chemistry*, *278*(34), 31564–31573. https://doi.org/10.1074/jbc.M211572200

Girardet, C., & Butler, A. A. (2014). Neural melanocortin receptors in obesity and related metabolic disorders. *Biochimica et Biophysica Acta (BBA) - Molecular Basis of Disease*, *1842*(3), 482–494. https://doi.org/10.1016/J.BBADIS.2013.05.004

Gong, L., Yao, F., Hockman, K., Heng, H. H., Morton, G. J., Takeda, K., … MacKenzie, R. G. (2008). Signal Transducer and Activator of Transcription-3 Is Required in Hypothalamic Agouti-Related Protein/Neuropeptide Y Neurons for Normal Energy Homeostasis. *Endocrinology*, *149*(7), 3346–3354. https://doi.org/10.1210/en.2007-0945

Gordon, D. E., Chia, J., Jayawardena, K., Antrobus, R., Bard, F., & Peden, A. A. (2017). VAMP3/Syb and YKT6 are required for the fusion of constitutive secretory carriers with the plasma membrane. *PLOS Genetics*, *13*(4), e1006698. https://doi.org/10.1371/journal.pgen.1006698

Goriounova, N. A., Heyer, D. B., Wilbers, R., Verhoog, M. B., Giugliano, M., Verbist, C., … Mansvelder, H. D. (2018). Large and fast human pyramidal neurons associate with intelligence. *ELife*, *7*. https://doi.org/10.7554/eLife.41714

Graham, F. L., Smiley, J., Russell, W. C., & Nairn, R. (1977). Characteristics of a human cell line transformed by DNA from human adenovirus type 5. *Journal of General Virology*, *36*(1), 59–72. https://doi.org/10.1099/0022-1317-36-1-59

Grandbarbe, L., Bouissac, J., Rand, M., Hrabé de Angelis, M., Artavanis-Tsakonas, S., & Mohier, E. (2003). Delta-Notch signaling controls the generation of neurons/glia from neural stem cells in a stepwise process. *Development (Cambridge, England)*, *130*(7), 1391–1402. Retrieved from http://www.ncbi.nlm.nih.gov/pubmed/12588854

Greco, S. J., Bryan, K. J., Sarkar, S., Zhu, X., Smith, M. A., Ashford, J. W., … Casadesus, G. (2010). Leptin Reduces Pathology and Improves Memory in a Transgenic Mouse Model of Alzheimer's Disease. *Journal of Alzheimer's Disease*, *19*(4), 1155–1167. https://doi.org/10.3233/JAD-2010-1308

Grüninger-Leitch, F., Schlatter, D., Küng, E., Nelböck, P., & Döbeli, H. (2002). Substrate and inhibitor profile of BACE (beta-secretase) and comparison with other mammalian aspartic proteases. *The Journal of Biological Chemistry*, *277*(7), 4687–4693. https://doi.org/10.1074/jbc.M109266200

Guerra, B., Santana, A., Fuentes, T., Delgado-Guerra, S., Cabrera-Socorro, A., Dorado, C., & Calbet, J. A. L. (2007). Leptin receptors in human skeletal muscle. *Journal of Applied Physiology*, *102*(5), 1786–1792. https://doi.org/10.1152/japplphysiol.01313.2006

Guglielmotto, M., Aragno, M., Autelli, R., Giliberto, L., Novo, E., Colombatto, S., … Tabaton, M. (2009). The up-regulation of BACE1 mediated by hypoxia

and ischemic injury: role of oxidative stress and HIF1α. *Journal of Neurochemistry*, *108*(4), 1045–1056. https://doi.org/10.1111/j.1471-4159.2008.05858.x

Guo, S. (2014). Insulin signaling, resistance, and metabolic syndrome: insights from mouse models into disease mechanisms. *Journal of Endocrinology*, *220*(2), T1–T23. https://doi.org/10.1530/JOE-13-0327

Haapalinna, F., Paajanen, T., Penttinen, J., Kokki, H., Kokki, M., Koivisto, A. M., … Herukka, S.-K. (2016). Low Cerebrospinal Fluid Amyloid-Beta Concentration Is Associated with Poorer Delayed Memory Recall in Women. *Dementia and Geriatric Cognitive Disorders Extra*, *6*(2), 303–312. https://doi.org/10.1159/000446425

Haass, C., Koo, E. H., Mellon, A., Hung, A. Y., & Selkoe, D. J. (1992). Targeting of cell-surface β-amyloid precursor protein to lysosomes: alternative processing into amyloid-bearing fragments. *Nature*, *357*(6378), 500–503. https://doi.org/10.1038/357500a0

Hall, A. M., Moore, R. Y., Lopez, O. L., Kuller, L., & Becker, J. T. (2008). Basal forebrain atrophy is a presymptomatic marker for Alzheimer's disease. *Alzheimer's & Dementia*, *4*(4), 271–279. https://doi.org/10.1016/J.JALZ.2008.04.005

Hamer, M., & Batty, G. D. (2019). Association of body mass index and waist-to-hip ratio with brain structure: UK Biobank study. *Neurology*, *92*(6), e594–e600. https://doi.org/10.1212/WNL.0000000000006879

Hamilton, D. L., Findlay, J. A., Montagut, G., Meakin, P. J., Bestow, D., Jalicy, S. M., & Ashford, M. L. J. (2014). Altered amyloid precursor protein processing regulates glucose uptake and oxidation in cultured rodent myotubes. *Diabetologia*, *57*(8), 1684–1692. https://doi.org/10.1007/s00125-014-3269-x

Hamilton, L. K., Dufresne, M., Joppé, S. E., Petryszyn, S., Aumont, A., Calon, F., … Fernandes, K. J. L. (2015). Aberrant Lipid Metabolism in the Forebrain Niche Suppresses Adult Neural Stem Cell Proliferation in an Animal Model of Alzheimer's Disease. *Cell Stem Cell*, *17*(4), 397–411. https://doi.org/10.1016/j.stem.2015.08.001

Han, X., M. Holtzman, D., W. McKeel, D., Kelley, J., & Morris, J. C. (2002). Substantial sulfatide deficiency and ceramide elevation in very early Alzheimer's disease: potential role in disease pathogenesis. *Journal of Neurochemistry*, *82*(4), 809–818. https://doi.org/10.1046/j.1471-4159.2002.00997.x

Haniu, M., Denis, P., Young, Y., Mendiaz, E. A., Fuller, J., Hui, J. O., … Citron, M. (2000). Characterization of Alzheimer's beta -secretase protein BACE. A pepsin family member with unusual properties. *The Journal of Biological Chemistry*, *275*(28), 21099–21106. https://doi.org/10.1074/jbc.M002095200

Hansen, C. G., Bright, N. A., Howard, G., & Nichols, B. J. (2009). SDPR induces membrane curvature and functions in the formation of caveolae. *Nature Cell Biology*, *11*(7), 807–814. https://doi.org/10.1038/ncb1887

Hardt, R., Winter, D., Gieselmann, V., & Eckhardt, M. (2018). Identification of progesterone receptor membrane component-1 as an interaction partner and possible regulator of fatty acid 2-hydroxylase. *Biochemical Journal*, *475*(5), 853–871. https://doi.org/10.1042/BCJ20170963

Hardy, J. A., & Higgins, G. A. (1992). Alzheimer's disease: the amyloid cascade hypothesis. *Science (New York, N.Y.)*, *256*(5054), 184–185. Retrieved from http://www.ncbi.nlm.nih.gov/pubmed/1566067

Harold, D., Jehu, L., Turic, D., Hollingworth, P., Moore, P., Summerhayes, P.,

… Williams, J. (2007). Interaction between theADAM12 andSH3MD1 genes may confer susceptibility to late-onset Alzheimer's disease. *American Journal of Medical Genetics Part B: Neuropsychiatric Genetics*, *144B*(4), 448–452. https://doi.org/10.1002/ajmg.b.30456

Harrison, S M, Harper, A. J., Hawkins, J., Duddy, G., Grau, E., Pugh, P. L., … Dingwall, C. (2003). BACE1 (beta-secretase) transgenic neurochernical deficits ind knockout mice: identification of and behavioral changes. *Molecular and Cellular Neuroscience*, *24*(3), 646–655. https://doi.org/10.1016/s1044-7431(03)00227-4

Harrison, Steve M, Harper, A. J., Hawkins, J., Duddy, G., Grau, E., Pugh, P. L., … Dingwall, C. (2003). BACE1 (beta-secretase) transgenic and knockout mice: identification of neurochemical deficits and behavioral changes. *Molecular and Cellular Neurosciences*, *24*(3), 646–655. Retrieved from http://www.ncbi.nlm.nih.gov/pubmed/14664815

Hata, Y., Butz, S., & Südhof, T. C. (1996). CASK: a novel dlg/PSD95 homolog with an N-terminal calmodulin-dependent protein kinase domain identified by interaction with neurexins. *The Journal of Neuroscience : The Official Journal of the Society for Neuroscience*, *16*(8), 2488–2494. https://doi.org/10.1523/JNEUROSCI.16-08-02488.1996

He, Wanxia, Hu, J., Xia, Y., & Yan, R. (2014). β-site amyloid precursor protein cleaving enzyme 1(BACE1) regulates Notch signaling by controlling the cleavage of Jagged 1 (Jag1) and Jagged 2 (Jag2) proteins. *The Journal of Biological Chemistry*, *289*(30), 20630–20637. https://doi.org/10.1074/jbc.M114.579862

He, Wen, Li, X., Adekunbi, D., Liu, Y., Long, H., Wang, L., … O'Byrne, K. T. (2017). Hypothalamic effects of progesterone on regulation of the pulsatile and surge release of luteinising hormone in female rats. *Scientific Reports*, *7*(1), 8096. https://doi.org/10.1038/s41598-017-08805-1

He, X., Chang, W.-P., Koelsch, G., & Tang, J. (2002). Memapsin 2 (β-secretase) cytosolic domain binds to the VHS domains of GGA1 and GGA2: implications on the endocytosis mechanism of memapsin 2. *FEBS Letters*, *524*(1–3), 183–187. https://doi.org/10.1016/S0014-5793(02)03052-1

Head, B. P., & Insel, P. A. (2007). Do caveolins regulate cells by actions outside of caveolae? *Trends in Cell Biology*, *17*(2), 51–57. https://doi.org/10.1016/J.TCB.2006.11.008

Head, E. (2013). A canine model of human aging and Alzheimer's disease. *Biochimica et Biophysica Acta*, *1832*(9), 1384–1389. https://doi.org/10.1016/j.bbadis.2013.03.016

Hemming, M. L., Elias, J. E., Gygi, S. P., & Selkoe, D. J. (2009). Identification of β-Secretase (BACE1) Substrates Using Quantitative Proteomics. *PLoS ONE*, *4*(12), e8477. https://doi.org/10.1371/journal.pone.0008477

Heneka, M. T., Kummer, M. P., Stutz, A., Delekate, A., Schwartz, S., Vieira-Saecker, A., … Golenbock, D. T. (2013). NLRP3 is activated in Alzheimer's disease and contributes to pathology in APP/PS1 mice. *Nature*, *493*(7434), 674–678. https://doi.org/10.1038/nature11729

Heneka, M. T., Sastre, M., Dumitrescu-Ozimek, L., Dewachter, I., Walter, J., Klockgether, T., & Van Leuven, F. (2005). Focal glial activation coincides with increased BACE1 activation and precedes amyloid plaque deposition in APP[V717I] transgenic mice. *Journal of Neuroinflammation*, *2*(1), 22. https://doi.org/10.1186/1742-2094-2-22

Herber, J., Njavro, J., Feederle, R., Schepers, U., Müller, U. C., Bräse, S., …

Lichtenthaler, S. F. (2018). Click Chemistry-mediated Biotinylation Reveals a Function for the Protease BACE1 in Modulating the Neuronal Surface Glycoproteome. *Molecular & Cellular Proteomics*, *17*(8), 1487–1501. https://doi.org/10.1074/MCP.RA118.000608

Heyer, E. J., Mergeche, J. L., Bruce, S. S., & Connolly, E. S. (2013). Inflammation and cognitive dysfunction in type 2 diabetic carotid endarterectomy patients. *Diabetes Care*, *36*(10), 3283–3286. https://doi.org/10.2337/dc12-2507

Hippius, H., & Neundörfer, G. (2003). The discovery of Alzheimer's disease. *Dialogues in Clinical Neuroscience*, *5*(1), 101–108. Retrieved from http://www.ncbi.nlm.nih.gov/pubmed/22034141

Hitt, B. D., Jaramillo, T. C., Chetkovich, D. M., & Vassar, R. (2010). BACE1-/- mice exhibit seizure activity that does not correlate with sodium channel level or axonal localization. *Molecular Neurodegeneration*, *5*(1), 31. https://doi.org/10.1186/1750-1326-5-31

Hock, B., Böhme, B., Karn, T., Yamamoto, T., Kaibuchi, K., Holtrich, U., … Strebhardt, K. (1998). PDZ-domain-mediated interaction of the Eph-related receptor tyrosine kinase EphB3 and the ras-binding protein AF6 depends on the kinase activity of the receptor. *Proceedings of the National Academy of Sciences of the United States of America*, *95*(17), 9779–9784. Retrieved from http://www.ncbi.nlm.nih.gov/pubmed/9707552

Hoffmeister, A., Tuennemann, J., Sommerer, I., Mössner, J., Rittger, A., Schleinitz, D., … Blüher, M. (2013). Genetic and biochemical evidence for a functional role of BACE1 in the regulation of insulin mRNA expression. *Obesity*, *21*(12), E626–E633. https://doi.org/10.1002/oby.20482

Holden, K. F., Lindquist, K., Tylavsky, F. A., Rosano, C., Harris, T. B., & Yaffe, K. (2009). Serum leptin level and cognition in the elderly: Findings from the Health ABC Study. *Neurobiology of Aging*, *30*(9), 1483–1489. https://doi.org/10.1016/J.NEUROBIOLAGING.2007.11.024

Holsinger, R. M. D., Goense, N., Bohorquez, J., & Strappe, P. (2013). Splice variants of the Alzheimer's disease beta-secretase, BACE1. *Neurogenetics*, *14*(1), 1–9. https://doi.org/10.1007/s10048-012-0348-3

Holsinger, R. M. D., McLean, C. A., Beyreuther, K., Masters, C. L., & Evin, G. (2002). Increased expression of the amyloid precursor beta-secretase in Alzheimer's disease. *Annals of Neurology*, *51*(6), 783–786. https://doi.org/10.1002/ana.10208

Hook, V., Kindy, M., & Hook, G. (2007). Cysteine protease inhibitors effectively reduce in vivo levels of brain β-amyloid related to Alzheimer's disease. *Biological Chemistry*, *388*(2), 247–252. https://doi.org/10.1515/BC.2007.027

Hooper, C., Meimaridou, E., Tavassoli, M., Melino, G., Lovestone, S., & Killick, R. (2007). p53 is upregulated in Alzheimer's disease and induces tau phosphorylation in HEK293a cells. *Neuroscience Letters*, *418*(1), 34–37. https://doi.org/10.1016/j.neulet.2007.03.026

Hosoi, T., Okuma, Y., & Nomura, Y. (2000). Expression of Leptin Receptors and Induction of IL-1β Transcript in Glial Cells. *Biochemical and Biophysical Research Communications*, *273*(1), 312–315. https://doi.org/10.1006/BBRC.2000.2937

Hosoi, T., Okuma, Y., & Nomura, Y. (2002). *Leptin regulates interleukin-1b expression in the brain via the STAT3-independent mechanisms*. *Brain Research* (Vol. 949). Retrieved from www.elsevier.com/locate/bres

Hotta, K., Tanaka, K., Mino, A., Kohno, H., & Takai, Y. (1996). Interaction of the

Rho Family Small G Proteins with Kinectin, an Anchoring Protein of Kinesin Motor. *Biochemical and Biophysical Research Communications*, *225*(1), 69–74. https://doi.org/10.1006/bbrc.1996.1132

Hsu, P. J., Shou, H., Benzinger, T., Marcus, D., Durbin, T., Morris, J. C., & Sheline, Y. I. (2015). Amyloid burden in cognitively normal elderly is associated with preferential hippocampal subfield volume loss. *Journal of Alzheimer's Disease : JAD*, *45*(1), 27–33. https://doi.org/10.3233/JAD-141743

Hu, X, Zhou, X., He, W., Yang, J., Xiong, W., Wong, P., … Yan, R. (2010). BACE1 deficiency causes altered neuronal activity and neurodegeneration. *The Journal of Neuroscience : The Official Journal of the Society for Neuroscience*, *30*(26), 8819–8829. https://doi.org/10.1523/JNEUROSCI.1334-10.2010

Hu, Xiangyou, He, W., Luo, X., Tsubota, K. E., & Yan, R. (2013). BACE1 Regulates Hippocampal Astrogenesis via the Jagged1-Notch Pathway. *Cell Reports*, *4*(1), 40–49. https://doi.org/10.1016/J.CELREP.2013.06.005

Hu, Xiangyou, Hicks, C. W., He, W., Wong, P., Macklin, W. B., Trapp, B. D., & Yan, R. (2006). Bace1 modulates myelination in the central and peripheral nervous system. *Nature Neuroscience*, *9*(12), 1520–1525. https://doi.org/10.1038/nn1797

Huang, T.-N., & Hsueh, Y.-P. (2017). Calcium/calmodulin-dependent serine protein kinase (CASK), a protein implicated in mental retardation and autism-spectrum disorders, interacts with T-Brain-1 (TBR1) to control extinction of associative memory in male mice. *Journal of Psychiatry & Neuroscience : JPN*, *42*(1), 37–47. https://doi.org/10.1503/JPN.150359

Huang, X. F., Koutcherov, I., Lin, S., Wang, H. Q., & Storlien, L. (1996). Localization of leptin receptor mRNA expression in mouse brain. *Neuroreport*, *7*(15–17), 2635–2638. Retrieved from http://www.ncbi.nlm.nih.gov/pubmed/8981437

Hughes, T. F., Borenstein, A. R., Schofield, E., Wu, Y., & Larson, E. B. (2009). Association between late-life body mass index and dementia: The Kame Project. *Neurology*, *72*(20), 1741. https://doi.org/10.1212/WNL.0B013E3181A60A58

Hurley, J. H., Zhang, S., Bye, L. S., Marshall, M. S., DePaoli-Roach, A. A., Guan, K., … Yu, L. (2003). Insulin signaling inhibits the 5-HT 2C receptor in choroid plexus via MAP kinase. *BMC Neuroscience*, *4*(1), 10. https://doi.org/10.1186/1471-2202-4-10

Hussain, I., Hawkins, J., Shikotra, A., Riddell, D. R., Faller, A., & Dingwall, C. (2003). Characterization of the ectodomain shedding of the beta-site amyloid precursor protein-cleaving enzyme 1 (BACE1). *The Journal of Biological Chemistry*, *278*(38), 36264–36268. https://doi.org/10.1074/jbc.M304186200

Hussain, I., Powell, D., Howlett, D. R., Tew, D. G., Meek, T. D., Chapman, C., … Christie, G. (1999). Identification of a Novel Aspartic Protease (Asp 2) as β-Secretase. *Molecular and Cellular Neuroscience*, *14*(6), 419–427. https://doi.org/10.1006/MCNE.1999.0811

Huth, T., Schmidt-Neuenfeldt, K., Rittger, A., Saftig, P., Reiss, K., & Alzheimer, C. (2009). Non-proteolytic effect of β-site APP-cleaving enzyme 1 (BACE1) on sodium channel function. *Neurobiology of Disease*, *33*(2), 282–289. https://doi.org/10.1016/J.NBD.2008.10.015

Huttlin, E. L., Ting, L., Bruckner, R. J., Gebreab, F., Gygi, M. P., Szpyt, J., … Gygi, S. P. (2015). The BioPlex Network: A Systematic Exploration of the

Human Interactome. *Cell*, *162*(2), 425–440. https://doi.org/10.1016/j.cell.2015.06.043

Ikeda, W., Nakanishi, H., Miyoshi, J., Mandai, K., Ishizaki, H., Tanaka, M., … Takai, Y. (1999). Afadin: A key molecule essential for structural organization of cell-cell junctions of polarized epithelia during embryogenesis. *The Journal of Cell Biology*, *146*(5), 1117–1132. https://doi.org/10.1083/JCB.146.5.1117

Ishida-Takahashi, R., Uotani, S., Abe, T., Degawa-Yamauchi, M., Fukushima, T., Fujita, N., … Eguchi, K. (2004). Rapid inhibition of leptin signaling by glucocorticoids in vitro and in vivo. *The Journal of Biological Chemistry*, *279*(19), 19658–19664. https://doi.org/10.1074/jbc.M310864200

Ishii, M., Wang, G., Racchumi, G., Dyke, J. P., & Iadecola, C. (2014). Transgenic mice overexpressing amyloid precursor protein exhibit early metabolic deficits and a pathologically low leptin state associated with hypothalamic dysfunction in arcuate neuropeptide Y neurons. *The Journal of Neuroscience : The Official Journal of the Society for Neuroscience*, *34*(27), 9096–9106. https://doi.org/10.1523/JNEUROSCI.0872-14.2014

Isom, L. L., & Catterall, W. A. (1996). Na+ channel subunits and Ig domains. *Nature*, *383*(6598), 307–308. https://doi.org/10.1038/383307b0

Iwasawa, N., Negishi, M., & Oinuma, I. (2012). R-Ras controls axon branching through afadin in cortical neurons. *Molecular Biology of the Cell*, *23*(14), 2793–2804. https://doi.org/10.1091/mbc.E12-02-0103

Iwatsubo, T., Saido, T. C., Mann, D. M., Lee, V. M., & Trojanowski, J. Q. (1996). Full-length amyloid-beta (1-42(43)) and amino-terminally modified and truncated amyloid-beta 42(43) deposit in diffuse plaques. *The American Journal of Pathology*, *149*(6), 1823–1830. Retrieved from http://www.ncbi.nlm.nih.gov/pubmed/8952519

J. Aura Gimm, ‡, Xiuli An, *,#, Wataru Nunomura, 2and, & Narla Mohandas‡, #. (2002). Functional Characterization of Spectrin-Actin-Binding Domains in 4.1 Family of Proteins†. https://doi.org/10.1021/BI0256330

Jang, H., Arce, F. T., Ramachandran, S., Capone, R., Azimova, R., Kagan, B. L., … Lal, R. (2010). Truncated beta-amyloid peptide channels provide an alternative mechanism for Alzheimer's Disease and Down syndrome. *Proceedings of the National Academy of Sciences of the United States of America*, *107*(14), 6538–6543. https://doi.org/10.1073/pnas.0914251107

Jo, S. A., Ahn, K., Kim, E., Kim, H.-S., Jo, I., Kim, D. K., … Park, M. H. (2008). Association of BACE1 Gene Polymorphism with Alzheimer's Disease in Asian Populations: Meta-Analysis Including Korean Samples. *Dementia and Geriatric Cognitive Disorders*, *25*(2), 165–169. https://doi.org/10.1159/000112918

John, B. A., Meister, M., Banning, A., & Tikkanen, R. (2014). Flotillins bind to the dileucine sorting motif of β-site amyloid precursor protein-cleaving enzyme 1 and influence its endosomal sorting. *FEBS Journal*, *281*(8), 2074–2087. https://doi.org/10.1111/febs.12763

Johnson, D. K., Wilkins, C. H., & Morris, J. C. (2006a). Accelerated weight loss may precede diagnosis in Alzheimer disease. *Archives of Neurology*, *63*(9), 1312–1317. https://doi.org/10.1001/archneur.63.9.1312

Johnson, D. K., Wilkins, C. H., & Morris, J. C. (2006b). Accelerated Weight Loss May Precede Diagnosis in Alzheimer Disease. *Archives of Neurology*, *63*(9), 1312. https://doi.org/10.1001/archneur.63.9.1312

Johnston, J. M., Hu, W. T., Fardo, D. W., Greco, S. J., Perry, G., Montine, T. J., … Alzheimer's Disease Neuroimaging Initiative, the A. D. N. (2014). Low

plasma leptin in cognitively impaired ADNI subjects: gender differences and diagnostic and therapeutic potential. *Current Alzheimer Research*, *11*(2), 165–174. Retrieved from http://www.ncbi.nlm.nih.gov/pubmed/24359504

Joice, S. L., Mydeen, F., Couraud, P. O., Weksler, B. B., Romero, I. A., Fraser, P. A., & Easton, A. S. (2009). Modulation of blood-brain barrier permeability by neutrophils: in vitro and in vivo studies. *Brain Research*, *1298*, 13–23. https://doi.org/10.1016/j.brainres.2009.08.076

Jolivalt, C. G., Hurford, R., Lee, C. A., Dumaop, W., Rockenstein, E., & Masliah, E. (2010). Type 1 diabetes exaggerates features of Alzheimer's disease in APP transgenic mice. *Experimental Neurology*, *223*(2), 422–431. https://doi.org/10.1016/j.expneurol.2009.11.005

Jonas, M. C., Costantini, C., & Puglielli, L. (2008). PCSK9 is required for the disposal of non-acetylated intermediates of the nascent membrane protein BACE1. *EMBO Reports*, *9*(9), 916–922. https://doi.org/10.1038/embor.2008.132

Jonsson, T., Atwal, J. K., Steinberg, S., Snaedal, J., Jonsson, P. V., Bjornsson, S., … Stefansson, K. (2012). A mutation in APP protects against Alzheimer's disease and age-related cognitive decline. *Nature*, *488*(7409), 96–99. https://doi.org/10.1038/nature11283

Julien, C., Tremblay, C., Phivilay, A., Berthiaume, L., Émond, V., Julien, P., & Calon, F. (2010). High-fat diet aggravates amyloid-beta and tau pathologies in the 3xTg-AD mouse model. *Neurobiology of Aging*, *31*(9), 1516–1531. https://doi.org/10.1016/J.NEUROBIOLAGING.2008.08.022

Kadokura, A., Yamazaki, T., Lemere, C. A., Takatama, M., & Okamoto, K. (2009). Regional distribution of TDP-43 inclusions in Alzheimer disease (AD) brains: Their relation to AD common pathology. *Neuropathology*, *29*(5), 566–573. https://doi.org/10.1111/j.1440-1789.2009.01017.x

Kagan, B. L., Jang, H., Capone, R., Teran Arce, F., Ramachandran, S., Lal, R., & Nussinov, R. (2012). Antimicrobial Properties of Amyloid Peptides. *Molecular Pharmaceutics*, *9*(4), 708–717. https://doi.org/10.1021/mp200419b

Kang, E. L., Biscaro, B., Piazza, F., & Tesco, G. (2012). BACE1 protein endocytosis and trafficking are differentially regulated by ubiquitination at lysine 501 and the Di-leucine motif in the carboxyl terminus. *The Journal of Biological Chemistry*, *287*(51), 42867–42880. https://doi.org/10.1074/jbc.M112.407072

Kang, E. L., Cameron, A. N., Piazza, F., Walker, K. R., & Tesco, G. (2010). Ubiquitin regulates GGA3-mediated degradation of BACE1. *The Journal of Biological Chemistry*, *285*(31), 24108–24119. https://doi.org/10.1074/jbc.M109.092742

Katano, T., Takao, K., Abe, M., Yamazaki, M., Watanabe, M., Miyakawa, T., … Ito, S. (2018). Distribution of Caskin1 protein and phenotypic characterization of its knockout mice using a comprehensive behavioral test battery. *Molecular Brain*, *11*(1), 63. https://doi.org/10.1186/s13041-018-0407-2

Kheir, A. E. M., Imam, A., Omer, I. M., Hassan, I. M. A., Elamin, S. A., Awadalla, E. A., … Hamdoon, T. A. (2012). Meckel-Gruber syndrome: A rare and lethal anomaly. *Sudanese Journal of Paediatrics*, *12*(1), 93–96. Retrieved from http://www.ncbi.nlm.nih.gov/pubmed/27493335

Kim, D. I., KC, B., Zhu, W., Motamedchaboki, K., Doye, V., & Roux, K. J. (2014). Probing nuclear pore complex architecture with proximity-dependent biotinylation. *Proceedings of the National Academy of Sciences*,

111(24), E2453–E2461. https://doi.org/10.1073/pnas.1406459111

Kim, D. Y., Carey, B. W., Wang, H., Ingano, L. A. M., Binshtok, A. M., Wertz, M. H., … Kovacs, D. M. (2007). BACE1 regulates voltage-gated sodium channels and neuronal activity. *Nature Cell Biology*, *9*(7), 755–764. https://doi.org/10.1038/ncb1602

Kim, H.-J., Seo, S. W., Jeon, S., Kang, M., Kim, Y. J., Lee, J.-M., … Kim, C. (2014). ASSOCIATION OF BODY FAT PERCENTAGE AND WAIST-HIP RATIO WITH BRAIN CORTICAL THICKNESS IN 1,777 COGNITIVELY NORMAL SUBJECTS. *Alzheimer's & Dementia*, *10*(4), P715–P716. https://doi.org/10.1016/j.jalz.2014.05.1322

Kimberly, W. T., LaVoie, M. J., Ostaszewski, B. L., Ye, W., Wolfe, M. S., & Selkoe, D. J. (2003). Gamma-secretase is a membrane protein complex comprised of presenilin, nicastrin, Aph-1, and Pen-2. *Proceedings of the National Academy of Sciences of the United States of America*, *100*(11), 6382–6387. https://doi.org/10.1073/pnas.1037392100

Kirouac, L., Rajic, A. J., Cribbs, D. H., & Padmanabhan, J. (2017). Activation of Ras-ERK Signaling and GSK-3 by Amyloid Precursor Protein and Amyloid Beta Facilitates Neurodegeneration in Alzheimer's Disease. *ENeuro*, *4*(2). https://doi.org/10.1523/ENEURO.0149-16.2017

Kirschling, C. M., Kölsch, H., Frahnert, C., Rao, M. L., Maier, W., & Heun, R. (2003). Polymorphism in the BACE gene influences the risk for Alzheimer's disease. *Neuroreport*, *14*(9), 1243–1246. https://doi.org/10.1097/01.wnr.0000081879.23960.fd

Kizuka, Y., Kitazume, S., Fujinawa, R., Saito, T., Iwata, N., Saido, T. C., … Taniguchi, N. (2015). An aberrant sugar modification of BACE1 blocks its lysosomal targeting in Alzheimer's disease. *EMBO Molecular Medicine*, *7*(2), 175–189. https://doi.org/10.15252/emmm.201404438

Klein, D. M., Felsenstein, K. M., & Brenneman, D. E. (2009). Cathepsins B and L differentially regulate amyloid precursor protein processing. *The Journal of Pharmacology and Experimental Therapeutics*, *328*(3), 813–821. https://doi.org/10.1124/jpet.108.147082

Ko, M. H., & Puglielli, L. (2009). Two Endoplasmic Reticulum (ER)/ER Golgi Intermediate Compartment-based Lysine Acetyltransferases Post-translationally Regulate BACE1 Levels. *Journal of Biological Chemistry*, *284*(4), 2482–2492. https://doi.org/10.1074/jbc.M804901200

Koga, Y., & Ikebe, M. (2005). p116Rip decreases myosin II phosphorylation by activating myosin light chain phosphatase and by inactivating RhoA. *The Journal of Biological Chemistry*, *280*(6), 4983–4991. https://doi.org/10.1074/jbc.M410909200

Konrad, M. (2016). *Charakterisierung der Thioreduktase TXNDC15*. Saarland University. Retrieved from https://publikationen.sulb.uni-saarland.de/bitstream/20.500.11880/22309/1/Fertige_Doktorarbeit.pdf

Koo, E. H., & Squazzo, S. L. (1994). Evidence that production and release of amyloid beta-protein involves the endocytic pathway. *The Journal of Biological Chemistry*, *269*(26), 17386–17389. Retrieved from http://www.ncbi.nlm.nih.gov/pubmed/8021238

Koo, E. H., Squazzo, S. L., Selkoe, D. J., & Koo, C. H. (1996). Trafficking of cell-surface amyloid beta-protein precursor. I. Secretion, endocytosis and recycling as detected by labeled monoclonal antibody. *Journal of Cell Science*, *109 (Pt 5)*, 991–998. Retrieved from http://www.ncbi.nlm.nih.gov/pubmed/8743946

Kothari, V., Luo, Y., Tornabene, T., O'Neill, A. M., Greene, M. W., Geetha, T., &

Babu, J. R. (2017). High fat diet induces brain insulin resistance and cognitive impairment in mice. *Biochimica et Biophysica Acta (BBA) - Molecular Basis of Disease*, *1863*(2), 499–508. https://doi.org/10.1016/j.bbadis.2016.10.006

Koyama, A., Okereke, O. I., Yang, T., Blacker, D., Selkoe, D. J., & Grodstein, F. (2012). Plasma Amyloid-β as a Predictor of Dementia and Cognitive Decline. *Archives of Neurology*, *69*(7), 824–831. https://doi.org/10.1001/archneurol.2011.1841

Kravitz, E., Gaisler-Salomon, I., & Biegon, A. (2013). Hippocampal Glutamate NMDA Receptor Loss Tracks Progression in Alzheimer's Disease: Quantitative Autoradiography in Postmortem Human Brain. *PLoS ONE*, *8*(11), e81244. https://doi.org/10.1371/journal.pone.0081244

Krucker, T., Siggins, G. R., & Halpain, S. (2000). Dynamic actin filaments are required for stable long-term potentiation (LTP) in area CA1 of the hippocampus. *Proceedings of the National Academy of Sciences*, *97*(12), 6856–6861. https://doi.org/10.1073/pnas.100139797

Krug, M., Wagner, M., Staak, S., & Smalla, K. H. (1994). Fucose and fucose-containing sugar epitopes enhance hippocampal long-term potentiation in the freely moving rat. *Brain Research*, *643*(1–2), 130–135. Retrieved from http://www.ncbi.nlm.nih.gov/pubmed/7518325

Kuhn, P.-H., Koroniak, K., Hogl, S., Colombo, A., Zeitschel, U., Willem, M., … Lichtenthaler, S. F. (2012). Secretome protein enrichment identifies physiological BACE1 protease substrates in neurons. *The EMBO Journal*, *31*(14), 3157–3168. https://doi.org/10.1038/emboj.2012.173

Kurkinen, K. M. A., Marttinen, M., Turner, L., Natunen, T., Mäkinen, P., Haapalinna, F., … Hiltunen, M. (2016). SEPT8 modulates β-amyloidogenic processing of APP by affecting the sorting and accumulation of BACE1. *J Cell Sci*, *129*(11), 2224–2238. https://doi.org/10.1242/JCS.185215

Kwon, K., & Beckett, D. (2000). Function of a conserved sequence motif in biotin holoenzyme synthetases. *Protein Science*, *9*(8), 1530–1539. https://doi.org/10.1110/ps.9.8.1530

Ladror, U. S., Snyder, S. W., Wang, G. T., Holzman, T. F., & Krafft, G. A. (1994). Cleavage at the amino and carboxyl termini of Alzheimer's amyloid-beta by cathepsin D. *The Journal of Biological Chemistry*, *269*(28), 18422–18428. Retrieved from http://www.ncbi.nlm.nih.gov/pubmed/8034590

Laffin, B., & Petrash, J. M. (2012). Expression of the Aldo-Ketoreductases AKR1B1 and AKR1B10 in Human Cancers. *Frontiers in Pharmacology*, *3*, 104. https://doi.org/10.3389/fphar.2012.00104

Lambe, T., Simpson, R. J., Dawson, S., Bouriez-Jones, T., Crockford, T. L., Lepherd, M., … Cornall, R. J. (2009). Identification of a Steap3 endosomal targeting motif essential for normal iron metabolism. *Blood*, *113*(8), 1805–1808. https://doi.org/10.1182/blood-2007-11-120402

Lambourne, S. L., Sellers, L. A., Bush, T. G., Choudhury, S. K., Emson, P. C., Suh, Y.-H., & Wilkinson, L. S. (2005). Increased tau phosphorylation on mitogen-activated protein kinase consensus sites and cognitive decline in transgenic models for Alzheimer's disease and FTDP-17: evidence for distinct molecular processes underlying tau abnormalities. *Molecular and Cellular Biology*, *25*(1), 278–293. https://doi.org/10.1128/MCB.25.1.278-293.2005

Lammich, S, Kojro, E., Postina, R., Gilbert, S., Pfeiffer, R., Jasionowski, M., … Fahrenholz, F. (1999). Constitutive and regulated alpha-secretase cleavage of Alzheimer's amyloid precursor protein by a disintegrin

metalloprotease. *Proceedings of the National Academy of Sciences of the United States of America*, *96*(7), 3922–3927. https://doi.org/10.1073/PNAS.96.7.3922

Lammich, Sven, Schöbel, S., Zimmer, A.-K., Lichtenthaler, S. F., & Haass, C. (2004). Expression of the Alzheimer protease BACE1 is suppressed via its 5'-untranslated region. *EMBO Reports*, *5*(6), 620–625. https://doi.org/10.1038/sj.embor.7400166

Lange, J., Lunde, K. A., Sletten, C., Møller, S. G., Tysnes, O.-B., Alves, G., … Maple-Grødem, J. (2015). Association of a BACE1 Gene Polymorphism with Parkinson's Disease in a Norwegian Population. *Parkinson's Disease*, *2015*, 1–5. https://doi.org/10.1155/2015/973298

Laumet, G., Petitprez, V., Sillaire, A., Ayral, A.-M., Hansmannel, F., Chapuis, J., … Lambert, J.-C. (2010). A study of the association between the ADAM12 and SH3PXD2A (SH3MD1) genes and Alzheimer's disease. *Neuroscience Letters*, *468*(1), 1–2. https://doi.org/10.1016/J.NEULET.2009.10.040

LeBlanc, A., Liu, H., Goodyer, C., Bergeron, C., & Hammond, J. (1999). Caspase-6 role in apoptosis of human neurons, amyloidogenesis, and Alzheimer's disease. *The Journal of Biological Chemistry*, *274*(33), 23426–23436. https://doi.org/10.1074/JBC.274.33.23426

Lee, Y.-H., Tharp, W. G., Maple, R. L., Nair, S., Permana, P. A., & Pratley, R. E. (2008). Amyloid Precursor Protein Expression Is Upregulated in Adipocytes in Obesity. *Obesity*, *16*(7), 1493–1500. https://doi.org/10.1038/oby.2008.267

Lehnert, S., Hartmann, S., Hessler, S., Adelsberger, H., Huth, T., & Alzheimer, C. (2016). Ion channel regulation by β-secretase BACE1 – enzymatic andnon-enzymatic effects beyond Alzheimer's disease. *Channels*, *10*(5), 365. https://doi.org/10.1080/19336950.2016.1196307

Leroy, K., Yilmaz, Z., & Brion, J.-P. (2007). Increased level of active GSK-3? in Alzheimer's disease and accumulation in argyrophilic grains and in neurones at different stages of neurofibrillary degeneration. *Neuropathology and Applied Neurobiology*, *33*(1), 43–55. https://doi.org/10.1111/j.1365-2990.2006.00795.x

Lesage, S., Drouet, V., Majounie, E., Deramecourt, V., Jacoupy, M., Nicolas, A., … International Parkinson's Disease Genomics Consortium (IPDGC), the I. P. D. G. C. (2016). Loss of VPS13C Function in Autosomal-Recessive Parkinsonism Causes Mitochondrial Dysfunction and Increases PINK1/Parkin-Dependent Mitophagy. *American Journal of Human Genetics*, *98*(3), 500–513. https://doi.org/10.1016/j.ajhg.2016.01.014

Levy-Lahad, E., Wasco, W., Poorkaj, P., Romano, D. M., Oshima, J., Pettingell, W. H., … Wang, K. (1995). Candidate gene for the chromosome 1 familial Alzheimer's disease locus. *Science (New York, N.Y.)*, *269*(5226), 973–977. Retrieved from http://www.ncbi.nlm.nih.gov/pubmed/7638622

Lewis, F., Karlsberg Schaffer, S., Sussex, J., O'Neill, P., & Cockcroft, L. (2014). *The Trajectory of Dementia in the UK - Making a Difference*. Retrieved from https://www.ohe.org/publications/trajectory-dementia-uk-making-difference

Li, C., & Friedman, J. M. (1999). Leptin receptor activation of SH2 domain containing protein tyrosine phosphatase 2 modulates Ob receptor signal transduction. *Proceedings of the National Academy of Sciences of the United States of America*, *96*(17), 9677–9682. https://doi.org/10.1073/PNAS.96.17.9677

Li, G., Yin, H., & Kuret, J. (2004). Casein kinase 1 delta phosphorylates tau and disrupts its binding to microtubules. *The Journal of Biological Chemistry*,

279(16), 15938–15945. https://doi.org/10.1074/jbc.M314116200

Li, X.-L., Aou, S., Oomura, Y., Hori, N., Fukunaga, K., & Hori, T. (2002). Impairment of long-term potentiation and spatial memory in leptin receptor-deficient rodents. *Neuroscience*, *113*(3), 607–615. https://doi.org/10.1016/S0306-4522(02)00162-8

Liao, L., Cheng, D., Wang, J., Duong, D. M., Losik, T. G., Gearing, M., … Peng, J. (2004). Proteomic characterization of postmortem amyloid plaques isolated by laser capture microdissection. *The Journal of Biological Chemistry*, *279*(35), 37061–37068. https://doi.org/10.1074/jbc.M403672200

Lieb, W., Beiser, A. S., Vasan, R. S., Tan, Z. S., Au, R., Harris, T. B., … Seshadri, S. (2009). Association of Plasma Leptin Levels With Incident Alzheimer Disease and MRI Measures of Brain Aging. *JAMA*, *302*(23), 2565. https://doi.org/10.1001/jama.2009.1836

Lima, M. H. M., Ueno, M., Thirone, A. C. P., Rocha, E. M., Carvalho, C. R. O., & Saad, M. J. A. (2002). Regulation of IRS-1/SHP2 Interaction and AKT Phosphorylation in Animal Models of Insulin Resistance. *Endocrine*, *18*(1), 01–12. https://doi.org/10.1385/ENDO:18:1:01

Lin, D.-T., Makino, Y., Sharma, K., Hayashi, T., Neve, R., Takamiya, K., & Huganir, R. L. (2009). Regulation of AMPA receptor extrasynaptic insertion by 4.1N, phosphorylation and palmitoylation. *Nature Neuroscience*, *12*(7), 879–887. https://doi.org/10.1038/nn.2351

Lindner, C., Sigrüner, A., Walther, F., Bogdahn, U., Couraud, P. O., Schmitz, G., & Schlachetzki, F. (2012). ATP-binding cassette transporters in immortalised human brain microvascular endothelial cells in normal and hypoxic conditions. *Experimental & Translational Stroke Medicine*, *4*(1), 9. https://doi.org/10.1186/2040-7378-4-9

Linger, R. M. A., Keating, A. K., Earp, H. S., & Graham, D. K. (2008). TAM receptor tyrosine kinases: biologic functions, signaling, and potential therapeutic targeting in human cancer. *Advances in Cancer Research*, *100*, 35–83. https://doi.org/10.1016/S0065-230X(08)00002-X

Liu, H., Yang, H., Wang, D., Liu, Y., Liu, X., Li, Y., … Wang, G. (2009). Insulin regulates P-glycoprotein in rat brain microvessel endothelial cells via an insulin receptor-mediated PKC/NF-κB pathway but not a PI3K/Akt pathway. *European Journal of Pharmacology*, *602*(2–3), 277–282. https://doi.org/10.1016/j.ejphar.2008.11.026

Liu, K., Doms, R. W., & Lee, V. M.-Y. (2002). Glu11 site cleavage and N-terminally truncated A beta production upon BACE overexpression. *Biochemistry*, *41*(9), 3128–3136. Retrieved from http://www.ncbi.nlm.nih.gov/pubmed/11863452

Liu, L., Wang, J., Zhao, L., Nilsen, J., McClure, K., Wong, K., & Brinton, R. D. (2009). Progesterone Increases Rat Neural Progenitor Cell Cycle Gene Expression and Proliferation Via Extracellularly Regulated Kinase and Progesterone Receptor Membrane Components 1 and 2. *Endocrinology*, *150*(7), 3186–3196. https://doi.org/10.1210/en.2008-1447

Lord, G. M., Matarese, G., Howard, J. K., Baker, R. J., Bloom, S. R., & Lechler, R. I. (1998). Leptin modulates the T-cell immune response and reverses starvation-induced immunosuppression. *Nature*, *394*(6696), 897–901. https://doi.org/10.1038/29795

Loskutova, N., Honea, R. A., Brooks, W. M., & Burns, J. M. (2010). Reduced Limbic and Hypothalamic Volumes Correlate with Bone Density in Early Alzheimer's Disease. *Journal of Alzheimer's Disease*, *20*(1), 313–322. https://doi.org/10.3233/JAD-2010-1364

Lu, D. C., Rabizadeh, S., Chandra, S., Shayya, R. F., Ellerby, L. M., Ye, X., … Bredesen, D. E. (2000). A second cytotoxic proteolytic peptide derived from amyloid β-proteinprecursor. *Nature Medicine*, *6*(4), 397–404. https://doi.org/10.1038/74656

Lu, D. C., Soriano, S., Bredesen, D. E., & Koo, E. H. (2003). Caspase cleavage of the amyloid precursor protein modulates amyloid β-protein toxicity. *Journal of Neurochemistry*, *87*(3), 733–741. https://doi.org/10.1046/j.1471-4159.2003.02059.x

Lu, M., Sarruf, D. A., Talukdar, S., Sharma, S., Li, P., Bandyopadhyay, G., … Olefsky, J. M. (2011). Brain PPAR-γ promotes obesity and is required for the insulin–sensitizing effect of thiazolidinediones. *Nature Medicine*, *17*(5), 618–622. https://doi.org/10.1038/nm.2332

Lund, I. K., Hansen, J. A., Andersen, H. S., Møller, N. P. H., & Billestrup, N. (2005). Mechanism of protein tyrosine phosphatase 1B-mediated inhibition of leptin signalling. *Journal of Molecular Endocrinology*, *34*(2), 339–351. https://doi.org/10.1677/jme.1.01694

Luo, Y., Bolon, B., Kahn, S., Bennett, B. D., Babu-Khan, S., Denis, P., … Vassar, R. (2001). Mice deficient in BACE1, the Alzheimer's β-secretase, have normal phenotype and abolished β-amyloid generation. *Nature Neuroscience*, *4*(3), 231–232. https://doi.org/10.1038/85059

Luo, Y., Koles, K., Vorndam, W., Haltiwanger, R. S., & Panin, V. M. (2006). Protein *O* -Fucosyltransferase 2 Adds *O* -Fucose to Thrombospondin Type 1 Repeats. *Journal of Biological Chemistry*, *281*(14), 9393–9399. https://doi.org/10.1074/jbc.M511975200

Luo, Y., Nita-Lazar, A., & Haltiwanger, R. S. (2006). Two Distinct Pathways for *O* -Fucosylation of Epidermal Growth Factor-like or Thrombospondin Type 1 Repeats. *Journal of Biological Chemistry*, *281*(14), 9385–9392. https://doi.org/10.1074/jbc.M511974200

Lv, X., Li, W., Luo, Y., Wang, D., Zhu, C., Huang, Z.-X., & Tan, X. (2013). Exploring the differences between mouse mAβ1–42 and human hAβ1–42 for Alzheimer's disease related properties and neuronal cytotoxicity. *Chemical Communications*, *49*(52), 5865. https://doi.org/10.1039/c3cc40779a

Ly, P. T. T., Wu, Y., Zou, H., Wang, R., Zhou, W., Kinoshita, A., … Song, W. (2013). Inhibition of GSK3β-mediated BACE1 expression reduces Alzheimer-associated phenotypes. *The Journal of Clinical Investigation*, *123*(1), 224–235. https://doi.org/10.1172/JCI64516

Ma, J., Yan, R., Zu, X., Cheng, J.-M., Rao, K., Liao, D.-F., & Cao, D. (2008). Aldo-keto reductase family 1 B10 affects fatty acid synthesis by regulating the stability of acetyl-CoA carboxylase-alpha in breast cancer cells. *The Journal of Biological Chemistry*, *283*(6), 3418–3423. https://doi.org/10.1074/jbc.M707650200

Mackay ', E. A., Ehrhard ', A., Moniatte', M., Guenet', C., Tardif', C., Tarnus ', C., … Mamont', P. (1997). *A possible role for cathepsins D, E, and B in the processing of P-amyloid precursor protein in Alzheimer's disease*. *Eur. J. Biochem* (Vol. 244). Retrieved from https://febs.onlinelibrary.wiley.com/doi/pdf/10.1111/j.1432-1033.1997.00414.x

Maes, E., Hadiwikarta, W. W., Mertens, I., Baggerman, G., Hooyberghs, J., & Valkenborg, D. (2016). CONSTANd : A Normalization Method for Isobaric Labeled Spectra by Constrained Optimization. *Molecular & Cellular Proteomics*, *15*(8), 2779–2790. https://doi.org/10.1074/mcp.M115.056911

Maioli, S., Lodeiro, M., Merino-Serrais, P., Falahati, F., Khan, W., Puerta, E., … Alzheimer's Disease Neuroimaging Initiative. (2015). Alterations in brain leptin signalling in spite of unchanged CSF leptin levels in Alzheimer's disease. *Aging Cell*, *14*(1), 122–129. https://doi.org/10.1111/acel.12281

Malekizadeh, Y., Holiday, A., Redfearn, D., Ainge, J. A., Doherty, G., & Harvey, J. (2017). A Leptin Fragment Mirrors the Cognitive Enhancing and Neuroprotective Actions of Leptin. *Cerebral Cortex*, *27*(10), 4769–4782. https://doi.org/10.1093/cercor/bhw272

Mandai, K., Nakanishi, H., Satoh, A., Takahashi, K., Satoh, K., Nishioka, H., … Takai, Y. (1999). Ponsin/SH3P12: an l-afadin- and vinculin-binding protein localized at cell-cell and cell-matrix adherens junctions. *The Journal of Cell Biology*, *144*(5), 1001–1017. Retrieved from http://www.ncbi.nlm.nih.gov/pubmed/10085297

Marquez-Sterling, N. R., Lo, A. C., Sisodia, S. S., & Koo, E. H. (1997). Trafficking of cell-surface beta-amyloid precursor protein: evidence that a sorting intermediate participates in synaptic vesicle recycling. *The Journal of Neuroscience : The Official Journal of the Society for Neuroscience*, *17*(1), 140–151. Retrieved from http://www.ncbi.nlm.nih.gov/pubmed/8987743

Mars, R. B., & Grol, M. J. (2007). Dorsolateral prefrontal cortex, working memory, and prospective coding for action. *The Journal of Neuroscience : The Official Journal of the Society for Neuroscience*, *27*(8), 1801–1802. https://doi.org/10.1523/JNEUROSCI.5344-06.2007

Martin, H.-J., & Maser, E. (2009). Role of human aldo–keto-reductase AKR1B10 in the protection against toxic aldehydes. *Chemico-Biological Interactions*, *178*(1–3), 145–150. https://doi.org/10.1016/J.CBI.2008.10.021

Maruyama, M., Arai, H., Sugita, M., Tanji, H., Higuchi, M., Okamura, N., … Sasaki, H. (2001). Cerebrospinal Fluid Amyloid β1–42 Levels in the Mild Cognitive Impairment Stage of Alzheimer's Disease. *Experimental Neurology*, *172*(2), 433–436. https://doi.org/10.1006/EXNR.2001.7814

Marwarha, G., Dasari, B., Prasanthi, J. R. P., Schommer, J., & Ghribi, O. (2010). Leptin reduces the accumulation of Abeta and phosphorylated tau induced by 27-hydroxycholesterol in rabbit organotypic slices. *Journal of Alzheimer's Disease : JAD*, *19*(3), 1007–1019. https://doi.org/10.3233/JAD-2010-1298

Matus, A., Ackermann, M., Pehling, G., Byers, H. R., & Fujiwara, K. (1982). High actin concentrations in brain dendritic spines and postsynaptic densities. *Proceedings of the National Academy of Sciences of the United States of America*, *79*(23), 7590–7594. https://doi.org/10.1073/pnas.79.23.7590

Mavrakis, M., Azou-Gros, Y., Tsai, F.-C., Alvarado, J., Bertin, A., Iv, F., … Lecuit, T. (2014). Septins promote F-actin ring formation by crosslinking actin filaments into curved bundles. *Nature Cell Biology*, *16*(4), 322–334. https://doi.org/10.1038/ncb2921

Maximov, A., Tang, T. S., & Bezprozvanny, I. (2003). Association of the type 1 inositol (1,4,5)-trisphosphate receptor with 4.1N protein in neurons. *Molecular and Cellular Neurosciences*, *22*(2), 271–283. Retrieved from http://www.ncbi.nlm.nih.gov/pubmed/12676536

May, P. C., Dean, R. A., Lowe, S. L., Martenyi, F., Sheehan, S. M., Boggs, L. N., … Audia, J. E. (2011). Robust central reduction of amyloid-β in humans with an orally available, non-peptidic β-secretase inhibitor. *Journal of Neuroscience*, *31*(46), 16507–16516.

https://doi.org/10.1523/JNEUROSCI.3647-11.2011
Mayorquin, L. C., Rodriguez, A. V., Sutachan, J., & Albarracín, S. L. (2018). Connexin-Mediated Functional and Metabolic Coupling Between Astrocytes and Neurons. *Frontiers in Molecular Neuroscience*, *11*, 118. https://doi.org/10.3389/fnmol.2018.00118
McDuff, T., & Sumi, S. M. (1985). Subcortical degeneration in Alzheimer's disease. *Neurology*, *35*(1), 123–126. Retrieved from http://www.ncbi.nlm.nih.gov/pubmed/3917560
McEwen, B. S. (1999). Stress and Hippocampal Plasticity. *Annual Review of Neuroscience*, *22*(1), 105–122. https://doi.org/10.1146/annurev.neuro.22.1.105
McGrath, L. T., McGleenon, B. M., Brennan, S., McColl, D., McILroy, S., & Passmore, A. P. (2001). Increased oxidative stress in Alzheimer's disease as assessed with 4-hydroxynonenal but not malondialdehyde. *QJM : Monthly Journal of the Association of Physicians*, *94*(9), 485–490. Retrieved from http://www.ncbi.nlm.nih.gov/pubmed/11528012
Meakin, P. J., Harper, A. J., Hamilton, D. L., Gallagher, J., McNeilly, A. D., Burgess, L. A., … Ashford, M. L. J. (2012). Reduction in BACE1 decreases body weight, protects against diet-induced obesity and enhances insulin sensitivity in mice. *The Biochemical Journal*, *441*(1), 285–296. https://doi.org/10.1042/BJ20110512
Meakin, P. J., Jalicy, S. M., Montagut, G., Allsop, D. J. P., Cavellini, D. L., Irvine, S. W., … Ashford, M. L. J. (2018). Bace1-dependent amyloid processing regulates hypothalamic leptin sensitivity in obese mice. *Scientific Reports*, *8*(1), 55. https://doi.org/10.1038/s41598-017-18388-6
Meakin, P. J., Mezzapesa, A., Benabou, E., Haas, M. E., Bonardo, B., Grino, M., … Peiretti, F. (2018). The beta secretase BACE1 regulates the expression of insulin receptor in the liver. *Nature Communications*, *9*(1), 1306. https://doi.org/10.1038/s41467-018-03755-2
Mei, L., & Xiong, W.-C. (2008). Neuregulin 1 in neural development, synaptic plasticity and schizophrenia. *Nature Reviews Neuroscience*, *9*(6), 437–452. https://doi.org/10.1038/nrn2392
Mellon, P. L., Windle, I., Goldsmith, P. C., Padula, C. A., Roberts, J. L., & Weiner+, R. I. (1990). *Immortalization of Hypothalamic GnRH Neurons by Genetically Targeted Tumorigenesis*. *Neuron* (Vol. 5). Retrieved from https://www.cell.com/neuron/pdf/0896-6273(90)90028-E.pdf?_returnURL=https%3A%2F%2Flinkinghub.elsevier.com%2Fretrieve%2Fpii%2F089662739090028E%3Fshowall%3Dtrue
Mercer, J. G., Hoggard, N., Williams, L. M., Lawrence, C. B., Hannah, L. T., & Trayhurn, P. (1996). Localization of leptin receptor mRNA and the long form splice variant (Ob-Rb) in mouse hypothalamus and adjacent brain regions by in situ hybridization. *FEBS Letters*, *387*(2–3), 113–116. https://doi.org/10.1016/0014-5793(96)00473-5
Miller, A. A., & Spencer, S. J. (2014). Obesity and neuroinflammation: A pathway to cognitive impairment. *Brain, Behavior, and Immunity*, *42*, 10–21. https://doi.org/10.1016/j.bbi.2014.04.001
Milner, T. A., Lee, A., Aicher, S. A., & Rosin, D. L. (1998). Hippocampal beta2A-adrenergic receptors are located predominantly presynaptically but are also found postsynaptically and in selective astrocytes. *The Journal of Comparative Neurology*, *395*(3), 310–327. https://doi.org/10.1002/(SICI)1096-9861(19980808)395:3<310::AID-CNE4>3.0.CO;2-5

Mohandas, N., Jap, B. K., Han, B.-G., Nunomura, W., & Takakuwa, Y. (2000). Protein 4.1R core domain structure and insights into regulation of cytoskeletal organization. *Nature Structural Biology*, *7*(10), 871–875. https://doi.org/10.1038/82819

Moir, R. D., Lathe, R., & Tanzi, R. E. (2018). The antimicrobial protection hypothesis of Alzheimer's disease. *Alzheimer's & Dementia*, *14*(12), 1602–1614. https://doi.org/10.1016/j.jalz.2018.06.3040

Montague, C. T., Prins, J. B., Sanders, L., Digby, J. E., & O'rahilly, S. (1997). *Depot-and Sex-Specific Differences in Human Leptin mRNA Expression Implications for the Control of Regional Fat Distribution*. *Diabetes* (Vol. 46). Retrieved from http://diabetes.diabetesjournals.org/content/diabetes/46/3/342.full.pdf?casa_token=G9glRjMFBRgAAAAA:8b_Y7DclKwrlJFvrbiidLDBLXEzKqr6G3cGEikIt8f2w9sfBqT8jx0dWwcqGqw34kpjJk5iVzUWaV0E

Moore, D. B., Gillentine, M. A., Botezatu, N. M., Wilson, K. A., Benson, A. E., & Langeland, J. A. (2014a). Asynchronous Evolutionary Origins of Aβ and BACE1. *Molecular Biology and Evolution*, *31*(3), 696–702. https://doi.org/10.1093/molbev/mst262

Moore, D. B., Gillentine, M. A., Botezatu, N. M., Wilson, K. A., Benson, A. E., & Langeland, J. A. (2014b). Asynchronous Evolutionary Origins of Aβ and BACE1. *Molecular Biology and Evolution*, *31*(3), 696–702. https://doi.org/10.1093/molbev/mst262

Moran, C., Beare, R., Phan, T. G., Bruce, D. G., Callisaya, M. L., Srikanth, V., & Alzheimer's Disease Neuroimaging Initiative (ADNI). (2015). Type 2 diabetes mellitus and biomarkers of neurodegeneration. *Neurology*, *85*(13), 1123–1130. https://doi.org/10.1212/WNL.0000000000001982

Mori, H., Takio, K., Ogawara, M., & Selkoe, D. J. (1992). Mass spectrometry of purified amyloid beta protein in Alzheimer's disease. *The Journal of Biological Chemistry*, *267*(24), 17082–17086. Retrieved from http://www.ncbi.nlm.nih.gov/pubmed/1512246

Morioka, T., Asilmaz, E., Hu, J., Dishinger, J. F., Kurpad, A. J., Elias, C. F., … Kulkarni, R. N. (2007). Disruption of leptin receptor expression in the pancreas directly affects beta cell growth and function in mice. *The Journal of Clinical Investigation*, *117*(10), 2860–2868. https://doi.org/10.1172/JCI30910

Moult, P. R., Cross, A., Santos, S. D., Carvalho, A.-L., Lindsay, Y., Connolly, C. N., … Harvey, J. (2010). Leptin Regulates AMPA Receptor Trafficking via PTEN Inhibition. *Journal of Neuroscience*, *30*(11), 4088–4101. https://doi.org/10.1523/JNEUROSCI.3614-09.2010

Moult, P. R., Milojkovic, B., & Harvey, J. (2009). Leptin reverses long-term potentiation at hippocampal CA1 synapses. *Journal of Neurochemistry*, *108*(3), 685–696. https://doi.org/10.1111/j.1471-4159.2008.05810.x

Mounzih, K., Lu, R., & Chehab, F. F. (1997). Leptin Treatment Rescues the Sterility of Genetically Obese ob/ob Males. *Endocrinology*, *138*(3), 1190–1193. https://doi.org/10.1210/endo.138.3.5024

Mouton-Liger, F., Paquet, C., Dumurgier, J., Bouras, C., Pradier, L., Gray, F., & Hugon, J. (2012). Oxidative stress increases BACE1 protein levels through activation of the PKR-eIF2α pathway. *Biochimica et Biophysica Acta (BBA) - Molecular Basis of Disease*, *1822*(6), 885–896. https://doi.org/10.1016/J.BBADIS.2012.01.009

Mowrer, K. R., & Wolfe, M. S. (2008). Promotion of BACE1 mRNA Alternative Splicing Reduces Amyloid β-Peptide Production. *Journal of Biological*

Chemistry, *283*(27), 18694–18701. https://doi.org/10.1074/jbc.M801322200

Mueller-Steiner, S., Zhou, Y., Arai, H., Roberson, E. D., Sun, B., Chen, J., … Gan, L. (2006). Antiamyloidogenic and neuroprotective functions of cathepsin B: implications for Alzheimer's disease. *Neuron*, *51*(6), 703–714. https://doi.org/10.1016/j.neuron.2006.07.027

Müller, T., Meyer, H. E., Egensperger, R., & Marcus, K. (2008). The amyloid precursor protein intracellular domain (AICD) as modulator of gene expression, apoptosis, and cytoskeletal dynamics—Relevance for Alzheimer's disease. *Progress in Neurobiology*, *85*(4), 393–406. https://doi.org/10.1016/J.PNEUROBIO.2008.05.002

Murphy, T., Yip, A., Brayne, C., Easton, D., Evans, J. G., Xuereb, J., … Rubinsztein, D. C. (2001). The BACE gene: genomic structure and candidate gene study in late-onset Alzheimer's disease. *Neuroreport*, *12*(3), 631–634. Retrieved from http://www.ncbi.nlm.nih.gov/pubmed/11234778

Müssig, K., Staiger, H., Fiedler, H., Moeschel, K., Beck, A., Kellerer, M., & Häring, H.-U. (2005). Shp2 is required for protein kinase C-dependent phosphorylation of serine 307 in insulin receptor substrate-1. *The Journal of Biological Chemistry*, *280*(38), 32693–32699. https://doi.org/10.1074/jbc.M506549200

Myers, M. G., Mendez, R., Shi, P., Pierce, J. H., Rhoads, R., & White, M. F. (1998). The COOH-terminal tyrosine phosphorylation sites on IRS-1 bind SHP-2 and negatively regulate insulin signaling. *The Journal of Biological Chemistry*, *273*(41), 26908–26914. https://doi.org/10.1074/JBC.273.41.26908

Nagy, A., Rossant, J., Nagy, R., Abramow-Newerly, W., Roder, J. C., Zhang, W., … Südhof, T. C. (1993). Derivation of completely cell culture-derived mice from early-passage embryonic stem cells. *Proceedings of the National Academy of Sciences*, *90*(18), 8424–8428. https://doi.org/10.1073/pnas.90.18.8424

Nagy, T. R., Gower, B. A., Trowbridge, C. A., Dezenberg, C., Shewchuk, R. M., & Goran, M. I. (1997). Effects of Gender, Ethnicity, Body Composition, and Fat Distribution on Serum Leptin Concentrations in Children. *The Journal of Clinical Endocrinology & Metabolism*, *82*(7), 2148–2152. https://doi.org/10.1210/jcem.82.7.4077

Nakamura, T., Nakamura, K., Lasser-Ross, N., Barbara, J. G., Sandler, V. M., & Ross, W. N. (2000). Inositol 1,4,5-trisphosphate (IP3)-mediated Ca2+ release evoked by metabotropic agonists and backpropagating action potentials in hippocampal CA1 pyramidal neurons. *The Journal of Neuroscience : The Official Journal of the Society for Neuroscience*, *20*(22), 8365–8376. Retrieved from http://www.ncbi.nlm.nih.gov/pubmed/11069943

Nakanishi, H., Tominaga, K., Amano, T., Hirotsu, I., Inoue, T., & Yamamoto, K. (1994). Age-Related Changes in Activities and Localizations of Cathepsins D, E, B, and L in the Rat Brain Tissues. *Experimental Neurology*, *126*(1), 119–128. https://doi.org/10.1006/exnr.1994.1048

Nakatsu, F., Baskin, J. M., Chung, J., Tanner, L. B., Shui, G., Lee, S. Y., … De Camilli, P. (2012). PtdIns4P synthesis by PI4KIIIα at the plasma membrane and its impact on plasma membrane identity. *The Journal of Cell Biology*, *199*(6), 1003–1016. https://doi.org/10.1083/jcb.201206095

Nam, S.-Y., Kratzsch, J., Wook Kim, K., Rae Kim, K., Lim, S.-K., & Marcus, C. (2001). Cerebrospinal Fluid and Plasma Concentrations of Leptin, NPY, andα -MSH in Obese Women and Their Relationship to Negative Energy

Balance. *The Journal of Clinical Endocrinology & Metabolism*, *86*(10), 4849–4853. https://doi.org/10.1210/jcem.86.10.7939

Narita, K., Kosaka, H., Okazawa, H., Murata, T., & Wada, Y. (2009). Relationship Between Plasma Leptin Level and Brain Structure in Elderly: A Voxel-Based Morphometric Study. *Biological Psychiatry*, *65*(11), 992–994. https://doi.org/10.1016/j.biopsych.2008.10.006

Nelson, P. T., Dickson, D. W., Trojanowski, J. Q., Jack, C. R., Boyle, P. A., Arfanakis, K., … Schneider, J. A. (2019). Limbic-predominant age-related TDP-43 encephalopathy (LATE): consensus working group report. *Brain*. https://doi.org/10.1093/brain/awz099

Neth, B. J., & Craft, S. (2017). Insulin Resistance and Alzheimer's Disease: Bioenergetic Linkages. *Frontiers in Aging Neuroscience*, *9*, 345. https://doi.org/10.3389/fnagi.2017.00345

Ng, A., Uribe, R. A., Yieh, L., Nuckels, R., & Gross, J. M. (2009). Zebrafish mutations in gart and paics identify crucial roles for de novo purine synthesis in vertebrate pigmentation and ocular development. *Development (Cambridge, England)*, *136*(15), 2601–2611. https://doi.org/10.1242/dev.038315

Nguyen, J. C. D., Killcross, A. S., & Jenkins, T. A. (2014). Obesity and cognitive decline: role of inflammation and vascular changes. *Frontiers in Neuroscience*, *8*, 375. https://doi.org/10.3389/fnins.2014.00375

Nichols, B. (2003). Caveosomes and endocytosis of lipid rafts. *Journal of Cell Science*, *116*(Pt 23), 4707–4714. https://doi.org/10.1242/jcs.00840

Niedowicz, D. M., Reeves, V. L., Platt, T. L., Kohler, K., Beckett, T. L., Powell, D. K., … Murphy, M. P. (2014). Obesity and diabetes cause cognitive dysfunction in the absence of accelerated β-amyloid deposition in a novel murine model of mixed or vascular dementia. *Acta Neuropathologica Communications*, *2*(1), 64. https://doi.org/10.1186/2051-5960-2-64

Nijenhuis, W. A. J., Oosterom, J., & Adan, R. A. H. (2001). AgRP(83–132) Acts as an Inverse Agonist on the Human-Melanocortin-4 Receptor. *Molecular Endocrinology*, *15*(1), 164–171. https://doi.org/10.1210/mend.15.1.0578

Nikolaev, A., McLaughlin, T., O'Leary, D. D. M., & Tessier-Lavigne, M. (2009). APP binds DR6 to trigger axon pruning and neuron death via distinct caspases. *Nature*, *457*(7232), 981–989. https://doi.org/10.1038/nature07767

Nishioka, H., Mizoguchi, A., Nakanishi, H., Mandai, K., Takahashi, K., Kimura, K., … Takai, Y. (2000). Localization of l-afadin at puncta adhaerentia-like junctions between the mossy fiber terminals and the dendritic trunks of pyramidal cells in the adult mouse hippocampus. *The Journal of Comparative Neurology*, *424*(2), 297–306. Retrieved from http://www.ncbi.nlm.nih.gov/pubmed/10906704

Nistor, M., Don, M., Parekh, M., Sarsoza, F., Goodus, M., Lopez, G. E., … Head, E. (2007). Alpha- and beta-secretase activity as a function of age and beta-amyloid in Down syndrome and normal brain. *Neurobiology of Aging*, *28*(10), 1493–1506. https://doi.org/10.1016/j.neurobiolaging.2006.06.023

Niswender, K. D., Morton, G. J., Stearns, W. H., Rhodes, C. J., Myers, M. G., & Schwartz, M. W. (2001). Key enzyme in leptin-induced anorexia. *Nature*, *413*(6858), 794–795. https://doi.org/10.1038/35101657

Nomura, I., Takechi, H., & Kato, N. (2012). Intraneuronally injected amyloid beta inhibits long-term potentiation in rat hippocampal slices. *Journal of Neurophysiology*, *107*(9), 2526–2531.

https://doi.org/10.1152/jn.00589.2011
Nordstedt, C., Caporaso, G. L., Thyberg, J., Gandy, S. E., & Greengard, P. (1993). Identification of the Alzheimer beta/A4 amyloid precursor protein in clathrin-coated vesicles purified from PC12 cells. *The Journal of Biological Chemistry*, *268*(1), 608–612. Retrieved from http://www.ncbi.nlm.nih.gov/pubmed/8416966
Nowotny, P., Kwon, J. M., Chakraverty, S., Nowotny, V., Morris, J. C., & Goate, A. M. (2001). Association studies using novel polymorphisms in BACE1 and BACE2. *Neuroreport*, *12*(9), 1799–1802. Retrieved from http://www.ncbi.nlm.nih.gov/pubmed/11435901
O'Connor, T., Sadleir, K. R., Maus, E., Velliquette, R. A., Zhao, J., Cole, S. L., … Vassar, R. (2008). Phosphorylation of the translation initiation factor eIF2alpha increases BACE1 levels and promotes amyloidogenesis. *Neuron*, *60*(6), 988–1009. https://doi.org/10.1016/j.neuron.2008.10.047
Oania, R., & McEvoy, L. K. (2015). Plasma leptin levels are not predictive of dementia in patients with mild cognitive impairment. *Age and Ageing*, *44*(1), 53–58. https://doi.org/10.1093/ageing/afu160
Ohba, C., Okamoto, N., Murakami, Y., Suzuki, Y., Tsurusaki, Y., Nakashima, M., … Saitsu, H. (2014). PIGN mutations cause congenital anomalies, developmental delay, hypotonia, epilepsy, and progressive cerebellar atrophy. *Neurogenetics*, *15*(2), 85–92. https://doi.org/10.1007/s10048-013-0384-7
Okumura, M., Kadokura, H., & Inaba, K. (2015). Structures and functions of protein disulfide isomerase family members involved in proteostasis in the endoplasmic reticulum. *Free Radical Biology and Medicine*, *83*, 314–322. https://doi.org/10.1016/J.FREERADBIOMED.2015.02.010
Oleskevich, S., Descarries, L., & Lacaille, J. C. (1989). Quantified distribution of the noradrenaline innervation in the hippocampus of adult rat. *The Journal of Neuroscience : The Official Journal of the Society for Neuroscience*, *9*(11), 3803–3815. https://doi.org/10.1523/JNEUROSCI.09-11-03803.1989
Papayannopoulos, V., Metzler, K. D., Hakkim, A., & Zychlinsky, A. (2010). Neutrophil elastase and myeloperoxidase regulate the formation of neutrophil extracellular traps. *The Journal of Cell Biology*, *191*(3), 677–691. https://doi.org/10.1083/jcb.201006052
Pappolla, M. A., Bryant-Thomas, T. K., Herbert, D., Pacheco, J., Fabra Garcia, M., Manjon, M., … Refolo, L. M. (2003). Mild hypercholesterolemia is an early risk factor for the development of Alzheimer amyloid pathology. *Neurology*, *61*(2), 199–205. Retrieved from http://www.ncbi.nlm.nih.gov/pubmed/12874399
Parra, M., Gascard, P., Walensky, L. D., Gimm, J. A., Blackshaw, S., Chan, N., … Conboy, J. G. (2000). Molecular and functional characterization of protein 4.1B, a novel member of the protein 4.1 family with high level, focal expression in brain. *The Journal of Biological Chemistry*, *275*(5), 3247–3255. https://doi.org/10.1074/jbc.275.5.3247
Pasternak, S. H., Bagshaw, R. D., Guiral, M., Zhang, S., Ackerley, C. A., Pak, B. J., … Mahuran, D. J. (2003). Presenilin-1, nicastrin, amyloid precursor protein, and gamma-secretase activity are co-localized in the lysosomal membrane. *The Journal of Biological Chemistry*, *278*(29), 26687–26694. https://doi.org/10.1074/jbc.m304009200
Pastorino, L., Ikin, A. F., Nairn, A. C., Pursnani, A., & Buxbaum, J. D. (2002). The Carboxyl-Terminus of BACE Contains a Sorting Signal That Regulates BACE Trafficking but Not the Formation of Total A.

https://doi.org/10.1006/mcne.2001.1065
Paz-Filho, G. J., Babikian, T., Asarnow, R., Delibasi, T., Esposito, K., Erol, H. K., … Licinio, J. (2008). Leptin replacement improves cognitive development. *PloS One*, *3*(8), e3098. https://doi.org/10.1371/journal.pone.0003098
Pelkmans, L. (2005). Secrets of caveolae-and lipid raft-mediated endocytosis revealed by mammalian viruses. https://doi.org/10.1016/j.bbamcr.2005.06.009
Pellegrini, L., Passer, B. J., Tabaton, M., Ganjei, J. K., & D'Adamio, L. (1999). Alternative, non-secretase processing of Alzheimer's beta-amyloid precursor protein during apoptosis by caspase-6 and -8. *The Journal of Biological Chemistry*, *274*(30), 21011–21016. https://doi.org/10.1074/JBC.274.30.21011
Perez, R. G., Soriano, S., Hayes, J. D., Ostaszewski, B., Xia, W., Selkoe, D. J., … Koo, E. H. (1999). Mutagenesis identifies new signals for beta-amyloid precursor protein endocytosis, turnover, and the generation of secreted fragments, including Abeta42. *The Journal of Biological Chemistry*, *274*(27), 18851–18856. https://doi.org/10.1074/JBC.274.27.18851
Petersen, S. L., Intlekofer, K. A., Moura-Conlon, P. J., Brewer, D. N., Del Pino Sans, J., & Lopez, J. A. (2013). Novel progesterone receptors: neural localization and possible functions. *Frontiers in Neuroscience*, *7*, 164. https://doi.org/10.3389/fnins.2013.00164
Phillips-Krawczak, C. A., Singla, A., Starokadomskyy, P., Deng, Z., Osborne, D. G., Li, H., … Burstein, E. (2015). COMMD1 is linked to the WASH complex and regulates endosomal trafficking of the copper transporter ATP7A. *Molecular Biology of the Cell*, *26*(1), 91–103. https://doi.org/10.1091/mbc.E14-06-1073
Piechotta, A., Parthier, C., Kleinschmidt, M., Gnoth, K., Pillot, T., Lues, I., … Stubbs, M. T. (2017). Structural and functional analyses of pyroglutamate-amyloid-β-specific antibodies as a basis for Alzheimer immunotherapy. *The Journal of Biological Chemistry*, *292*(30), 12713–12724. https://doi.org/10.1074/jbc.M117.777839
Pinteaux, E., Inoue, W., Schmidt, L., Molina-Holgado, F., Rothwell, N. J., & Luheshi, G. N. (2007). Leptin induces interleukin-1β release from rat microglial cells through a caspase 1 independent mechanism. *Journal of Neurochemistry*, *102*(3), 826–833. https://doi.org/10.1111/j.1471-4159.2007.04559.x
Piquet, J., Toussay, X., Hepp, R., Lerchundi, R., Le Douce, J., Faivre, É., … Cauli, B. (2018). Supragranular Pyramidal Cells Exhibit Early Metabolic Alterations in the 3xTg-AD Mouse Model of Alzheimer's Disease. *Frontiers in Cellular Neuroscience*, *12*, 216. https://doi.org/10.3389/fncel.2018.00216
Plant, L. D., Boyle, J. P., Smith, I. F., Peers, C., & Pearson, H. A. (2003). The production of amyloid beta peptide is a critical requirement for the viability of central neurons. *The Journal of Neuroscience : The Official Journal of the Society for Neuroscience*, *23*(13), 5531–5535. https://doi.org/10.1523/JNEUROSCI.23-13-05531.2003
Plucinska, K., Crouch, B., Koss, D., Robinson, L., Siebrecht, M., Riedel, G., & Platt, B. (2014). Knock-In of Human BACE1 Cleaves Murine APP and Reiterates Alzheimer-like Phenotypes. *Journal of Neuroscience*, *34*(32), 10710–10728. https://doi.org/10.1523/JNEUROSCI.0433-14.2014
Plucińska, K., Dekeryte, R., Koss, D., Shearer, K., Mody, N., Whitfield, P. D., … Platt, B. (2016). Neuronal human BACE1 knockin induces systemic

diabetes in mice. *Diabetologia*, *59*(7), 1513–1523. https://doi.org/10.1007/s00125-016-3960-1

Pohle, W., Acosta, L., Rüthrich, H., Krug, M., & Matthies, H. (1987). Incorporation of [3H]fucose in rat hippocampal structures after conditioning by perforant path stimulation and after LTP-producing tetanization. *Brain Research*, *410*(2), 245–256. Retrieved from http://www.ncbi.nlm.nih.gov/pubmed/3594237

Poirier, G. L., Amin, E., Good, M. A., & Aggleton, J. P. (2011). Early-onset dysfunction of retrosplenial cortex precedes overt amyloid plaque formation in Tg2576 mice. *Neuroscience*, *174*, 71–83. https://doi.org/10.1016/j.neuroscience.2010.11.025

Popp, J., Meichsner, S., Kölsch, H., Lewczuk, P., Maier, W., Kornhuber, J., … Lütjohann, D. (2013). Cerebral and extracerebral cholesterol metabolism and CSF markers of Alzheimer's disease. *Biochemical Pharmacology*, *86*(1), 37–42. https://doi.org/10.1016/j.bcp.2012.12.007

Pothuizen, H. H. J., Aggleton, J. P., & Vann, S. D. (2008). Do rats with retrosplenial cortex lesions lack direction? *European Journal of Neuroscience*, *28*(12), 2486–2498. https://doi.org/10.1111/j.1460-9568.2008.06550.x

Power, D. A., Noel, J., Collins, R., & O'Neill, D. (2001). Circulating Leptin Levels and Weight Loss in Alzheimer's Disease Patients. *Dementia and Geriatric Cognitive Disorders*, *12*(2), 167–170. https://doi.org/10.1159/000051252

Prabhu, Y., Burgos, P. V, Schindler, C., Farías, G. G., Magadán, J. G., & Bonifacino, J. S. (2012). Adaptor protein 2-mediated endocytosis of the β-secretase BACE1 is dispensable for amyloid precursor protein processing. *Molecular Biology of the Cell*, *23*(12), 2339–2351. https://doi.org/10.1091/mbc.E11-11-0944

Preece, P., Virley, D. J., Costandi, M., Coombes, R., Moss, S. J., Mudge, A. W., … Cairns, N. J. (2003). β-Secretase (BACE) and GSK-3 mRNA levels in Alzheimer's disease. *Molecular Brain Research*, *116*(1–2), 155–158. https://doi.org/10.1016/S0169-328X(03)00233-X

Prince, M., Knapp, M., Guerchet, M., McCrone, P., Prina, M., Comas-Herrera, A., … Salimkumar, D. (2007). *Dementia UK Second edition - Overview*. London. Retrieved from http://eprints.lse.ac.uk/59437/1/Dementia_UK_Second_edition_-_Overview.pdf

Puglielli, L., Ellis, B. C., Saunders, A. J., & Kovacs, D. M. (2003). Ceramide stabilizes beta-site amyloid precursor protein-cleaving enzyme 1 and promotes amyloid beta-peptide biogenesis. *The Journal of Biological Chemistry*, *278*(22), 19777–19783. https://doi.org/10.1074/jbc.M300466200

Puzzo, D., Privitera, L., Fa', M., Staniszewski, A., Hashimoto, G., Aziz, F., … Arancio, O. (2011). Endogenous amyloid-β is necessary for hippocampal synaptic plasticity and memory. *Annals of Neurology*, *69*(5), 819–830. https://doi.org/10.1002/ana.22313

Qi, H., Prabakaran, S., Cantrelle, F.-X., Chambraud, B., Gunawardena, J., Lippens, G., & Landrieu, I. (2016). Characterization of Neuronal Tau Protein as a Target of Extracellular Signal-regulated Kinase. *Journal of Biological Chemistry*, *291*(14), 7742–7753. https://doi.org/10.1074/jbc.M115.700914

Rangel, L., Lospitao, E., Ruiz-Sáenz, A., Alonso, M. A., & Correas, I. (2017). Alternative polyadenylation in a family of paralogous EPB41 genes generates protein 4.1 diversity. *RNA Biology*, *14*(2), 236.

https://doi.org/10.1080/15476286.2016.1270003

Ratter, J. M., Rooijackers, H. M. M., Tack, C. J., Hijmans, A. G. M., Netea, M. G., De Galan, B. E., & Stienstra, R. (2017). *Pro-inflammatory effects of hypoglycemia in humans with or without diabetes Running title: Pro-inflammatory effects of hypoglycemia*. Retrieved from http://diabetes.diabetesjournals.org/content/diabetes/early/2017/01/19/db16-1091.full.pdf

Rehker, J., Rodhe, J., Nesbitt, R. R., Boyle, E. A., Martin, B. K., Lord, J., … Brkanac, Z. (2017). Caspase-8, association with Alzheimer's Disease and functional analysis of rare variants. *PLOS ONE*, *12*(10), e0185777. https://doi.org/10.1371/journal.pone.0185777

Renner, M., Lacor, P. N., Velasco, P. T., Xu, J., Contractor, A., Klein, W. L., & Triller, A. (2010). Deleterious Effects of Amyloid β Oligomers Acting as an Extracellular Scaffold for mGluR5. *Neuron*, *66*(5), 739–754. https://doi.org/10.1016/j.neuron.2010.04.029

Rinaldi, F., Hartfield, E. M., Crompton, L. A., Badger, J. L., Glover, C. P., Kelly, C. M., … Caldwell, M. A. (2014). Cross-regulation of Connexin43 and β-catenin influences differentiation of human neural progenitor cells. *Cell Death & Disease*, *5*(1), e1017–e1017. https://doi.org/10.1038/cddis.2013.546

Roberds, S. L., Anderson, J., Basi, G., Bienkowski, M. J., Branstetter, D. G., Chen, K. S., … McConlogue, L. (2001). BACE knockout mice are healthy despite lacking the primary beta-secretase activity in brain: implications for Alzheimer's disease therapeutics. *Human Molecular Genetics*, *10*(12), 1317–1324. https://doi.org/10.1093/hmg/10.12.1317

Rogers, G. W., Edelman, G. M., & Mauro, V. P. (2004). Differential utilization of upstream AUGs in the -secretase mRNA suggests that a shunting mechanism regulates translation. *Proceedings of the National Academy of Sciences*, *101*(9), 2794–2799. https://doi.org/10.1073/pnas.0308576101

Roux, K. J., Kim, D. I., Raida, M., & Burke, B. (2012). A promiscuous biotin ligase fusion protein identifies proximal and interacting proteins in mammalian cells. *The Journal of Cell Biology*, *196*(6), 801–810. https://doi.org/10.1083/jcb.201112098

Russell, C. D., Petersen, R. N., Rao, S. P., Ricci, M. R., Prasad, A., Zhang, Y., … Fried, S. K. (1998). Leptin expression in adipose tissue from obese humans: depot-specific regulation by insulin and dexamethasone. *American Journal of Physiology-Endocrinology and Metabolism*, *275*(3), E507–E515. https://doi.org/10.1152/ajpendo.1998.275.3.E507

Russo, C., Violani, E., Salis, S., Venezia, V., Dolcini, V., Damonte, G., … Schettini, G. (2002). Pyroglutamate-modified amyloid beta-peptides--AbetaN3(pE)--strongly affect cultured neuron and astrocyte survival. *Journal of Neurochemistry*, *82*(6), 1480–1489. Retrieved from http://www.ncbi.nlm.nih.gov/pubmed/12354296

Ruth, M. R., Proctor, S. D., & Field, C. J. (2009). Feeding long-chain n-3 polyunsaturated fatty acids to obese leptin receptor-deficient JCR:LA-cp rats modifies immune function and lipid-raft fatty acid composition. *British Journal of Nutrition*, *101*(09), 1341. https://doi.org/10.1017/S0007114508076277

Ryu, B. R., Ko, H. W., Jou, I., Noh, J. S., & Gwag, B. J. (1999). Phosphatidylinositol 3-kinase-mediated regulation of neuronal apoptosis and necrosis by insulin and IGF-I. *Journal of Neurobiology*, *39*(4), 536–546. Retrieved from http://www.ncbi.nlm.nih.gov/pubmed/10380075

Saeed, A. A., Genové, G., Li, T., Lütjohann, D., Olin, M., Mast, N., … Björkhem, I. (2014). Effects of a disrupted blood-brain barrier on cholesterol homeostasis in the brain. *The Journal of Biological Chemistry*, *289*(34), 23712–23722. https://doi.org/10.1074/jbc.M114.556159

Saftig, P., Peters, C., von Figura, K., Craessaerts, K., Van Leuven, F., & De Strooper, B. (1996). Amyloidogenic processing of human amyloid precursor protein in hippocampal neurons devoid of cathepsin D. *The Journal of Biological Chemistry*, *271*(44), 27241–27244. https://doi.org/10.1074/JBC.271.44.27241

Sambamurti, K., KINSEY, R., MALONEY, B., GE, Y.-W., & LAHIRI, D. K. (2004). Gene structure and organization of the human β-secretase (BACE) promoter. *The FASEB Journal*, *18*(9), 1034–1036. https://doi.org/10.1096/fj.03-1378fje

Sanchez-Alvarez, L., Visanuvimol, J., McEwan, A., Su, A., Imai, J. H., & Colavita, A. (2011). VANG-1 and PRKL-1 Cooperate to Negatively Regulate Neurite Formation in Caenorhabditis elegans. *PLoS Genetics*, *7*(9), e1002257. https://doi.org/10.1371/journal.pgen.1002257

Sankaranarayanan, S., Holahan, M. A., Colussi, D., Crouthamel, M.-C., Devanarayan, V., Ellis, J., … Simon, A. J. (2009). First Demonstration of Cerebrospinal Fluid and Plasma A Lowering with Oral Administration of a -Site Amyloid Precursor Protein-Cleaving Enzyme 1 Inhibitor in Nonhuman Primates. *Journal of Pharmacology and Experimental Therapeutics*, *328*(1), 131–140. https://doi.org/10.1124/jpet.108.143628

Sannerud, R., Declerck, I., Peric, A., Raemaekers, T., Menendez, G., Zhou, L., … Annaert, W. (2011). ADP ribosylation factor 6 (ARF6) controls amyloid precursor protein (APP) processing by mediating the endosomal sorting of BACE1. *Proceedings of the National Academy of Sciences*, *108*(34), E559–E568. https://doi.org/10.1073/pnas.1100745108

Santos-Alvarez, J., Goberna, R., & Sánchez-Margalet, V. (1999). Human Leptin Stimulates Proliferation and Activation of Human Circulating Monocytes. *Cellular Immunology*, *194*(1), 6–11. https://doi.org/10.1006/CIMM.1999.1490

Sarasa, M., & Pesini, P. (2009). Natural Non-Trasgenic Animal Models for Research in Alzheimer's Disease. *Current Alzheimer Research*, *6*(2), 171. https://doi.org/10.2174/156720509787602834

Sasaki, A., Yasukawa, H., Suzuki, A., Kamizono, S., Syoda, T., Kinjyo, I., … Yoshimura, A. (1999). Cytokine-inducible SH2 protein-3 (CIS3/SOCS3) inhibits Janus tyrosine kinase by binding through the N-terminal kinase inhibitory region as well as SH2 domain. *Genes to Cells*, *4*(6), 339–351. https://doi.org/10.1046/j.1365-2443.1999.00263.x

Sastre, M., Dewachter, I., Rossner, S., Bogdanovic, N., Rosen, E., Borghgraef, P., … Heneka, M. T. (2006). Nonsteroidal anti-inflammatory drugs repress β-secretase gene promoter activity by the activation of PPARγ. *Proceedings of the National Academy of Sciences*, *103*(2), 443–448. https://doi.org/10.1073/PNAS.0503839103

Savonenko, A. V, Melnikova, T., Laird, F. M., Stewart, K.-A., Price, D. L., & Wong, P. C. (2008). Alteration of BACE1-dependent NRG1/ErbB4 signaling and schizophrenia-like phenotypes in BACE1-null mice. *Proceedings of the National Academy of Sciences of the United States of America*, *105*(14), 5585–5590. https://doi.org/10.1073/pnas.0710373105

Schaper, F., Gendo, C., Eck, M., Schmitz, J., Grimm, C., Anhuf, D., … Heinrich, P. C. (1998). Activation of the protein tyrosine phosphatase SHP2 via the

interleukin-6 signal transducing receptor protein gp130 requires tyrosine kinase Jak1 and limits acute-phase protein expression. *The Biochemical Journal*, *335 (Pt 3)*(Pt 3), 557–565. https://doi.org/10.1042/bj3350557

Scheller, J., Chalaris, A., Schmidt-Arras, D., & Rose-John, S. (2011). The pro- and anti-inflammatory properties of the cytokine interleukin-6. *Biochimica et Biophysica Acta (BBA) - Molecular Cell Research*, *1813*(5), 878–888. https://doi.org/10.1016/J.BBAMCR.2011.01.034

Schilling, S., Zeitschel, U., Hoffmann, T., Heiser, U., Francke, M., Kehlen, A., … Rossner, S. (2008). Glutaminyl cyclase inhibition attenuates pyroglutamate Aβ and Alzheimer's disease–like pathology. *Nature Medicine*, *14*(10), 1106–1111. https://doi.org/10.1038/nm.1872

Schneider, A., Rajendran, L., Honsho, M., Gralle, M., Donnert, G., Wouters, F., … Simons, M. (2008). Flotillin-Dependent Clustering of the Amyloid Precursor Protein Regulates Its Endocytosis and Amyloidogenic Processing in Neurons. *Journal of Neuroscience*, *28*(11), 2874–2882. https://doi.org/10.1523/JNEUROSCI.5345-07.2008

Schneider, M., Al-Shareffi, E., & Haltiwanger, R. S. (2017). Biological functions of fucose in mammals. *Glycobiology*, *27*(7), 601–618. https://doi.org/10.1093/glycob/cwx034

Schoonenboom, N. S., Mulder, C., Van Kamp, G. J., Mehta, S. P., Scheltens, P., Blankenstein, M. A., & Mehta, P. D. (2005). Amyloid 38, 40, and 42 Species in Cerebrospinal Fluid: More of the Same? https://doi.org/10.1002/ana.20508

Schürks, M., Buring, J. E., Ridker, P. M., Chasman, D. I., & Kurth, T. (2011). Genetic Determinants of Cardiovascular Events among Women with Migraine: A Genome-Wide Association Study. *PLoS ONE*, *6*(7), e22106. https://doi.org/10.1371/journal.pone.0022106

Schwartz, M. W., Peskind, E., Raskind, M., Boyko, E. J., & Porte, D. (1996). Cerebrospinal fluid leptin levels: Relationship to plasma levels and to adiposity in humans. *Nature Medicine*, *2*(5), 589–593. https://doi.org/10.1038/nm0596-589

Scott, C., Keating, L., Bellamy, M., & Baines, A. J. (2001). Protein 4.1 in forebrain postsynaptic density preparations. *European Journal of Biochemistry*, *268*(4), 1084–1094. https://doi.org/10.1046/j.1432-1327.2001.01968.x

Seabrook, G. R., Smith, D. W., Bowery, B. J., Easter, A., Reynolds, T., Fitzjohn, S. M., … Hill, R. G. (1999). Mechanisms contributing to the deficits in hippocampal synaptic plasticity in mice lacking amyloid precursor protein. *Neuropharmacology*, *38*(3), 349–359. Retrieved from http://www.ncbi.nlm.nih.gov/pubmed/10219973

Sezgin, E., Levental, I., & Eggeling, C. (2017). Liquid-liquid phase separation The mystery of membrane organization: composition, regulation and roles of lipid rafts. *NATURE REVIEWS | MOLECULAR CELL BIOLOGY*, *18*, 361. https://doi.org/10.1038/nrm.2017.16

Shaheen, R., Szymanska, K., Basu, B., Patel, N., Ewida, N., Faqeih, E., … Alkuraya, F. S. (2016). Characterizing the morbid genome of ciliopathies. *Genome Biology*, *17*(1), 242. https://doi.org/10.1186/s13059-016-1099-5

Shanley, L. J., Irving, A. J., & Harvey, J. (2001). Leptin enhances NMDA receptor function and modulates hippocampal synaptic plasticity. *The Journal of Neuroscience : The Official Journal of the Society for Neuroscience*, *21*(24), RC186. https://doi.org/10.1523/JNEUROSCI.21-24-J0001.2001

Shao, L., Moloney, D. J., & Haltiwanger, R. (2003). Fringe Modifies *O* -Fucose on Mouse Notch1 at Epidermal Growth Factor-like Repeats within the Ligand-binding Site and the Abruptex Region. *Journal of Biological Chemistry*, *278*(10), 7775–7782. https://doi.org/10.1074/jbc.M212221200

Sharma, A. N., Elased, K. M., Garrett, T. L., & Lucot, J. B. (2010). Neurobehavioral deficits in db/db diabetic mice. *Physiology & Behavior*, *101*(3), 381–388. https://doi.org/10.1016/j.physbeh.2010.07.002

Sharman, M. J., Moussavi Nik, S. H., Chen, M. M., Ong, D., Wijaya, L., Laws, S. M., … Verdile, G. (2013). The Guinea Pig as a Model for Sporadic Alzheimer's Disease (AD): The Impact of Cholesterol Intake on Expression of AD-Related Genes. *PLoS ONE*, *8*(6), e66235. https://doi.org/10.1371/journal.pone.0066235

Shen, L., Liang, F., Walensky, L. D., & Huganir, R. L. (2000). Regulation of AMPA receptor GluR1 subunit surface expression by a 4. 1N-linked actin cytoskeletal association. *The Journal of Neuroscience : The Official Journal of the Society for Neuroscience*, *20*(21), 7932–7940. https://doi.org/10.1523/JNEUROSCI.20-21-07932.2000

Shepardson, N. E., Shankar, G. M., & Selkoe, D. J. (2011). Cholesterol Level and Statin Use in Alzheimer Disease. *Archives of Neurology*, *68*(10), 1239. https://doi.org/10.1001/archneurol.2011.203

Shi, J., Zhang, S., Tang, M., Liu, X., Li, T., Wang, Y., … Ma, C. (2004). The 1239G/C polymorphism in exon 5 ofBACE1 gene may be associated with sporadic Alzheimer's disease in Chinese Hans. *American Journal of Medical Genetics*, *124B*(1), 54–57. https://doi.org/10.1002/ajmg.b.20087

Shi, X. P., Chen, E., Yin, K. C., Na, S., Garsky, V. M., Lai, M. T., … Gardell, S. J. (2001). The pro domain of beta-secretase does not confer strict zymogen-like properties but does assist proper folding of the protease domain. *The Journal of Biological Chemistry*, *276*(13), 10366–10373. https://doi.org/10.1074/JBC.M009200200

Shiba, T., Kametaka, S., Kawasaki, M., Shibata, M., Waguri, S., Uchiyama, Y., & Wakatsuki, S. (2004). Insights into the Phosphoregulation of β-Secretase Sorting Signal by the VHS Domain of GGA1. *Traffic*, *5*(6), 437–448. https://doi.org/10.1111/j.1600-0854.2004.00188.x

Shima, H., Matsumoto, M., Ishigami, Y., Ebina, M., Muto, A., Sato, Y., … Igarashi, K. (2017). S-Adenosylmethionine Synthesis Is Regulated by Selective N6-Adenosine Methylation and mRNA Degradation Involving METTL16 and YTHDC1. *Cell Reports*, *21*(12), 3354–3363. https://doi.org/10.1016/j.celrep.2017.11.092

Siegel, S. J., Bieschke, J., Powers, E. T., & Kelly, J. W. (2007). The oxidative stress metabolite 4-hydroxynonenal promotes Alzheimer protofibril formation. *Biochemistry*, *46*(6), 1503–1510. https://doi.org/10.1021/bi061853s

Silva, S. V, Zhang, P., Haberl, M. G., Labrousse, V., Grosjean, N., Blanchet, C., … Mulle, C. (2019). Hippocampal Mossy Fibers Synapses in CA3 Pyramidal Cells Are Altered at an Early Stage in a Mouse Model of Alzheimer's Disease. *Journal of Neuroscience*, *39*(21), 4193–4205. https://doi.org/10.1523/JNEUROSCI.2868-18.2019

Sinha, S., Anderson, J. P., Barbour, R., Basi, G. S., Caccavello, R., Davis, D., … John, V. (1999). Purification and cloning of amyloid precursor protein β-secretase from human brain. *Nature*, *402*(6761), 537–540. https://doi.org/10.1038/990114

Sjölander, A., Zetterberg, H., Andreasson, U., Minthon, L., & Blennow, K.

(2010). BACE1 gene variants do not influence BACE1 activity, levels of APP or Aβ isoforms in CSF in Alzheimer's disease. *Molecular Neurodegeneration*, *5*(1), 37. https://doi.org/10.1186/1750-1326-5-37

Slieker, L. J., Sloop, K. W., Surface, P. L., Kriauciunas, A., LaQuier, F., Manetta, J., … Stephens, T. W. (1996). Regulation of expression of ob mRNA and protein by glucocorticoids and cAMP. *The Journal of Biological Chemistry*, *271*(10), 5301–5304. https://doi.org/10.1074/JBC.271.10.5301

Snowden, S. G., Ebshiana, A. A., Hye, A., An, Y., Pletnikova, O., O'Brien, R., … Thambisetty, M. (2017). Association between fatty acid metabolism in the brain and Alzheimer disease neuropathology and cognitive performance: A nontargeted metabolomic study. *PLOS Medicine*, *14*(3), e1002266. https://doi.org/10.1371/journal.pmed.1002266

Sohn, J.-W. (2015). Network of hypothalamic neurons that control appetite. *BMB Reports*, *48*(4), 229–233. https://doi.org/10.5483/BMBREP.2015.48.4.272

Sokol, D. K., Demao Chen, D., Farlow, M. R., Dunn, D. W., Maloney, B., Zimmer, J. A., & Lahiri, D. K. (2006). High Levels of Alzheimer Beta-Amyloid Precursor Protein (APP) in Children With Severely Autistic Behavior and Aggression. *Journal of Child Neurology*, *21*(6), 444–449. https://doi.org/10.1177/08830738060210062201

Sperbera, B. R., Leight, S., Goedert, M., & Lee, V. M.-Y. (1995). Glycogen synthase kinase-3β phosphorylates tau protein at multiple sites in intact cells. *Neuroscience Letters*, *197*(2), 149–153. https://doi.org/10.1016/0304-3940(95)11902-9

Spruston, N. (2008). Pyramidal neurons: dendritic structure and synaptic integration. *Nature Reviews Neuroscience*, *9*(3), 206–221. https://doi.org/10.1038/nrn2286

Stahl, R., Schilling, S., Soba, P., Rupp, C., Hartmann, T., Wagner, K., … Kins, S. (2014). Shedding of APP limits its synaptogenic activity and cell adhesion properties. *Frontiers in Cellular Neuroscience*, *8*, 410. https://doi.org/10.3389/fncel.2014.00410

Stampfer, M. J. (2006). Cardiovascular disease and Alzheimer's disease: common links. *Journal of Internal Medicine*, *260*(3), 211–223. https://doi.org/10.1111/j.1365-2796.2006.01687.x

Stefansson, H., Sigurdsson, E., Steinthorsdottir, V., Bjornsdottir, S., Sigmundsson, T., Ghosh, S., … Stefansson, K. (2002). Neuregulin 1 and susceptibility to schizophrenia. *American Journal of Human Genetics*, *71*(4), 877–892. https://doi.org/10.1086/342734

Stępień, M., Stępień, A., Wlazeł, R. N., Paradowski, M., Banach, M., & Rysz, J. (2014). Obesity indices and inflammatory markers in obese non-diabetic normo- and hypertensive patients: a comparative pilot study. *Lipids in Health and Disease*, *13*(1), 29. https://doi.org/10.1186/1476-511X-13-29

Stouffer, M. A., Woods, C. A., Patel, J. C., Lee, C. R., Witkovsky, P., Bao, L., … Rice, M. E. (2015). Insulin enhances striatal dopamine release by activating cholinergic interneurons and thereby signals reward. *Nature Communications*, *6*(1), 8543. https://doi.org/10.1038/ncomms9543

Stützer, I., Selevsek, N., Esterházy, D., Schmidt, A., Aebersold, R., Stoffel, M., & Zürich, E. (2013). Discovery of β-Secretase Substrates in β-Cells 1 Systematic Proteomic Analysis Identifies Beta-site Amyloid Precursor Protein Cleaving Enzyme 2 and 1 (BACE2 and BACE1) Substrates in Pancreatic Beta-cells*. https://doi.org/10.1074/jbc.M112.444703

Succol, F., Fiumelli, H., Benfenati, F., Cancedda, L., & Barberis, A. (2012).

Intracellular chloride concentration influences the GABAA receptor subunit composition. *Nature Communications*, *3*(1), 738. https://doi.org/10.1038/ncomms1744

Sugawara, K., Shibasaki, T., Mizoguchi, A., Saito, T., & Seino, S. (2009). Rab11 and its effector Rip11 participate in regulation of insulin granule exocytosis. *Genes to Cells*, *14*(4), 445–456. https://doi.org/10.1111/j.1365-2443.2009.01285.x

Sun, X., Wang, Y., Qing, H., Christensen, M. A., Liu, Y., Zhou, W., … Song, W. (2005). Distinct transcriptional regulation and function of the human BACE2 and BACE1 genes. *The FASEB Journal*, *19*(7), 739–749. https://doi.org/10.1096/fj.04-3426com

Sutherland, C., Leighton, I. A., & Cohen, P. (1993). Inactivation of glycogen synthase kinase-3 beta by phosphorylation: new kinase connections in insulin and growth-factor signalling. *The Biochemical Journal*, *296 (Pt 1)*, 15–19. Retrieved from http://www.ncbi.nlm.nih.gov/pubmed/8250835

Swart, I., Jahng, J. W., Overton, J. M., & Houpt, T. A. (2002). Hypothalamic NPY, AGRP, and POMC mRNA responses to leptin and refeeding in mice. *American Journal of Physiology-Regulatory, Integrative and Comparative Physiology*, *283*(5), R1020–R1026. https://doi.org/10.1152/ajpregu.00501.2001

Szczepanik, A. M., Rampe, D., & Ringheim[2], G. E. (2001). *Amyloid-b peptide fragments p3 and p4 induce pro-in¯ammatory cytokine and chemokine production in vitro and in vivo*. *Journal of Neurochemistry*. Retrieved from https://onlinelibrary.wiley.com/doi/pdf/10.1046/j.1471-4159.2001.00240.x

Takami, M., Nagashima, Y., Sano, Y., Ishihara, S., Morishima-Kawashima, M., Funamoto, S., & Ihara, Y. (2009). gamma-Secretase: successive tripeptide and tetrapeptide release from the transmembrane domain of beta-carboxyl terminal fragment. *The Journal of Neuroscience : The Official Journal of the Society for Neuroscience*, *29*(41), 13042–13052. https://doi.org/10.1523/JNEUROSCI.2362-09.2009

Takeuchi, H., Jin, S., Wang, J., Zhang, G., Kawanokuchi, J., Kuno, R., … Suzumura, A. (2006). Tumor necrosis factor-alpha induces neurotoxicity via glutamate release from hemichannels of activated microglia in an autocrine manner. *The Journal of Biological Chemistry*, *281*(30), 21362–21368. https://doi.org/10.1074/jbc.M600504200

Talbot, K., Wang, H.-Y., Kazi, H., Han, L.-Y., Bakshi, K. P., Stucky, A., … Arnold, S. E. (2012). Demonstrated brain insulin resistance in Alzheimer's disease patients is associated with IGF-1 resistance, IRS-1 dysregulation, and cognitive decline. *The Journal of Clinical Investigation*, *122*(4), 1316–1338. https://doi.org/10.1172/JCI59903

Tamayev, R., Akpan, N., Arancio, O., Troy, C. M., & D'Adamio, L. (2012). Caspase-9 mediates synaptic plasticity and memory deficits of Danish dementia knock-in mice: caspase-9 inhibition provides therapeutic protection. *Molecular Neurodegeneration*, *7*(1), 60. https://doi.org/10.1186/1750-1326-7-60

Tan, W., Wang, Y., Gold, B., Chen, J., Dean, M., Harrison, P. J., … Law, A. J. (2007). Molecular cloning of a brain-specific, developmentally regulated neuregulin 1 (NRG1) isoform and identification of a functional promoter variant associated with schizophrenia. *The Journal of Biological Chemistry*, *282*(33), 24343–24351. https://doi.org/10.1074/jbc.M702953200

Tanahashi, H., & Tabira, T. (2001). Three novel alternatively spliced isoforms of the human beta-site amyloid precursor protein cleaving enzyme (BACE)

and their effect on amyloid beta-peptide production. *Neuroscience Letters*, *307*(1), 9–12. https://doi.org/10.1016/S0304-3940(01)01912-7

Tanahashi, H., & Tabira, T. (2007). A novel beta-site amyloid precursor protein cleaving enzyme (BACE) isoform regulated by nonsense-mediated mRNA decay and proteasome-dependent degradation. *Neuroscience Letters*, *428*(2–3), 103–108. https://doi.org/10.1016/j.neulet.2007.09.033

Tartaglia,', L. A., Dembski, M., Weng, X., Deng, N., Culpepper, J., Devos, R., … Tepper', R. I. (1995). *Identification and Expression Cloning of a Leptin Receptor, OB-R*. *Cell* (Vol. 83). Retrieved from https://www.cell.com/cell/pdf/0092-8674(95)90151-5.pdf?_returnURL=https%3A%2F%2Flinkinghub.elsevier.com%2Fretrieve%2Fpii%2F0092867495901515%3Fshowall%3Dtrue

Taylor, C. J., Ireland, D. R., Ballagh, I., Bourne, K., Marechal, N. M., Turner, P. R., … Abraham, W. C. (2008). Endogenous secreted amyloid precursor protein-α regulates hippocampal NMDA receptor function, long-term potentiation and spatial memory. *Neurobiology of Disease*, *31*(2), 250–260. https://doi.org/10.1016/J.NBD.2008.04.011

Texidó, L., Martín-Satué, M., Alberdi, E., Solsona, C., & Matute, C. (2011). Amyloid β peptide oligomers directly activate NMDA receptors. *Cell Calcium*, *49*(3), 184–190. https://doi.org/10.1016/j.ceca.2011.02.001

Thakker, D. R., Sankaranarayanan, S., Weatherspoon, M. R., Harrison, J., Pierdomenico, M., Heisel, J. M., … Shafer, L. L. (2015). Centrally Delivered BACE1 Inhibitor Activates Microglia, and Reverses Amyloid Pathology and Cognitive Deficit in Aged Tg2576 Mice. *Journal of Neuroscience*, *35*(17), 6931–6936. https://doi.org/10.1523/JNEUROSCI.2262-14.2015

Thaler, J. P., Guyenet, S. J., Dorfman, M. D., Wisse, B. E., & Schwartz, M. W. (2013). Hypothalamic inflammation: marker or mechanism of obesity pathogenesis? *Diabetes*, *62*(8), 2629–2634. https://doi.org/10.2337/db12-1605

Thirumangalakudi, L., Prakasam, A., Zhang, R., Bimonte-Nelson, H., Sambamurti, K., Kindy, M. S., & Bhat, N. R. (2008). High cholesterol-induced neuroinflammation and amyloid precursor protein processing correlate with loss of working memory in mice. *Journal of Neurochemistry*, *106*(1), 475–485. https://doi.org/10.1111/j.1471-4159.2008.05415.x

Todd, S., McKnight, A. J., Liu, W. W., Carson, R., Heggarty, S., McGuinness, B., … Johnston, J. A. (2008). BACE1 Polymorphisms Do Not Influence Platelet Membrane β-secretase Activity or Genetic Susceptibility for Alzheimer's Disease in the Northern Irish Population. *NeuroMolecular Medicine*, *10*(4), 368–376. https://doi.org/10.1007/s12017-008-8045-y

Tögel, M., Wiche, G., & Propst, F. (1998). Novel features of the light chain of microtubule-associated protein MAP1B: microtubule stabilization, self interaction, actin filament binding, and regulation by the heavy chain. *The Journal of Cell Biology*, *143*(3), 695–707. Retrieved from http://www.ncbi.nlm.nih.gov/pubmed/9813091

Toh, W. H., Chia, P. Z. C., Hossain, M. I., & Gleeson, P. A. (2018). GGA1 regulates signal-dependent sorting of BACE1 to recycling endosomes, which moderates Aβ production. *Molecular Biology of the Cell*, *29*(2), 191–208. https://doi.org/10.1091/mbc.E17-05-0270

Tollervey, J. R., Wang, Z., Hortobágyi, T., Witten, J. T., Zarnack, K., Kayikci, M., … Ule, J. (2011). Analysis of alternative splicing associated with aging and neurodegeneration in the human brain. *Genome Research*, *21*(10), 1572. https://doi.org/10.1101/GR.122226.111

Tomita, T., Takikawa, R., Koyama, A., Morohashi, Y., Takasugi, N., Saido, T. C., … Ihara, Y. (1999). C terminus of presenilin is required for overproduction of amyloidogenic Abeta42 through stabilization and endoproteolysis of presenilin. *The Journal of Neuroscience : The Official Journal of the Society for Neuroscience*, *19*(24), 10627–10634. https://doi.org/10.1523/jneurosci.1575-04.2005

Toth, A. B., Terauchi, A., Zhang, L. Y., Johnson-Venkatesh, E. M., Larsen, D. J., Sutton, M. A., & Umemori, H. (2013). Synapse maturation by activity-dependent ectodomain shedding of SIRPα. *Nature Neuroscience*, *16*(10), 1417–1425. https://doi.org/10.1038/nn.3516

Turkia, H. Ben, Tebib, N., Azzouz, H., Abdelmoula, M. S., Bouguila, J., Sanhaji, H., … Ben Dridi, M. F. (2008). Phenotypic spectrum of fucosidosis in Tunisia. *Journal of Inherited Metabolic Disease*, *31*(S2), 313–316. https://doi.org/10.1007/s10545-008-0891-0

Udayar, V., Buggia-Prévot, V., Guerreiro, R. L., Siegel, G., Rambabu, N., Soohoo, A. L., … Hardy, J. (2013). A Paired RNAi and RabGAP Overexpression Screen Identifies Rab11 as a Regulator of β-Amyloid Production. *Cell Reports*, *5*(6), 1536–1551. https://doi.org/10.1016/j.celrep.2013.12.005

Ule, J., Ule, A., Spencer, J., Williams, A., Hu, J.-S., Cline, M., … Darnell, R. B. (2005). Nova regulates brain-specific splicing to shape the synapse. *Nature Genetics*, *37*(8), 844–852. https://doi.org/10.1038/ng1610

Urbanc, B., Cruz, L., Yun, S., Buldyrev, S. V., Bitan, G., Teplow, D. B., & Stanley, H. E. (2004). In silico study of amyloid -protein folding and oligomerization. *Proceedings of the National Academy of Sciences*, *101*(50), 17345–17350. https://doi.org/10.1073/pnas.0408153101

Van Heek, M., Compton, D. S., France, C. F., Tedesco, R. P., Fawzi, A. B., Graziano, M. P., … Jr. (1997). Diet-induced obese mice develop peripheral, but not central, resistance to leptin. *The Journal of Clinical Investigation*, *99*(3), 385–390. https://doi.org/10.1172/JCI119171

Vandal, M., White, P. J., Tremblay, C., St-Amour, I., Chevrier, G., Emond, V., … Calon, F. (2014). Insulin reverses the high-fat diet-induced increase in brain Aβ and improves memory in an animal model of Alzheimer disease. *Diabetes*, *63*(12), 4291–4301. https://doi.org/10.2337/db14-0375

Vann, S. D., & Aggleton, J. P. (2002). Extensive cytotoxic lesions of the rat retrosplenial cortex reveal consistent deficits on tasks that tax allocentric spatial memory. *Behavioral Neuroscience*, *116*(1), 85–94. Retrieved from http://www.ncbi.nlm.nih.gov/pubmed/11895186

Vann, S. D., Aggleton, J. P., & Maguire, E. A. (2009). What does the retrosplenial cortex do? *Nature Reviews Neuroscience*, *10*(11), 792–802. https://doi.org/10.1038/nrn2733

Vassar, R, Bennett, B. D., Babu-Khan, S., Kahn, S., Mendiaz, E. A., Denis, P., … Citron, M. (1999). Beta-secretase cleavage of Alzheimer's amyloid precursor protein by the transmembrane aspartic protease BACE. *Science (New York, N.Y.)*, *286*(5440), 735–741. https://doi.org/10.1126/SCIENCE.286.5440.735

Vassar, Robert, Kuhn, P.-H., Haass, C., Kennedy, M. E., Rajendran, L., Wong, P. C., & Lichtenthaler, S. F. (2014). Function, therapeutic potential and cell biology of BACE proteases: current status and future prospects. *Journal of Neurochemistry*, *130*(1), 4–28. https://doi.org/10.1111/jnc.12715

Venegas, C., Kumar, S., Franklin, B. S., Dierkes, T., Brinkschulte, R., Tejera, D., … Heneka, M. T. (2017). Microglia-derived ASC specks cross-seed

amyloid-β in Alzheimer's disease. *Nature*, *552*(7685), 355–361. https://doi.org/10.1038/nature25158

Verberne, A. J. M., Sabetghadam, A., & Korim, W. S. (2014). Neural pathways that control the glucose counterregulatory response. *Frontiers in Neuroscience*, *8*, 38. https://doi.org/10.3389/fnins.2014.00038

Vetrivel, K. S., Meckler, X., Chen, Y., Nguyen, P. D., Seidah, N. G., Vassar, R., … Thinakaran, G. (2009). Alzheimer disease Abeta production in the absence of S-palmitoylation-dependent targeting of BACE1 to lipid rafts. *The Journal of Biological Chemistry*, *284*(6), 3793–3803. https://doi.org/10.1074/jbc.M808920200

Viet, M. H., Ngo, S. T., Lam, N. S., & Li, M. S. (2011). Inhibition of Aggregation of Amyloid Peptides by Beta-Sheet Breaker Peptides and Their Binding Affinity. *The Journal of Physical Chemistry B*, *115*(22), 7433–7446. https://doi.org/10.1021/jp1116728

Vignal, E., Blangy, A., Martin, M., Gauthier-Rouviere, C., & Fort, P. (2001). Kinectin Is a Key Effector of RhoG Microtubule-Dependent Cellular Activity. *Molecular and Cellular Biology*, *21*(23), 8022–8034. https://doi.org/10.1128/MCB.21.23.8022-8034.2001

Vitureira, N., & Goda, Y. (2013). The interplay between Hebbian and homeostatic synaptic plasticity. *The Journal of Cell Biology*, *203*(2), 175–186. https://doi.org/10.1083/jcb.201306030

Viwatpinyo, K., & Chongthammakun, S. (2009). Activation of group I metabotropic glutamate receptors leads to brain-derived neurotrophic factor expression in rat C6 cells. *Neuroscience Letters*, *467*(2), 127–130. https://doi.org/10.1016/j.neulet.2009.10.020

Vogel, M. J., Peric-Hupkes, D., & van Steensel, B. (2007). Detection of in vivo protein–DNA interactions using DamID in mammalian cells. *Nature Protocols*, *2*(6), 1467–1478. https://doi.org/10.1038/nprot.2007.148

Volloch, V., & Rits, S. (2018). Results of Beta Secretase-Inhibitor Clinical Trials Support Amyloid Precursor Protein-Independent Generation of Beta Amyloid in Sporadic Alzheimer's Disease. *Medical Sciences*, *6*(2), 45. https://doi.org/10.3390/medsci6020045

von Arnim, C. A. F., Kinoshita, A., Peltan, I. D., Tangredi, M. M., Herl, L., Lee, B. M., … Hyman, B. T. (2005). The Low Density Lipoprotein Receptor-related Protein (LRP) Is a Novel β-Secretase (BACE1) Substrate. *Journal of Biological Chemistry*, *280*(18), 17777–17785. https://doi.org/10.1074/jbc.M414248200

Wahle, T., Prager, K., Raffler, N., Haass, C., Famulok, M., & Walter, J. (2005). GGA proteins regulate retrograde transport of BACE1 from endosomes to the trans-Golgi network. *Molecular and Cellular Neuroscience*, *29*(3), 453–461. https://doi.org/10.1016/J.MCN.2005.03.014

Walensky, L. D., Blackshaw, S., Liao, D., Watkins, C. C., Weier, H. U., Parra, M., … Snyder, S. H. (1999). A novel neuron-enriched homolog of the erythrocyte membrane cytoskeletal protein 4.1. *The Journal of Neuroscience : The Official Journal of the Society for Neuroscience*, *19*(15), 6457–6467. Retrieved from http://www.ncbi.nlm.nih.gov/pubmed/10414974

Walker, J. M., Dixit, S., Saulsberry, A. C., May, J. M., & Harrison, F. E. (2017). Reversal of high fat diet-induced obesity improves glucose tolerance, inflammatory response, β-amyloid accumulation and cognitive decline in the APP/PSEN1 mouse model of Alzheimer's disease. *Neurobiology of Disease*, *100*, 87–98. https://doi.org/10.1016/J.NBD.2017.01.004

Walsh, D. M., Klyubin, I., Fadeeva, J. V., Cullen, W. K., Anwyl, R., Wolfe, M. S.,

… Selkoe, D. J. (2002). Naturally secreted oligomers of amyloid β protein potently inhibit hippocampal long-term potentiation in vivo. *Nature*, *416*(6880), 535–539. https://doi.org/10.1038/416535a

Walter, J., Fluhrer, R., Hartung, B., Willem, M., Kaether, C., Capell, A., … Haass, C. (2001). Phosphorylation regulates intracellular trafficking of beta-secretase. *The Journal of Biological Chemistry*, *276*(18), 14634–14641. https://doi.org/10.1074/jbc.M011116200

Wang, F., Flanagan, J., Su, N., Wang, L. C., Bui, S., Nielson, A., … Luo, Y. (2012). RNAscope: a novel in situ RNA analysis platform for formalin-fixed, paraffin-embedded tissues. *The Journal of Molecular Diagnostics*, *14*(1), 22–29. https://doi.org/10.1016/j.jmoldx.2011.08.002

Wang, H.-W., Pasternak, J. F., Kuo, H., Ristic, H., Lambert, M. P., Chromy, B., … Trommer, B. L. (2002). Soluble oligomers of beta amyloid (1-42) inhibit long-term potentiation but not long-term depression in rat dentate gyrus. *Brain Research*, *924*(2), 133–140. Retrieved from http://www.ncbi.nlm.nih.gov/pubmed/11750898

Wang, H, Liu, C., Debnath, G., Baines, A. J., Conboy, J. G., Mohandas, N., & An, X. (2010). Comprehensive characterization of expression patterns of protein 4.1 family members in mouse adrenal gland: implications for functions. *Histochemistry and Cell Biology*, *134*(4), 411–420. https://doi.org/10.1007/s00418-010-0749-z

Wang, Haizhi, Sang, N., Zhang, C., Raghupathi, R., Tanzi, R. E., & Saunders, A. (2015). Cathepsin L Mediates the Degradation of Novel APP C-Terminal Fragments. *Biochemistry*, *54*(18), 2806–2816. https://doi.org/10.1021/acs.biochem.5b00329

Wang, J. Y., Miller, S. J., & Falls, D. L. (2001). The N-terminal region of neuregulin isoforms determines the accumulation of cell surface and released neuregulin ectodomain. *The Journal of Biological Chemistry*, *276*(4), 2841–2851. https://doi.org/10.1074/jbc.M005700200

Wang, R, & Reddy, P. H. (2017). Role of glutamate and NMDA receptors in Alzheimer's disease. *Journal of Alzheimer's Disease : JAD*, *57*(4), 1041. https://doi.org/10.3233/JAD-160763

Wang, Ruishan, Chen, S., Liu, Y., Diao, S., Xue, Y., You, X., … Liao, F.-F. (2015). All- *trans* -retinoic Acid Reduces *BACE1* Expression under Inflammatory Conditions via Modulation of Nuclear Factor κB (NFκB) Signaling. *Journal of Biological Chemistry*, *290*(37), 22532–22542. https://doi.org/10.1074/jbc.M115.662908

Wang, Ruishan, Li, J. J., Diao, S., Kwak, Y.-D., Liu, L., Zhi, L., … Liao, F.-F. (2013a). Metabolic stress modulates Alzheimer's β-secretase gene transcription via SIRT1-PPARγ-PGC-1 in neurons. *Cell Metabolism*, *17*(5), 685–694. https://doi.org/10.1016/j.cmet.2013.03.016

Wang, Ruishan, Li, J. J., Diao, S., Kwak, Y.-D., Liu, L., Zhi, L., … Liao, F.-F. (2013b). Metabolic Stress Modulates Alzheimer's β-Secretase Gene Transcription via SIRT1-PPARγ-PGC-1 in Neurons. *Cell Metabolism*, *17*(5), 685–694. https://doi.org/10.1016/j.cmet.2013.03.016

Wang, Xiangchun, Gu, J., Miyoshi, E., Honke, K., & Taniguchi, N. (2006). Phenotype Changes of Fut8 Knockout Mouse: Core Fucosylation Is Crucial for the Function of Growth Factor Receptor(s). *Methods in Enzymology*, *417*, 11–22. https://doi.org/10.1016/S0076-6879(06)17002-0

Wang, Xinlu, Fei, F., Qu, J., Li, C., Li, Y., & Zhang, S. (2018). The role of septin 7 in physiology and pathological disease: A systematic review of current status. *Journal of Cellular and Molecular Medicine*, *22*(7), 3298–3307.

https://doi.org/10.1111/jcmm.13623
Wang, Z., Wang, B., Yang, L., Guo, Q., Aithmitti, N., Songyang, Z., & Zheng, H. (2009). Presynaptic and Postsynaptic Interaction of the Amyloid Precursor Protein Promotes Peripheral and Central Synaptogenesis. *Journal of Neuroscience*, *29*(35), 10788–10801. https://doi.org/10.1523/JNEUROSCI.2132-09.2009
Ward, D. M., Pevsner, J., Scullion, M. A., Vaughn, M., & Kaplan, J. (2000). Syntaxin 7 and VAMP-7 are Soluble *N* -Ethylmaleimide–sensitive Factor Attachment Protein Receptors Required for Late Endosome–Lysosome and Homotypic Lysosome Fusion in Alveolar Macrophages. *Molecular Biology of the Cell*, *11*(7), 2327–2333. https://doi.org/10.1091/mbc.11.7.2327
Ward, M. A., Carlsson, C. M., Trivedi, M. A., Sager, M. A., & Johnson, S. C. (2005). The effect of body mass index on global brain volume in middle-aged adults: a cross sectional study. *BMC Neurology*, *5*(1), 23. https://doi.org/10.1186/1471-2377-5-23
Watterson, K. R., Bestow, D., Gallagher, J., Hamilton, D. L., Ashford, F. B., Meakin, P. J., & Ashford, M. L. J. (2013). Anorexigenic and orexigenic hormone modulation of mammalian target of rapamycin complex 1 activity and the regulation of hypothalamic agouti-related protein mRNA expression. *Neuro-Signals*, *21*(1–2), 28–41. https://doi.org/10.1159/000334144
Weidemann, A., Paliga, K., Dürrwang, U., Reinhard, F. B., Schuckert, O., Evin, G., & Masters, C. L. (1999). Proteolytic processing of the Alzheimer's disease amyloid precursor protein within its cytoplasmic domain by caspase-like proteases. *The Journal of Biological Chemistry*, *274*(9), 5823–5829. https://doi.org/10.1074/JBC.274.9.5823
Wen, Y., Yu, W. H., Maloney, B., Bailey, J., Ma, J., Marié, I., … Duff, K. (2008). Transcriptional regulation of beta-secretase by p25/cdk5 leads to enhanced amyloidogenic processing. *Neuron*, *57*(5), 680–690. https://doi.org/10.1016/j.neuron.2008.02.024
Westmark, C. J., & Malter, J. S. (2007). FMRP Mediates mGluR5-Dependent Translation of Amyloid Precursor Protein. *PLoS Biology*, *5*(3), e52. https://doi.org/10.1371/journal.pbio.0050052
Wheeler, D. W., White, C. M., Rees, C. L., Komendantov, A. O., Hamilton, D. J., & Ascoli, G. A. (2015). Hippocampome.org: a knowledge base of neuron types in the rodent hippocampus. *ELife*, *4*. https://doi.org/10.7554/eLife.09960
White, H., Pieper, C., & Schmader, K. (1998). The association of weight change in Alzheimer's disease with severity of disease and mortality: A longitudinal analysis. *Journal of the American Geriatrics Society*, *46*(10), 1223–1227. https://doi.org/10.1111/j.1532-5415.1998.tb04537.x
White, H., Pieper, C., Schmader, K., & Fillenbaum, G. (1996). Weight Change in Alzheimer's Disease. *Journal of the American Geriatrics Society*, *44*(3), 265–272. https://doi.org/10.1111/j.1532-5415.1996.tb00912.x
Whitmer, R. A., Gustafson, D. R., Barrett-Connor, E., Haan, M. N., Gunderson, E. P., & Yaffe, K. (2008). Central obesity and increased risk of dementia more than three decades later. *Neurology*, *71*(14), 1057–1064. https://doi.org/10.1212/01.wnl.0000306313.89165.ef
Whitmer, Rachel A, Gunderson, E. P., Barrett-Connor, E., Quesenberry, C. P., Yaffe, K., & Yaffe, K. (2005). Obesity in middle age and future risk of dementia: a 27 year longitudinal population based study. *BMJ (Clinical*

Research Ed.), *330*(7504), 1360. https://doi.org/10.1136/bmj.38446.466238.E0

Wickham, L., Benjannet, S., Marcinkiewicz, E., Chretien, M., & Seidah, N. G. (2005). beta-Amyloid protein converting enzyme 1 and brain-specific type II membrane protein BRI3: binding partners processed by furin. *Journal of Neurochemistry*, *92*(1), 93–102. https://doi.org/10.1111/j.1471-4159.2004.02840.x

Willems, P. J., Seo, H.-C., Coucke, P., Tonlorenzi, R., & O'Brien, J. S. (1999). Spectrum of mutations in fucosidosis. *European Journal of Human Genetics*, *7*(1), 60–67. https://doi.org/10.1038/sj.ejhg.5200272

Winkler, S., & Rösen-Wolff, A. (2015). Caspase-1: an integral regulator of innate immunity. *Seminars in Immunopathology*, *37*(4), 419–427. https://doi.org/10.1007/s00281-015-0494-4

Winocur, G, & Greenwood, C. E. (1999). The effects of high fat diets and environmental influences on cognitive performance in rats. *Behavioural Brain Research*, *101*(2), 153–161. Retrieved from http://www.ncbi.nlm.nih.gov/pubmed/10372571

Winocur, Gordon, & Greenwood, C. E. (2005). Studies of the effects of high fat diets on cognitive function in a rat model. *Neurobiology of Aging*, *26*(1), 46–49. https://doi.org/10.1016/j.neurobiolaging.2005.09.003

Wolfe, M. S., Xia, W., Ostaszewski, B. L., Diehl, T. S., Kimberly, W. T., & Selkoe, D. J. (1999). Two transmembrane aspartates in presenilin-1 required for presenilin endoproteolysis and γ-secretase activity. *Nature*, *398*(6727), 513–517. https://doi.org/10.1038/19077

Wong, H.-K., Sakurai, T., Oyama, F., Kaneko, K., Wada, K., Miyazaki, H., … Nukina, N. (2005). beta Subunits of voltage-gated sodium channels are novel substrates of beta-site amyloid precursor protein-cleaving enzyme (BACE1) and gamma-secretase. *The Journal of Biological Chemistry*, *280*(24), 23009–23017. https://doi.org/10.1074/jbc.M414648200

Wong, M.-L., Licinio, J., Yildiz, B. O., Mantzoros, C. S., Prolo, P., Kling, M., & Gold, P. W. (2004). Simultaneous and Continuous 24-Hour Plasma and Cerebrospinal Fluid Leptin Measurements: Dissociation of Concentrations in Central and Peripheral Compartments. *The Journal of Clinical Endocrinology & Metabolism*, *89*(1), 258–265. https://doi.org/10.1210/jc.2003-031275

Wood, P. L., Locke, V. A., Herling, P., Passaro, A., Vigna, G. B., Volpato, S., … Zuliani, G. (2016). Targeted lipidomics distinguishes patient subgroups in mild cognitive impairment (MCI) and late onset Alzheimer's disease (LOAD). *BBA Clinical*, *5*, 25–28. https://doi.org/10.1016/j.bbacli.2015.11.004

Wood, W. G., Li, L., Müller, W. E., & Eckert, G. P. (2014). Cholesterol as a causative factor in Alzheimer's disease: a debatable hypothesis. *Journal of Neurochemistry*, *129*(4), 559–572. https://doi.org/10.1111/jnc.12637

Woods, D. F., Hough, C., Peel, D., Callaini, G., & Bryant, P. J. (1996). Dlg protein is required for junction structure, cell polarity, and proliferation control in Drosophila epithelia. *The Journal of Cell Biology*, *134*(6), 1469–1482. https://doi.org/10.1083/JCB.134.6.1469

Wozny, C., Breustedt, J., Wolk, F., Varoqueaux, F., Boretius, S., Zivkovic, A. R., … Ivanovic, A. (2009). The function of glutamatergic synapses is not perturbed by severe knockdown of 4.1N and 4.1G expression. *Journal of Cell Science*, *122*(5), 735–744. https://doi.org/10.1242/JCS.037382

Wu, J., Anwyl, R., & Rowan, M. J. (1995). beta-Amyloid selectively augments

NMDA receptor-mediated synaptic transmission in rat hippocampus. *Neuroreport*, *6*(17), 2409–2413. Retrieved from http://www.ncbi.nlm.nih.gov/pubmed/8747164

Xu, A. W., Ste-Marie, L., Kaelin, C. B., & Barsh, G. S. (2007). Inactivation of Signal Transducer and Activator of Transcription 3 in Proopiomelanocortin (Pomc) Neurons Causes Decreased Pomc Expression, Mild Obesity, and Defects in Compensatory Refeeding. *Endocrinology*, *148*(1), 72–80. https://doi.org/10.1210/en.2006-1119

Xu, W. L., Atti, A. R., Gatz, M., Pedersen, N. L., Johansson, B., & Fratiglioni, L. (2011). Midlife overweight and obesity increase late-life dementia risk: a population-based twin study. *Neurology*, *76*(18), 1568–1574. https://doi.org/10.1212/WNL.0b013e3182190d09

Yamazaki, T., Koo, E. H., & Selkoe, D. J. (1996). Trafficking of cell surface beta-amyloid precursor protein: retrograde and transcytotic transport in cultured neurons. *The Journal of Cell Science*, *129*(2), 431–442. https://doi.org/10.1083/jcb.129.2.431

Yan, R, Munzner, J. B., Shuck, M. E., & Bienkowski, M. J. (2001). BACE2 functions as an alternative alpha-secretase in cells. *The Journal of Biological Chemistry*, *276*(36), 34019–34027. https://doi.org/10.1074/jbc.M105583200

Yan, Riqiang. (2017). Physiological Functions of the β-Site Amyloid Precursor Protein Cleaving Enzyme 1 and 2. *Frontiers in Molecular Neuroscience*, *10*, 97. https://doi.org/10.3389/fnmol.2017.00097

Yan, Riqiang, Bienkowski, M. J., Shuck, M. E., Miao, H., Tory, M. C., Pauley, A. M., … Gurney, M. E. (1999). Membrane-anchored aspartyl protease with Alzheimer's disease β-secretase activity. *Nature*, *402*(6761), 533–537. https://doi.org/10.1038/990107

Yasojima, K., Kuret, J., DeMaggio, A. J., McGeer, E., & McGeer, P. L. (2000). Casein kinase 1 delta mRNA is upregulated in Alzheimer disease brain. *Brain Research*, *865*(1), 116–120. Retrieved from http://www.ncbi.nlm.nih.gov/pubmed/10814741

Ye, K., Compton, D. A., Lai, M. M., Walensky, L. D., & Snyder, S. H. (1999). Protein 4.1N binding to nuclear mitotic apparatus protein in PC12 cells mediates the antiproliferative actions of nerve growth factor. *The Journal of Neuroscience : The Official Journal of the Society for Neuroscience*, *19*(24), 10747–10756. Retrieved from http://www.ncbi.nlm.nih.gov/pubmed/10594058

Ye, K., Hurt, K. J., Wu, F. Y., Fang, M., Luo, H. R., Hong, J. J., … Snyder, S. H. (2000). Pike. A nuclear gtpase that enhances PI3kinase activity and is regulated by protein 4.1N. *Cell*, *103*(6), 919–930. Retrieved from http://www.ncbi.nlm.nih.gov/pubmed/11136977

Yeates, E. F. A., & Tesco, G. (2016). The Endosome-associated Deubiquitinating Enzyme USP8 Regulates BACE1 Enzyme Ubiquitination and Degradation. *The Journal of Biological Chemistry*, *291*(30), 15753–15766. https://doi.org/10.1074/jbc.M116.718023

Yu, G., Nishimura, M., Arawaka, S., Levitan, D., Zhang, L., Tandon, A., … St George-Hyslop, P. (2000). Nicastrin modulates presenilin-mediated notch/glp-1 signal transduction and βAPP processing. *Nature*, *407*(6800), 48–54. https://doi.org/10.1038/35024009

Yu, M., Liu, Y., Shen, J., Lv, D., & Zhang, J. (2016). Meta-analysis of BACE1 gene rs638405 polymorphism and the risk of Alzheimer's disease in Caucasion and Asian population. *Neuroscience Letters*, *616*, 189–196.

https://doi.org/10.1016/J.NEULET.2016.01.059
Yu, Y. J., Zhang, Y., Kenrick, M., Hoyte, K., Luk, W., Lu, Y., … Watts, R. J. (2011). Boosting brain uptake of a therapeutic antibody by reducing its affinity for a transcytosis target. *Science Translational Medicine*, *3*(84), 84ra44. https://doi.org/10.1126/scitranslmed.3002230
Zade, D., Beiser, A., McGlinchey, R., Au, R., Seshadri, S., Palumbo, C., … Milberg, W. (2013). Apolipoprotein Epsilon 4 Allele Modifies Waist-to-Hip Ratio Effects on Cognition and Brain Structure. *Journal of Stroke and Cerebrovascular Diseases*, *22*(2), 119–125. https://doi.org/10.1016/J.JSTROKECEREBROVASDIS.2011.06.020
Zakrzewska, K. E., Cusin, I., Sainsbury, A., Rohner-Jeanrenaud, F., & Jeanrenaud, B. (1997). Glucocorticoids as counterregulatory hormones of leptin: toward an understanding of leptin resistance. *Diabetes*, *46*(4), 717–719. https://doi.org/10.2337/DIAB.46.4.717
Zarkesh-Esfahani, H., Pockley, A. G., Wu, Z., Hellewell, P. G., Weetman, A. P., & Ross, R. J. M. (2004). Leptin Indirectly Activates Human Neutrophils via Induction of TNF-α. *The Journal of Immunology*, *172*(3), 1809–1814. https://doi.org/10.4049/JIMMUNOL.172.3.1809
Zenaro, E., Pietronigro, E., Bianca, V. Della, Piacentino, G., Marongiu, L., Budui, S., … Constantin, G. (2015). Neutrophils promote Alzheimer's disease–like pathology and cognitive decline via LFA-1 integrin. *Nature Medicine*, *21*(8), 1–30. https://doi.org/10.1038/nm.3913
Zhai, X., Li, Y., Liang, P., Li, L., Zhou, Y., Zhang, W., … Wei, G. (2018). PI3K/AKT/Afadin signaling pathway contributes to pathological vascularization in glioblastomas. *Oncology Letters*, *15*(2), 1893–1899. https://doi.org/10.3892/ol.2017.7461
Zhang, B., Hu, Y., & Ma, J. (2009). Anti-inflammatory and Antioxidant Effects of SERPINA3K in the Retina. *Investigative Opthalmology & Visual Science*, *50*(8), 3943. https://doi.org/10.1167/iovs.08-2954
Zhang, B., & Ma, J. (2008). SERPINA3K Prevents Oxidative Stress Induced Necrotic Cell Death by Inhibiting Calcium Overload. *PLoS ONE*, *3*(12), e4077. https://doi.org/10.1371/journal.pone.0004077
Zhang, E. E., Chapeau, E., Hagihara, K., & Feng, G.-S. (2004). Neuronal Shp2 tyrosine phosphatase controls energy balance and metabolism. *Proceedings of the National Academy of Sciences*, *101*(45), 16064–16069. https://doi.org/10.1073/pnas.0405041101
Zhou, Yan, Du, G., Hu, X., Yu, S., Liu, Y., Xu, Y., … Yuan, J. (2005). Nectin-like molecule 1 is a protein 4.1N associated protein and recruits protein 4.1N from cytoplasm to the plasma membrane. *Biochimica et Biophysica Acta (BBA) - Biomembranes*, *1669*(2), 142–154. https://doi.org/10.1016/j.bbamem.2005.01.013
Zhou, Yandong, Nwokonko, R. M., Cai, X., Loktionova, N. A., Abdulqadir, R., Xin, P., … Gill, D. L. (2018). Cross-linking of Orai1 channels by STIM proteins. *Proceedings of the National Academy of Sciences*, *115*(15), E3398–E3407. https://doi.org/10.1073/PNAS.1720810115
Zohar, O., Pick, C. G., Cavallaro, S., Chapman, J., Katzav, A., Milman, A., & Alkon, D. L. (2005). Age-dependent differential expression of BACE splice variants in brain regions of tg2576 mice. *Neurobiology of Aging*, *26*(8), 1167–1175. https://doi.org/10.1016/j.neurobiolaging.2004.10.005

Chapter 10

Appendix

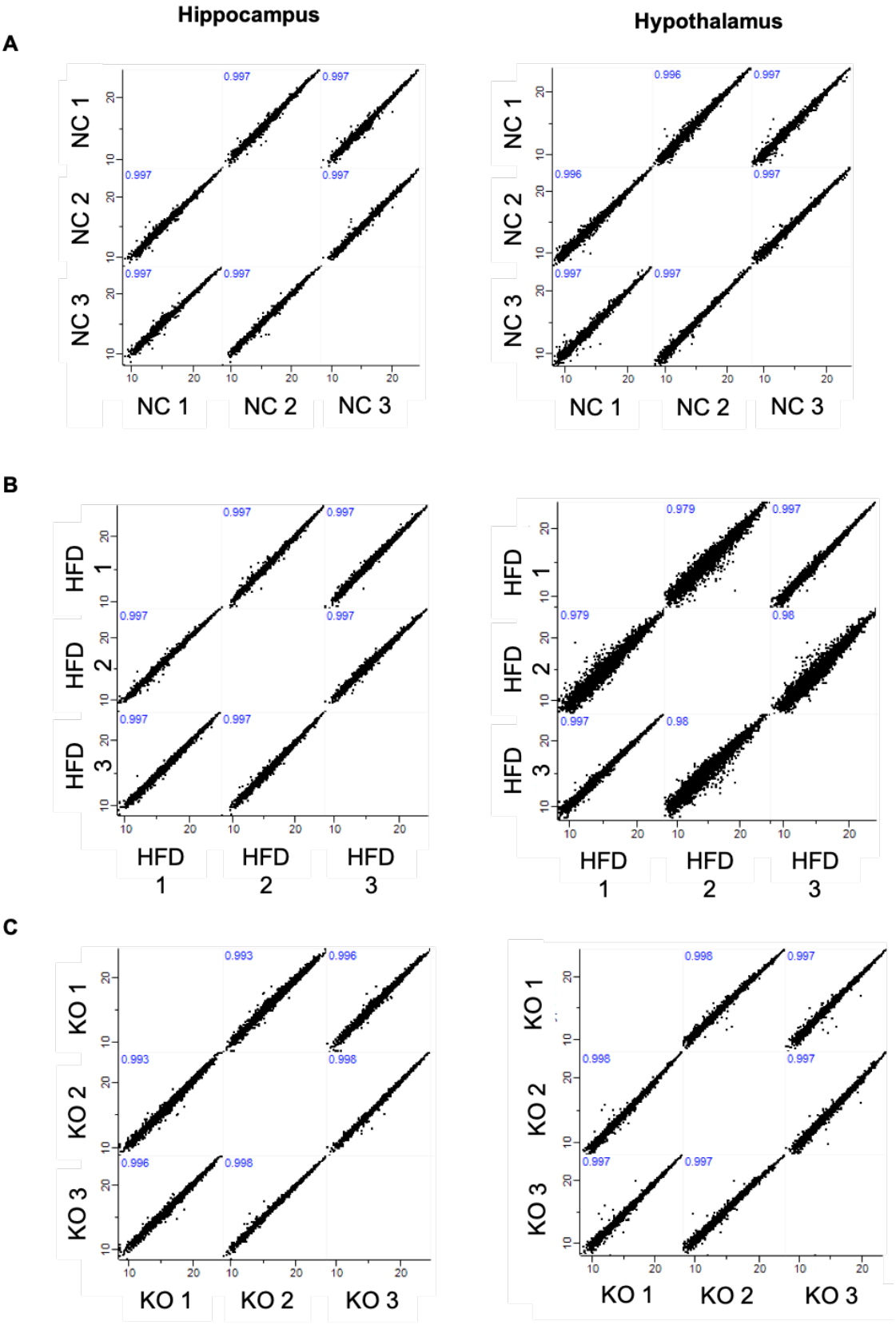

Figure S1 Pearson's correlations of replicates within the Wild-type normal chow (WT NC) (**A**), WT high-fat (WT HFD) (**B**), and BACE1 knock-out HFD (KO) (**C**) groups by semi-quantitative analysis. Pearson's correlation coefficients show very good correlation between replicates of each group with HFD replicate 2 exhibiting greater proteomic variability in the hypothalamus compared to other replicates within this group.

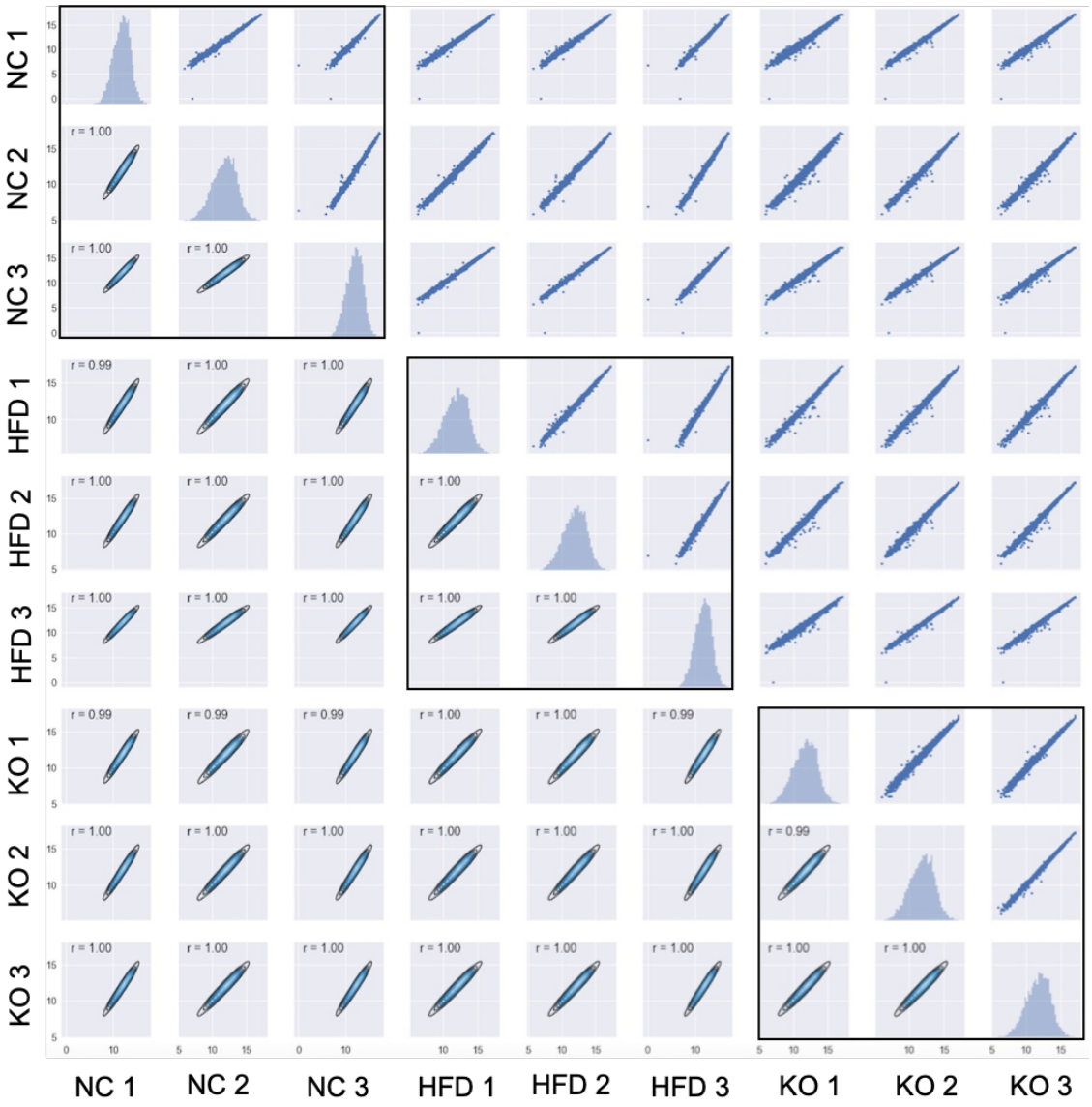

Figure S2 Pearson's correlations of replicates within the hippocampus of Wild-type normal chow (NC) (**A**), WT high-fat (HFD) (**B**), and BACE1 knock-out HFD (KO) groups by quantitative analysis. Pearson's correlation coefficients show very good correlation between replicates of each group with r≧0.99.

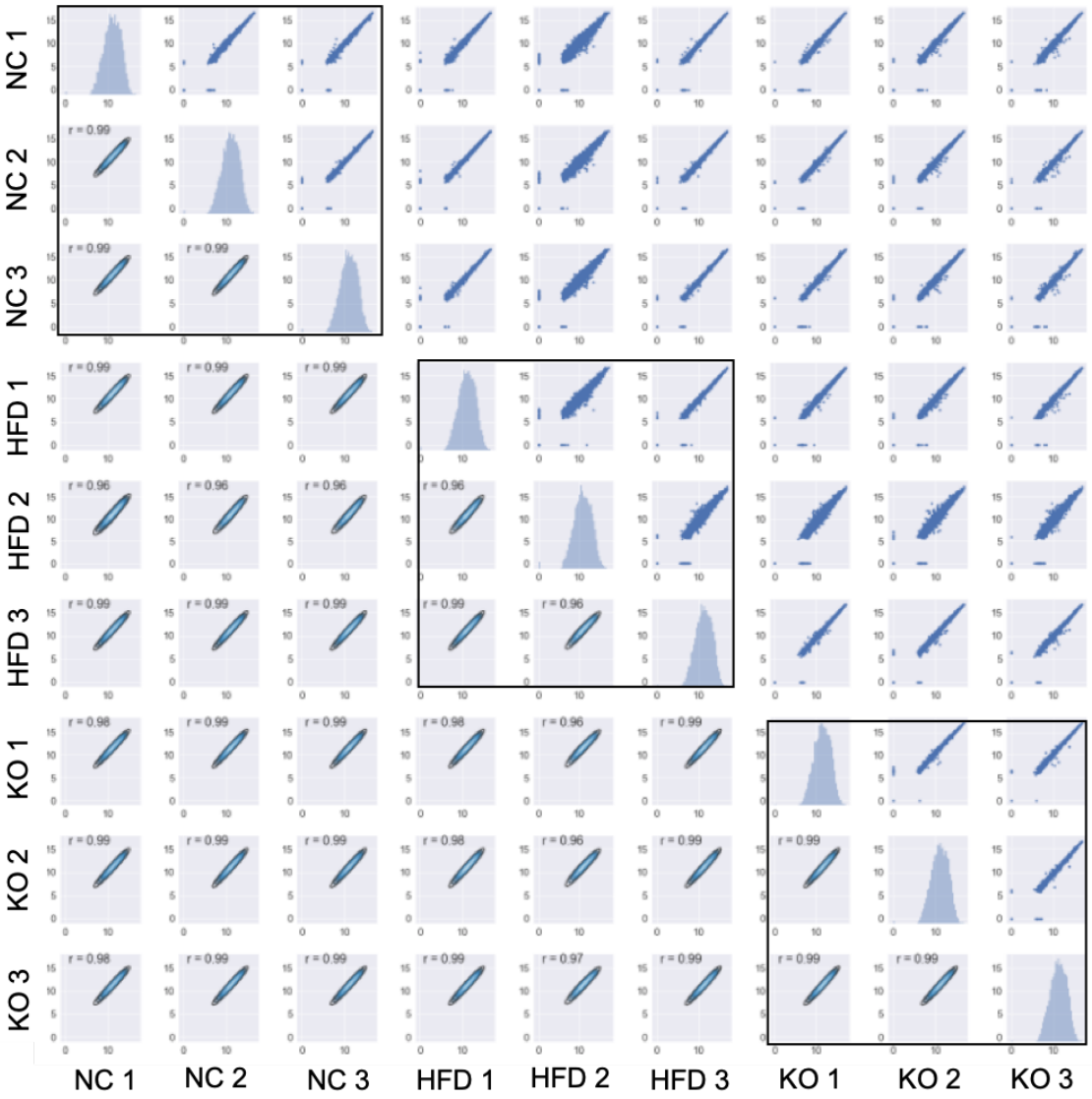

Figure S3 Pearson's correlations of replicates within the hypothalamus of Wild-type normal chow (NC) (**A**), WT high-fat (HFD) (**B**), and BACE1 knock-out HFD (KO) groups by quantitative analysis. Pearson's correlation coefficients show good correlation between replicates of each group with r≧0.96. HFD replicate 2 showed greater proteomic variability compared to the other replicates within that group.

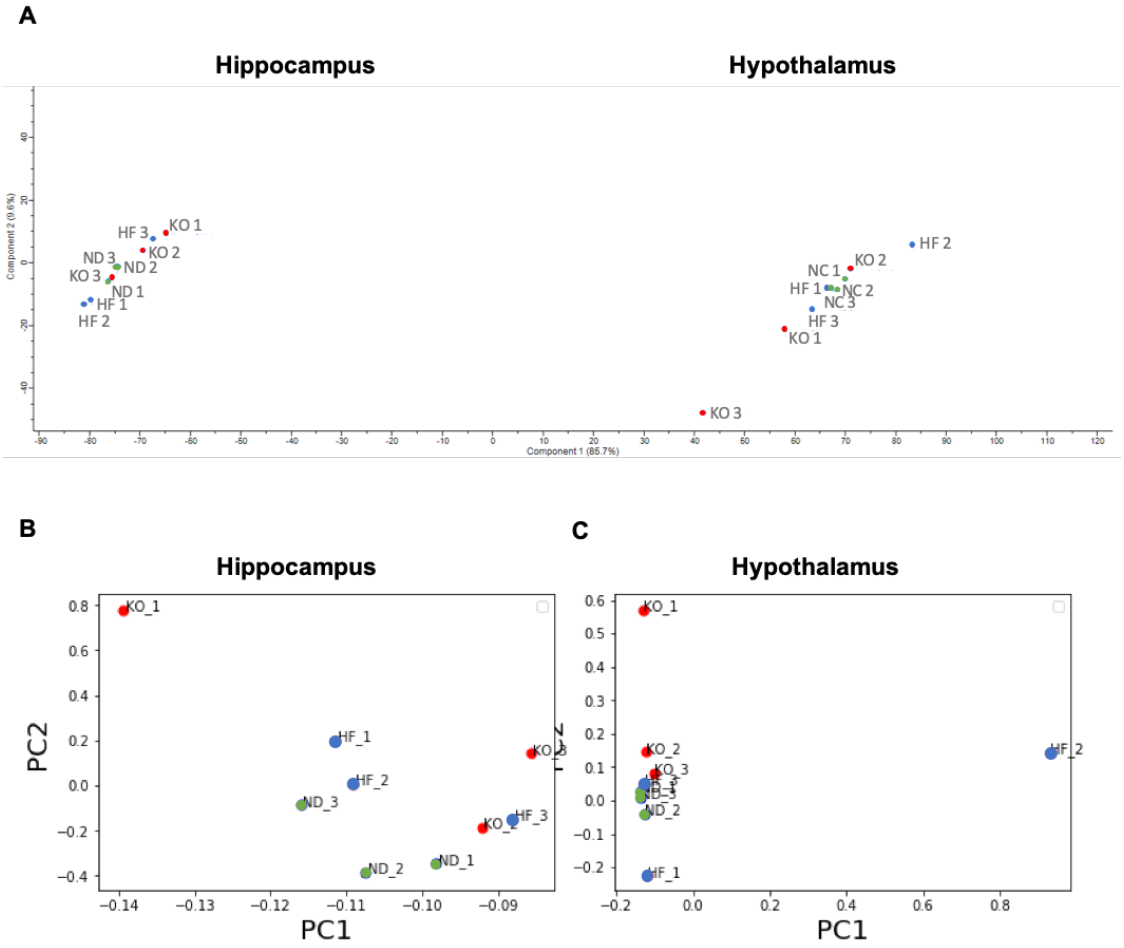

Figure S4 (**A**) Principle component analysis (PCA) using semi-quantitative analysis revealed greatest variability between the hippocampal and hypothalamic samples by component 1 with little variability in component 2. Little variability was seen between Wild-type normal chow (ND), Wild-type high-fat and BACE1 KO high-fat (KO) groups. PCA using quantitative analysis revealed very little variability in either component in either the hippocampus with the majority of variance between samples being due to component 2. (**B**) In the hypothalamus, WT HF sample 3 indicated variability in both component 1 and 2 whilst variability between the other samples was very small. The majority of which was due to differences in component 1. (**C**)

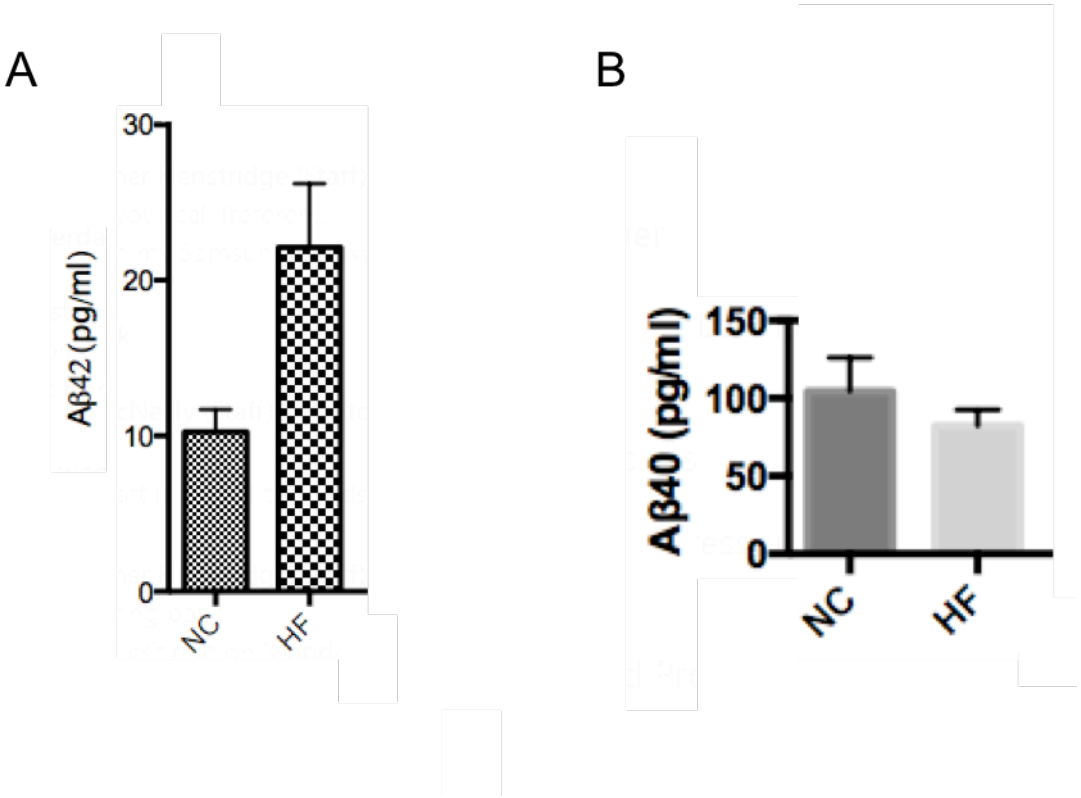

Figure S5 Amyloid beta content of serum after 20week dietary intervention. Both Amyloid-β 1-42 (A) and Amyloid-β 1-40 (B) expression in the blood of mice challenged with a 20 week HF diet and NC controls. Aβ42 increases from approx. 10 to 20pg/ml with dietary intervention whilst Aβ40 reduces from approx. 100 to 80pg/ml with HFD.